Manipulation of host cell signaling pathways and translation factors during poxvirus infection

A thesis submitted for the degree of Ph.D.

Dublin City University

by

Izabela Zaborowska M.Sc.

The research work described in this thesis

was carried out under the supervision of

Dr. Derek Walsh

National Institute for Cellular Biotechnology

Dublin City University

Republic of Ireland

2010

I hereby certify that this material, which I now submit for assessment on the programme of study leading to the award of Ph.D. is entirely my own work, that I have exercised reasonable care to ensure that the work is original, and does not to the best of my knowledge breach any law of copyright, and has not been taken from the work of others save and to the extent that such work has been cited and acknowledged within the text of my work.

Signed: _____ ID No.: _____ Date: _____

ABSTRACT

Poxviruses are large double-stranded DNA viruses that replicate exclusively in the cytoplasm of infected cells in distinct sites termed viral factories, with Vaccinia Virus (VacV) acting as the laboratory prototype for those that infect humans. Despite encoding proteins responsible for DNA replication and mRNA transcription, like all viruses they remain dependent on the host-cell translational machinery to produce viral proteins. Although recent studies have shown that VacV stimulates mTOR activity and redistributes translation factors to viral factories, how this is accomplished and its importance to VacV replication remain unknown.

Here, we demonstrate that VacV activates the PI3 kinase (PI3K) to stimulate its downstream substrate mTOR, thereby inactivating the translational repressor protein, 4E-BP1. This provides the first evidence that VacV activates PI3K signal pathway in a manner distinct from other poxviruses studied, such as myxoma virus, which directly stimulates Akt activity in a PI3K-independent mode. Using specific inhibitors we dissect the role of various components of PI3K/Akt pathway and show that rapamycin-insensitive mTORC1 and mTORC2 activity is responsible for stimulating the formation of the translation initiation factor, eIF4F, which drives cap-dependent translation in infected and uninfected cells. We also show that eIF4F is important but not absolutely essential for viral protein synthesis. In addition, we demonstrate that inactivation of the PI3K by either LY294002 or wortmannin does not cause apoptosis in human or monkey cell lines.

In an attempt to understand how VacV causes the redistribution of host translation initiation factors to viral factories, we performed immunoprecipitation-based screens and identified the product of the VacV I3L gene, the single-stranded DNA (ssDNA) binding protein, I3 as interacting with eIF4F. We demonstrate that I3 binds eIF4G directly *in vivo* and *in vitro* within the eIF4G C-terminal domain. PAA, a DNA polymerase inhibitor that blocks viral factory formation and entry into late stages of infection, did not significantly affect the ability of I3 to interact with eIF4F, although it did block re-localization of these factors. Cloned I3 was able to mediate the binding of initiation factors to ssDNA in cell extracts, suggesting that I3 sequesters host translation factors within viral factories as they form. Our attempt to recover VacV ΔI3L mutants using the Vac-Bac/λ system was unsuccessful, suggesting that the I3L gene product (I3) is essential during VacV infection.

Overall, our results provide new insights into how VacV manipulates host signaling and translation initiation factor function and their importance in viral protein synthesis and replication, highlighting a novel approach by a DNA virus to manipulate the host-cell translation initiation machinery.

Acknowledgements

First of all I would like to thank my supervisor, Dr. Derek Walsh, who introduced me to the magic world of science. With his enthusiasm, optimism and brilliant ideas he provided me support and encouragement during these years of my research, his guidance has been invaluable.

Thanks also to Prof. Martin Clynes and all others in the Centre who contributed to this thesis, especially Mick for helping with protein identification, and Finbarr for assistance with the microscopes and "lending" the antibodies. Many thanks to Joe for his excellent technical assistance. I am also grateful to Mairead, Carol, Yvonne, and Sree for being incredibly kind, helpful and having things in hand.

I appreciatively thank Prof. Michael Clemens and Dr. Niall Barron for their constructive comments and critical insights on my thesis, and for being the members of my examining committee. Thanks to Rob for the helpful discussions, Kerstin and Patricia for all the girly talks and gossip. Many thanks to all my friends, especially Monika and Marta for their support during my every crisis.

A special thank you goes to Suraj for his patience, motivational lectures and a company in every joy and sadness I've been through during the past 3 years of my studies.

Lastly, and most importantly, I would like to thank my parents, Wanda and Adam for supporting me in all my decisions and always believing in me. To them I dedicate this dissertation.

To my parents

Dla Rodziców

Abbreviations

4E-BP	-	eIF4E-binding protein
Ab	-	antibody
ATP	-	adenosine triphosphate
BrdU	-	bromodeoxyuridine
BSA	-	bovine Serum albumin
BSC40	-	monkey epithelial kidney cells
C_2 domain	-	protein kinase C homology domain 2
cDNA	-	complementary DNA
C-terminus	-	carboxy-terminus
DEPC	-	diethyl pyrocarbonate
DMEM	-	Dulbecco's modified Eagle's medium
DMSO	-	dimethyl sulfoxide
DNA	-	deoxyribonucleic acid
ds	-	double stranded
DNAse	-	deoxyribonuclease
dNTP	-	deoxynucleotide triphosphate
DTT	-	dithiothreitol
EDTA	-	ethylene diamine tetracetic acid
eIF	-	eukaryotic initiation factor
FBS	-	fetal bovine serum
FKBP12	-	FK506-binding protein, molecular mass of 12 kDa
g	-	gram
GST	-	glutathione-S-transferase
HEK	-	human embryonic kidney
HEPES	-	N-[2-Hydroxyethyl]piperazine-N'-[2-ethanesulphonic acid]
IC_{50}	-	inhibitory concentration 50%
IPTG	-	isopropyl β-D-1-thiogalactopyranoside
IRES	-	internal ribosome entry site
kDa	-	kilo Daltons
kb	-	kilobase
kbp	-	kilobase pair
M	-	mole
MAb	-	monoclonal antibody
MAPK	-	microtubule associated protein kinase

Met	-	methionine
Met-tRNA$_i$	-	methionyl-initiator transfer ribonucleic acid
min	-	minute
mRNA	-	messenger RNA
miRNA	-	micro ribonucleic acid
ml	-	mililitre
mm	-	milimetre
mM	-	mili mole
Mnk	-	MAP kinase interacting kinase
mTOR	-	mammalian target of rapamycin
MW	-	molecular weight
μ	-	micro
NHDF	-	normal human diploid fibroblast
N-terminus	-	amino-terminus
OD	-	optical density
P	-	phospho-
PAA	-	phosphonoacetic acid
PABP	-	poly(A)-binding protein
PBS	-	phosphate buffered saline
PCR	-	polymerase chain reaction
PDK1	-	phosphoinositide-dependent kinase 1
PI	-	phosphoinositide
PI3K	-	phosphoinositide-3 kinase
PIP$_2$	-	phosphatidylinositol-4,5-biphosphate
PIP$_3$	-	phosphatidylinositol-3,4,5-triphosphate
PtdIns	-	phosphatidylinositol
PTEN	-	phosphatase and tensin homolog deleted on chromosome 10
raptor	-	regulatory-associated protein of mTOR
rictor	-	rapamycin-independent companion of mTOR
RNA	-	ribonucleic acid
RNAse	-	ribonuclease
RNAi	-	RNA interference
RNAsin	-	ribonuclease inhibitor
rpm	-	revolution(s) per minute
SDS	-	sodium dodecyl sulphate
SDS-PAGE	-	sodium dodecyl sulphate-polyacrylamide gel electrophoresis
sec	-	second

siRNA	-	small interfering ribonucleic acid
SSB	-	single-strand DNA-binding
ssDNA	-	single-stranded DNA
ssRNA	-	single-stranded RNA
TBS	-	tris buffered saline
TCA	-	trichloroacetic acid
TE	-	Tris-EDTA
TEMED	-	N, N, N', N'-tetramethyl-ethylenediamine
UHP	-	ultra high purity
UTR	-	untranslated region
V	-	volt
VacV	-	Vaccinia virus
VarV	-	Variola virus
WB	-	Western blot
xg	-	times gravity

Table of contents

Section 1.0

Introduction

1.1 The *Poxviridae* family

Poxviruses are mysterious and fascinating microbes that distinguish themselves from other DNA viruses on account of their enormous size, complex morphology, and unique replication cycle in the cytoplasm. Members of the family of poxviruses (*Poxviridae*) infect diverse genera of the animal kingdom from insects to mammals. Two of them, variola virus and molluscum contagiosum virus infect only humans, but other members of the family, such as monkeypox, can be transmitted from animals to humans as zoonoses and have been reported to subsequently transmit from human to human (Moss, 2007).

1.1.1 Classification of Poxviruses

The *Poxviridae* are divided into two subfamilies: the poxviruses of vertebrates (*Chordopoxvirinae*) consisting of eight genera, and the poxviruses of insects (*Entomopoxvirinae*) consisting of three genera (Table 1.1). The genetic connection between poxvirus subfamilies was confirmed by DNA sequencing and bioinformatic analysis; moreover, a genetic relation with other large DNA viruses belonging to the families *Asfaviridae*, *Iridoviridae*, *Phycodnaviridae*, and recently discovered *Mimiviruses* has been suggested (Iyer *et al.*, 2001; Suzan-Monti *et al.*, 2006). Poxviruses pathogenic for humans belong to four diverse genera of the vertebrate poxvirus family, and the majority of them are orthopoxviruses. Therefore, the *Orthopoxvirus* genus has been of interest to scientists for many years, becoming the best known and the most widely studied amongst eleven genera comprising the Poxvirus family.

Family	Subfamily	Genus	Type species
Poxviridae	*Chordopoxvirinae*	*Orthopoxvirus*	*Vaccinia virus, Variola virus*
		Parapoxvirus	*Orf virus*
		Avipoxvirus	*Fowlpox virus*
		Capripoxvirus	*Sheeppox virus*
		Leporipoxvirus	*Myxoma virus*
		Suipoxvirus	*Swinepox virus*
		Molluscipoxvirus	*Molluscum contagiosum virus*
		Yatapoxvirus	*Yaba monkey tumor virus*
	Entomopoxvirinae	*Alphaentomopoxvirus*	*Melolontha melolontha entomopoxvirus*
		Betaentomopoxvirus	*Amsacta moorei entomopoxvirus*
		Gammaentomopoxvirus	*Chironomus luridus entomopoxvirus*

Table 1.1 Classification of Poxviruses (Data of *Virus Taxonomy*, 2000)

The laboratory prototype of orthopoxviruses used in this study is vaccinia virus (VacV), which has been employed to eliminate the smallpox epidemic of the 18th and 19th centuries (see next paragraph).

1.1.2 Smallpox disease

Smallpox, also called variola, is one of the most devastating diseases known, affects only humans, and is caused by variola virus (VarV). The name "variola" is derived from a term "variolation", which was a practice of inhaling material from the dried pox scabs or inoculating this material directly beneath the skin to stimulate the immune system against smallpox. There are two clinical forms of smallpox: variola major, concerning more than 90% cases and with the case-fatality rate varied from 5 to 40%, and variola minor, a milder form of smallpox with a mortality rate of about 0.1-2%. Outbreaks of variola minor were observed independently of variola major outbreaks and located mostly in South America and South Africa (Shchelkunov *et al.*, 2005). However, biological distinctions between diverse forms of variola still lack a complete explanation.

Transmission of VarV follows inhalation or other close contact with infected persons or their belongings, such as blankets (Damon, 2007). Infectious forms of the virus occur in the pustules formed during the incubation period, as illustrated on Fig. 1.1.1. During the first hour of the incubation period virus infects pulmonary macropahges, then spreads from the lungs to local lymph nodes where it multiplies, and is borne by blood. The virus also replicates in the spleen, bone marrow and lymph tissue. Finally, leucocytes with multiplied virus appear in dermal and mucosal vessels, leading to characteristic skin and mucosal symptoms (de los Rios and Jimenez-Gomez, 2007).

Infection begins with high fever (38-40^{0}C) and chills, often accompanied by malaise, headache, lumbar pain, and less frequently by nausea, vomiting, abdominal pain and delirium. The rash arises within 4 days of infection and begins with small red spots on the tongue and in the mouth. These spots evolve to sores that break open and spread the

virus into the mouth and throat, and soon after to the skin beginning on the face and extending to arms, legs and entire body within 24 hours. By the third day of the rash it becomes raised bumps, filled with a thick, opaque fluid containing infectious virions. During the next 5 days the bumps evolve to round pustules, which then begin to form crusts and scabs. The scabs begin to fall off, releasing infectious virions and leaving the marks on the skin. The patient remains contagious until the last scab falls off (de los Rios and Jimenez-Gomez, 2007).
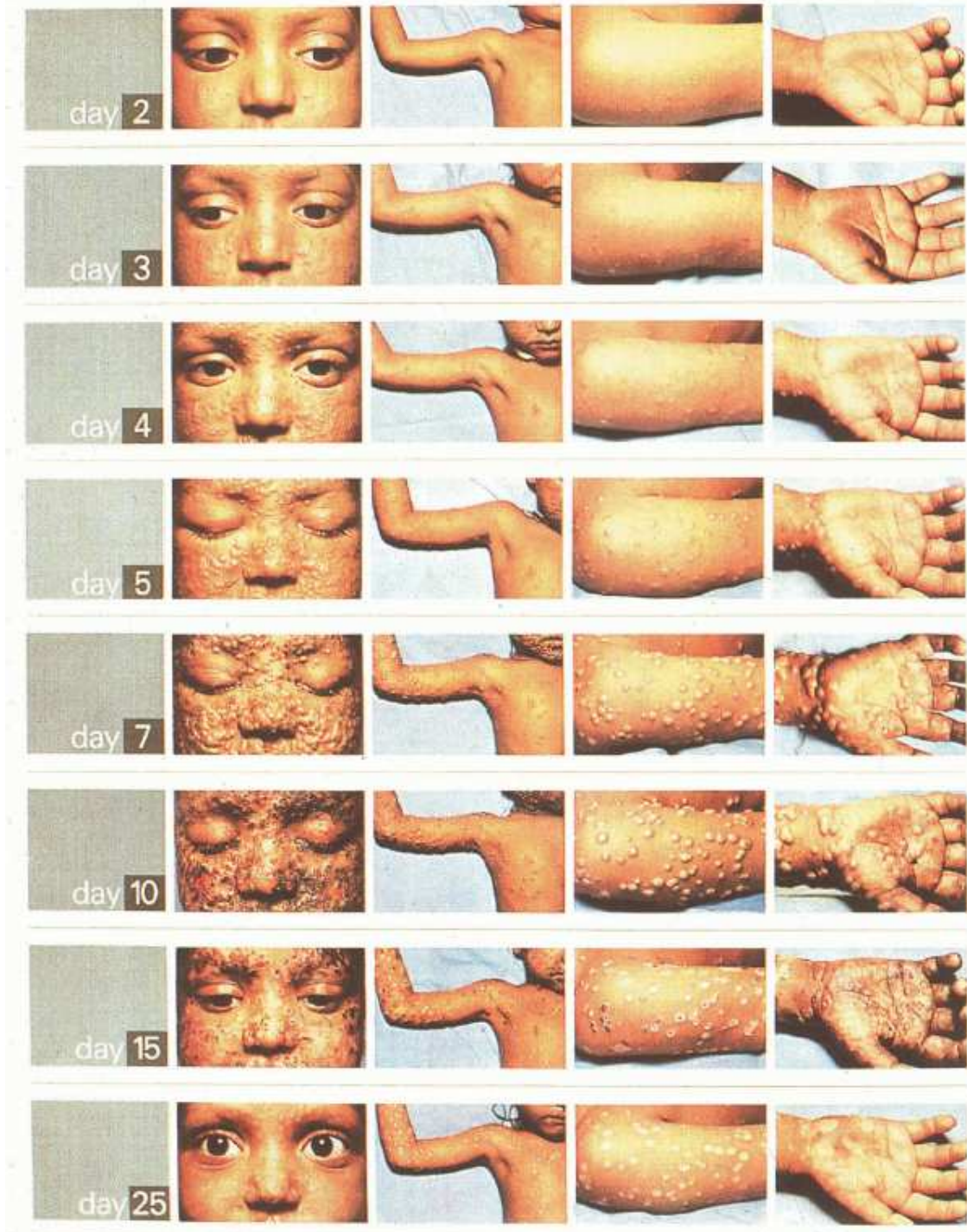
Figure 1.1.1 A poster showing the stages of rash during smallpox infection. Multilingual versions of the poster were prepared and distributed in 1970, during smallpox eradication programme (From Fenner *et al*., 1988)

1.1.2.1 Smallpox in human history

Smallpox has had a massive impact on human history for more than 2000 years. The virus causing smallpox probably originated in either Egypt or India. Examination of the Egyptian mummies, as well as analysis of the ancient Indian Sanskrit describing the smallpox-like disease suggest that smallpox existed on those lands as early as 1000-1400 B.C. (Hopkins, 2002). By 1000 A.D. smallpox spread in Europe, North Africa and East Asia, but did not become a major problem until the 17th century (Carmichael and Silverstein, 1987). During the 17th and 18th centuries smallpox was introduced by Europeans into North and South America, Australia and South Africa, becoming a worldwide issue.

Until recently, smallpox was the most infectious and deadly epidemic disease of humans, with a mortality rate exceeding 30%. In the previous century alone smallpox killed more than 300 million people around the world and most likely would have been killing millions until now if not for the recognition that vaccination with cowpox or vaccinia virus protects from smallpox infection, which has been observed and published by Edward Jenner in 1798. The live vaccine was applied intradermally by scarifying the skin on the arm. The virus replicated at the site of scarification stimulating both antibody-mediated and T cell-mediated protective immunity against smallpox and other orthopoxviruses such as monkeypox (Dimmock *et al*., 2007). Smallpox was completely eradicated in 1977 through the international vaccination campaigns carried out by the World Health Organization (WHO). The remaining stocks of VarV have been destroyed with the exception of two reservoirs in United States and Russia (WHO, 1999) under the supervision of WHO. Smallpox became a history, and the only epidemic disease known that has been completely eradicated by vaccination.

1.1.2.2 Poxviruses still endanger

Although variola virus does not occur naturally in the environment anymore, there is a concern that if unknown stocks of VarV exist, they can be used as a potential and very dangerous biological weapon in bioterrorism. There is also a possibility of genetically engineering orthopoxvirus strains such as monkeypox virus to create a smallpox-like disease. Since WHO stopped the routine vaccination against smallpox in 1980 due to the mass side effects and complications caused by vaccinia virus, the effects of a smallpox outbreak on our current population would be profound.

In addition, other orthopoxvirus infections, such as monkeypox, have been reported in humans. A recent outbreak of the monkeypox disease occurred in the United States in 2003, when 72 humans were diagnosed with monkeypox after contact with wild prairie dogs (Shchelkunov *et al*., 2005). Monkeypox virus can spread between humans and cause a serious, smallpox-like disease (Fig. 1.1.2).

Figure 1.1.2 Human monkeypox. The day 8 of the monkeypox infection on a 7-year-old girl (From Breman *et al*., 1980)

Considering the facts described above, further research in poxviruses is essential in terms of investigating new antiviral agents and improved vaccines.

1.1.3 Vaccinia virus

A remarkable poxvirus that is not host-species specific is vaccinia virus (VacV), a laboratory prototype of poxviruses, which, together with cowpox virus, has been used for immunisation against smallpox. Since VacV and VarV belong to the same *Orthopoxvirus* genus, they are closely related genetically, morphologically, and cover a similar host range. VacV is the most widely studied poxvirus and has greatly contributed to the expansion of general knowledge on infectious diseases and immunity; it was the first animal virus seen under the microscope, precisely titered, grown in tissue culture, physically purified, and chemically analyzed (Moss, 2007). Furthermore, VacV has been used as a live recombinant expression vector for protein synthesis *in vivo* and *in vitro* (Moss, 1996) providing a new tool in gene therapy, developing vaccines against various infectious diseases, and cancer therapy (Mastrangelo *et al*., 2000).

1.1.3.1 The origin of VacV

Although VacV biology has been widely studied and the virus was used for millions of vaccinations, its origin and natural host remain a mystery. Some scientists believe that VacV is a laboratory strain with no natural reservoir, and could be a result of a cowpox virus transformation during vaccination (Shchelkunov *et al*., 2005). Furthermore, Bedson and Dumbell (1964) were able to obtain recombinants of variola and cowpox viruses with properties similar to VacV, suggesting its origin. Another hypothesis proposes that VacV is a derivative of other animal viruses that have disappeared from

the environment such as horsepox virus (Shchelkunov *et al*., 2005). Vaccinia-like viruses were also isolated from buffaloes in India at the late 1960s- early 1970s, and most recently in 1992-96 (Kolhapure *et al*., 1997), and also from dairy cattle and humans in Brazil during the outbreak in 1990s (Damaso *et al.*, 2000). Those isolates could be the derivatives of the vaccinia-like viruses originally existing in nature, but most likely they are mutated vaccine strains accidentally introduced into the environment during smallpox eradication and vaccination. Some of those naturally occurring strains became subspecies of VacV, such as buffalopox and rabbitpox virus (*Virus Taxonomy*, 2000).

Summarizing, the origin of VacV needs further investigation including the analysis of genomic structures of VacV and related orthopoxviruses, which will probably solve that point of issue.

1.1.3.2   Virion structure and entry

The orthopoxvirus virions exist in four different forms, depending on the stage of maturity: immature virions (IV), mature virions (MV), wrapped virions (WV), and extracellular virions (EV). The last three forms are infectious and differ in the number of membranes and thus surface antigens (reviewed by Smith *et al.*, 2002). The vaccinia virion is very large in comparison to other animal viruses. Reconstruction of the intracellular mature virion (MV) by cryo-electron tomography carried out recently by Cyrklaff and colleagues (2005) revealed its brick-shape with rounded edges and dimensions of approximately 360x270x250 nm (Fig. 1.1.3 A, B). Each MV is surrounded by a lipid membrane which is 5-6 nm thick and contains at least one, but most frequently two lateral bodies built up by a heterogeneous protein layer and

attached to the outer membrane. The central part of the virion possesses a dumbbell-shaped core with the wall composed of two layers (Fig. 1.1.3 C, D; Fig. 1.1.4). The outer membrane of the core appears continuous, but pore-like structures were identified on the inner core membrane that may be involved in releasing the viral mRNA into the cytoplasm shortly after infection (Griffiths *et al*., 2001), indicating that VacV entirely uncoats the outer core membrane before getting into the cytoplasm.
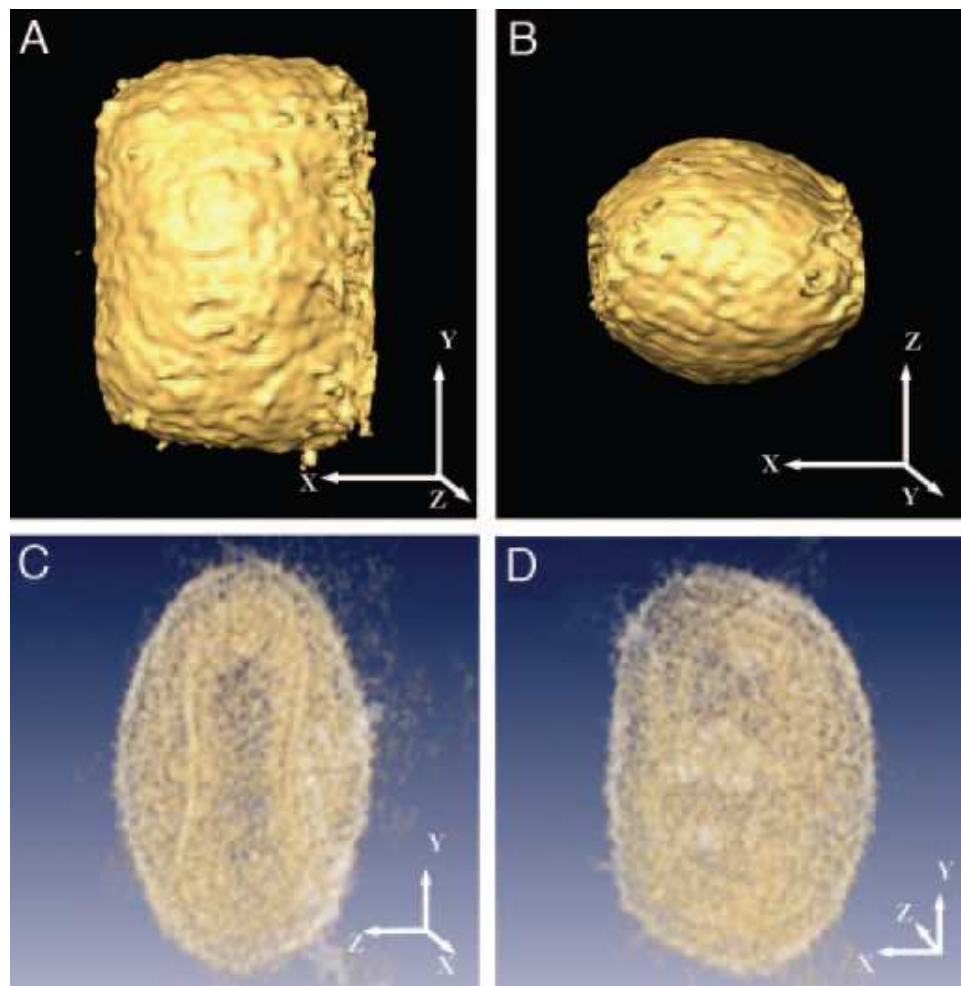
Figure 1.1.3 Images of the VacV mature virion (MV) reconstructed by cryo-electron tomography. (A, B) Two orthogonal views along perpendicular axes, highlighting the outer shape and size of the virion. (C, D) Translucent illustration of the virion showing the complex internal structure of the core. (From Cyrklaff *et al*., 2005)
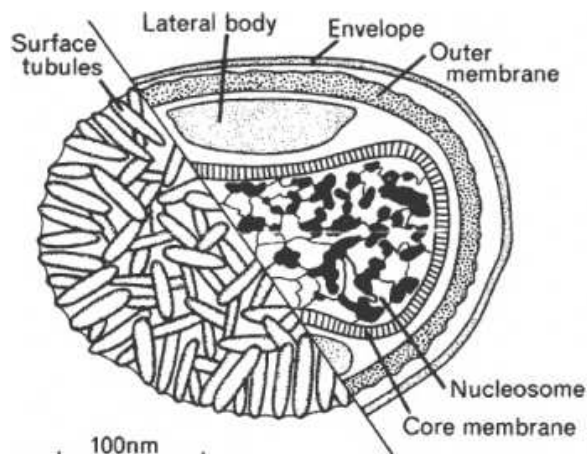
Figure 1.1.4 Schematic diagram of the structure of orthopoxvirus mature virion (MV).
Virion is brick-shaped and surrounded by two lipid membranes. Viral genome DNA and a
number of proteins within the core are organized as a nucleosome. Lateral bodies are attached to
the outer lipoprotein membrane, which is 12 nm thick. The outer membrane surface
appears to consist of irregularly shaped tubules. (From Damon, 2007)

The viral genome is situated in the core. In the tomographic reconstructions the contents
of the core separate in two phases, one of which is denser, contains DNA, and was
found to concentrate near the core membrane, while the lower density volume is free of
DNA and is most likely occupied by enzymes and factors needed for synthesis of early
viral mRNA (Cyrklaff *et al*., 2005).

Investigations of the mechanism(s) used by VacV to enter cells are complicated by the
existence of multiple infectious forms that differ from one another by their outer
membrane. MVs have a single outer membrane while EVs possess an additional
antigenically distinct outer membrane that must be disrupted prior to or during entry
(Moss, 2007). MV enters the cell by fusion of the lipoprotein membrane with the
plasma membrane or following endocytosis, while entry of the EV is still a matter of
some debate. However, it is known that virus entry is facilitated by interaction of viral

proteins with specific cell surface receptors, which can determine tropism (Sieczkarski and Whittaker, 2005; reviewed in Moss, 2006).

The outer membrane of MV is covered with irregularly shaped, randomly located surface tubules (Fig. 1.1.4) in lengths of about 50-100 nm, consisting of a single, 58 kDa polypeptide (Muller and Williamson, 1987). Surface tubules were shown to inhibit cellular protein synthesis both *in vivo* and when added to the rabbit reticulocyte lysate (Mbuy *et al.*, 1982).

1.1.3.3 Life cycle

Unlike most other DNA viruses, poxviruses replicate exclusively in the cytoplasm of infected cells rather than in the nucleus, in structures called viral factories or virosomes, and can even replicate in enucleated cells (Prescott *et al.*, 1971; Pennington and Follett, 1974). A single virion contains a complete transcription system essential for the synthesis of viral mRNA which is capped, methylated and polyadenylated (Moss, 2007). A great number of viral core-associated enzymes and factors have been identified including RNA polymerase, DNA helicase, topoisomerase, vaccinia early transcription factor (VETF), capping and methylating enzymes, and many more. VacV also encodes protein kinases and a protein phosphatase, suggesting the role of protein phosphorylation in the regulation of its life cycle (Traktman, 1996).

The VacV life cycle starts after fusion with the cell membrane and releasing the core into the cytoplasm (Fig. 1.1.7). The early genes are transcribed and translated immediately, while the core translocates on microtubules to specific cytoplasmic compartments and forms a viral factory, where intermediate-to-late protein synthesis as well as viral DNA replication occur. The viral factory is also a place where the early

VacV proteins accumulate (Kovacs and Moss, 1996, Domi and Beaud, 2000; Katsafanas and Moss, 2007). As soon as the late genes are transcribed, virion assembly begins with the formation of distinct membrane structures. The newly synthesized viral particles containing structural proteins, enzymes and early transcription factors are wrapped by membranes derived from virus-modified trans-Golgi or endosomal cisternae, containing at least seven viral proteins (Moss, 2007), and released from the cell through exocytosis. Some enveloped virions remain attached to the cell surface and induce the growth of actin tails beneath virions on the plasma membrane to facilitate virus spread into neighbouring cells (Smith and Law, 2004).

1.1.3.4 Virion assembly

The assembly of vaccinia virions begins in viral factories that form close to the nucleus. The core of the immature virion (IV) originates from the crescent-shaped precursors, and subsequently condenses and differentiates to form a mature virion (MV). The difference in morphology between those two types of virions has been illustrated in Figure 1.1.5. MV is an infectious virion and can be released by cell lysis. However, these virions are not sufficient for the efficient virus spread, and the additional enveloped forms of the virions are required for this process. A number of MVs are wrapped by modified trans-Golgi (Schmelz *et al.*, 1994) or endosomal (Tooze *et al.*, 1993; van Eijl *et al.*, 2002) cisternae to form intracellular wrapped virions (WV), which then translocate to the cell surface through microtubules. WVs can remain on the cell surface as a Cell-associated Enveloped Virion (CEV), or be released from the cell through exocytosis, resulting in loss of the outer membrane and forming the extracellular mature virion (EV) (Moss and Ward, 2001; Smith *et al.*, 2002).
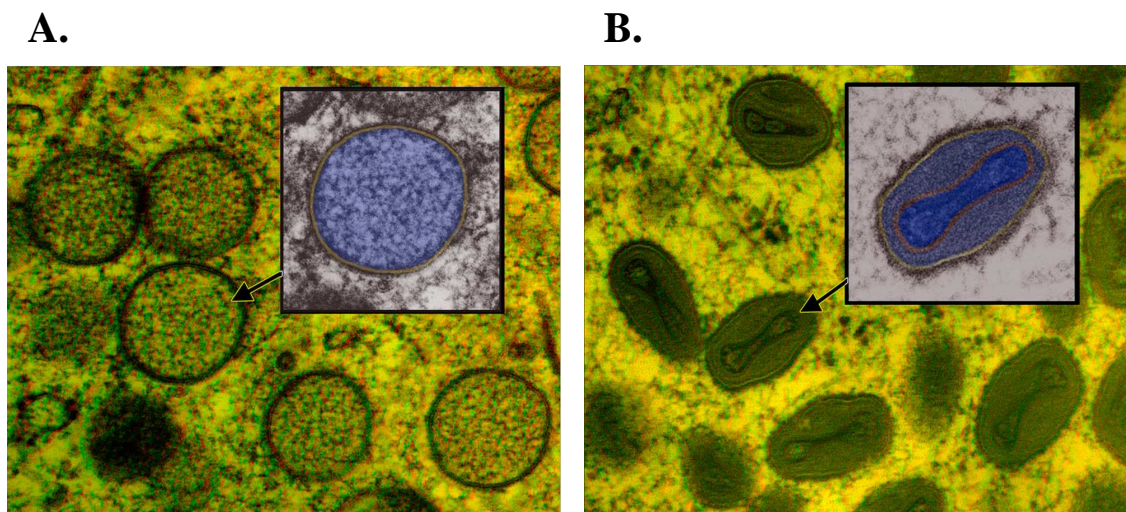
Figure 1.1.5 Images of vaccinia virions in cells infected overnight, acquired by using a three-dimensional electron microscopy system. A. Immature virions (IV) with one selected and color coded with membrane in yellow and core in blue. **B.** Mature virions (MV) with characteristic dumbbell-shaped core. One virion selected and color coded with membrane in yellow and core in two shades of blue, separated by a palisade layer in red. (From Heuser, 2005)

VacV can spread from cell-to-cell in several ways. Direct spread can be mediated by cell lysis, release of MV and re-infection of adjacent cells. In turn, CEV particles present on the cell surface can be driven into neighbouring cells by actin tails, which are formed in response to expression of the proteins encoded by A33R, A34R or A36R genes (Smith and Low, 2004).

1.1.3.5 Genome organization

Because poxviruses replicate in the cytoplasm of infected cells and hence are extremely self-sufficient, the mature virions contain the complete package of enzymes needed for synthesis of early viral mRNA. The nuclear material of VacV is a linear double-stranded DNA molecule with the approximate length of 190 kb and encodes more than 200 genes (Goebel *et al*., 1990; Lefkowitz *et al*., 2005). The vaccinia genome has A+T-

rich, covalently closed hairpin ends that connect the two DNA strands (Baroudy *et al*., 1982; Condit *et al*., 1996). As a result, when the DNA is fully denatured, a circular single-stranded molecule is generated. Furthermore, VacV genome contains quite large (approximately 10 kbp) inverted terminal repetitions (ITRs), which comprise identical but oppositely oriented sequences at both ends of the genome and exist in variable lengths (Garon *et al*., 1978). Next to the ends of the ITRs, short tandem repeated sequences occur (Wittek and Moss, 1980), which are thought to participate in recombination events (Traktman, 1996). The ITRs include a highly conserved DNA sequence of less than 100 bp required for the resolution of the VacV hairpin terminus (DeLange and McFadden, 1987; Merchlinsky, 1990), and a number of open reading frames (ORFs). The structure of the VacV genome is illustrated in Figure 1.1.6.

Vaccinia genes are very tightly packed in the genome; the gaps between coding sequences usually do not exceed 50 nt. Moreover, vaccinia genes do not contain introns, most likely as a consequence of the cytoplasmic site of replication, which makes analysis of the genomic sequences much simpler. There is no specific order of the genes location on the genome with respect to function, although Mackett and Archard (1979) illustrated that essential genes required for virus growth aggregate around the central part of the genome, which comprises around 60% of the total genome. Genes situated outside this region are generally not required for virus replication, but seem to be related to immune modulation and providing each poxvirus species unique and specific characteristics.

Figure 1.1.6 Schematic illustration of the VacV genome. A. A structure of the entire linear double-stranded DNA genome illustrates the hairpin ends and the location of inverted terminal repetitions comprising the tandem repeated sequences. **B**. The nucleotide sequences of the inverted and complementary forms of the terminal loops. (From Moss, 2007)
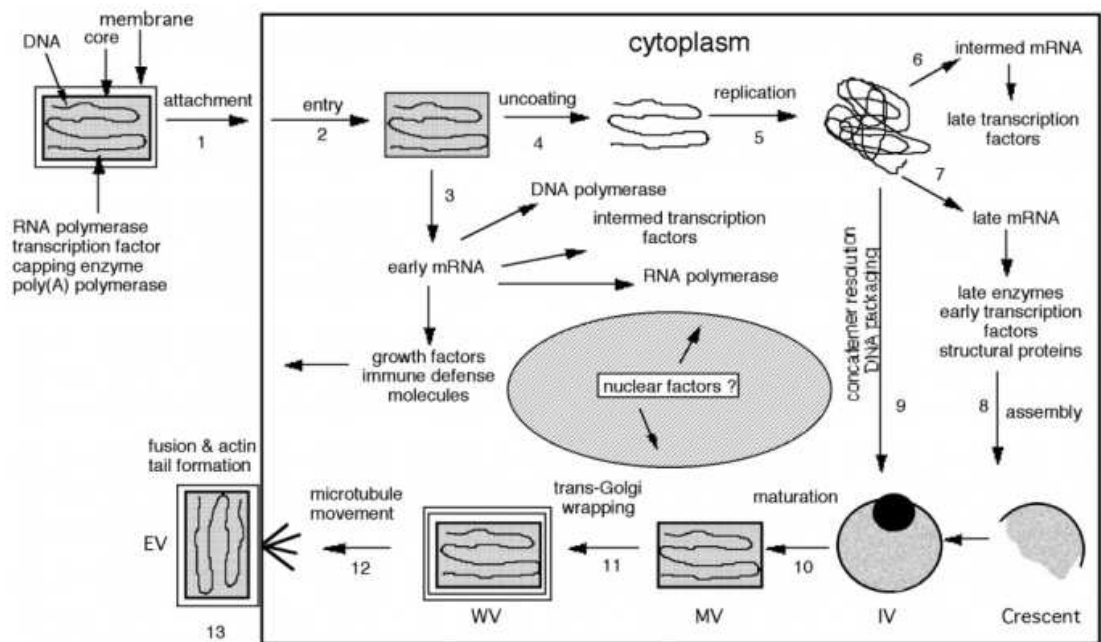
Figure 1.1.7 Replication cycle of vaccinia virus. A single virion containing DNA, enzymes and transcription factors attaches to a cell (1) and fuses with the cell membrane (2). Virion releases the core, and synthesizes early mRNA that is translated into various proteins (3). After uncoating (4) the DNA is replicated to form concatemeric molecules (5). Intermediate genes are transcribed and the mRNA is translated and to form late transcription factors (6). The late genes are transcribed, and the mRNA is translated and forms structural proteins, enzymes and early transcription factors (7). Virion assembly begins with the formation of the crescent-shaped precursors (8). The concatemeric DNA intermediates resolve into unit genomes, which are packed in immature virions (IV) (9). Maturation leads to the formation of infectious intracellular mature virions (MV) (10). MVs are enveloped by trans-Golgi membranes and the wrapped virions (WV) are transported to the cell surface on microtubules (11, 12). After fusion with the cell membrane extracellular enveloped virions (EV) are released from the cell, followed by actin tail formation beneath the EV (13). (From Moss, 2007)

1.1.3.6 DNA replication

As mentioned before, the vaccinia virus genome is a linear double-stranded DNA molecule with the approximate length of 190 kb that is unusual in having covalently closed ends, which means that the molecule does not have free 5' or 3' termini. Consequently, denaturation of DNA results in the formation of a circular single-stranded molecule. VacV DNA is extremely AT-rich (67%), especially on the termini, and is not methylated. Although the detailed biochemistry of VacV replication is not yet established, the unique structure of the VacV genome and the presence of concatemer junctions suggest a similar model of replication to the rolling hairpin model proposed for a single-stranded parvovirus DNA (Tattersall and Ward, 1976). Replication of VacV DNA does not only provide progeny genomes, but also is an obligatory step leading to the activation of viral intermediate gene transcription (Vos and Stunnenberg, 1988; Keck *et al.*, 1990). In turn, it is thought that optimal DNA replication requires the synthesis of viral and/or cellular proteins that are made at intermediate and late times after infection.

Vaccinia DNA replication begins one to two hours after infection with the introduction of a nick (cleavage at the phosphodiester bond between two nucleotides) near one or both ends of the termini, presumably within 200 bp of the end of the molecule (Du and Traktman, 1996). Strand cleavage provides a free 3'-OH end, which acts as a primer terminus for the viral DNA polymerase (Fig. 1.1.8). Strand extension proceeds towards the hairpin telomere, leading to the formation of a dimeric tail-to-tail concatemer, which is then resolved to monomer progeny genomes and packed into newly synthesized virions.
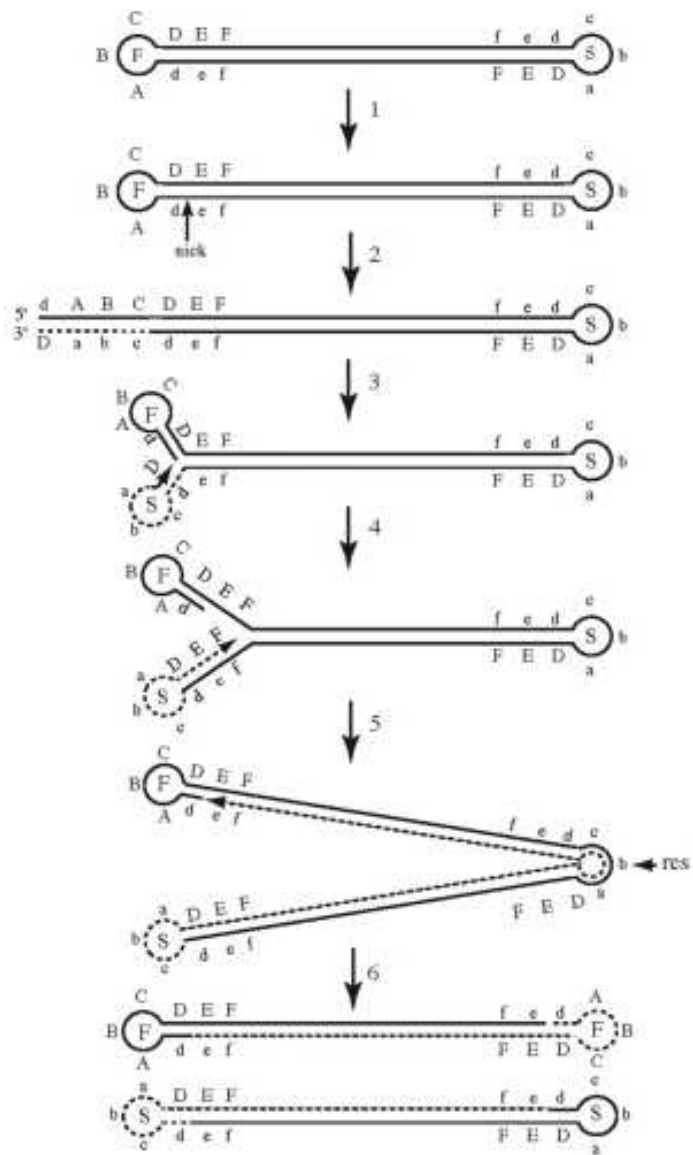
Figure 1.1.8 Schematic model for poxviral DNA replication. F and S indicate the fast and slow electrophoretic mobilities of DNA fragments containing complementary and inverted hairpin sequences. Newly synthesized DNA shown as dashed lines, with arrowhead at the 3'-OH termini. Complementary sequences are labeled with upper and lower case. "Res" indicates the resolution sites within the concatemer junction. (From Moss, 2007)

In spite of the fact that poxviruses are relatively self-sufficient and encode proteins responsible for DNA replication and mRNA transcription, like all viruses they remain completely dependent on the host-cell translational machinery to produce viral proteins. Consequently, they have to compete with the host-cell in utilising the protein synthesis factors. Virus influence affects all host-cell translational processes including initiation, elongation, termination, and signaling pathways, but the majority of the viral strategies are focused on translation initiation (Gale *et al*., 2000).

1.2 Translation initiation in eukaryotes

Translation is a multistep and multifactorial process leading to the synthesis of proteins, the molecules highly important for every living organism. Such an important process needs to be precisely monitored and regulated, and can enable the rapid manipulation of protein production without involving new mRNA synthesis, processing, or export. Although translational rates can be controlled at each of the three levels (initiation, elongation, termination) the majority of the regulation affects the initiation step, when the ribosome is recruited to the mRNA (Mathews *et al*., 2007). This fact seems to be logical and agrees with the biological principle which says that it is easier and more efficient to govern the process at its outset than to interrupt it in midstream and have to struggle with the activated apparatus and the accumulation of intermediates.

The regulation of translational rates (the frequency of mRNA translation) plays a key role in many fundamental biological processes including cell growth, development and response to stress agents. Modulation of initiation can influence both the overall rate of protein synthesis as well as the relative rates of synthesis of different proteins. Control of the overall rate of translation is potentially important for cell growth during G1 phase of the cell cycle, while the concentrations of the growing number of specific proteins involved in cell proliferation and differentiation control are now considered to be modulated, at least in part, at the translational level (Mathews *et al.*, 2007).

Usually, translation in eukaryotes is cap-dependent and starts with recognition of the 5' end of the mRNA and association of initiation factors. However, translation of some cellular mRNAs does not involve the cap and occurs through internal ribosome entry mechanism, which involves the internal association of ribosome subunits at or near the initiation codon without requiring entry from 5' end of the mRNA. Internal ribosome

22

entry sites (IRES) were first discovered in viral mRNAs (Jang *et al.*, 1988; Pelletier and Sonenberg, 1988), and the first cellular IRES was documented a few years later (Macejak and Sarnow, 1991).

The key elements involved in cap-dependent translation initiation are eukaryotic initiation factors (eIFs), the 80S ribosome and a messenger ribonucleic acid (mRNA).

1.2.1 The structure of eukaryotic mRNA

The mRNA is an RNA molecule that carries codes from the DNA in the nucleus to the region of protein synthesis in the cytoplasm. The translational efficiency of eukaryotic mRNA is limited by the rate of translation initiation, which is in turn determined by structural characteristics of mRNA that affect recruitment of ribosomes, scanning to the initiation codon, and recognition of initiation codon. Eukaryotic mRNA associates dynamically with proteins mediating nuclear export, subcellular localization, stability, and translation initiation or suppression. Broadly, the mRNA molecule is divided into a coding sequence that is flanked by non-coding regions located in the 5' or 3' untranslated regions (UTRs) that determine stability and translational efficiency. The majority of mRNAs transcribed in the nucleus contain a 5'-terminal $m^7G[5']ppp[5']N$ cap (where m^7G represents 7-methylguanylate, p represents phosphate group and N is any nucleotide), and a 3'poly(A) tail.

1.2.1.1 Cap structure

All eukaryotic mRNAs and small nuclear ribonucleic acids (snRNAs) that are transcribed in the nucleus are modified at their 5' ends by binding a 7-methylguanosine

to the first transcribed nucleotide. 7-methylguanosine is linked by the 5'-5'-triphosphate bridge to the first nucleoside (Muthukrishnan *et al.*, 1975) (Fig. 1.1.9). This modification is essential for efficient gene expression and viability for all living organisms from yeasts to humans, and is often referred to as "capping", and the enzymes catalyzing that process are referred to as "capping enzymes"(Cowling, 2010). The guanosine is methylated on the 7 position directly by a methyl transferase to produce the 7-methylguanosine cap, abbreviated as m^{7}G.
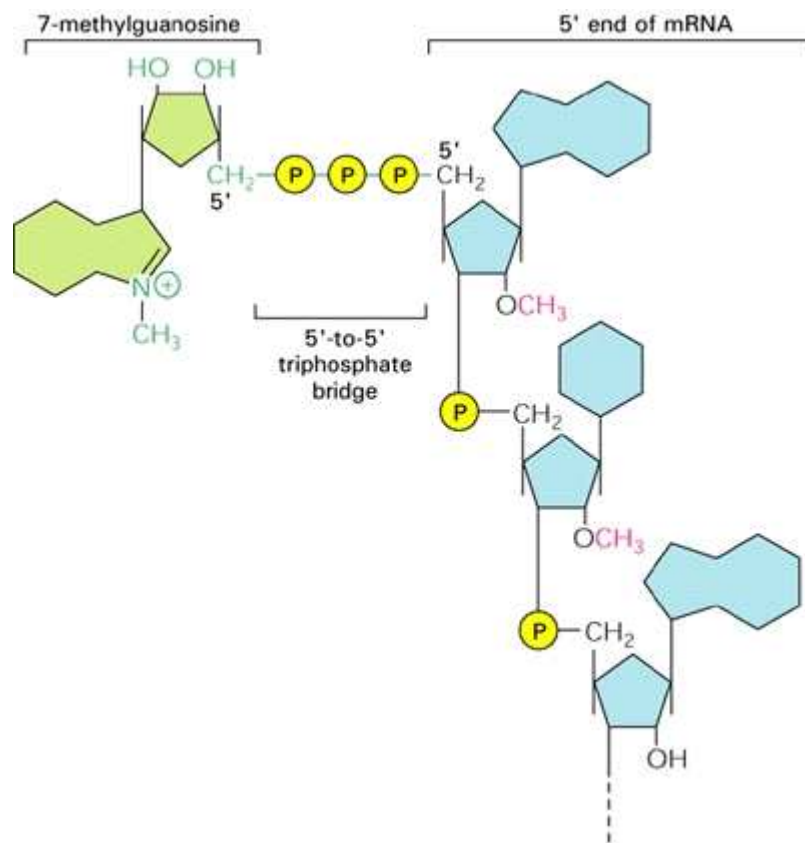
Figure 1.1.9 Structures of the cap at the 5' end of eukaryotic mRNA. The guanosine is methylated on position 7 by the methyl transferase and connected to the 5' end of the mRNA via the unusual 5'-to-5' triphosphate linkage. (From *Molecular biology of the cell*, 2002)

The 7-methylguanosine is required for translation of the majority of the mRNAs, with the exception of a group of mRNA translated by IRES (Spriggs *et al.*, 2008). The presence of m^{7}G is critical for mRNA recognition by eIF4F complex and the ribosome in the initiation stage of protein synthesis. The cap was also reported to stabilize mRNA against exonucleases, to promote transcription, splicing, polyadenylation, and nuclear export of RNA. Capping occurs in the cell nucleus and is a highly regulated process controlled by several cellular factors (reviewed by Cowling, 2010).

Some viruses, including vaccinia virus, encode a polypeptide containing all three enzymes required for capping (triphosphatase, guanylyltransferase, methyltransferase) which allows the efficient capping and cap methylation of the viral mRNAs (Shuman, 2002).

1.2.1.2 Poly(A) Tail

mRNA is modified at the 3' end by addition of the poly(A) tail in a process called polyadenylation (Shatkin and Manley, 2000). The poly(A) tail consists of multiple adenosine phosphates which only have adenine bases, and ranges from 50 bases long in yeasts to 300 bases in higher eukaryotes (Pestova *et al.*, 2007). However, most histone mRNAs and some viral RNAs (reovirus, rotavirus) do not contain this structure (Marzluff, 1992; Poncet *et al.*, 1993). The poly(A) tail plays an important role in translation efficiency, promoting the recruitment of 43S preinitiation complexes to the mRNA (Tarun and Sachs, 1995), and in mRNA stability, protecting the mRNA from enzymatic degradation in the cytoplasm (Guhaniyogi and Brewer, 2001). Poly(A)-mediated translation initiation and the cap/poly(A) synergy require poly(A)-binding protein (PABP) (Tarun and Sachs, 1995) and its interaction with eIF4G (Tarun *et al.*,

1997), leading to the formation of the "closed loop configuration" of the mRNA molecule which stabilizes the translation initiation complexes on the mRNA and facilitates the scanning process. Moreover, Munroe and Jacobson (1990) implicated the role of poly(A)-tail and PABP in enhancing the 60S ribosomal subunit recruitment.

Both the cap and poly(A) tail are important but not essential for translation, as mRNAs lacking any of these structures are still translated only less efficiently (Gingras *et al.*, 1999).

1.2.2   Mechanism of cap-dependent translation initiation

Following transcription, post-transcriptional modification and nucleo-cytoplasmic export, eukaryotic mRNA is competent for translation. The ribosome does not bind to mRNA directly, but involves a series of protein:protein and protein:RNA interactions resulting in the formation of an initiation factor:ribosome complex (Morley, 2001). Generally, translation initiation of eukaryotic mRNA occurs by a scanning mechanism, which starts with the recognition of the 5' terminus of the mRNA and the cap structure, and scanning of the ribosome towards the initiation codon (Kozak, 1989).

To do this, the methionine initiation transfer-RNA (Met-tRNA$_i$) and initiation factor 2 (eIF2) associate with the 40S ribosomal subunit to form a 43S pre-initiation complex (Fig. 1.1.10). The complex then binds to mRNA through interactions with the translation initiation factor complex eIF4F, forming the 48S initiation complex and migrates to the AUG starting codon. The large (60S) ribosomal subunit joins the 48S initiation complex forming the final 80S initiation complex which begins translation of the coding sequences (Pain, 1996).
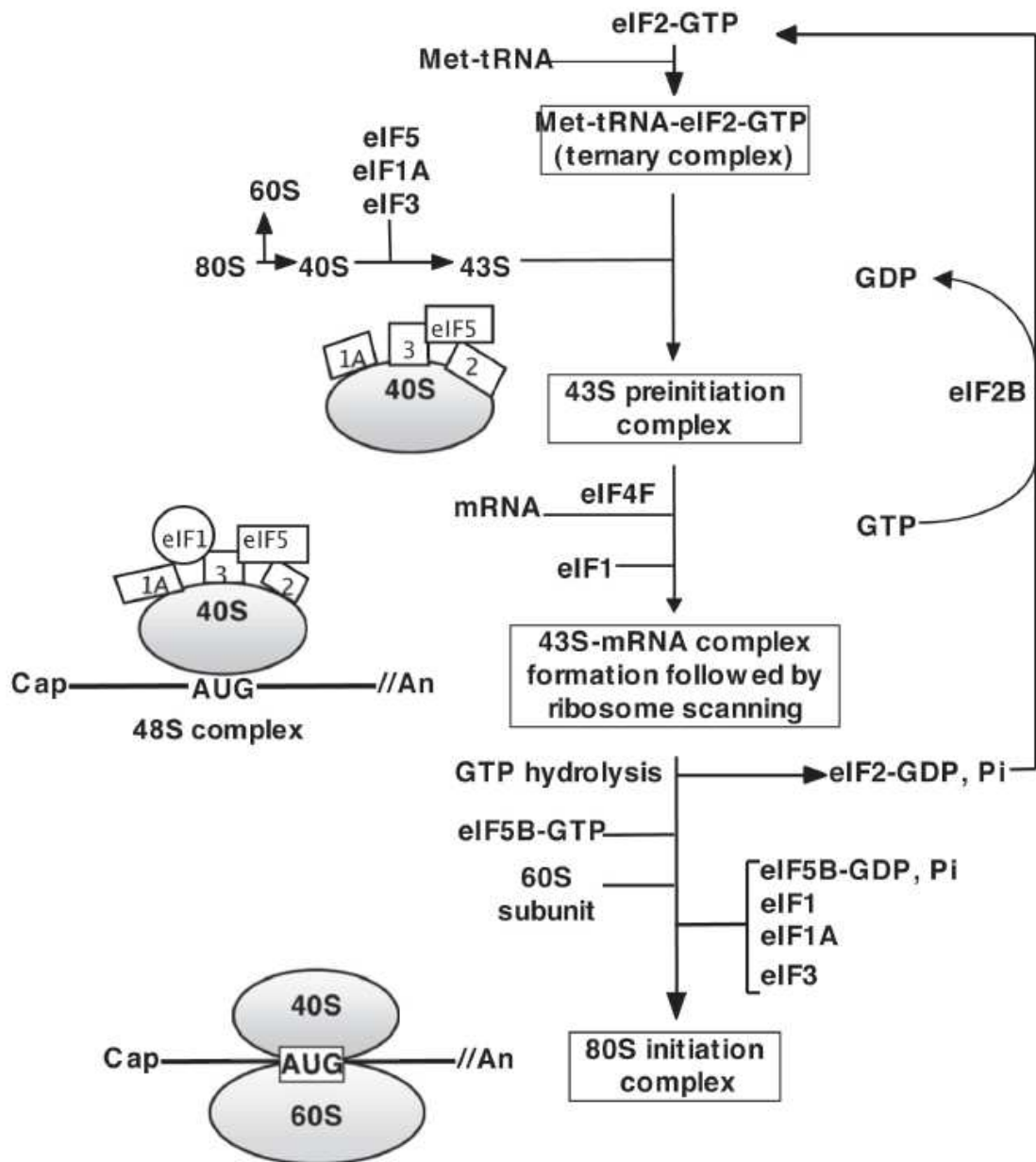
Figure 1.1.10 Mechanism of translation initiation. A ternary complex is formed by binding the initiation factor eIF2 together with GTP to the Met-tRNA$_f$. A ternary complex associates with a 40S ribosomal subunit carrying eIF3 to form a 43S pre-initiation complex, which then binds to mRNA at the 5' terminal m^{7}GTP cap, and migrates along mRNA towards the AUG codon. The mRNA binding to this complex involves participation of the eIF4E, eIF4G, eIF4A, and the helicase-stimulatory factor eIF4B. In the final step, Met-tRNA$_f$ interacts with the AUG codon, facilitated by eIF2 and eIF4B to form the 48S initiation complex. Then the 60S ribosomal subunit binds to the mRNA together with eIF5 using the energy from the hydrolysis of two GTP molecules to two GDP molecules. The final 80S initiation complex is formed by joining the larger (60S) ribosomal subunit to the initiation complex. (From Lopez-Lastra *et al.*, 2005)

27

1.2.3 eIF4F initiation complex

A key step in translation initiation is association of the pre-initiation complex with an mRNA mediated by initiation factors eIF4. Within the eukaryotic translation initiation factors (eIFs), the eIF4F complex plays a critical role in regulating the translation of capped messages (Sonenberg and Hinnebusch, 2009). The eIF4F complex together with associated proteins are localized to the 5' end of mRNA and unwind mRNA secondary structure, allowing interaction of the 43S initiation complex with the AUG start codon (Fig. 1.1.11). However, the exact mechanism leading to the assembly of eIF4F on the mRNA cap structure is still a matter of some debate (Morley, 1994; Pain, 1996; Gingras *et al.*, 1999).

eIF4F consists of three subunits: eIF4G, a large scaffolding protein on which the complex is built; eIF4E, a small cap-binding protein; and eIF4A, an RNA helicase that facilitates ribosomal scanning. Each of those subunits plays a unique and crucial role in initiating cap-dependent translation. Regulation of eIF4G and eIF4E activities significantly affects translational rates, therefore it has been a focus of many research groups recently.
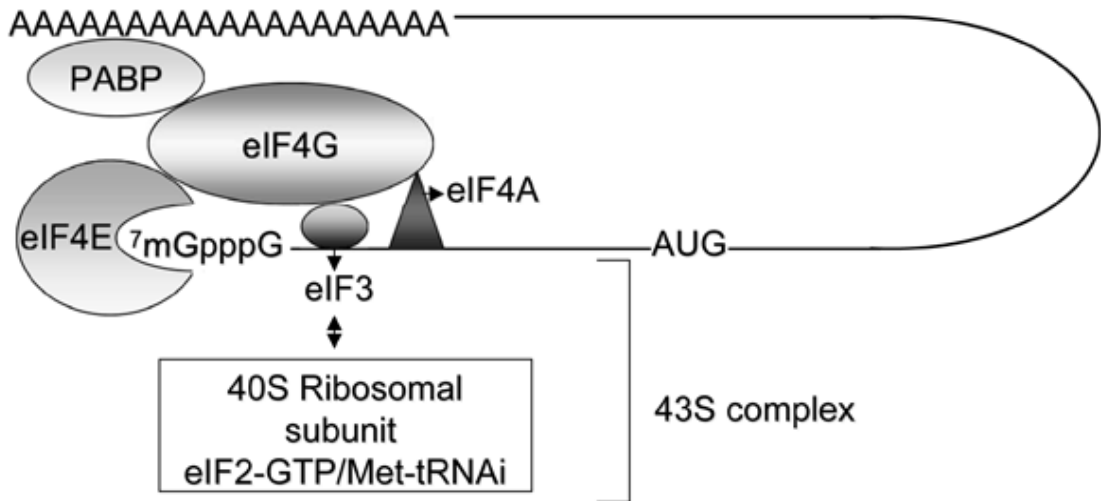
Figure 1.1.11 Mechanism of 48S initiation complex formation. In this schematic closed-loop model of translation initiation the eIF4F complex interacts with both the 5'end of mRNA and the poly(A) tail (through PABP), and recruits the 40S ribosomal subunit through binding with eIF3. (From Lopez-Lastra *et al*,. 2005)

1.2.3.1 eIF4G

There are two isoforms of eIF4G in mammals: eIF4GI and eIF4GII, which are 46% identical, have molecular masses of 171 kDa and 176 kDa, respectively, and exhibit similar biochemical activities (Gingras *et al.*, 1999). Human eIF4G was initially isolated as part of a large protein complex, identified later as eIF4F, that could restore protein synthesis in cell extracts derived from poliovirus-infected HeLa cells (Prevot *et al.*, 2003). eIF4G interacts with many different cellular and viral proteins and plays an important role in gathering initiation factors to begin the effective process of protein synthesis.

1.2.3.1.1 eIF4G structure

eIF4G is a large scaffold protein on which the eIF4F complex is built. It possesses binding sites for the remaining eIF4F components: eIF4E and eIF4A, and also other key translation initiation factors such as eIF3 complex and poly(A)-binding protein (PABP) (Fig. 1.1.12). Furthermore, binding sites for MAP-kinase-interacting kinase-1 and -2 (MNK1/2) were identified on the C-terminal region of eIF4GI and eIF4GII (Pyronnet *et al.*, 1999). It has been shown that complexes between these proteins exhibit enhanced mRNA cap-binding and RNA helicase activities.

Three domains of eIF4G have been identified that are comparable in size: the N-terminal fragment, characterized by its cleavage by picornaviral proteases; the middle domain that is critical for assembly of the translation machinery; and the C-terminal part which appears to function as a translation modulator (Prevot *et al.*, 2003).
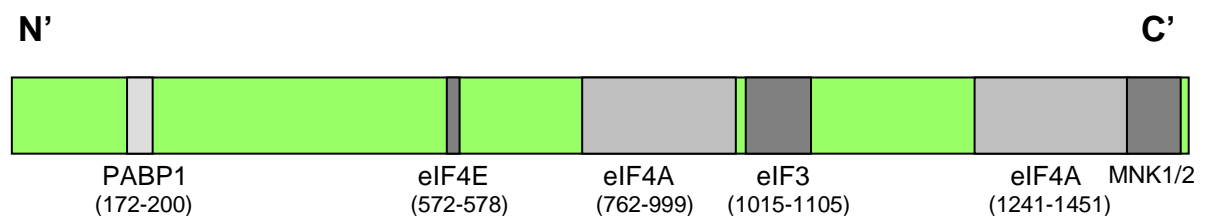
Figure 1.1.12 Schematic illustration of eIF4G binding sites for PABP1, eIF4E, eIF4A, eIF3 and MNK1. Amino acid location of each binding site is indicated in brackets. (Data of Hinton *et al.*, 2007)

1.2.3.1.1.1   eIF4G–PABP interaction

The eIF4G-PABP interaction enhances the formation of 48S and 80S complexes and ribosome recycling through mRNA circularization, thus is important for the contribution of the poly(A)-tail in translation initiation at the 5' end (Tarun and Sachs, 1995) (see paragraph 1.2.1.2). Moreover, Kahvejian *et al.* (2005) showed that PABP enhances translation and stimulates ribosome recruitment to the mRNA, both 40S and 60S subunits, and that an interaction between PABP and eIF4G is essential for this enhancement.

1.2.3.1.1.2   eIF4G – eIF4E interaction

The best characterized binding site on eIF4G is that for eIF4E, which is placed within the N-terminal half of the gene (Fig. 1.1.12) at the position 572-578 in human eIF4GI (Gingras *et al.*, 1999). This eIF4G fragment binds to the dorsal, convex surface of eIF4E behind the cap-binding slot by interacting with a number of evolutionarily conserved residues through hydrogen bonds, salt bridges, and van der Waals contacts (Marcotrigiano *et al.*, 1999). The role of eIF4E is to recognize and associate with the 7-Methyl-Gppp cap, and association with eIF4G stimulates this binding (Haghighat and Sonenberg, 1997). Interaction between eIF4E and eIF4G is regulated by eIF4E-binding proteins (4E-BPs), which block the eIF4G-binding site on eIF4E (Ptushkina *et al.*, 1999). Furthermore, it has been suggested that PABP-binding to eIF4G may stimulate eIF4E-cap interaction (von Der Haar *et al.*, 2000).

1.2.3.1.1.3   eIF4A, eIF3 and Mnk1/2- binding sites

The carboxy-terminal part of the eIF4G molecule contains eIF4A- and eIF3- and MNK1/2- binding sites. There are two independent binding sites for eIF4A, one is located in the middle portion of eIF4G, which also possesses the RNA- and eIF3-binding sites (Lamphear *et al.*, 1995), and the other is located in the COOH-terminal part of eIF4G, which also binds the eIF4E kinases Mnk1 and Mnk 2 (Pyronnet *et al.*, 1999). Although there are two binding sites, eIF4G only binds one eIF4A molecule (Rhoads, 2009). eIF4A is a 46-kDa polypeptide that exhibits RNA-dependent ATPase and RNA helicase activities (Gingras *et al.*, 1999), which is thought to unwind secondary structure in the 5′-untranslated region of the mRNA. The helicase activity of eIF4A is noticeably stimulated by two RNA-binding initiation factors, eIF4B and eIF4H (Rozen *et al.*, 1990). The eIF3-eIF4G1 interaction is thought to form a link between the 40S subunit and mRNA. Hinton *et al.* (2007) demonstrated that eIF4G lacking either the eIF4A-binding sites or eIF3-binding site was still able to interact with eIF4E, but resulted in significant decrease of translational rates. The eIF4G-Mnk1/2 interaction is important for eIF4E phosphorylation (see section 1.2.3.2.2.3).

1.2.3.2   eIF4E

The smallest subunit of the eIF4F complex was discovered in 1978 as a 24 kDa cap binding protein termed cap binding protein I (CBPI), later renamed eIF4E, and was the first eIF4F component identified; the other components were isolated during eIF4E purification by affinity chromatography (Sonenberg *et al.*, 1978; Tahara *et al.*, 1981; McKendrick *et al.*, 1999). eIF4E exists in both free form and as a part of an eIF4F

complex, and was shown to form nuclear bodies in addition to its cytoplasmic localization (Rousseau *et al.*, 1996).

1.2.3.2.1 Structure of eIF4E

The three-dimensional structure of eIF4E illustrates a cupped hand-shaped molecule, which consists of one α/β domain. The secondary structure includes three long and one short α helices and an 8-stranded, antiparallel β sheet (Marcotrigiano *et al.*, 1997). The cap recognition occurs via interaction between two highly conserved tryptophan residues on the concave surface, whereas the majority of the interacting partners, such as eIF4G and eIF4E-binding proteins (4E-BPs), bind via the convex face of eIF4E involving tryptophan 73 (Goodfellow and Roberts, 2008).

Interaction between eIF4E and eIF4G is a key step in cap-dependent translation initiation. This interaction enables eIF4G to bring eIF4F complex and ribosome to mRNA and start protein synthesis. Both eIF4G and 4E-BP1, the translational repressor, compete with each other for the binding site on eIF4E. Moreover, association of one of those proteins with eIF4E results in conformational changes in eIF4E, and leads to enhanced association of eIF4E with the cap (Volpon *et al.*, 2006). The nature of the structural changes during cap-binding has not been fully understood, although evaluations of CD difference spectra noticed with human cap-bound and apo-eIF4E (free eIF4E) suggested that a region of approximately 40 amino acids undergoes large-scale structural rearrangements (Cohen *et al.*, 2001).

1.2.3.2.2 Function of eIF4E

eIF4E was discovered as a protein promoting translation initiation, and the majority of the study on its structure, function, and regulation has been evaluated with this in mind. eIF4E is an essential factor for cap-dependent translation that mediates 5' 7-Methyl-Gppp cap recognition by the eIF4F complex and recruitment of mRNA to the ribosome, which results in formation of the 43S pre-initiation complex followed by scanning of the mRNA. In addition, eIF4E is thought to be the first factor interacting with the mRNA to initiate translation. It is well known that eIF4E stimulates translation of capped mRNA, although mRNAs differ in their dependence on eIF4E (reviewed by Goodfellow and Roberts, 2008; Rhoads, 2009). Moreover, Svitkin *et al.* (1996) demonstrated that depletion of eIF4E (together with associated proteins) from the cell extracts significantly reduced translation of capped mRNA.

Apart from its function in cap recognition, eIF4E plays also a crucial role in nuclear transport. The majority (up to 68%) of the total cellular eIF4E is localized in the nucleus, in distinct sites termed nuclear bodies, where it is involved in the export of the mRNAs (Iborra *et al.*, 2001; Strudwick and Borden, 2002). eIF4E enters the nucleus by associating with the eIF4E-binding protein known as 4E-transporter or 4E-T (Dostie *et al.*, 2000). Once in the nucleus, eIF4E interacts with several proteins which regulate cap-binding and mRNA export. One of such proteins is PML (promyelocytic leukaemia protein) which associates with eIF4E via its RING domain. Nuclear eIF4E was found to co-localize with PML in complexes termed PML nuclear bodies (Lai and Borden, 2000). Changes in those complexes appear to be a result of stress such as viral infection (Regadand Chelbi-Alix, 2001) hence it is thought that PML regulates mRNA transport mediated by eIF4E in response to stress (Culjkovic *et al.*, 2007).

Surprisingly, overexpression of eIF4E does not cause an overall increase in translational rates, but leads to deregulation of cellular growth and induces cell transformation (Mader and Sonenberg, 1995; de Benedetti and Harris, 1999). Conversely, increased expression of translational repressor 4E-BP1 can reverse the transformed phenotype and induce apoptotic cell death (Li *et al.*, 2002; Proud, 2005). High levels of eIF4E have been detected in a number of cancers and malignant transformation (de Benedetti and Graff, 2004), however, the role of eIF4E in tumor progression still needs to be determined. It was suggested that overexpressed eIF4E observed in malignant transformation promotes the synthesis of growth stimulatory and antiapoptotic proteins (Clemens, 2004; Mamane *et al.*, 2004). Another hypothesis says that overexpression of eIF4E may promote the export and selective translation of some mRNAs encoding proteins involved in cell proliferation and tumorigenesis (Topisirovic *et al.*, 2003; Goodfellow and Roberts, 2008).

1.2.3.2.3   eIF4E-Binding Proteins

eIF4E was originally discovered as a single polypeptide bound to the 7-Methyl-Gppp cap, but since it was found in complexes with eIF4G it was renamed as a subunit of eIF4F. However, the number of eIF4E-binding proteins has grown recently and many of the newly discovered roles of eIF4E are mediated by its interaction with those new binding partners.

The specific and high affinity interaction between eIF4E and eIF4G leads to recruitment of eIF4F complex to mRNA, which allows the activation of eIF4A-driven unwinding machinery. The association of eIF4G with cap-bound protein enables initiation and stimulates cap-dependent translation. In contrast, binding of 4E-BP1, the translational

repressor, to eIF4E disrupts eIF4F formation and thereby inhibits cap-dependent translation, whereas cap-independent translation may actually be enhanced by the 4E-BPs (Svitkin *et al.*, 2005).

The 4E-BPs are small (approximately 10-12 kDa), acidic, heat-stable proteins, discovered in 1994 by using Far-Western hybridization technique (Pause *et al.*, 1994), which enabled the isolation of cDNAs encoding two small (~12kDa) proteins associating with eIF4E and sharing 56% identity. These proteins, named 4E-BP1 and 4E-BP2 were shown to inhibit cap-dependent translation both *in vivo* and *in vitro*. In addition, Pause *et al.* (1994) demonstrated that binding of 4E-BPs to eIF4E does not alter the affinity of eIF4E for the cap structure. Instead, it prevents the association between eIF4E and eIF4G and thus the assembly of eIF4F complexes (Haghighat *et al.*, 1995). Both eIF4G and 4E-BPs possess a small amino acid motif (YXXXXLφ, where X is any amino acid, and φ is an aliphatic residue Leu, Met or Phe) which interacts with eIF4E (Mader *et al.*, 1995). Deletion or mutation of this sequence was shown to abolish interaction with eIF4E. Four years after the discovery of 4E-BP1 and 4E-BP2 proteins, Paulin *et al.* (1998) reported a new member of the 4E-BP family termed 4E-BP3 which shares approximately 58% identity with 4E-BP1/2. However, 4E-BP1 is the most widely studied, and is thought to be a prototype of the 4E-BPs family.

Another eIF4E-binding protein that disrupts eIF4F is Maskin, which is thought to repress translation of cyclin B1 and c-Mos mRNA in *Xenopus* oocytes through the interaction with the RNA-binding protein CPEB [CPE-binding protein] and eIF4E (de Moor and Richter, 1999; Cao and Richter, 2002; Pascreau *et al.*, 2005). CPEB interacts with the cytoplasmic polyadenylation element (CPE), a small sequence in the 3' UTR of mRNAs, and mediates cytoplasmic polyadenylation. Despite rather weak association of

Maskin with eIF4E, Maskin does disrupt the eIF4G-eIF4E interaction. Therefore, the CPEB–Maskin–eIF4E complex inhibits the translation of CPE-containing mRNAs specifically (Stebbins-Boaz *et al.*, 1999). As soon as frog oocytes are induced to complete meiosis, CPEB stimulates growth of poly(A) tail. The newly elongated poly(A) tail is then bound through PABP, which in turn associates with eIF4G. PABP-bound eIF4G displaces Maskin from eIF4E, thereby inducing translation (Cao and Richter, 2002).

Selected proteins interacting with eIF4E are also involved in embryogenesis. In *Drosophila melanogaster* the product of the fs (2)cup gene (Cup), a nucleocytoplasmic shuttling protein, was found to directly associate with eIF4E which promotes retention of the Cup protein in the cytoplasm (Zappavigna *et al.*, 2004). Cup is required for the proper accumulation and localization of eIF4E within the cytoplasm of developing oocytes. It was demonstrated that the Cup–eIF4E complex plays a crucial role in ovary-specific developmental programs. Furthermore, the role of eIF4E-binding proteins in mammalian neurogenesis has recently been revealed. Jung *et al.* (2006) demonstrated that neuroguidin (Ngd) binds to eIF4E and inhibits translation of CPE-containing mRNAs. Ngd occurs in axons and dendrites of the mammalian nervous system and contains three eIF4E-binding motifs.

Another eIF4E-binding protein discovered ten years ago is eIF4E transporter (4E-T), which was shown to mediate the nuclear import of eIF4E via the importin αβ pathway (Dostie *et al.*, 2000). 4E-T is thought to function to inhibit translation and promote recruitment of P-body through a third unrelated pathway specific for mammalian cells. 4E-T binds to eIF4E through the same site on eIF4E that associates with eIF4G and 4E-BP1 (Dostie *et al.*, 2000). Furthermore, overexpression of 4E-T was shown to inhibit

cap-dependent, but not cap-independent translation (Ferraiuolo *et al.*, 2005), which may involve at least two mechanisms. First, binding of 4E-T prevents eIF4E from binding to eIF4G, which would negatively affect translation initiation (Dostie *et al.*, 2000). Second, interaction between eIF4E and 4E-T results in accumulation of eIF4E in P-bodies (Farraiuolo *et al.*, 2005), separating the associated mRNA from the translation apparatus. Noteworthy, depletion of 4E-T by RNA interference results in loss of P-bodies and stabilization of at least some RNAs (Farraiuolo *et al.*, 2005).

In the case of viruses, VPg proteins of plant potyviruses and human caliciviruses also interact with eIF4E, which reduces eIF4E affinity for the cap and inhibits host translation (Leonard *et al.*, 2000; Goodfellow *et al.*, 2005).

1.2.3.2.4   eIF4E regulation

Since eIF4E plays an important role in cap recognition and association of the initiation complex with mRNA, it is a key target for the regulation of protein synthesis. eIF4E activity is regulated by at least three different mechanisms: (1) modulation of its abundance, (2) phosphorylation, and (3) binding of translational repressor proteins (Gingras *et al.*, 1999).

1.2.3.2.4.1   Regulation of eIF4E abundance and turnover

The mechanisms regulating eIF4E gene expression are not completely understood, but transcriptional activation appears to be an important part of this regulation. Expression of eIF4E has been shown to be correlated with c-Myc expression during the cell cycle (Rosenwald *et al.*, 1993). In addition, in cells overexpressing c-Myc an increased level

of eIF4E mRNA has been observed, and transcription of the eIF4E gene was responsive to activation of a Myc-estrogen fusion protein. Furthermore, two functional Myc-binding sites (E boxes) have been characterized in the eIF4E promoter, and both of them are required for promoter activity (Jones *et al.*, 1996).

The c-Myc protein is a member of the nuclear oncoproteins and functions as a transcriptional factor that activates a great number of genes. Moreover, its function in regulating cell proliferation and growth has been described (Adhikary and Eilers, 2005). Since eIF4E itself is a key regulator of cell growth and proliferation, it appears to be an important downstream target of c-Myc. Recent findings suggest that the role of Myc during cell growth and proliferation is related to an increase in eIF4F activity. C-Myc mRNA is complex and effectively translated during eIF4F stimulation, forming a feedforward relationship and providing a possible molecular mechanism of cell transformation by Myc (Lin *et al.*, 2009). Therefore, developing therapeutics that inhibit eIF4F and/or Myc could be a potential treatment for a wide range of human cancers.

1.2.3.2.4.2   Regulation by phosphorylation

eIF4E is phosphorylated on Ser209 in response to extracellular stimuli such as growth factors, hormones and mitogens (Joshi *et al.*, 1995). Phosphorylation of eIF4E is regulated by extracellular signal-regulated kinases (ERKs) and mitogen-activated protein kinases (p38/MAPK). The ERK signaling cascade is stimulated by growth factors, hormones, cytokines or mitogen treatment. A putative role for the ERK pathway in eIF4E phosphorylation was suggested after demonstrating an increased phosphorylation of eIF4E in ras- or src-transformed cells (Frederickson *et al.*, 1991; Rinker-Schaeffer *et al.*, 1992). However, Flynn and Proud (1996) demonstrated that

ERK cannot phosphorylate eIF4E *in vitro*, which suggested indirect role of ERK in eIF4E phosphorylation. The p38/MAPK pathway is activated by various types of cellular stress such as heat shock and exposure to arsenite or anisomycin. Stimulation of this pathway was shown to enhance eIF4E phosphorylation (Morley and McKendrick, 1997; Wang *et al.*, 1998). It was later discovered that both ERK and p38/MAPK kinases regulate the eIF4E phosphorylation indirectly through phosphorylation of Mnks (Mnk1/2) – the kinases interacting with the scaffold protein eIF4G and directly phosphorylating eIF4E on Ser209 (Waskiewicz *et al.*, 1997; Wang *et al.*, 1998; Pyronnet *et al.*, 1999). Free Mnk1/2 does not phosphorylate eIF4E efficiently, but does so through interaction with eIF4G. The C-terminal region of eIF4G contains a binding site for both Mnk1 and Mnk2, whereas no such a binding site was determined on eIF4E (Pyronnet *et al.*, 1999), which suggests that eIF4E is regulated by phosphorylation only as a part of eIF4F complex, by eIF4G placing Mnk1/2 and eIF4E in proximity to one another.

The biological significance of eIF4E phosphorylation is not completely understood. Phosphorylation of eIF4E has been reported to enhance its binding affinity for the cap and mRNA (Minich *et al.*, 1994), which may lead to the increased translational rates observed after eIF4E phosphorylation (Bonneau and Sonenberg, 1987; Morley *et al.*, 1993; Dyer *et al.*, 2003), and formation of more stable eIF4F complex (Bu *et al.*, 1993). The most recent studies demonstrate that eIF4E phosphorylation decreases its affinity for the cap (Scheper *et al.*, 2004). However, while some reports show a strong correlation between eIF4E phosphorylation and translational stimulation, other studies illustrate no effect of eIF4E phosphorylation on translation (McKendrick *et al.*, 2001; Morley and Naegele, 2002), or even its negative effect on protein synthesis (Knauf *et al.*, 2001).

Overall, it is not clear how eIF4E phosphorylation controls the function of eIF4E. Although phosphorylation of eIF4E is not critical for high levels of translation, the most recent studies demonstrate that it does control cell transformation (Furic *et al.*, 2010) and viral mRNA translation (Walsh *et al.*, 2008).

1.2.3.2.4.3   Regulation by translational inhibitors

The third mechanism regulating eIF4E is through its interaction with a family of inhibitory binding proteins, 4E-BPs. 4E-BPs act in their hypophosphorylated form as competitive inhibitors of eIF4G binding to eIF4E (Gingras *et al.*, 2004; Proud, 2004). Interaction of 4E-BP1 with eIF4E inhibits cap-dependent translation both *in vivo* and *in vitro*. In contrast, activation of the PI3K/Akt/mTOR pathway causes phosphorylation of the 4E-BPs at multiple sites, decreases its affinity for eIF4E and thus releases the cap-binding protein which is then incorporated into the eIF4F complex by interaction with N-terminal region of eIF4G (see Fig. 1.2.1). Interaction between 4E-BP1 and eIF4E does not appear to alter the affinity of eIF4E for the cap since eIF4E-4E-BP1 complexes were found to associate with the cap (Pause *et al.*, 1994).

The phosphorylation of 4E-BP1 is regulated by a wide range of extracellular stimuli including growth factors, hormones, cytokines, mitogens, and G-protein coupled receptor ligands (Gingras *et al.*, 1999). During early adenovirus and VacV infection 4E-BP1 also becomes hyperphosphorylated, which results in an increase of translation rates (Gingras and Sonenberg, 1997; Walsh *et al.*, 2008). An increase in 4E-BP1 phosphorylation is correlated with a decrease of binding affinity to eIF4E. Phosphorylation of 4E-BP1 occurs at multiple sites and is regulated by mTORC1 to control the release of eIF4E which then interacts with eIF4G promoting eIF4F

formation (Gingras *et al.*, 1999). Furthermore, recent studies have shown that phosphorylation of 4E-BP1 stimulates its ubiquitination, which leads to protein degradation (Elia *et al.*, 2008). In contrast, physiological stresses that inhibit translation and cause dephosphorylation of 4E-BP1, such as DNA damage, amino-acid starvation or the activation of p53 might actually stabilize 4E-BP1. Tilleray *et al.* (2006) reported that induction of p53 leads to accumulation of hypophosphorylated 4E-BP1, and a similar effect has been observed in cells treated with the proapoptotic cytokine TRAIL (Elia *et al.*, 2008).

1.2.4   Signaling pathways regulating protein synthesis

Translation rates are chiefly regulated at the initiation stage, and precisely controlled in response to extracellular stimuli, environmental stress, hormone/growth factor signals, and availability of nutrients and amino acids (Raught and Gingras, 2007). Since protein synthesis consumes a high proportion of cellular metabolic energy, the status of energy of the cell can also modulate translation factors. The aforementioned agents regulate the translational apparatus via phosphorylation of translation factors and related proteins, which may affect the basic activity of translation factors or their ability to bind other components (other factors, ribosome, RNA). These changes are mostly controlled by signaling pathways regulating the activities of kinases and effector proteins. These pathways include:

I.   The phosphatidylinositide 3-kinase (PI3K) pathway

II.   The mammalian target of rapamycin (mTOR) pathway

III.   The ERK and p38 MAP kinase pathways (Wang and Proud, 2007)

In this study, we are interested mostly in the first two pathways, the PI 3-kinase (PI3K) and the mTOR pathway.

1.2.4.1 The PI 3K/Akt/mTORC1 pathway

The PI3K pathway plays a key role in the transduction of signals from extracellular stimuli such as hormones, growth factors, mitogens, and cytokines to regulate cell growth, proliferation and survival. The PI3Ks are lipid kinases generating second messengers by phosphorylation of the phosphatidyl group at the 3' position of the inositol ring to form phosphatidylinositol phosphate (PIP), phosphatidylinositol biphosphate (PIP2) or phosphatidylinositol triphosphate (PIP3) (Fig. 1.2.1) (Vivanco and Sawyers, 2002; Engelman *et al.*, 2006). Phosphatidylinositol (PI) is a component of eukaryotic cell membranes and is unique among phospholipids because it can be phosphorylated at multiple free hydroxyls. A number of phosphorylated derivatives of PI, termed phosphoinositides, have been identified in eukaryotic cells from yeast to mammals, and are thought to be involved in regulation of many cellular processes such as proliferation, cytoskeletal organization, survival, glucose transport, and platelet function. The enzymes that phosphorylate PI and its derivatives are termed phosphoinositide kinases. Although PI represents only a small group among total cellular phospholipids, it plays a significant role in signal transduction as a precursor of several second-messenger molecules (Fruman *et al.*, 1998).
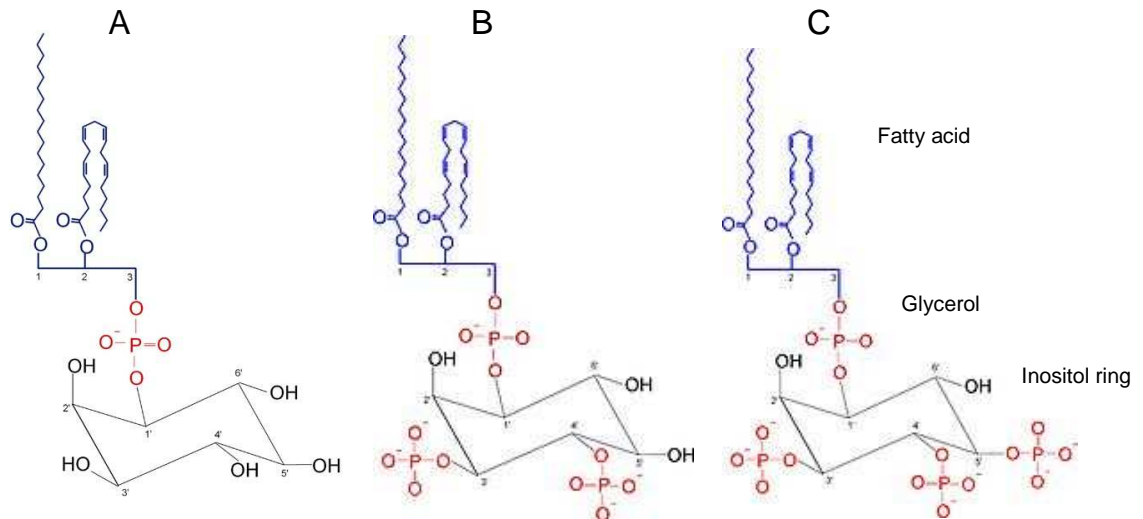
Figure 1.2.1 Chemical structures of phosphatidylinositol (A), phosphatidylinositol-3,4-biphosphate (PIP2) (B), and phosphatidylinositol-3,4,5-triphospahte (PIP3) (C). Phosphatidylinositol (PI) is a glycerophospholipid that contains a glycerol backbone, two non-polar fatty acid tails, and a phosphate group substituted with an inositol polar head group. The inositol can be phosphorylated to form phosphatidylinositol phosphate (PIP), phosphatidylinositol biphosphate (PIP2) or phosphatidylinositol triphosphate (PIP3). (www.medlibrary.org/medwiki/Phosphatidylinositol)

PI3Ks consist of three classes of kinases based on their primary structure and substrate specificity. Class I PI3Ks can be divided into class IA and class IB, depending on the receptors to which they link. Class IA consists of the catalytic subunit (p110, comprising three isoforms α, β, δ) and an adaptor/regulatory subunit p85 containing two SH2 domains, which are essential for their activation by tyrosine kinase receptors. Class IB PI3Kγ has a p101 subunit, which is required for maximal Gβγ-stimulated formation of PIP$_3$ (Stephens *et al.*, 1997; Maier *et al.*, 1999). Catalytic subunits form heterodimers with various regulatory subunits and can use PI 3,4-bis-phosphate (PIP$_2$) as a substrate to generate the second messenger PI 3,4,5-tri-phosphate PIP$_3$.

Class II PI3Ks are large (170-210 kDa) proteins that share 45-50% similarity with class I PI3Ks (Fruman *et al.*, 1998). Class II consists of three subunits named PI3KC2α, PI3KC2β and PI3KC2γ, which contain a C-terminal region with homology to C2 domains[1]. These enzymes can be activated by chemokines, cytokines, insulin, epidermal growth factor (EGF) or platelet-derived growth factor (PDGF) (Turner *et al.*, 1998; Brown *et al.*, 1999; Arcaro *et al.*, 2000; Ktori *et al.*, 2003), and preferably phosphorylate PI and PI-4-P. The mechanism regulating the activity of class II PI3Ks and their function have not been fully explored, although it was reported that PI3KC2β might be involved in lysophosphatidic acid-induced cell migration of cancer cells (Maffucci *et al.*, 2005). Class III PI3Ks phosphorylate only PI and consist of the Vps34 enzyme. These proteins may play a role in the regulation of mTORC1 by amino acids (Nobukuni *et al.*, 2005).

The PI3K pathway starts with the PI 3-kinase. Activation of PI3K leads to activation of Akt (PKB) through its phosphorylation (at T308 and S473) which, in turn, phosphorylates a number of substrates including TSC-2, an upstream regulator of mTORC1 (Wand and Proud, 2007) (Fig. 1.2.2). Akt phosphorylation is mediated by mammalian target of rapamycin complex 2 (mTORC2) and phosphoinositide-dependent protein kinase 1 (PDK1) acting as downstream effectors for PI3K pathway (Alessi *et al.*, 1996; Sarbassov *et al.*, 2005). Akt consists of three isoforms (α, β, γ) composed of N-terminal central catalytic domain and C-terminal hydrophobic domain. Both Akt and PDK1 are recruited to the plasma membrane through interactions with PIP3, where PDK1 activates Akt by phosphorylating threonine 308. Activated Akt is an essential mediator for the regulation of proliferation and growth by PI3K.

---

[1] A C2 domain (Protein kinase C homology domain 2) is a Ca^{2+}-binding motif of approximately 130 residues in length. C2 domain is involved in targeting proteins to the cell membrane, and can bind a variety of different ligands and substrates including phospholipids, inositol phosphatases, and intracellular proteins (Nalefski and Falke, 1996).
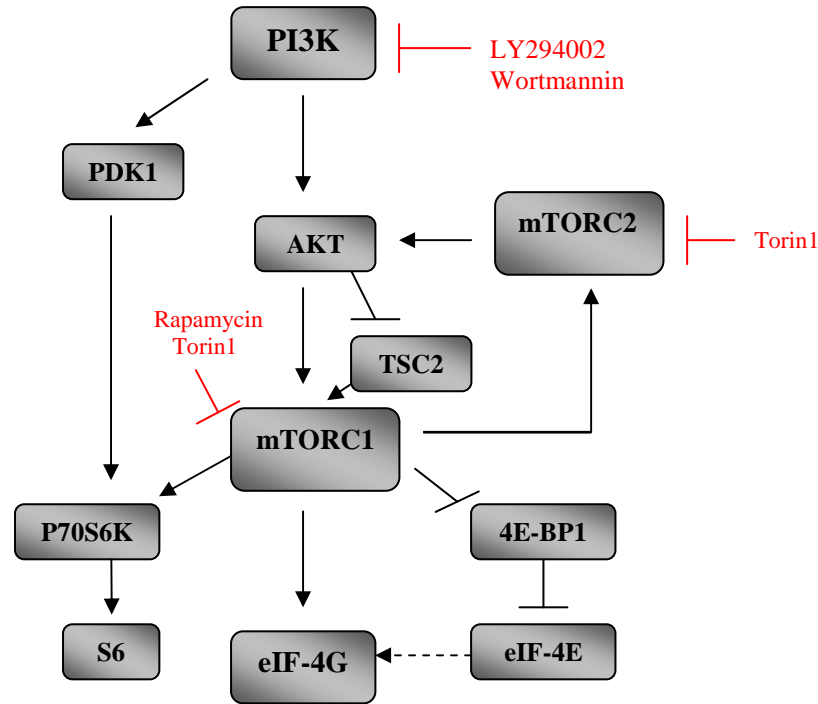
Figure 1.2.2 The PI3K/Akt/mTOR pathway and its pharmacological inhibitors. PI3K is activated through cytokines, chemokines, insulin or growth factors, and then phosphorylates its downstream substrates. PDK1 and Akt are recruited to the cell membrane where PDK1 phosphorylates Akt on Thr308 and Ser473. Akt then can activate mTORC1 directly or indirectly by phosphorylation and inactivation of TSC2, which normally inhibits mTORC1 when dephosphorylated. mTORC1 activates p70S6 kinase-1, which directly phosphorylates ribosomal protein S6 and leads to increased protein translation. mTORC1 also phosphorylates 4E-BP1, causing its dissociation from eIF4E, and freeing eIF4E to participate in formation of the translation initiation complex by binding to eIF4G, which is also phosphorylated by mTORC1. mTORC1 indirectly (through p70S6K) stimulates phosphorylation of mTORC2, which then inhibits Akt. T-bars represent suppression. Inhibitors marked in red.

Akt phosphorylates a number of factors such as proapoptotic protein Bad, caspase-9, glycogen synthase kinase 3β, and FKHR, which leads to the suppression of such processes as cell growth, survival, and proliferation (Datta *et al.*, 1997; Cardone *et al.*, 1998; Pap and Cooper, 1998), and also regulates the activity of transcription factors stimulating the expression of several cell death genes. For instance, phosphorylation of

Bad causes its dissociation from Bcl-X$_l$ and its sequestration by 14-3-3 proteins, thus preventing it from translocation to the mitochondria, an event necessary for its proapoptotic function (Kennedy *et al.*, 1999; Yang *et al.*, 2001). As part of the proapoptotic role, activated death receptors have been shown to attenuate survival signaling events, thus potentiating cell death (Yousefi *et al.*, 2003).

Furthermore, PI3K is thought to play a major role in cancer pathogenesis. The most important proteins involved in proliferation and tumorigenesis are p110α and its regulatory subunit p85 belonging to class IA PI3Ks. The activity of PI3K is counteracted by the phosphatase PTEN (phosphatase and tensin homolog deleted on chromosome 10), which acts as a tumor suppressor. PTEN and p85 were shown to be mutationally inactivated in a wide range of malignant human cancers, but mostly in prostate and endometrial cancers, melanomas, and glioblastomas, thereby constitutively activating PI3K (Vivanco and Sawyers, 2002; Bader *et al.*, 2005). Hyperactivation of Akt isoforms α, β, and γ by PIP3 or other kinases, such as PDK1 or PDK2, has been reported in many human cancers. Noteworthy, mutated PI3 kinases are thought to be ideal drug targets, thus specific inhibitors of these mutants could have a significant therapeutic effect (reviewed by Bader *et al.*, 2005*).

Precise regulation of the PI3K/Akt pathway is essential to coordinate the balance between protein synthesis and protein degradation in response to nutrient availability.

1.2.4.1.1   Inhibitors of the PI3 kinase

The PI 3-kinase has two widely used specific inhibitors, LY294002 and wortmannin, which have been crucial in establishing the roles of PI3K in cellular processes. LY294002 and wortmannin are structurally unrelated and they both target the p110

catalytic subunit of PI3K effectively blocking this kinase. Unfortunately, the poor solubility and high toxicity have limited their clinical use. However, LY294002 and wortmannin provide a powerful preclinical tool to study the cellular consequences of PI3K inhibition.

LY294002 (2-(4-Morpholinyl)-8-phenyl-4H-I-benzopyran-4-one) is a synthetic compound that was derived from the naturally occurring bioflavonoid quercetin (Vlahos *et al.*, 1994). LY294002 competitively inhibits the ATP-binding site of PI3K, but does not inhibit several other ATP-requiring enzymes. This drug has been used in studies of cardiovascular, neuronal, immune, and diabetes-related cell function for more than a decade, and it is more widely used in cell biology than wortmannin due to its higher stability in solution. An IC_{50}[2] for this inhibitor of approximately 1µM has been measured for a class IA PI3K, and 19 µM for class II (Vlahos *et al.*, 1994; Walker *et al.*, 2000). As such, LY294002 is widely used in many studies, including our own, over ranges of 20-50 µM to ensure complete inhibition of both Class I and Class II PI3Ks.
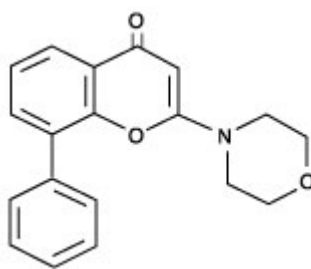
Figure 1.2.3 Chemical structure of LY294002. (www.medlibrary.org/medwiki/LY294002)

Wortmannin is a natural small molecule product isolated in 1957 from the fungus *Penicillium wortmanii*, and reacts covalently with a residue in the active site of PI3K inactivating it irreversibly (Powis *et al*., 1994; Walker *et al.*, 2000). Wortmannin was

---

[2] IC_{50} – half maximal inhibitory concentration

shown to act as a noncompetitive PI3K inhibitor with respect to ATP, and has low IC_{50}

lying between 1-10 nM for class I PI3K which makes it more potent inhibitor than

LY294002. In contrast to LY294002, wortmannin was shown to cause large

conformational rearrangement in the active site of PI3K (Walker *et al.*, 2000).

Figure 1.2.4 Chemical structure of wortmannin (www.medlibrary.org/medwiki/wortmannin)
Wortmannin inhibits all PI3K isoforms and has shown antitumor activity against a variety of
human cancers (Schultz *et al.*, 1995; Lemke *et al.*, 1999; Teranishi *et al.*, 2009) but due to the
fact that it is a biologically unstable molecule, wortmannin seems not to be a good drug
candidate. However, the use of wortmannin analogs such as PX-866 has recently been reported
to have a potential therapeutic role in human glioblastoma (Koul *et al.*, 2010). Because of its
instability, wortmannin is often used at a very broad range of concentrations, often depending
upon how long the treatment time of the experiment is.

1.2.4.2 mTOR

Another downstream target of PI3K/Akt is mammalian target of rapamycin (mTOR), a

kinase that plays a central role in the regulation of cell growth and size, proliferation,

nutrient responses, survival, and protein synthesis (Hay and Sonenberg, 2004). mTOR is

evolutionarily conserved serine/threonine kinase, which in humans is encoded by the

FRAP1 gene. mTOR was discovered as the molecular target of rapamycin, an

antifungal agent used clinically as an immunosuppressant and more recently as an

anticancer drug (Heitman *et al.*, 1991; Kunz *et al.*, 1993; Fasolo and Sessa, 2008).

Rapamycin binds to a small, ubiquitously expressed protein FKBP12 (FK506-Binding

Protein, molecular mass of 12 kDa), which then binds and inhibits mTOR in a poorly understood mechanism (Gingras *et al.*, 2007). Recent research indicates that deregulation of the mTOR pathway occurs in a majority of human cancers (Chiang and Abraham, 2004; Guertin and Sabatini, 2007; Engelman, 2009), suggesting that rapamycin analogs may be potent therapeutic agents.

A single TOR molecule is a high molecular-weight protein containing several distinct and conserved structural domains. The N-terminus possesses 20 tandem HEAT (Huntington, EF3, A subunit of PP2A, TOR1) repeats that are involved in protein-protein interactions (Andrade and Bork, 1995). The C-terminal half of mTOR contains a kinase domain that shares sequence similarity with the catalytic domain of PI3K, and also the FATC (FRAP, ATM, TRAP, C-terminal) domain that is essential for mTOR activity (Peterson *et al.*, 2000; Takahashi *et al.*, 2000). mTOR interacts with several different proteins including raptor and rictor, and forms two different types of complexes: mTORC1 and mTORC2.

The downstream signaling of mTOR requires the associated factors: **r**egulatory **a**ssociated **p**rotein of m**TOR** (raptor), and G protein β-subunit-like protein (GβL) (Hara *et al.*, 2002; Kim *et al.*, 2003). These three components constitute the mTORC1 complex, which interacts with downstream substrates through raptor. Raptor associates with both N- and C-terminal domains of mTOR, while GβL binds specifically to the carboxyl end of this factor. Noteworthy, treatment with rapamycin disrupts only association with raptor, while it does not affect GβL binding to mTOR (Kim *et al.*, 2003). In mammals, mTORC1 regulates the activity of several translation factors (eIF4G, eIF4B), translation inhibitors (4E-BP), and ribosomal S6 kinases. mTORC1 regulates the availability of initiation factor eIF4E through the phosphorylation of the

4E-binding protein (4E-BP) leading to an increase in protein synthesis. mTORC1 also activates, either directly or indirectly, p70 S6 kinase (p70S6K), which in turn phosphorylates ribosomal protein S6 (Gingras *et al.*, 2007).

In the case of mTORC2, while it also contains GβL, raptor is replaced by a large adaptor protein named **r**apamycin-**i**ndependent **c**ompanion of m**TOR** (rictor) (Sarbassov *et al.*, 2004). mTORC2, in contrast to mTORC1, is resistant to rapamycin treatment and does not activate either S6K1 or 4E-BP1. Instead, it was shown to phosphorylate and activate PKB/Akt on Ser473 by a mechanism similar to activation of S6K1 by mTORC1 (Fig. 1.2.1) (Sarbassov *et al.*, 2005).

Signaling towards mTORC1 can be activated by various agents including insulin, growth factors, and amino acids. The mechanism of mTORC2 regulation was not known until recently, when Julien *et al.* (2010) discovered that phosphorylation of rictor requires mTORC1 activity. Rictor has been shown to be phosphorylated directly by p70S6K *in vivo* and *in vitro*, in a rapamycin-insensitive manner. Because mTORC2 was shown to phosphorylate Akt, it appears to form part of a feedback loop between mTOR and Akt.

1.3 Manipulation of cellular translational apparatus by viruses

As mentioned before, all viruses remain dependent on the host-cell translation machinery to synthesize viral proteins, for the reason that protein synthesis requires specific proteins that cannot be encoded within viral genomes. As a result, viruses developed various tricks and strategies to take control of translation factors, optimize viral mRNA translation, and avoid host-cell antiviral responses, and consequently viruses compete with the cell at the translational level (Schneider and Mohr, 2003). Some of such recently discovered strategies are discussed later in Section 4.

Viruses can be broadly divided into two classes, RNA and DNA viruses. The strategies used by each class of viruses are briefly characterized below.

1.3.1 RNA viruses

RNA viruses can contain either positive- or negative-sense genome, the latter of which must be transcribed to form positive sense mRNA which is then translated into proteins using host cell ribosomes. Unlike DNA viruses, and despite the need for using the host cell ribosomes for protein synthesis, many RNA viruses produce mRNA which lacks either the 7-Methyl cap or the poly(A) tail. The lack of these structures, particularly the 5'mRNA cap, results in the necessity to develop novel mechanisms to ensure translation of viral mRNA.

1.3.1.1 The closed-loop model of translation initiation

As mentioned before, experimental evidence suggests that mRNA circularization is required for efficient cellular protein synthesis. However, a number of viruses, such as

rotaviruses, generate mRNA that lacks a 3'poly(A) tail. Rotavirus is a member of *Reoviridae* and contains 11 double-stranded RNA segments. Each segment is transcribed into mRNA that possess a 5'cap structure but lacks a 3'poly(A) tail. Instead, the 3'end contains a tetranucleotide motif which is recognized by the virus encoded NSP3 protein (Piron *et al.*, 1998; Vende *et al.*, 2000). NSP3 binds specifically to the conserved viral 3'end and to the scaffold protein eIF4G. In addition, eIF4G displays higher affinity for NSP3 than for PABP and as a consequence the interaction between eIF4G and PABP is disrupted in rotavirus-infected cells (Groft and Burley, 2002), which results in reduced efficiency of host mRNA translation and circularization-mediated enhancement of viral protein synthesis. Another virus lacking 3'poly(A) tail is Dengue virus, a mosquito-borne member of the family Flaviviridae. In this case PABP was found to interact with the 5'UTR of the viral mRNA to bring about its circularization (Polacek *et al.*, 2009).

1.3.1.2 IRES

One of the mechanisms used by some RNA and DNA viruses to initiate protein synthesis is use of an IRES (Internal Ribosome Entry Site), which is a sequence of nucleotides that allows initiation of the translation process in the middle of mRNA, on highly structured regions located within the 5'UTRs (Pelletier and Sonenberg, 1988), without involving 5'mRNA cap. The entry of ribosomes at an internal site of mRNA was first found in picornaviruses (poliovirus) (Pelletier and Sonenberg, 1988) and encephalomyocarditis virus (EMCV) (Jang *et al.*, 1988), and occurs in a growing number of viral mRNAs including those of hepatitis C virus (HCV) (Tsukiyama-Kohara *et al.*, 1992; Wang *et al.*, 1993), flaviviruses (Lemon and Honda, 1997), and

retroviruses (Balvay *et al.*, 2007). IRES has even been proposed for some herpesviruses mRNAs (Low *et al.*, 2001). It was also suggested that some mammalian mRNAs also have IRES (reviewed by Carter *et al.*, 2000).

Surprisingly, there is no general mechanism used by these viruses. In HCV-infected cells IRES directly binds to 40S ribosomal subunit, while picornavirus IRESes do not attract 40S directly, but rather through high-affinity eIF4G-binding site (Hellen and Sarnow, 2001). Viral IRESes have been divided into four groups (Kieft, 2008; Hellen, 2009) based on their secondary structure, requirement for eIFs, the location of the start codon relative to the site of the 40S ribosomal subunit recruitment, and the ability to operate in rabbit reticulocyte lysate with or without supplementation (Kieft, 2008). There is a number of different mechanisms of initiation used by viral IRES elements, however, no viral proteins have been found to be essential for IRES function, although the protease 2A encoded by poliovirus is thought to play a stimulatory role (Hambidge and Sarnow, 1992).

In contrast to cap-dependent translation, translation initiation mediated by IRES elements is independent of the cap, and is therefore independent of eIF4F integrity. As such, these viruses often inactivate eIF4F by cleaving eIF4G or PABP, or dephosphorylating 4E-BP1.

1.3.2 DNA viruses

In contrast to many RNA viruses that inactivate eIF4F function, an increasing number of DNA viruses are being found to stimulate the assembly of translation initiation complexes to maximize viral protein production. These include herpes simplex virus (HSV), human cytomegalovirus (HCMV), VacV, and African swine fever virus (ASFV)

(Kudchodkar *et al*., 2004; Walsh and Mohr, 2004; O'Shea *et al*., 2005; Walsh *et al*., 2005; Walsh *et al*., 2008; Castello *et al*., 2009). In all of these cases viruses activate mTOR to phosphorylate 4E-BP1 and stimulate eIF4F assembly. In the case of human papillomavirus (HPV), little is known about its effects on eIF4F, however, it has been shown that HPV de-regulates eIF4E and 4E-BP1 through mTOR activation, which may contribute to cell transformation (Oh *et al.*, 2006). Another example of eIF4F manipulation is adenovirus-encoded 100k protein, which binds to the C-terminus of eIF4G and evicts Mnk, leading to dephosphorylation of eIF4E (Cuesta *et al.*, 2000; Cuesta *et al.*, 2004). 100k protein also binds to the viral mRNA to promote its translation by the process of "shunting" in which ribosomes physically bypass parts of the 5' untranslated region to reach the initiation codon (Yueh and Schneider, 1996; Xi *et al.*, 2004). In addition, a number of other viral factors have been shown to interact with eIF4F and regulate its function during infection (discussed in Section 4).

In contrast to other DNA viruses, only the *Poxviridae* and *Asfarviridae*, with its only member ASFV, replicate exclusively in the cytoplasm of infected cells. Recent studies have shown that besides stimulating eIF4F assembly both VacV and ASFV cause a unique redistribution of host translation factors to viral replication compartments (Katsafanas and Moss, 2007; Walsh *et al*., 2008; Castello *et al*., 2009). How this impressive rearrangement of the host translation system is accomplished remains unknown, and is part of the aim of this study.

1.4 Aims of thesis

Previous studies by a number of researchers showed that poxviruses stimulate eIF4F formation and commandeer components of this host translation initiation complex by redistributing and concentrating them within viral factories by an unknown mechanism.

This thesis aimed to analyze the signaling pathways activated by vaccinia virus and leading to eIF4F complex assembly in infected cells. We intended to evaluate the effect of VacV on PI3K/Akt/mTOR pathway, which is the key pathway regulating protein synthesis in cells, but had not been studied in VacV-infected cells. Investigation of its changes would provide valuable information not only about vaccinia virus strategies, but also the cellular signaling and translational machinery in general.

Finally, we aimed to identify possible viral/cellular protein(s) involved in redistribution of translation factors during VacV infection. In order to do this it was essential to screen components of the eIF4F complex in VacV-infected cells to search for such protein(s). The next step would be to clone and express that protein(s) in cells to determine its function and importance in VacV replication. As a last point we planned to find the regions of the protein(s) responsible for its function.

Section 2.0

Material and Methods

2.1 Equipment

Applied Biosystems 2720 Thermal Cycler

Centrifuge Beckman Avanti J-25I

Container with printed label, 30 ml (greiner bio-one)

Gene Pulser II Electroporator (Bio-Rad Laboratories)

Hotplate stirrer (SB162, Stuart)

Laminar flow cabinet (Lamin Air, Model 1.2, Holten)

Leica DFC 500 microscope

Microcentrifuge Sigma 1-15 PK

Microcentrifuge Galaxy 14D, VWR

Microprocessor ph meter (pH210, HANNA instruments)

Mini see-saw rocker (SSM4, Stuart)

Micropipettes 1-10 µl, 10-100 µl, 20-200 µl, 100-1000 µl (VWR)

Pipettes 1 ml, 2 ml, 5 ml (costar, USA)

Pipettes 10 ml, 25 ml (greiner bio-one)

Power Supply (PowerPac™ HV, catalogue no. 164-5056, BIO-RAD)

Speed Gel SG 200 gel dryer (Savant, Farmingdale, NY)

Steri-cycle CO2 Incubator (Thermo Electron Corporation)

Tips, natural bevelled (TipOne, Starlab)

Vortex Mixer (PV-1, Grant Bio)

Vacuum Millipore

2.2 Antibodies

Table 2.1 Primary antibodies used in immunocytochemical studies

Antibody	Host	Supplier, #catalogue no.	Dilution
Akt	Rabbit	Cell Signalling #9272	1/1000
Phospho-Akt Ser473	Rabbit	Cell Signalling #9271	1/1000
Phospho-Akt Thr308	Rabbit	Cell Signalling #9275	1/1000
Phospho-Erk	Rabbit	Cell Signalling #9101	1/1000
mTOR	Rabbit	Cell Signalling #2972)	1/1000
p70 S6 Kinase	Rabbit	Cell Signalling #9202	1/1000
4E-BP1	Rabbit	Cell Signalling #9452	1/1000
Caspase 3	Rabbit polyclonal	Cell Signaling #9662	1/1000
Cleaved Caspase 3	Rabbit polyclonal	Cell Signaling #9661	1/1000
Parp	Rabbit polyclonal	Cell Signaling #9542	1/1000
Cleaved Parp	Rabbit polyclonal	Cell Signaling #9541	1/1000
PABP	Rabbit polyclonal	Cell Signaling #4992	1/1000
PABP	Rabbit monoclonal	Gift (Simon Morley)	1/3000
Phospho-eIF4G	Rabbit polyclonal	Cell Signaling #2441	1/1000
eIF-4E	Mouse monoclonal	BD Labs #610269	1/1000
P-eIF2α	Rabbit polyclonal	Cell Signaling #9721	1/1000
eIF-4G	Rabbit polyclonal	Gift (Ian Mohr)	1/5000
Vaccinia virus	Rabbit	Virostat # 8101	1/1000
I3	Rabbit	Gift (J. Krijnse-Locker)	1/2000
FLAG	Rabbit	Sigma-Aldrich	1/1000

2.3 Water

Ultrapure water was used in the preparation of all media and solutions. Water was first pretreated using activated carbon and pre-filtration, and then purified by a reverse osmosis system (Milipore Milli-RO 10 Plus, Elgastat UHP) with a standard of 12-18 MΩ/cm resistance.

2.4 Sterilization

Water, glassware, lids and all thermostable solutions were sterilised by autoclaving at 121° C for 20 minutes under pressure of 1 bar. Thermolabile solutions and drugs were filtered through a 0.45 μm sterile filter (Milipore, Millex-hv, SLHV033RB). Low protein-binding filters were used for all protein-containing solutions.

2.5 Cell culture

2.5.1 Medium

Cells were cultured in Dulbecco's Modified Eagle's Medium (DMEM) (Sigma) supplemented with 2 mM L-glutamine (Invitrogen, UK), 1 mM sodium pyruvate (Invitrogen, UK), 50 units of penicillin, and 50 μg per ml of streptomycin (both Invitrogen, UK). Medium with 5 % fetal bovine serum (FBS) (Sigma) was used for culturing cells, whereas 0.2 % FBS supplementation was added to the medium for starving NHDFs.

2.5.2 Cell lines

The utilized cell lines were (1) primary normal human diploid fibroblasts (NHDFs) (Clonetics, Walkersville, Maryland, United States), (2) HEK-293 cells, and (3) BSC40

cells (which are monkey epithelial kidney cells), both kindly provided by Dr. I. Mohr, New York University.

Table 2.2 Cell lines used in the study

Cell line	Cell type	Basal medium	Source
NHDF	Normal human diploid fibroblasts	DMEM	Clonetics
HEK-293	Transformed human embryonic kidney cells	DMEM	Dr. I. Mohr
BSC40	Monkey epithelial kidney cells	DMEM	Dr. I. Mohr

NHDFs were used to carry out the majority of the experiments as we were interested in the effects of viral infection on normal human cells. NHDFs express low levels of translation factors that are noticeably activated during infection. We also used serum starvation to study both actively cycling and resting states of NHDFs.

HEK-293 is a hypotriploid human cell line established from primary human embryonic kidney cells, which were transformed with human adenovirus 5 DNA (Graham *et al.*, 1977). On account of the presence of increased quantities of translational factors, characteristic for transformed cell lines, HEK-293 cells were used in this study to perform the majority of the binding assays.

BSC40 is a high-temperature tolerant derivative of BS-C-1 established by Brockman and Nathans (1974), which supports the growth of vaccinia virus for titering.

2.5.3 Cell passaging

Cells were grown in a CO_2 incubator at 37° C and 5 % CO_2 until confluent. A 10 cm^2 dish of cells was then quickly washed with PBS and treated with 1 ml of trypsin. After an incubation of five to ten minutes at 37° C cells were resuspended in the appropriate amount of medium and mixed well. NHDFs were split 1:3, 293 cells were split 1:10 and seeded into new tissue culturing containers.

2.5.4 Cell starvation

For serum starvation, confluent cultures of NHDFs were washed three times in PBS then cultured in DMEM containing 0.2 % FBS for 5 days, when more than 98 % of the cells are in the G_1 phase of the cell cycle. Starvation of NHDFs was used to simulate the resting state of cells.

2.5.5 Cell harvesting

For the preparation of whole cell extracts from cultures seeded in 6-well plates or on 35 mm^2 dishes, cells were lysed in 250 µl of working sample buffer to solubilize total cellular proteins. Working sample buffer was prepared from the stock of 2 x Laemmli buffer.

1 x working buffer	2 x Laemmli buffer
50 % 2x Laemmli	12.5 % 1M Tris, pH 6.8
45 % UHP water	20 % SDS (20 %)
5 % β-Mercaptoethanol	40 % Glycerol (50 %)
4 µl 8 % bromophenol blue per ml buffer	27.5 % UHP water

The working sample buffer contains a negatively charged detergent sodium dodecylsulfate as well as β-Mercaptoethanol being the reducing agent. The tensid SDS binds to the proteins hydrophobic regions and leads to an unfolding of the polypeptide chains. Other subunits are also released from the protein. Anionic SDS interacts proportionally to the protein's molecular weight and confers its negative charge. β-Mercaptoethanol is added to analyse the polypeptide's linear form. This reducing agent cleaves the disulfide bond between two thiol groups. The samples were boiled after harvesting for three minutes to destroy remaining secondary and tertiary structures. All proteins are now showing an ellipsoid structure and are generally not separated by their conformation but by their size. After heating the samples, they were cooled, vortexed, centrifuged and stored at -20° C until further usage.

2.5.6 Cell freezing

To allow long term storage of cell stocks, cells were frozen and cryo-preserved in liquid nitrogen at temperature below -180° C. Once frozen properly, such stocks should last indefinitely.

- ➢ Cells to be frozen were harvested in the log phase of growth (i.e. actively growing and approximately 60-70 % confluent) by centrifugation at 1200 rpm for 5 min.
- ➢ Pelleted cells were carefully re-suspended in freezing medium (FBS containing 10 % DMSO) (Sigma) and transferred into cryovials (Greiner).
- ➢ Cryovials were immediately placed in isopropanol freezing container, as DMSO is toxic to cells at room temperature, and set at -80° C for 24 h.
- ➢ Cryovials were then transferred into liquid nitrogen containers, where they were stored until required.

2.5.7 Cell thawing

Immediately prior to removal of a cryovial from the liquid nitrogen stores for thawing, a sterile universal tube containing growth medium was prepared for the rapid transfer and dilution of thawed cells to reduce their exposure time to DMSO freezing solution.

➢ The cryovial was quickly thawed at 37° C water bath.

➢ When thawed, the DMSO-cell suspension was quickly transferred to the media-containing universal.

➢ The suspension was centrifuged at 1200 rpm for 5 min, the DMSO-containing supernatant removed, and the pellet re-suspended in fresh growth medium.

➢ Thawed cells were placed on 10 cm^2 dish and allowed to attach overnight.

➢ After 24 h the cells were re-fed with fresh growth medium to remove any residual traces of DMSO.

2.6 Cell fixation

Cells were washed 1x with cold PBS. The fixing solution was made by diluting the Formaldehyde Solution 37 % (Sigma) in PBS in a ratio of 1:10, and 2 ml of the solution was added to cells for 10 min. Cells were then washed 3x in cold PBS and stored in 2 ml of PBS at 4° C.

2.7 Virus

Vaccinia virus Western Reserve (VacV WR) was a kind gift of Dr. Stewart Shuman, Memorial Sloan-Kettering, New York, and was propagated and titered on permissive BSC40 cells as described below.

2.7.1 Growing viral stocks

Virus was grown in confluent 10 cm^2 dishes using BSC40s, the cell line that supports the growth of VacV (Brockman and Nathans, 1974).

- One day before infection BSC40 cells grown in 5 % FBS were seeded on 10 cm^2 dishes by splitting 1:2 each confluent 10 cm^2 dish. The next day medium was changed to 2 % FBS, which supports virus growth.

- The stock tube of VacV was trypsinized for 30 min at 37° C in an equal volume of 0.25 % trypsin (diluted 1:10 in PBS). Trypsinization reaction was then neutralized by adding an equal or larger volume of medium containing 2 % FBS.

- Cells were infected at moi 0.05 and virus was grown at 37° C for 2-3 days (the virus is highly cell associated so growing stocks at lower temperature doesn't have any advantage). Medium was replaced with an equal volume of serum-free DMEM, and cells were scraped very carefully, to avoid splashing the virus around. Cells together with serum-free medium were collected in a 50 ml Falcon tube and placed at -80° C.

- To harvest the virus, cells were freeze/thawed by placing the tube in a 37° C waterbath, a total of three times. Medium containing the virus was then aliquoted in 1ml aliquots and stored at -80° C.

2.7.2 Titering virus

Virus was titered using confluent BSC40 cells grown in DMEM 5 % FBS in 6-well plates.

- The day before titering, BSC40 cells were seeded at 5x10^5 cells per well of a 6-well plate.

- The virus was thawed and trypsinized with an equal volume of 0.25 % trypsin; mixed well by pipetting up and down and incubated for 30 min at 37° C. Trypsinization reaction was then neutralized by adding 500 ul DMEM 2 % FBS.

- Serial dilutions of virus in DMEM 2 % FBS were made, and 500 ul of each dilution was then added to cells containing 1.5 ml 2 % FBS DMEM, and mixed gently.

- Cells were placed at 37° C, and on day 3 plates were fixed by aspirating medium and adding 10 % TCA (Trichloroacetic acid) (Sigma) for 10 min. Staining the plates was performed by aspirating 10 % TCA and adding Crystal Violet stain (Merck) for 15 min, followed by rotating plates on orbital rotator. Plates were then washed using tap-water and left to dry.

2.8 SDS-PAGE

(Sodium dodecylsulfate polyacrylamide gel electrophoresis)

To fractionate the samples, an acrylamide percentage was chosen depending on the size of the proteins to examine. To look at proteins with a high MW like eIF4G a 10 % gel was used while the different phosphorylation states of 4E-BP1 were much better resolved in a 17.5 % gel. The increasing percentage of acrylamide made it harder for large proteins with a low electrophoretic mobility to pass through the gel while small proteins were separated more clearly.

Table 2.3 Ingredients for SDS-PAGE resolving gel

	7.5 %	10 %	12.5 %	17.5 %
Water (ml)	2.75	2.22	1.55	-
1 M Tris pH 8.7 (ml)	2.5	3.75	3.75	3.75
30 % Acrylamide (ml)	0.95	3.34	4.15	5.85
2 % Bis-Acrylamide (ml)	3.75	0.67	0.5	0.365
20 % SDS (µl)	50	50	50	50
10 % APS (µl)	33.35	33.35	33.35	33.35
TEMED (µl)	8.35	8.35	8.35	8.35

Table 2.4 Ingredients for SDS-PAGE stacking gel (5 ml)

Water (ml)	3.175
1M Tris pH 6.8 (ml)	625
30% Acrylamide (ml)	850
2% Bis-Acrylamide (ml)	350
20% SDS (µl)	25
10% APS (µl)	25
TEMED (µl)	12.5

All ingredients (40 % Acrylamide, 2 % Bis-Acrylamide and TEMED from Merck; Tris, SDS and APS from Sigma) were mixed according to Tables 2.3 and 2.4, and the resolving gel was poured between two vertical glass plates. The vertical construction minimizes oxygen absorption which limits the polymerization. Approximately 500 µl of water-saturated iso-butanol (Sigma) was added on top to overlay the resolving gel and prevent further oxygen uptake. After one hour alcohol was washed out, the stacking gel was poured on top, the comb inserted and once everything was set, gels were transferred

to the electrophoresis chamber. The chambers were filled with 1x electrode buffer (0.25 M Tris, 2.5 M Glycine [Sigma], 1 % SDS), and bubbles that could influence the electric current were removed with the help of syringes filled with buffer. The marker was prepared in working sample buffer using 3 µl of Precision Plus Protein Dual Colour Standards (Bio-Rad) per lane. After loading 5 to 14 µl of the sample the gel was run at 150 volts to resolve the proteins.

2.9 Western blotting (Immunoblotting)

The western blot or protein immunoblot is used for highly sensitive detection as well as quantification of immobilized proteins. The SDS-PAGE separated proteins are transferred to a nitrocellulose membrane via wet electroblotting, immobilized and immunochemically detected. For that the gel was carefully fixed between a piece of chromatography paper and a nitrocellulose membrane. The sandwich made of the chromatography paper, the gel, the nitrocellulose membrane, second piece of chromatography paper, and two sponges on each side was stabilized between two plastic scaffolds and then transferred to a chamber filled with 1x transfer buffer mixed with 20 % methanol (Merck). The methanol in the buffer helps removing SDS from protein-detergent complexes and increases the affinity between proteins and the membrane.

5 X wet western transfer buffer	1 X transfer buffer:
124 mM Tris	20 % 5x wet western transfer buffer
960 mM Glycine	20 % methanol
0.05 % SDS	60 % UHP water

An electric current induced by 57 volts for one hour transferred the proteins out of the gel onto the membrane. Big proteins such as eIF4G needed three hours of transfer. Afterwards the membrane was washed in 1 X TBS-T (tris-buffered saline with Tween 20) (1.5 M NaCl, 0.5 M Tris, 0.1 % Tween 20, pH adjusted to 7.4 using concentrated HCl) to remove remaining SDS.

To detect proteins, the membrane was blocked in 1x TBS-T with 3 % dried skimmed milk powder with less then 1 % fat (Marvel, Premier International Foods, UK) or 3 % bovine serum albumin (BSA) (Sigma). The blocking prevented non-specific binding of antibodies used for detection of the target protein to the membrane. After washing, the membrane was incubated with primary antibodies at 4° C over night. The next day the membrane was washed 3 times for five minutes with 1 x TBS-T to remove the remaining primary antibodies and incubated with appropriate horseradish peroxidase-conjugated secondary antibodies in 1 x TBS-T with 3 % dried skimmed milk powder or 3 % BSA for one hour. The horseradish peroxidase catalysed the oxidation of luminol when activated by hydrogen peroxide. The product of this reaction is very unstable and decomposes immediately. It emits blue light that leads to a dark region which corresponds to the protein bands of interest when exposed to X-ray film. The brightness of the light is proportional to the amount of protein present. After washing the membrane 3 times for five minutes it was subjected to chemiluminescence western blotting substrate according to the manufacturer's instructions (Pierce ECL, Thermo Scientific), fixed between cling films, exposed to x-ray film, and developed in the dark room using Kodak developer/fixer solutions.

2.10 Metabolic labelling

Radioactive medium was made by using the following components:

1 ml Methionine/Cysteine-free DMEM (Sigma)

10 μl L-Glutamine (Gibco)

10 μl Pen-Strep (Gibco)

10 μl NaPyruvate (Gibco)

25 μl HEPES, pH 8 (sterile, TC grade)

All ingredients were mixed by gently swirling, and warmed up at 37°C. ^{35}S-Methionine (Perkin Elmer) was thawed and 7 μl (0.017 mCi) was added per 1ml of medium (or 20 μl in the case of immunoprecipitation assay), and gently mixed. Old medium was aspirated off from cells, and radioactive medium was added with the amount of 1ml per 35 mm dish. If the cells were infected, the pipette used for applying the medium was carefully placed in 1 % virkon several times, to inactivate the virus before placing the pipette into radioactive waste. The dish was then carefully placed in the designated container for labeling, together with the opened 35 mm dish containing activated charcoal, and incubated at 37°C in cell culture incubator for 1 h. After labeling, the dish was carefully removed and transferred to the safety cabinet. Radioactive medium was removed by pipette, mixed with virkon to inactivate the virus, and placed into liquid disposal container for ^{35}S waste. Cells were lysed in appropriate lysis buffer (Laemmli buffer to make total cell extracts, NP40 buffer for immunoprecipitation assay). All tubes, pipettes and used dishes were placed in the solid waste disposal area for ^{35}S waste.

2.11 Gel fixation and drying

Resolved SDS-PAGE gels containing samples that had been labelled with ^{35}S-methionine/-cysteine were placed in destain solution (Table 2.5) for 20 min at room temperature. The gel was dried on cardboard at 80° C for two hours under vacuum with a Speed Gel SG 200 gel dryer to remove the water in the gel. The dried gel was then exposed to x-ray film at -80° C for the appropriate exposure time and developed using Kodak developer/fixer solutions.

Table 2.5 Ingredients of destain solution

Destain solution
25 % Methanol
10 % Acetic Acid
65 % UHP water

2.12 Immunoprecipitation

Anti-eIF4G and anti-PABP immunoprecipitation from metabolically labeled cell extracts was performed as follows. After labeling, soluble cell extracts were prepared in NP-40 lysis buffer (NLB) and centrifuged at 10000xg for 10 min at 4° C. Extracts were treated with a cocktail of nucleases (RNAse A, RNase T1 and Micrococcal Nuclease) then precleared with 5 μl normal rabbit serum and incubated with 2 μl primary antibody for 1 h. Then samples were added to Protein A Sepharose beads (GE Healthcare) and incubated for another hour at 4° C. Beads were washed 3 times in NP-40 buffer and boiled in Laemmli buffer.

NP-40 lysis buffer (10 ml)

500 μl of 1 M HEPES/KOH pH 7.4 containing 40 mM EDTA

400 μl of 2.5 M NaCl (Sigma)

80 μl of 0.25 M Na_3VO_4 (Calbiochem)

250 μl of 1 M Glycerophosphate (Calbiochem)

125 μl of 2 % NP-40

10 μl of 1.5 M $MgCl_2$ (Sigma)

8.56 ml Water

1 protease inhibitor cocktail tablet (CompleteR Mini-tablets, Roche)

2.13 7-methyl GTP sepharose 4B chromatography

10^7 cells were washed in PBS then lysed in 600 μl NLB, treated with RNAse A and precleared with 80 μl packed-bed volume (pbv) BSA-blocked sepharose 4B (Amersham) for 1 h. Input samples were taken from precleared extracts and the remaining sample was incubated with 50 μl pbv BSA-blocked 7-Methyl GTP-Sepharose (Amersham) for 1 h then washed in NP-40 lysis buffer, and boiled in Laemmli buffer.

2.14 ssDNA-binding assay

3×10^7 cells were washed in PBS then lysed in NLB and centrifuged at 10000 xg for 10 min at 4° C. Extracts were treated with RNAse A (50 μg) for 20 min at room temperature, then treated with RNAse Inhibitor (Sigma-Aldrich). Extracts were precleared for 1 h with 20 μl p.b.v. anti-biotin antibody conjugated sepharose 4B (Sigma-Aldrich). Precleared extracts were then programmed with 7.5 μg

phosphothioate-stabilized 5'-biotin conjugated ssDNA (sequence: ataattaataacaccatagaccaccgcccgaaggg) (Sigma) and 20 μl p.b.v. anti-biotin antibody-conjugated sepharose 4B for 2 h at 4°C. Resin was recovered and washed extensively in NLB before boiling in Laemmli buffer.

2.15 Transfections

Cells were seeded in antibiotic-free medium and transfected using Fugene HD Transfection Reagent (Roche) according to the manufacturer's instructions.

2.16 Immunofluorescence

Cells were seeded on glass-bottom 35 mm dishes (Lennox). On day 2 cells were transfected with 0.5 μg pGFP-I3L. On day 3 cells were infected overnight (16-20 h) at the indicated moi. Cells were then fixed in 3.7 % formaldehyde/PBS for 20 min, washed extensively with PBS and permeabilized in 0.1 % Triton for 20 min. After washing, dishes were blocked in a mixture of 3 % BSA and 1 % Donkey Serum in TBS for 40 min, then probed for 1h with anti-eIF4G antiserum (1:3000) in 3 % BSA and 1 % Donkey Serum in TBS-0.1 % Tween (TBS-T). Dishes were washed three times with TBS-T then probed for 40 min with TRITC (rhodamine isothiocyanate derivative)-conjugated cross-adsorbed donkey anti-rabbit secondary (Jackson ImmunoResearch) (1:1000) in 3 % BSA and 1 % Donkey Serum in TBS-T. Samples were washed three times with TBS-T, DNA was stained with Hoescht for 5 min and washed again in TBS-T. Images were captured on a Leica DFC 500 microscope.

2.17 Coomassie staining

After resolution of samples by SDS-PAGE, gels were sequentially soaked in coomassie stain overnight.

<u>Coomassie stain:</u>   50 % MeOH

                               10 % Acetic acid (Merck)

                             0.25 % Coomassie Brilliant blue (Biochemica)

The following day gels were washed in destain solution (see Table 2.5) for 90 min, frequently changing the solution at first, and stored in destain solution.

2.18 Silver Staining and Mass Spectrometry Analysis

After resolution of samples by SDS-PAGE, gels were sequentially soaked for 10 min each time in 50 % Methanol (Merck), 5 % Methanol, 30 μM DTT, 0.1 % (w/v) $AgNO_3$ (Sigma), then visualized with 3 % (w/v) Na_2CO_3. Bands were excised from silver stained gels and destained using a 1:1 mixture of 30 mM potassium ferricyanide/100 mM sodium thiosulfate solution. In-gel digestion using sequence grade trypsin (Promega) at a concentration of 12.5 ng/μl trypsin in 10 mM ammonium bicarbonate containing 10 % (vol/vol) acetonitrile was carried out overnight at 37° C. Tryptic peptides generated were extracted and analyzed by LC-MS/MS using an LTQ ion trap mass spectrometer (Thermo Fisher Scientific). The data generated was searched using BioWorks 3.3.1 (Thermo Fisher Scientific) against a subset of human and viral proteins from the SwissProt database.

2.19 Isoelectric focusing

Isoelectric focusing (IEF) is an electrophoretic method of protein separation based on their isoelectric point (pI). The pI is the pH at which the protein has no net charge and does not move in an electric field. The net charge is the sum of all positive and negative charges of the protein. Proteins carry positive, negative or zero net electrical charge, depending on the pH of their surroundings. IEF gels create a pH gradient to separate the proteins according to their unique pI (Garfin, 2003). This description of the procedure was kindly given to us by Dr. Simon Morley (University of Sussex), and is besed on the vertical slab version of IEF published by Savinova and Jagus (1997).

Firstly, a 50 ml stock of incomplete gel mix was made, filtered using a 0.22 µl filter (large syringe and pressure, not vacuum) and stored at 4° C.

Table 2.6 The components of the incomplete gel mixture.

42.8 ml pure water	24.13 ml H2O
4.86 g acrylamide	12.17 ml 40 % Acrylamide
274.3 mg bis-acrylamide	13.7 ml 2 % Bis-acrylamide
1.71 g CHAPS	1.71 g of CHAPS

2.19.1 Making and pouring the gel

The gel was mixed as outlined in table 2.7 leaving out the APS and TEMED. The mixture was gently heated at 37° C waterbath to dissolve the urea. Once urea was

dissolved, the APS and TEMED was added, and the gel was poured right to the top of
plates, combs added and gels were allowed to set.

Table 2.7 The components of the gel used for IEF.

1 Gel (6 ml)	2 Gels (12 ml)
3.5 ml Incomplete gel mix	7 ml incomplete gel mix
3.24 g urea	6.48 g urea
0.45 ml ampholines*	0.9 ml ampholines
20 µl 10 % APS	40 µl 10 % APS
10 µl TEMED	10 µl TEMED

 * pH range 3-10.

2.19.2 Sample buffer and sample preparation

7x sample buffer was made as described in table 2.8. 1 ml aliquots were stored at -20° C
to be reused when needed.

Table 2.8 The components of the 5 ml stock

Components	Volume
21 % (v/v) ampholines (same as for gels)	1.05 ml
14 % (v/v) ß-mercaptoethanol	0.7 ml
35 % (w/v) CHAPS	1.75 g
H_2O	3.0 ml

For sample preparation 1x sample buffer was made as described below.

1x sample buffer: 143 μl of 7 x sample buffer

                            0.54 g urea (gives 9 M final)

                            550 μl MilliQ water

Running buffers were prepared as described below (Tab. 2.9).

Table 2.9 The components of the running buffer

Cathode (outer chamber)	0.05 M Histidine (= 3.88g/500ml)
Anode (inner chamber)	0.01 M Glutamic Acid (= 0.073g/500ml)

500 ml of each buffer was freshly made. The buffers were chilled as the high voltage used during IEF can increase buffer temperature and warp the gels.

2.19.3 Running the gels

Once gel was set, the combs were removed and wells were washed out thoroughly with water. 20-25 μl of 1x sample buffer was added to each well. The wells were then carefully overlayed with 10 μl 6 M urea followed by glutamic acid. The inner chamber of the IEF apparatus was filled with 0.01 M glutamic aid and the outer chamber was filled with 250 ml 0.05 M histidine. The apparatus was placed in a plastic container and surrounded with ice to maintain a low temperature. The gels were then prefocused for a total of 1 h on reverse polarity at the following voltage:

-    20 min at 200 V

-    20 min at 300 V

-    20 min at 400 V

After prefocusing the wells were washed out thoroughly with water. Before the end of the prefocus stage the samples were prepared by boiling and allowing cooling. A 1:1 dilution of sample with 1x IEF sample buffer was prepared. The samples were then vortexed immediately and 25 µl of sample was loaded into each well. The sample was overlayed with urea and glutamic acid as for prefocusing and IEF was performed by increasing voltages in 50 V increments every 20 min starting at 500 up to 750 V, each one for 20 min, then run at 1000 V for another 20 min. Again, as for prefocus, IEF was run on reverse polarity. After electrophoresis the gel was transferred to nitrocellulose and probed with antieIF4E antiserum as described for Western Blotting.

2.20 Cloning procedure and plasmids

2.20.1 Purification of I3 from VacV-infected cells

Since VacV genes do not have introns, genomic DNA can be used for cloning. To prepare template for cloning, DNA was first isolated from uninfected or VacV-infected BSC40 cells, as described by Roper (2004). Cells were harvested by scraping in PBS, centrifuged, and lysed in buffer 1 (40 µM Tris-EDTA [pH 9], 1.5 M NaCl, H_2O) and buffer 2 (40 µM Tris-EDTA [pH 9], 7.5 % SDS, H_2O). Cells were then incubated with proteinase K to remove proteins from the DNA. Finally, proteinase K was heat-inactivated to avoid degradation of DNA polymerases used in PCR reaction, and DNA was purified by a phenol-chloroform extraction.

The I3L gene was then amplified from VacV genomic DNA by PCR using specific primers as described below.

2.20.2 PCR reaction

Primers were dissolved in TE buffer to make a 100 pMol/µl stock, from which the working primer stock of 10 pMol/µl was prepared. The target sequence was amplified in a 50 µl reaction using the KOD XL DNA polymerase kit (Novagen) and the PCR conditions as indicated in table 2.10. The PCR was performed using 2720 Thermal Cycler (Applied Biosystems). The amplified PCR product was gel purified using Qiagen kit and following the manufacturer's instructions. All necessary ingredients were supplied with the kit.

Table 2.10 PCR conditions used in this study

Step of PCR reaction	Temperature [^{o}C]	Time [sec]	Cycles
Initial denaturation	94	300	1
Denaturation	94	15	35
Annealing	60.3	30	35
Elongation	72	60	35

2.20.3 Restriction enzyme digestion of plasmid DNA

2 µl of each isolated product sample was run out on a 1 % agarose gel to check for degradation. 1 µl of the product, together with the same amount of the plasmid backbone, was then digested using 0.2 µl of the specific restriction enzymes. The 10 µl digestion reaction was carried out for 1 h at 37° C. The backbone was then SAP (Shrimp Alkaline Phosphatase) treated for 20 min at 37° C. SAP was inactivated by heating the

reaction to 65° C for 10 min. 1 µl of each digestion reaction (backbone and PCR digestion) was then run on 1 % agarose gel to check the sizes.

2.20.4 Ligation of target DNA into a suitable vector

Ligation of the target DNA into a plasmid backbone (in a ratio 1:1) was carried out in a 10 µl reaction including T4 DNA ligase (1 µl), ligase buffer 10x (1 µl), and usually 1 µl of both target DNA and backbone plasmid. Three different types of plasmids were used in this study: the mammalian expression vectors pCI-neo and pGFP-N, and the bacterial expression plasmid pET-15b containing the *lac* operon. Ligation reaction was carried out at 16° C for 1 h. To provide the control, an additional reaction containing backbone plasmid but no insert DNA was included.

2.20.5 Transformation of bacteria

1 µl of the ligation reaction was transformed into appropriate bacteria, DH5α or BL21(DE3) (both Invitrogen), following the manufacturer's instructions. Bacteria were thawed on ice very slowly, mixed with the ligation reaction and heat-shocked by placing the transformation into the 37° C/42° C waterbath for approximately 30 sec, then returned on ice for 2 min. Cells were then cultured in 1 ml SOC at 37° C in a shaking incubator for 1 hour to recover and begin expressing resistance marker gene. 20 µl and 200 µl of the transformation reaction was then plated on LB Agar (Sigma) containing the appropriate antibiotic. Bacterial culture was then spread on the plate using sterile glass beads, and plates were incubated overnight at 37° C. The next day single colonies were isolated and inoculated in 3 ml LB broth (Sigma) containing the appropriate antibiotic. The cultures were incubated overnight at 37° C in a shaking incubator, and the next day minipreps were made from the bacterial pellet.

2.20.6 DNA miniprep of plasmid DNA

Overnight bacterial cultures were centrifuged at 17000 xg and the minipreps were made using the QIAprep System (Qiagen) and following the manufacturer's instructions. Three basic steps of the procedure include:

➤ Preparation and clearing of a bacterial lysate

➤ Adsorption of DNA onto the QIAprep membrane

➤ Washing and elution of plasmid DNA

DNA was eluted in 30-50 µl Buffer EB (10 mM Tris-Cl, pH 8.5). Plasmid DNA purified by this system does not require phenol extraction or ethanol precipitation, and can be used directly for restriction enzyme digestion and sequencing.

2.20.7 Plasmid DNA restriction enzyme digestion and sequencing

To confirm the orientation of the inserted DNA in the plasmid, restriction digestion was then carried out using the enzyme from the original cloning and one enzyme outside the insert. The digestion reaction was then run on 1 % agarose to check the orientation of the insert.

In order to fully confirm the orientation of the inserted DNA in the plasmid and exclude mutations, the samples were sent to be sequenced.

2.20.8 Plasmids, restriction enzymes and primers used in this study

2.20.8.1 Generation of His-tagged I3L

To generate His-tagged I3L the following primers were used, containing EcoR1 and Sal1 restriction sites for cloning. The His sequence is italicized.

Forward: GCAACT GAATTC CGCCGCC ATG *cat cat cat cat cat cat*

AGTAAGGTAATCAAGAAG

Reverse: GCAACT GTCGAC TCTAGT TCA TAC ATT GAA TAT TGG CTT TTC

2.20.8.2 Generation of FLAG-tagged I3L

To generate FLAG-tagged I3L the following primers were used, containing EcoR1 and Sal1 restriction sites for cloning. The FLAG sequence is italicized.

Forward: GCAACT GAATTC CGCCGCC ATG AGTAAGGTAATCAAGAAG

Reverse: GCAACT GTCGAC TCTAGT TCA *ctt gtc gtc atc gtc ttt gta gtc* TAC ATT GAA TAT TGG CTT TTC

2.20.8.3 Generation of GFP-tagged I3L

To generate pGFP-I3L the following primers were used, containing EcoR1 and Kpn1 restriction sites, to amplify I3L from viral DNA.

Forward: GCAACT GA ATT CTC GCC GCC ATG AGT AAG GTA ATC AAG AAG

Reverse: GGC CCG CGG TAC CGT TAC ATT GAA TAT TGG CTT TTC

The amplified PCR product was gel purified and digested then ligated into the EcoR1-Kpn1 cloning site of the mammalian expression plasmid, pGFP-N (Clontech).

2.20.8.4 Generation of FLAG-tagged actin

FLAG-Actin was amplified from cDNA prepared from RNA isolated from human cells. The following primers, containing EcoR1 and Sal1 restriction sites, were used to amplify the gene and ligate it into the EcoR1-Sal1 cloning site of pCI-Neo. The FLAG sequence is italicized.

Forward: GCAACT GAATTC CGCCGCCATGTGCGACGAAGACGAGACC

Reverse:GCAACTGTCGACTCTAGTTCA*cttgtcgtcatcgtctttgtagtc*GAAGCATTTGCG GTGGAC

Ligations were transformed into DH5α cells and individual colonies were isolated. Recovered plasmids were analyzed by restriction digestion then sequenced to ensure cloning fidelity.

2.20.8.5 Generation of I3L fragments

To generate purified his-tagged full length I3 and fragments thereof the I3L gene was PCR amplified using the following primers containing Not1 and Nde1 cloning sites:

Full Length I3:

Forward: GCAACTCATATGAGTAAGGTAATCAAGAAG

Reverse: GCAACTGCGGCCGCGACTAGTTCATACATTGAATATTGGCTTTTC

I3-F1:

Forward: GCAACTCATATGAGTAAGGTAATCAAGAAG

Reverse: GCAACT GCGGCCGC GACTAGT TCA atc aat gat tag ttt ctt gag

I3-F2:

Forward: GCAACTCATATGAGTAAGGTAATCAAGAAG

Reverse: GCAACT GCGGCCGC GACTAGT TCAaac ata ttc tac cat ggc tcc

I3-F3:

Forward: GCAACTCATATGAGTAAGGTAATCAAGAAG

Reverse: GCAACT GCGGCCGCGACTAGTTCAatacaacataggactagccgc

I3-F4:

Forward: GCAACTCATATGAGTAAGGTAATCAAGAAG

Reverse: GCAACT GCGGCCGC GACTAGT TCA aca att agc gta ttg aga agc

I3-F5:

Forward: GCAACTCATATGtct atc tct ata aaa ctt act g

Reverse: GCAACTGCGGCCGCGACTAGTTCATACATTGAATATTGGCTTTTC

PCR products were digested with Not1 and Nde1 and ligated into Not1/Nde1 cloning sites in the bacterial expression plasmid, pET-15b. Ligations were transformed into DH5α cells and individual colonies were isolated. Recovered plasmids were analyzed by restriction digestion then sequenced to ensure cloning fidelity. Plasmids were then transformed into BL-21(DE3) cells (Invitrogen).

2.21 Protein purification

Overnight starter cultures were used to inoculate 250 ml cultures (LB broth containing ampicillin) grown at room temperature until O.D. = 600 (approximately 5 h) then induced with 0.05 mM isopropyl β-D-1-thiogalactopyranoside (IPTG) for 60 min. IPTG is a non-metabolisable metabolite of lactose that triggers transcription of the *lac* operon. Cells were harvested by centrifugation at 6000 xg for 15 min at 4° C. The specific purification procedure was carried out for each protein as described below, and all proteins were then dialysed overnight, with buffer changes 2 h before and after the overnight dialysis. The components of dialysis buffer were as follows:

Dialysis buffer components: 20 mM HEPES-KOH pH 7.4

100 mM KCl

5 % Glycerol

UHP water

2.21.1 Purification of His-tagged I3 proteins

His-tagged I3 proteins were purified at room temperature using His-Talon columns (Clontech). Cell pellet was resuspended in xTractor buffer containing Benzonase (1 μl per 2 ml of buffer) and Protease Inhibitor Coctail, EDTA-free (Roche) (1 tablet per 15 ml of buffer) and lysed by sonication using a Branson probe 102C (5 pulses of 10 sec on, 10 sec off; performed on ice), then centrifuged at 27000 xg for 15 min (Beckman Avanti J-25I, JA17 rotor) at 4° C to separate soluble from insoluble proteins. Supernatant was collected and applied on the cartridge, which was previously equilibrated according to the manufacturer's instructions. Using a syringe attached to the Luer Lock Adapter, the sample was passed through the column, the resin was washed with the Wash Buffer provided with the kit, and eluted by applying 5 column volumes of Elution Buffer. The 1 ml fractions of the purified protein were collected and analyzed by performing a Bradford assay (Bio-Rad Protein Assay, Bio-Rad Laboratories) (Bradford, 1976). Fractions were snap-frozen in a dry ice-EtOH bath, and stored at -80° C.

2.21.2 Purification of GST-tagged eIF4G fragments

GST-tagged eIF4G fragments (kind gift of Dr. Robert Schneider, NYU Langone Medical Center) were purified from BL21(DE3) cells at 4° C by using the B-Per GST Fusion Protein Spin Purification Kit (Pierce). Cell pellet was resuspended in cold PBS containing Benzonase (1 μl per 2 ml of PBS) and Protease Inhibitor Coctail, EDTA-free (Roche) (1 tablet per 15 ml of PBS), lysed by sonication using a Branson probe 102C (5 pulses of 10 sec on, 10 sec off; performed on ice), and centrifuged at 27000 xg for 15 min (Beckman Avanti J-25I, JA17 rotor) to separate soluble from insoluble proteins. Supernatant was collected and incubated with 1ml Immobilized Glutathione (provided

with the kit) at 4^oC for 1 h, then centrifuged at 1200 xg (Sigma 1-15 PK) for 5 min at 4° C. The supernatant was removed and the gel slurry was resuspended with 0.25 ml Wash Buffer, transferred to a column provided with the kit, and centrifuged at 1200 xg for 2 min at 4^oC. Washing step was repeated once more, and the resin was then eluted using the Elution Buffer, according to the manufacturer's instructions. The 1 ml fractions of the purified protein were collected and analyzed by performing a Bradford assay (Bio-Rad Protein Assay, Bio-Rad Laboratories) (Bradford, 1976). Fractions were snap-frozen in a dry ice-EtOH bath, and stored at -80^oC.

2.21.3 Batch-purification of eIF4E

Untagged human eIF4E was batch-purified from BL21(DE3) cells at 4° C. Cell pellet was resuspended in cold PBS containing Protease Inhibitor Cocktail, EDTA-free (Roche) (1 tablet per 15 ml of PBS), lysed by sonication using a Branson probe 102C (5 pulses of 10 sec on, 10 sec off; performed on ice), and centrifuged at 27000 xg for 15 min (Beckman Avanti J-25I, JA17 rotor) to separate soluble from insoluble proteins. Supernatant was collected and snap-frozen in a dry ice-EtOH bath, and stored at -80^oC. When needed, lysates were thawed on ice, treated with benzonase and batch-purified by incubation with 7-Methyl GTP Sepharose 4B for 1h at 4^oC. The resin was then washed several times to remove unbound debris.

2.22 Generation of VacV mutant

Deletion of the I3L gene was carried out using a novel application of the VAC-BAC/λ system in which the complete VacV genome is cloned in a bacterial artificial chromosome (BAC), and rescued by fowlpox virus, a distantly related poxvirus (Domi

and Moss, 2002). A two-step procedure was used to replace the I3L ORF of the VAC-BAC plasmid with the ampicillin (Amp) resistance gene by homologous recombination in *E.coli* DH10B cells. In the first step I3L ORF was replaced with the Amp ORF. In the second step VAC-BAC ΔI3L plasmid was transfected into fowlpox virus-infected cells that are not permissive for fowlpox virus.

2.22.1 Deletion of I3L ORF

2.22.1.1 Primers and PCR

To amplify the ampicillin ORF from the pET plasmid by PCR the following primers containing approximately 18 bp of the 5' and 3' end of the amp gene and 50 bp of homologous sequences flanking the region where I3L overlaps the I2L and I4L ORFs were used:

Forward: AAAGTGAAAATATATATC ATTATATTACAAAGTACAA

TTATTTAGGTTTATCTTGA AGACGAAAGGGCC

Reverse: TCCGGAGACCCCATAAAT ACACCAAATATAGCGGC

GTACAACTTATCCATGAG ATTATCAAAAAGG

To confirm that ampicillin ORF replaced I3L ORF the following primers containing the I3L flanking sequences were used:

Forward: CAAAGTACAATTATTTAGG

Reverse: AATACACCAAATATAGCGG

The conditions used for the PCR reactions are described in table 2.6

2.22.1.2 Preparation of electrocompetent VAC-BAC cells

E.coli cells strain DH10B harboring VAC-BAC/λ plasmid (gift of A. Domi and B. Moss) needed to be specially treated in order to perform the efficient transformation through electroporation.

2.22.1.2.1 Activation of the recombination system

To induce expression of λ recombination genes in *E.coli* DH10B/VAC-BAC/λ, the protocol recommended by Domi and Moss (2005) was used. 50 ml of LB medium containing tetracycline (25 µg/ml) and chloramphenicol (34 µg/ml) was inoculated with 500 µl of an overnight culture of *E.coli* DH10B/VAC-BAC/λ and incubated at 32° C until OD_{600} was approximately 0.6. Then, the culture was induced at 42° C for 45 min. The cells were chilled on ice for about 10 min.

2.22.1.2.2 Cell wash

After activation of the recombination system, 15 ml cell aliquots were collected by centrifugation at 4° C, 2200 xg for 10 min (Beckman Avanti J-25I, JA14 rotor). After discarding supernatant the pellet was washed 3 times with ice-cold 10 % glycerol in UHP water, and resuspended in 50 µl of the same solution. Electrocompetent cells were then snap-frozen in a dry ice-EtOH bath, and stored at -80° C

2.22.1.3 Transformation of DH10B cells

Electrocompetent *E.coli* DH10B cells harboring VAC-BAC/λ plasmid were thawed on wet-ice, and 50 µl of the cells was mixed with 1 ng of the PCR amplified DNA (Amp ORF containing the flanking sequences), then gently transferred into the pre-chilled on ice electroporation (EP) cuvettes (Gene Pulser Cuvette, 0.1 cm electrode, Bio-Rad

Laboratories). EP cuvettes were kept on ice for 5min then dried and placed in the electroporator. Transformations were performed using a Gene Pulser II Electroporator (Bio-Rad Laboratories). The following EP parameters were used:

EP parameters: 200 Ω

2.0 kV

25 μF

10-12 MSec

Immediately after electroporation cells were diluted in 1 ml of SOC medium (Sigma), mixed gently by pipetting up and down and transferred to the 30 ml tube. Cells were incubated at 37° C shaking incubator for 1 h. Then, 200 μl cultures were plated on LB Agar plates containing Amp and chloramphenicol and incubated at 37° C overnight for selection of efficiently transformed cells.

2.22.1.4 BAC purification

In order to recover VAC-BAC/λ plasmid from DH10B cells, the BAC purification was performed using the QIAGEN Large-Construct Kit, which is based on the QIAGEN Anion-Exchange Resin.

The single colonies of the wildtype DH10B/VAC-BAC/λ cells and the recombinant DH10B/VAC-BACΔI3L/λ were used to inoculate a starter culture of 3 ml LB medium containing selective antibiotics (Amp and chloramphenicol). Cultures were incubated at 37° C for 6-8 h with vigorous shaking (225 rpm). Then, 0.5 ml of the starter culture was inoculated into 500 ml selective LB medium, and grown at 37° C for 16 h with vigorous shaking. Cells were harvested by centrifugation at 6000 xg for 15 min at 4° C (Beckman Avanti J-25I, JA17 rotor), and purified according to the manufacturer's instructions.

Basically, the protocol starts with modified alkaline lysis and integrated ATP-dependent exonuclease digestion, which ensures selective removal of contaminating genomic DNA. Following digestion, BAC was then bound to QIAGEN Resin under appropriate low-salt and pH conditions. RNA, proteins, dyes, and low-molecular-weight impurities were removed by a medium-salt wash. BAC was eluted in high-salt buffer and then concentrated and desalted by isopropanol precipitation. DNA was then diluted in TE buffer, measured on Nanodrop and stored at 4° C.

2.22.2 Rescue of infectious virus

To recover the recombinant virus BSC40 cells were infected with 0.1 PFU per cell of the helper fowlpox virus (FPV) to provide the transcription system, as infection cannot be initiated with viral DNA alone. At 2 hpi cells were transfected with 1 µg of the VAC-BAC or VAC-BAC-ΔI3L plasmid using Fugene HD Transfection Reagent (Roche) according to the manufacturer's instructions. Transfected cells were incubated at 37° C until the plaques could be seen (5-7 days). Cells were then fixed in formaldehyde as outlined before.

Section 3.0

Results

3.1 Kinetics of infection in a variety of cell lines

Three different cell types were used in this study:

(1) normal human diploid fibroblasts (NHDFs);

(2) human embryonic kidney 293 cells (HEK-293);

(3) transformed monkey kidney cells (BSC40s).

The kinetics of VacV infection needed to be established in each cell type in order to perform further experiments.

Cells were cultured on 35 mm dishes and mock-infected or infected with VacV with multiplicity of infection (moi) 5. After indicated time post infection (8, 16 or 25 hours) cells were metabolically labeled with [^{35}S]methionine-cysteine for 1 h, and lysed in Laemmli buffer. Cell extracts were fractionated by SDS-PAGE and gels were dried and exposed to x-ray film at -80° C. First, comparison of transformed lines (HEK-293 and BSC40s) indicated similar kinetics in each cell line (Fig. 3.1.1). At 8 hours post infection (hpi) significant inhibition of cellular protein synthesis was observed, while more complete host shut-off and robust translation of late viral proteins was evident by 16 hpi in both cell lines. By 25 hpi the patterns of protein synthesis were unchanged but had declined in intensity, demonstrating that late phases of infection were reached by 16 hpi in these cells.
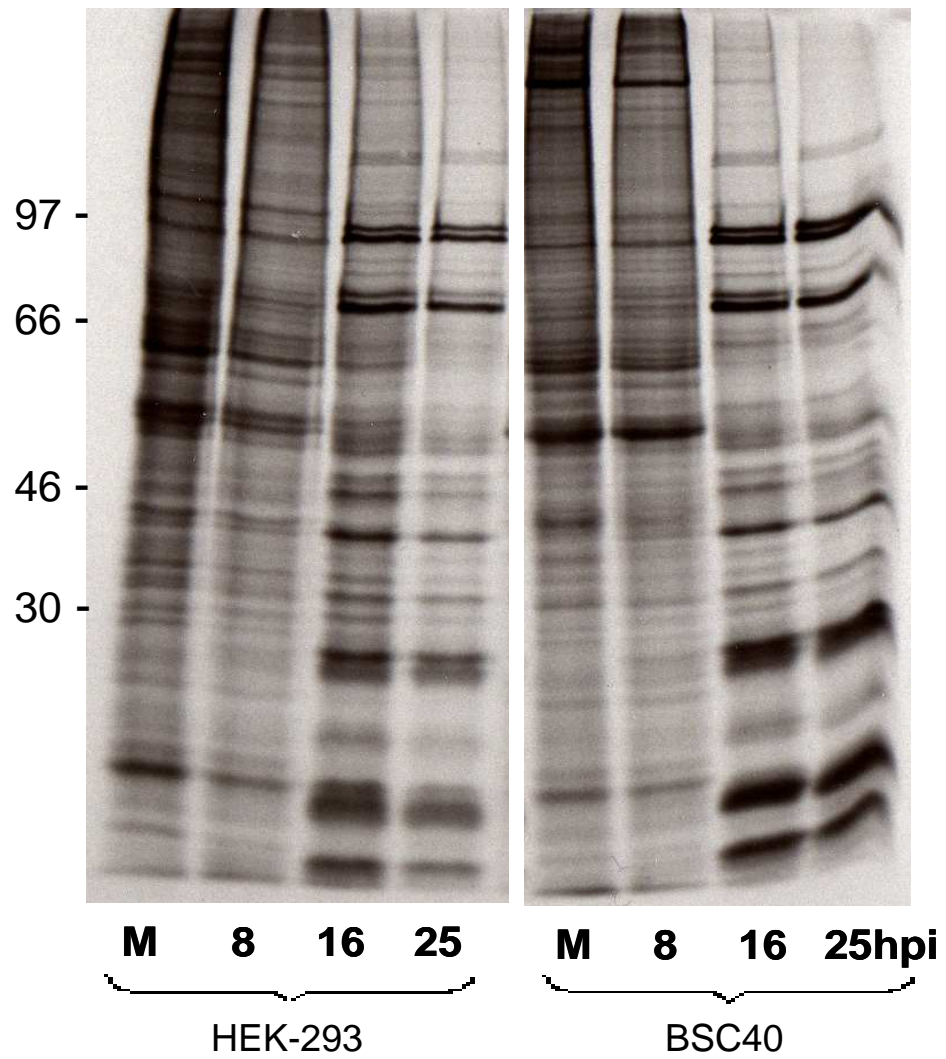
Figure 3.1.1 Autoradiograph illustrating the time-course of VacV protein synthesis in two transformed cell lines used in this study. Cells were metabolically labeled with [^{35}S]methionine-cysteine for 1 h prior to sampling. Molecular weight markers are indicated to the left. (M = mock)

The previous experiments were performed in transformed cells. However, to simulate the metabolic state of cells in the body more closely, we often use normal human diploid fibroblasts (NHDFs) and serum-starvation to growth-arrest these cells. This allows us to observe activation of signaling pathways and translation complexes that might be induced during viral infection, but also affects the kinetics of infection (Walsh *et al.*, 2008).

As such, cycling and serum-starved NHDFs were mock-infected or VacV-infected at moi 5. Extracts of cells metabolically labeled with [^{35}S]methionine-cysteine were made at 16 and 25 hpi, and analyzed as described above. In cycling NHDFs, late stage infection, as determined by host shut-off and viral protein synthesis patterns, were reached by 16hpi, similar to transformed lines. In contrast to cycling cells, in serum-starved NHDFs the highest level of viral protein synthesis was detected at 24-25 hpi (Fig. 3.1.2 a), while at 16 h host shut-off was incomplete and some intermediate protein synthesis remained detectable (marked by asterix). This indicates that reducing the cells metabolism by starvation extends the replication cycle of VacV. As can be seen in Fig. 3.1.2 b, western blotting showed that in serum-starved cells viral protein production reached the intermediate phase by 16 hpi with complete accumulation of the intermediate protein I3 (Fig. 3.1.2 c). However, while some structural proteins were produced, they continued to increase in abundance by 25 hpi, while others were only detected in 25 h but not 16 h samples.

The majority of further research was carried out using starved NHDFs infected for 16 or 24-25 hours, to analyze the middle or late phase of infection.
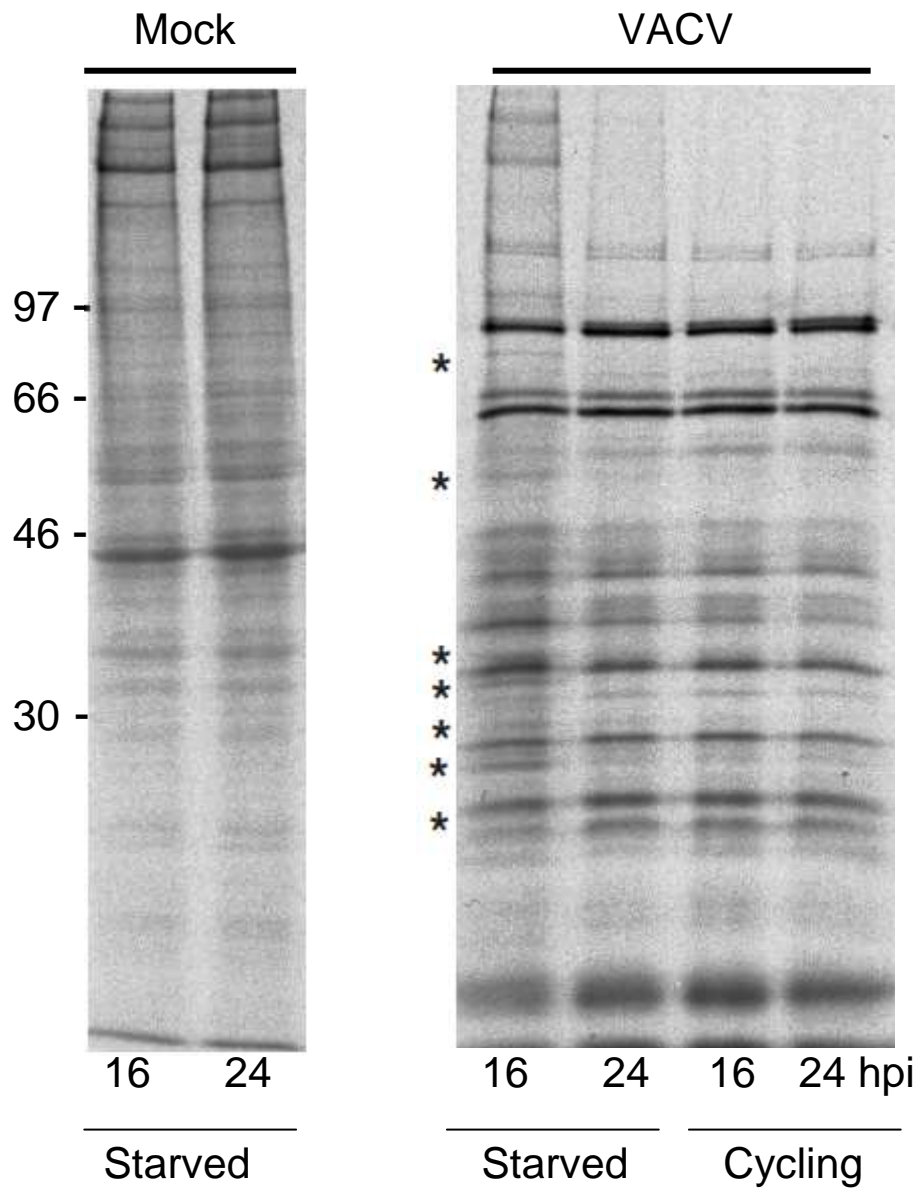
Figure 3.1.2 (a) Comparison of the kinetic of VacV infection in cycling and serum-starved NHDFs. Intermediate protein synthesis still detectable in serum-starved but not cycling cells at late stages of infection (16 hpi) are marked with asterix. Molecular weight markers are indicated to the left.
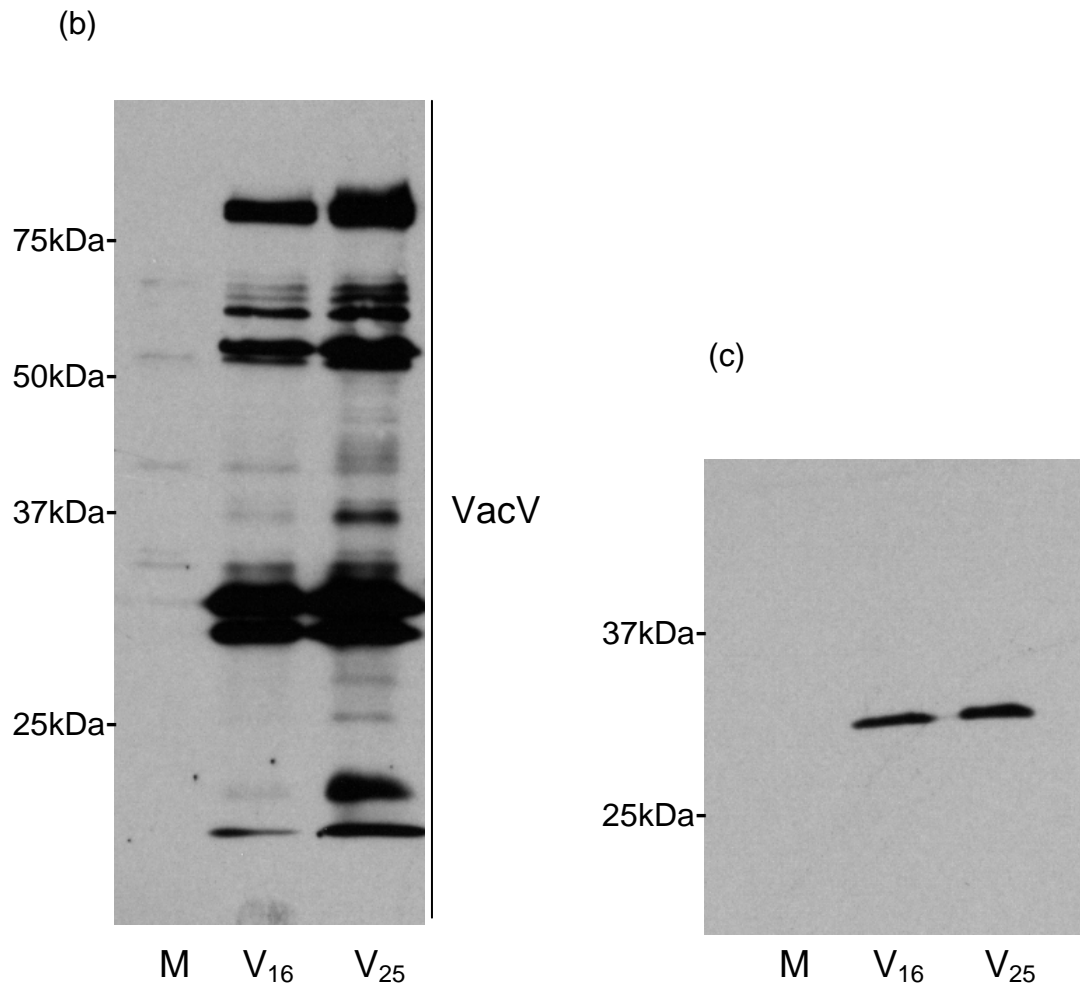
Figure 3.1.2 (b, c) Immunoblots illustrating the accumulation of total VacV proteins (b) and the intermediate protein I3 in serum-starved NHDFs (c) Molecular weight markers are indicated to the left. (M = mock, V_{16} = VacV-infected for 16 h, V_{25} = VacV-infected for 25 h)

3.2 Analysis of signaling and translation during vaccinia virus infection

3.2.1 Manipulation of the cellular PI3K pathway by vaccinia virus

It has recently been shown that VacV activates mTORC1 to phosphorylate 4E-BP1 (Walsh *et al.*, 2008). However, whether VacV activates mTORC1 directly or induces upstream signaling remained unknown so far. In this study we aimed to investigate the mechanism used by VacV to manipulate the PI3K/Akt/mTOR pathway that leads to the activation of mTORC1 and inhibition of the translational repressor 4E-BP1. To assign a role for the PI3 kinase in VacV translational strategies, the phosphorylation of its downstream effectors in the presence of specific inhibitors that block PI3K and mTORC1 (LY294002 and rapamycin, respectively) (Fig. 3.2.1) was evaluated.

Serum-starved normal human diploid fibroblasts (NHDFs) were pre-treated for 1 hour with equal volumes of the following inhibitors: dimethyl sulfoxide (DMSO) solvent control, 40 µM[3] LY294002 (LY), and 2 µM[4] rapamycin. Cells were then uninfected or infected with 10 PFU VacV, and phosphorylation of selected proteins was measured at 16 hpi by immunoblotting of whole cell extracts using specific antisera against phosphorylated forms of Akt (P-Akt) and ERK (P-ERK), or total forms of Akt (T-Akt), p70S6K and 4E-BP.

Interestingly, VacV caused increased phosphorylation of Akt in infected cells, while LY294002 completely blocked this process (Fig. 3.2.2). In addition, inhibitors did not affect the total level of Akt. The fold change (F.C.) in Akt phosphorylation was quantified by densitometry and averaged, and then presented relative to uninfected

---

[3] High concentration (40µM) of LY294002 was used because high doses of this drug were shown to inhibit both class I and class II of PI3 kinases, while low doses (2µM) inhibit only class I (Vlahos, 1994).
[4] High concentration (2µM) of rapamycin was used to make sure mTORC1 activity is completely inhibited. Concentrations are normally between 100-200 nM.

levels, arbitrarily set at 1. LY294002 also inhibited phosphorylation of mTOR downstream substrates: p70S6 kinase (p70S6K) and 4E-BP1, which are activated and phosphorylated in VacV-infected cells (Fig. 3.2.3). Similar effects of LY294002 were observed in uninfected, serum-starved NHDFs (not shown). Multiple phosphorylation of 4E-BP1 and p70S6K was detected by mobility shift analysis with high-percentage SDS-PAGE gels (hyper- and hypophosphorylated forms are indicated). The mTORC1 inhibitor, rapamycin, blocked VacV-induced phosphorylation of p70S6K and 4E-BP1, as reported previously (Walsh *et al.*, 2008), but did not reduce Akt phosphorylation which lies upstream of mTORC1 (Fig. 3.2.3).

The abundance of eIF4E, used as a loading control, remained unaltered and inhibitors did not significantly affect phosphorylation of ERK, a kinase outside of the PI3K pathway which phosphorylates the eIF4E kinase MNK1, and is known to be activated by VacV. This indicates the specificity of PI3K and mTOR inhibitors. The fold change (F.C.) in ERK phosphorylation was quantified by densitometry and averaged, and then presented relative to uninfected levels, arbitrarily set at 1 (Fig. 3.2.4).

These results reveal the importance of the host PI3 kinase in VacV-induced downstream signaling to mTORC1 and its substrates, 4E-BP1 and p70S6K. Therefore, we further examined the impact of PI3K inhibition on the formation of eIF4F complexes.
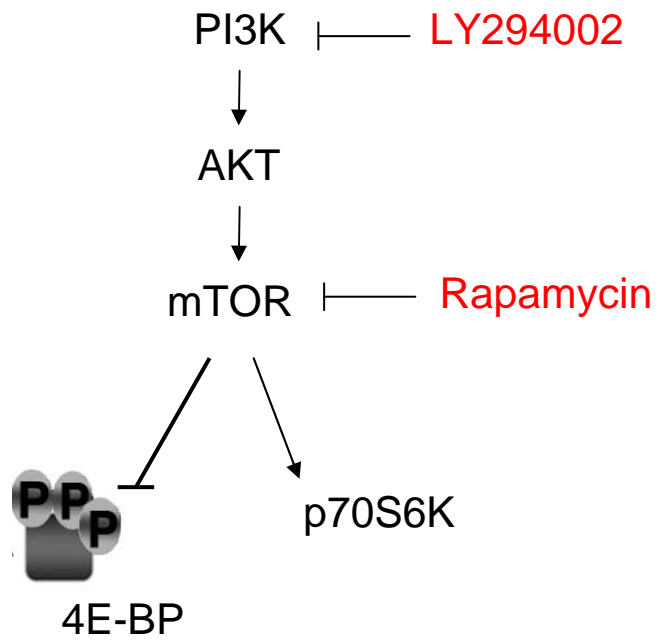
Figure 3.2.1 Simplistic PI3K pathway including key factors involved and points at which inhibitors function. T-bars represent suppression. Circled P's represent phosphorylation events.
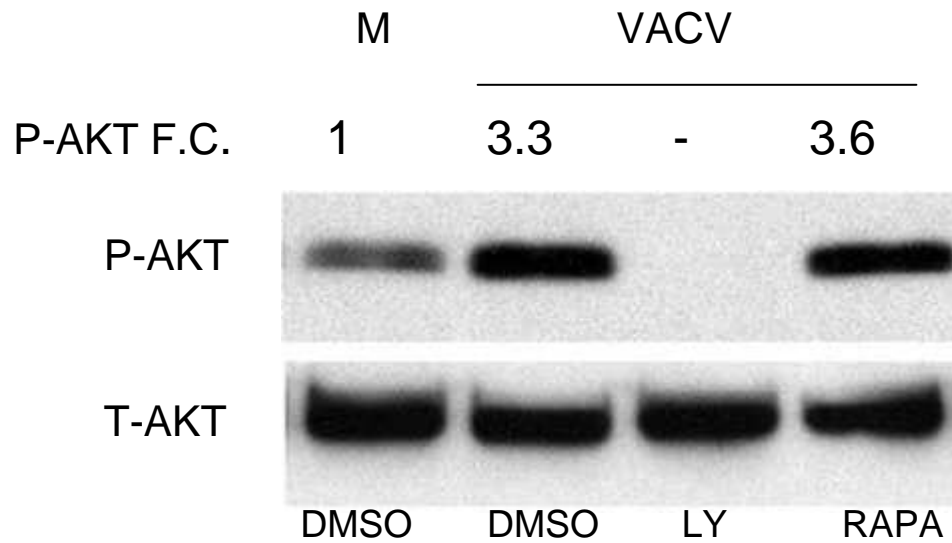
Figure 3.2.2 (a) Western blot analysis of AKT phosphorylation in mock (M) and VacV-infected cells (VACV) in a presence of indicated inhibitors. (F.C.= fold change measured by densitometry; LY = LY294002; Rapa = rapamycin)
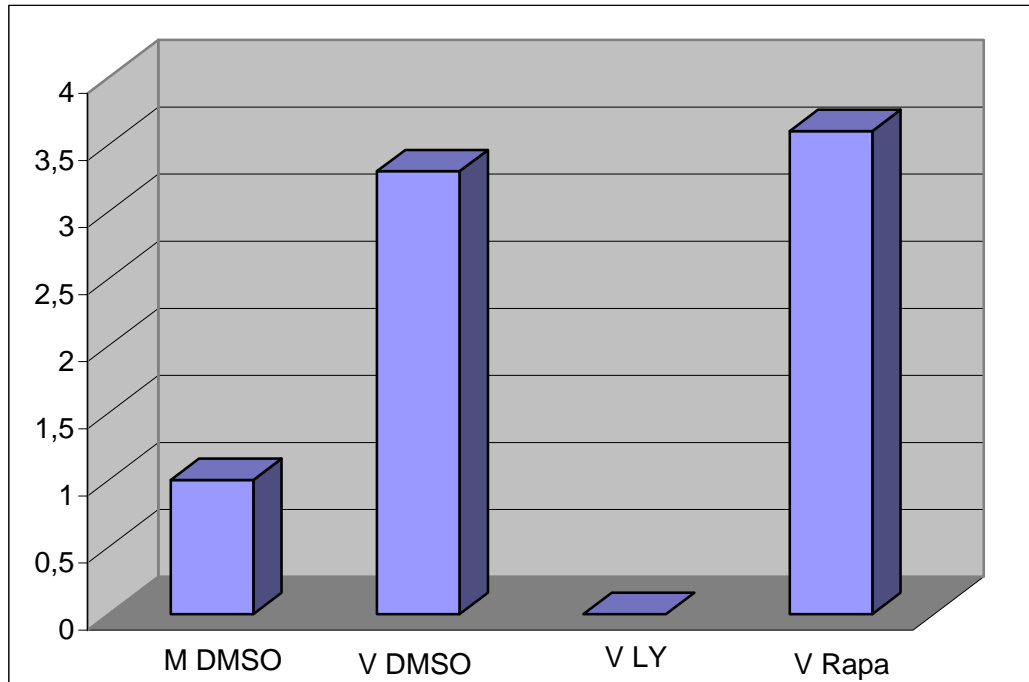

Figure 3.2.2 (b) Densitometry analysis of AKT phosphorylation in mock and VacV-infected cells in the presence of indicated inhibitors. (M = mock; V = VacV-infected; LY = LY294002, Rapa = rapamycin)
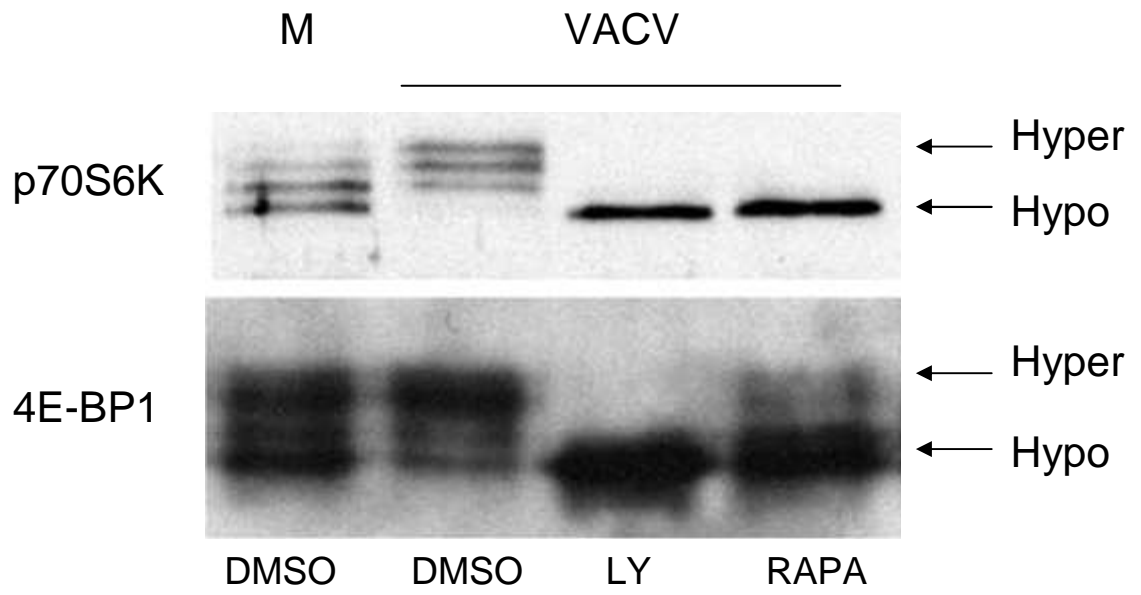
Figure 3.2.3 Immunoblot illustrating the LY294002 and rapamycin effects on mTOR's substrates phosphorylation in mock (M) and VacV-infected cells. (LY = LY294002, Rapa = rapamycin)
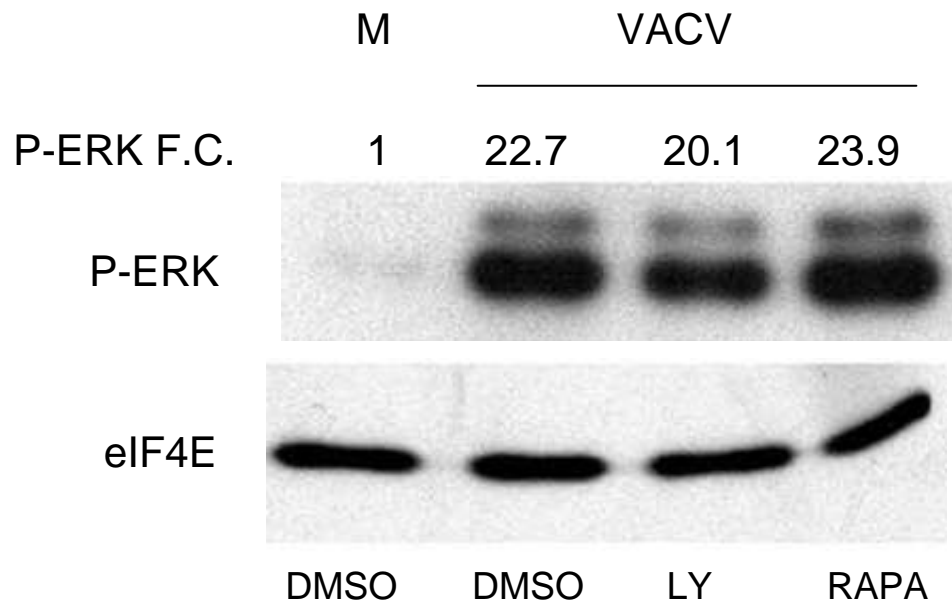
Figure 3.2.4 (a) Immunoblot illustrating phosphorylation of ERK in mock (M) and VacV-infected cells in the presence of indicated inhibitors. (F.C. = fold change measured by densitometry; LY = LY294002; Rapa = rapamycin)
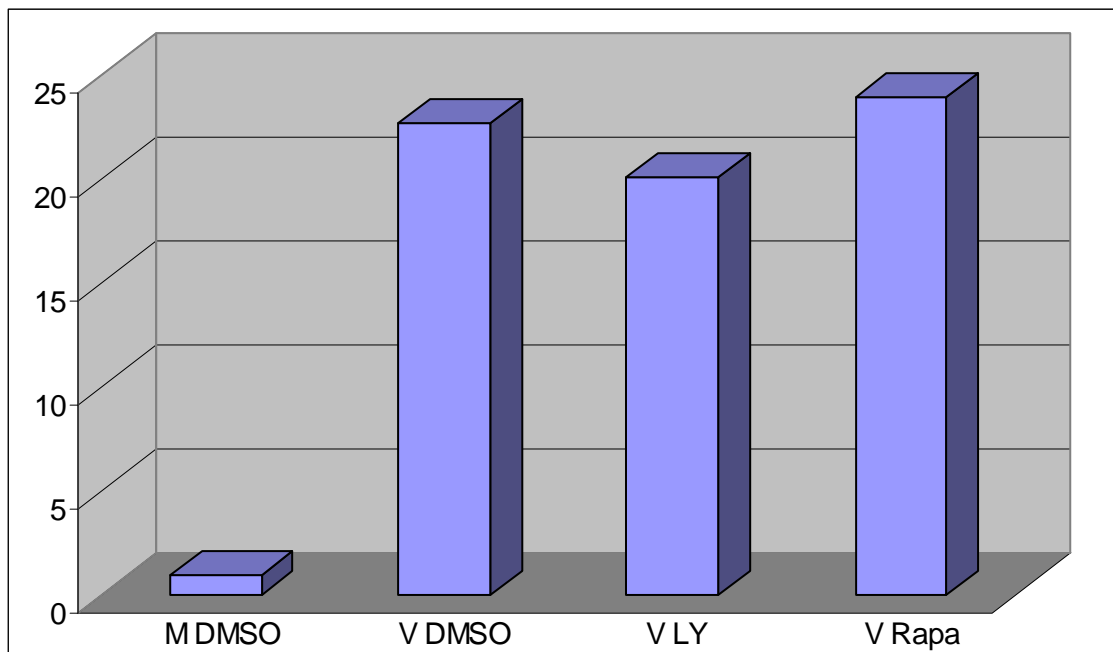

Figure 3.2.4 (b) Densitometry analysis of ERK phosphorylation in mock and VacV-infected cells in the presence of indicated inhibitors. (M = mock; V = VacV-infected; LY = LY294002, Rapa = rapamycin)

3.2.2 The effect of LY294002 and rapamycin on eIF4F complex formation in VacV-infected cells

3.2.2.1 The levels and binding of eIF4G, eIF4E and 4E-BP1

To examine the effect of LY294002 and rapamycin on the formation of eIF4F complex during VacV-infection, 7-methylguanosine cap binding assays were carried out. Serum-starved NHDFs were uninfected or infected with 10 PFU VacV in the presence of DMSO, 40 µM LY294002 or 2 µM rapamycin, and 16 hpi the soluble cell extract was made. eIF4E was recovered from the lysate by 7-methylguanosine GTP batch chromatography, as described in Section 2.2.8, and samples were fractionated by SDS-page and probed with antisera towards eIF4E, eIF4G and 4E-BP1 to establish the composition of eIF4E-bound complexes in each sample.

In mock-infected cells both eIF4G and 4E-BP1 naturally bound to individual eIF4E molecules and were recovered on cap resin. VacV significantly increased the amount of eIF4G in eIF4E-bound complexes and blocked the binding of 4E-BP1, as expected and reported previously (Walsh *et al.*, 2008). However, inhibition of PI3K resulted in a strong recruitment of 4E-BP1 to eIF4E and inhibition of eIF4G binding (Fig. 3.2.5 a). In addition, rapamycin only slightly affected binding of eIF4G, but did prevent 4E-BP1 phosphorylation by VacV, which can be observed in input samples as well. The levels of eIF4E remained constant. The fold change (F.C.) in eIF4G and 4E-BP1 binding was quantified by densitometry and averaged, and then presented relative to uninfected levels, arbitrarily set at 1 (Fig. 3.2.5 b, c).

These results demonstrated that by 16 hpi of serum-starved NHDFs, VacV increased levels of eIF4F in a PI3K-dependent manner.
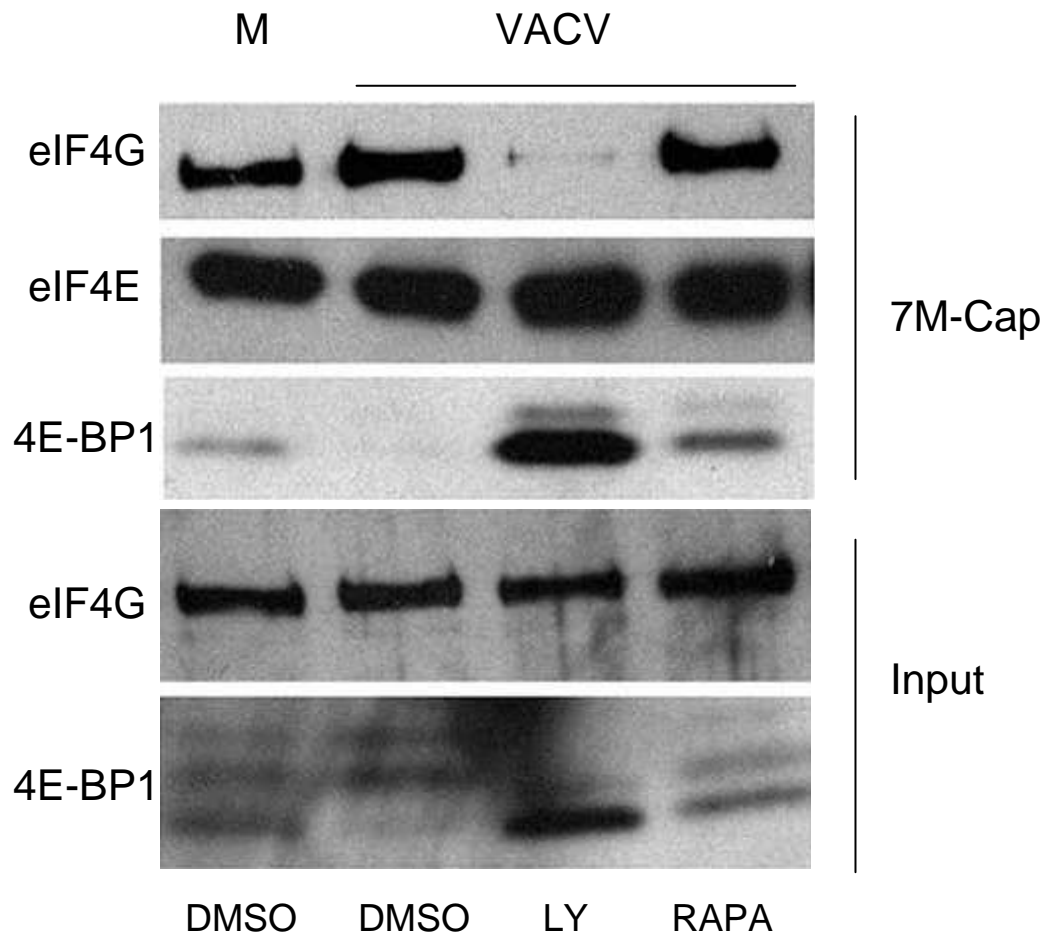
Figure 3.2.5 (a) Immunoblot illustrating eIF4F complex formation in mock (M) and VacV-infected cells in the presence of indicated inhibitors. (LY = LY294002, Rapa = rapamycin)
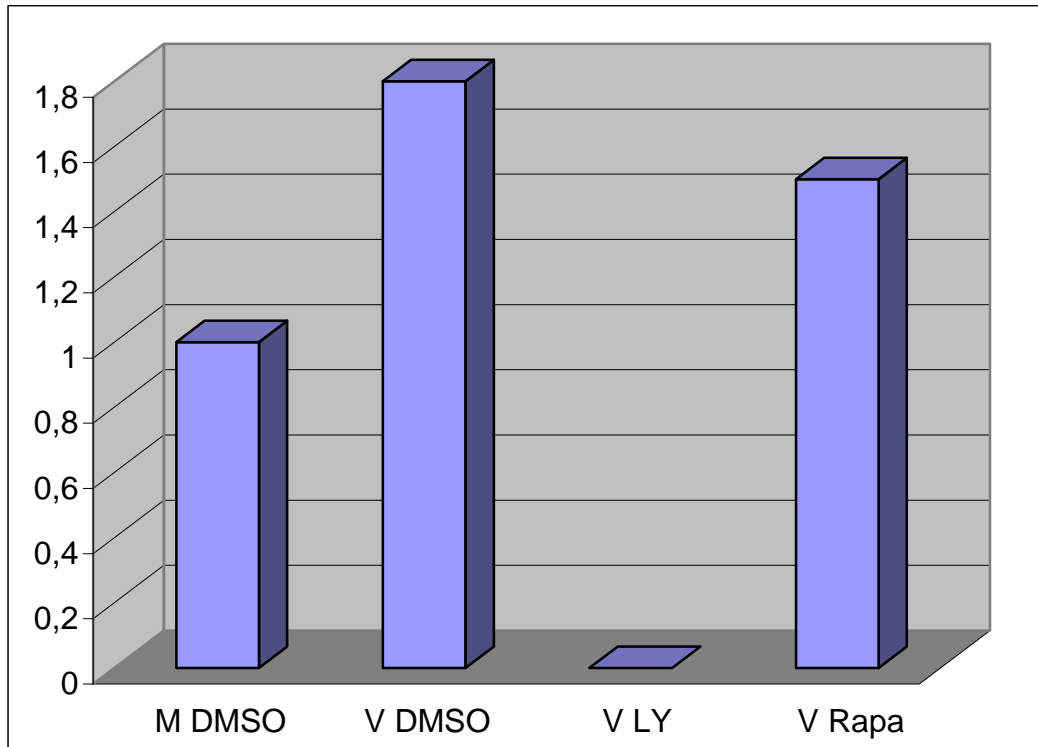
Figure 3.2.5 (b) Densitometry analysis of eIF4G binding to eIF4E in mock and VacV-infected cells in the presence of indicated inhibitors**.** (M = mock; V = VacV-infected; LY = LY294002, Rapa = rapamycin)
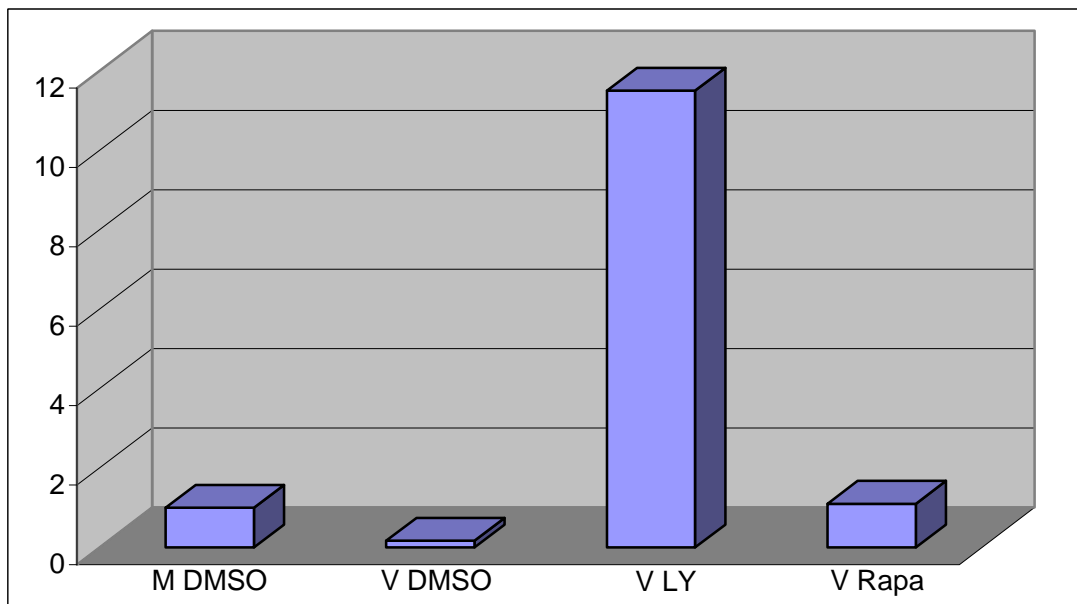
Figure 3.2.5 (c) Densitometry analysis of 4E-BP1 binding to eIF4E in mock and VacV-infected cells in the presence of indicated inhibitors**.** (M = mock; V = VacV-infected; LY = LY294002, Rapa = rapamycin)

3.2.2.2 The effects of inhibitors on the abundance of 4E-BP1 in VacV-infected NHDFs

VacV infection has been shown to decrease the abundance of 4E-BP1 in a rapamycin-sensitive manner (Walsh *et al.*, 2008). We therefore examined effects of PI3K inhibition on 4E-BP1 abundance in infected cells.

The total levels of 4E-BP1 in the samples described in the previous section were analyzed by immunoblotting using low-percentage (7.5 %) gel and with anti-4E-BP1 antiserum. Low percentage gel was used to prevent the resolution of multiple phosphorylated 4E-BP1 isoforms, and monitor the steady-state levels of 4E-BP1. This experiment demonstrated that in fact rapamycin blocked 4E-BP1 degradation in VacV-infected cells; however, LY294002 dramatically increased the abundance of this repressor bringing it to a higher level than observed in mock-infected cells (Fig. 3.2.6 a). The fold change (F.C.) of 4E-BP1 levels was quantified by densitometry and averaged, and then presented relative to uninfected levels, arbitrarily set at 1 (Fig. 3.2.6 b).
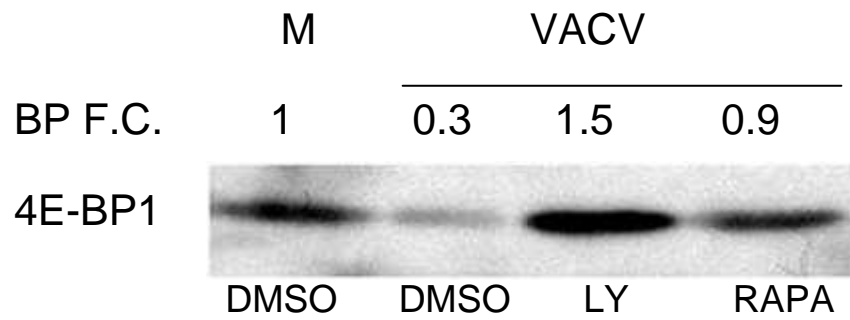
**Figure 3.2.6 (a)** Immunoblot illustrating the total 4E-BP1 levels in mock (M) and VacV-infected cells in the presence of indicated inhibitors. (F.C. = fold change measured by densitometry; LY = LY294002, Rapa = rapamycin)
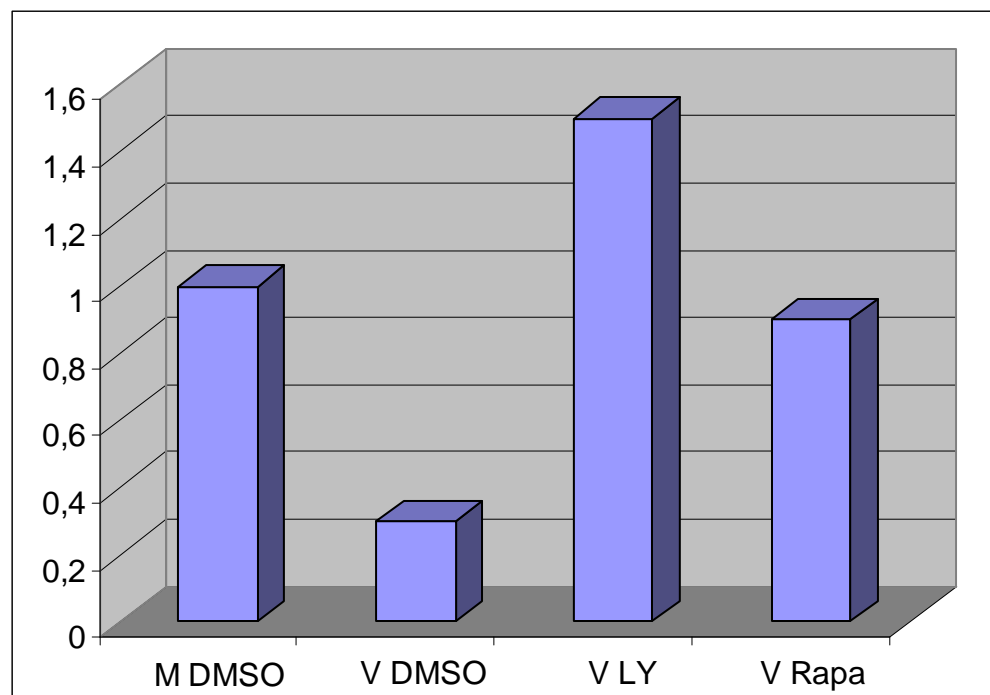

Figure 3.2.6 (b) Densitometry analysis of 4E-BP1 accumulation in VacV-infected cells in the presence of indicated inhibitors. (M = mock; V = VacV-infected; LY = LY294002, Rapa = rapamycin)

3.2.2.3 The effect of PI3K and mTORC1 inhibitors on eIF4E phosphorylation in VacV-infected cells

Since the PI3K inhibitor was found to significantly affect eIF4G association with eIF4E, the effect of LY294002 on eIF4E phosphorylation was examined. eIF4E is phosphorylated as part of eIF4F complex by eIF4G-associated kinase Mnk1/2, and this process is mediated by the MAPK/Erk signaling pathway (Wang *et al.*, 1998; Scheper *et al.*, 2001). Although the role of eIF4E phosphorylation in cellular translation has not been fully explored, it appears to play an important role in VacV protein synthesis. Walsh *et al.* (2008) demonstrated that inhibition of Mnk1 by CGP57380 significantly decreased VacV replication. Here, we examined if inhibition of PI3 kinase by LY294002 also impairs eIF4E phosphorylation.

Serum-starved NHDFs were pre-treated with LY294002 or rapamycin for 1 hour, then mock or VacV-infected at moi 10, and lysed in Laemmli buffer at 16 hpi. The lysates were resolved by isoelectric focusing to separate the phosphorylated and unphosphorylated forms of eIF4E and analyzed by immunoblotting using anti-eIF4E antiserum. As shown in Fig. 3.2.7, VacV infection enhanced phosphorylation of eIF4E, whereas LY294002 significantly reduced this event due to the collapse of eIF4F complexes in which eIF4E phosphorylation occurs. Rapamycin did not significantly affect eIF4E phosphorylation.
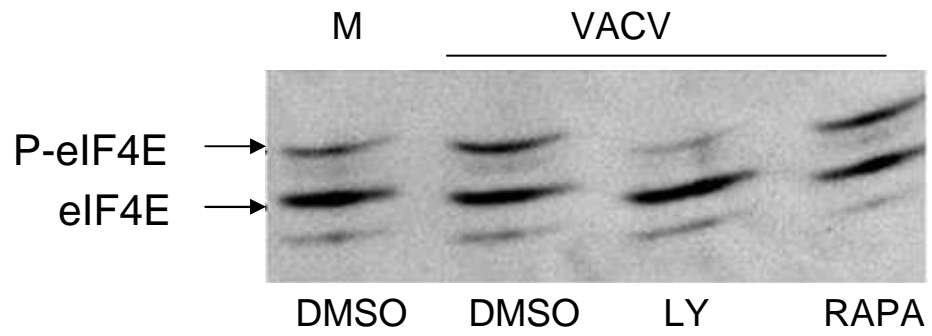
Figure 3.2.7 Immunoblot illustrating eIF4E phosphorylation in mock (M) and VacV-infected cells in the presence of indicated inhibitors. Migration of phosphorylated (P-eIF4E) and hypophosphrylated (eIF4E) eIF4E is indicated to the left. (LY = LY294002, Rapa = rapamycin)

3.2.2.4 The effect of the PI3K and mTORC1 inhibitors on eIF4G phosphorylation in VacV-infected cells

To investigate if other factors might be involved in eIF4F disruption caused by LY294002 in VacV-infected cells, the phosphorylation of eIF4G was examined. eIF4G is thought to be phosphorylated by a number of kinases including mTORC1 (Raught *et al.*, 2000; Ling *et al.*, 2005). Cell extracts were analyzed by western blotting using antisera against the total (T-eIF4G) or phosphorylated (P-eIF4G) forms of eIF4G. The results demonstrated that while the total levels of eIF4G remained constant, VacV evidently increased the accumulation of phosphorylated eIF4G (Fig. 3.2.8). Treating the cells with mTORC1 inhibitor prevented this stimulation maintaining phosphorylation at basal uninfected levels, whereas inhibition of PI3 kinase resulted in only modestly decreased eIF4G phosphorylation compared to uninfected levels. As such, dramatic loss of eIF4G phosphorylation did not occur specifically in LY294002-treated samples and is unlikely to contribute to the collapse of eIF4F.
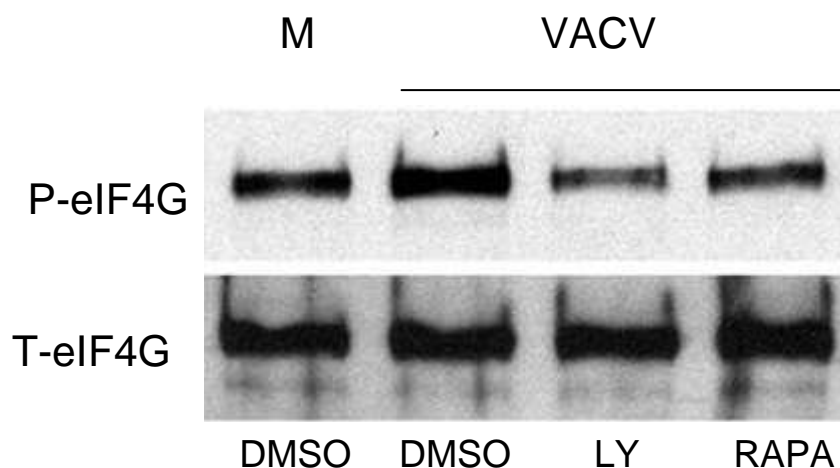

Figure 3.2.8 Immunoblot illustrating eIF4G phosphorylation in mock and VacV-infected cells in the presence of indicated inhibitors. (LY = LY294002, Rapa = rapamycin)

3.2.3 The effect of LY294002 and rapamycin on cellular stress response in VacV-infected cells

As mentioned before (section 1.2.2), initiation factor eIF2 catalyses Met-tRNA$_f$ binding to the 40S ribosomal subunit during the formation of the ternary complex. eIF2 consists of three subunits: α, β, and γ. Phosphorylation of the smallest (α) subunit can be caused by physiological stresses such as heat shock or virus infection, and leads to disruption in overall protein synthesis or cell death by apoptosis (Clemens, 2001). Therefore, increased phosphorylation of eIF2α is considered one of the indicators of cellular stress and/or apoptosis. Another such an indicator is thought to be cleavage of eIF4G, which is an early event in apoptosis and results in the production of modified eIF4F complex containing eIF4E, eIF4A, and the central fragment of eIF4G instead of the full length (Morley, 2001).

In the previous experiments no changes in eIF4G abundance were observed, suggesting that LY294002 was not inducing a cellular stress response. To further determine whether or not the observed LY294002 effect involves the cellular stress responses, the phosphorylation of eIF2α was examined. Serum-starved NHDFs were infected with 10 PFU VacV per cell in the presence of DMSO, LY294002 or rapamycin. At 16 hpi cells were lysed in Laemmli buffer and analyzed by immunoblotting using antisera against the phosphorylated forms of eIF2*alpha* (P- eIF2α). The results, illustrated in Fig. 3.2.9, did not show noticeable changes in the total eIF2α phosphorylation, demonstrating that the observed effects of LY294002 and rapamycin seem not to be a result of cellular stress responses.
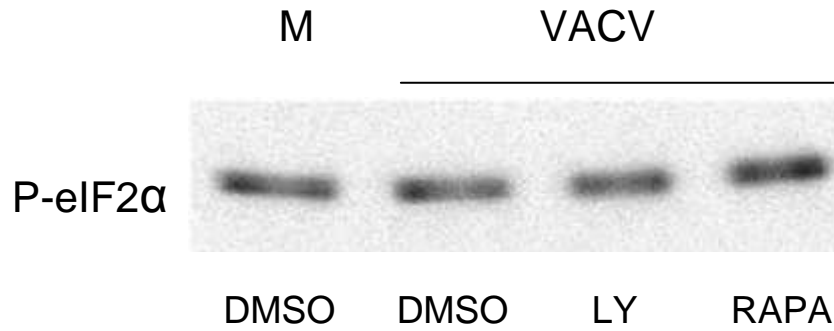
Figure 3.2.9 Immunoblot illustrating eIF2α phosphorylation in mock (M) and VacV-infected cells in the presence of indicated inhibitors. (LY = LY294002, RAPA = rapamycin)

Furthermore, looking at cells morphology in a phase contrast microscope confirmed that cells were indeed infected characterized by long cellular protrusions and cell-cell detachment. However, LY294002-treated cultures actually exhibited a reduced cytopathic effect compared to cells treated with DMSO (Fig. 3.2.10). This suggested that LY294002 protected infected cells from morphological changes caused by the virus, and that VacV could not carry out its normal replication cycle in cells where PI3 kinase was inhibited. In contrast, rapamycin did not protect the cells.
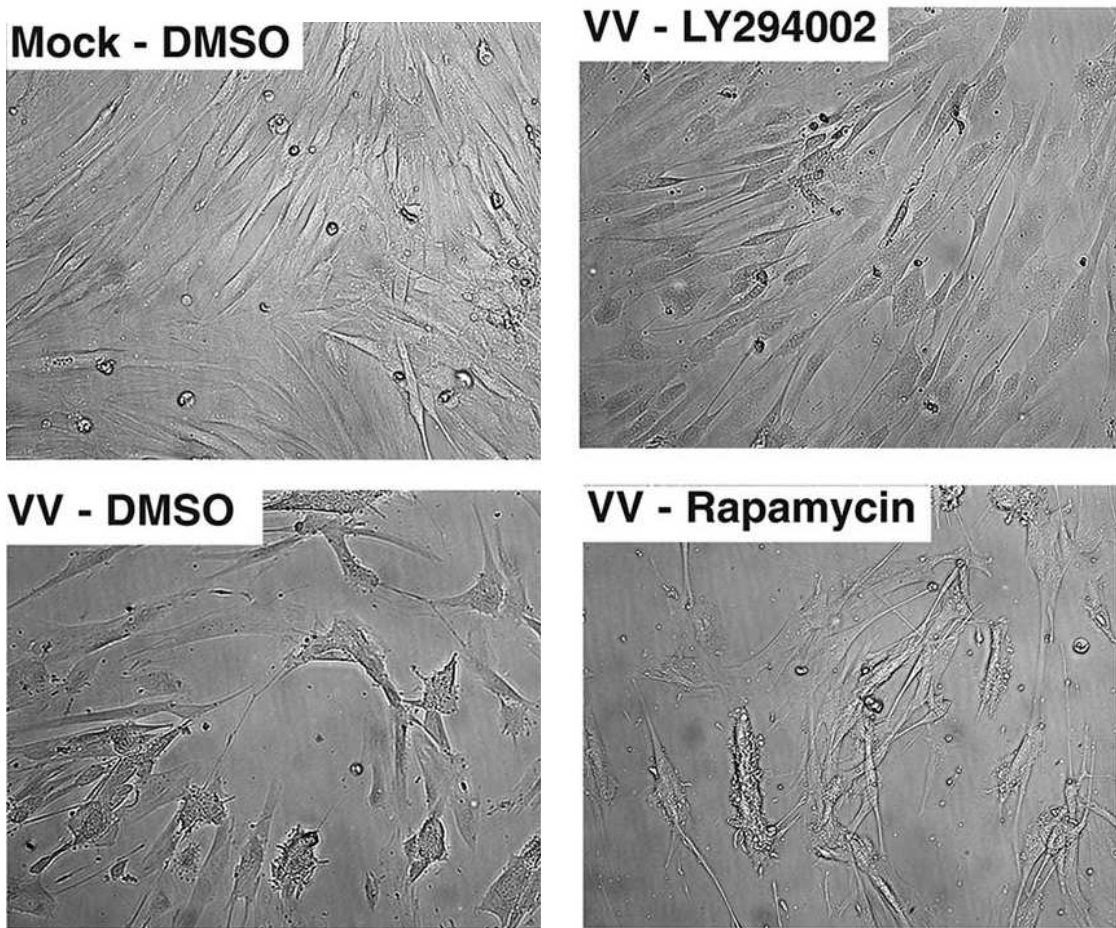
Figure 3.2.10 Phase contrast microscopy photographs of mock and VacV-infected serum-starved NHDFs treated with LY294002 or rapamycin.

3.2.4   The effect of LY294002 and rapamycin on VacV protein synthesis

Next, the effect of PI3K and mTORC1 inhibitors on total vaccinia virus protein synthesis was examined. Serum-starved NHDFs were mock- or VacV-infected in the presence of inhibitors, and at 16 hpi metabolically labeled with [^{35}S] methionine/cysteine for 1 hour. Then cells were lysed in Laemmli buffer and fractionated by SDS-PAGE; the gels were dried and exposed to X-ray film at -80° C or analyzed by immnoblotting using antiserum against vaccinia virus. As observed in Figure 3.2.11, the inhibition of PI3K had a huge effect on the protein synthesis in infected cells. The translational rates were significantly suppressed even at high input doses of the virus, suggesting that viral proteins could not be efficiently produced in the presence of LY294002, while rapamycin did not affect protein synthesis. Immunoblotting of the same samples using antiserum against VacV confirmed the inhibition of protein production by LY294002.
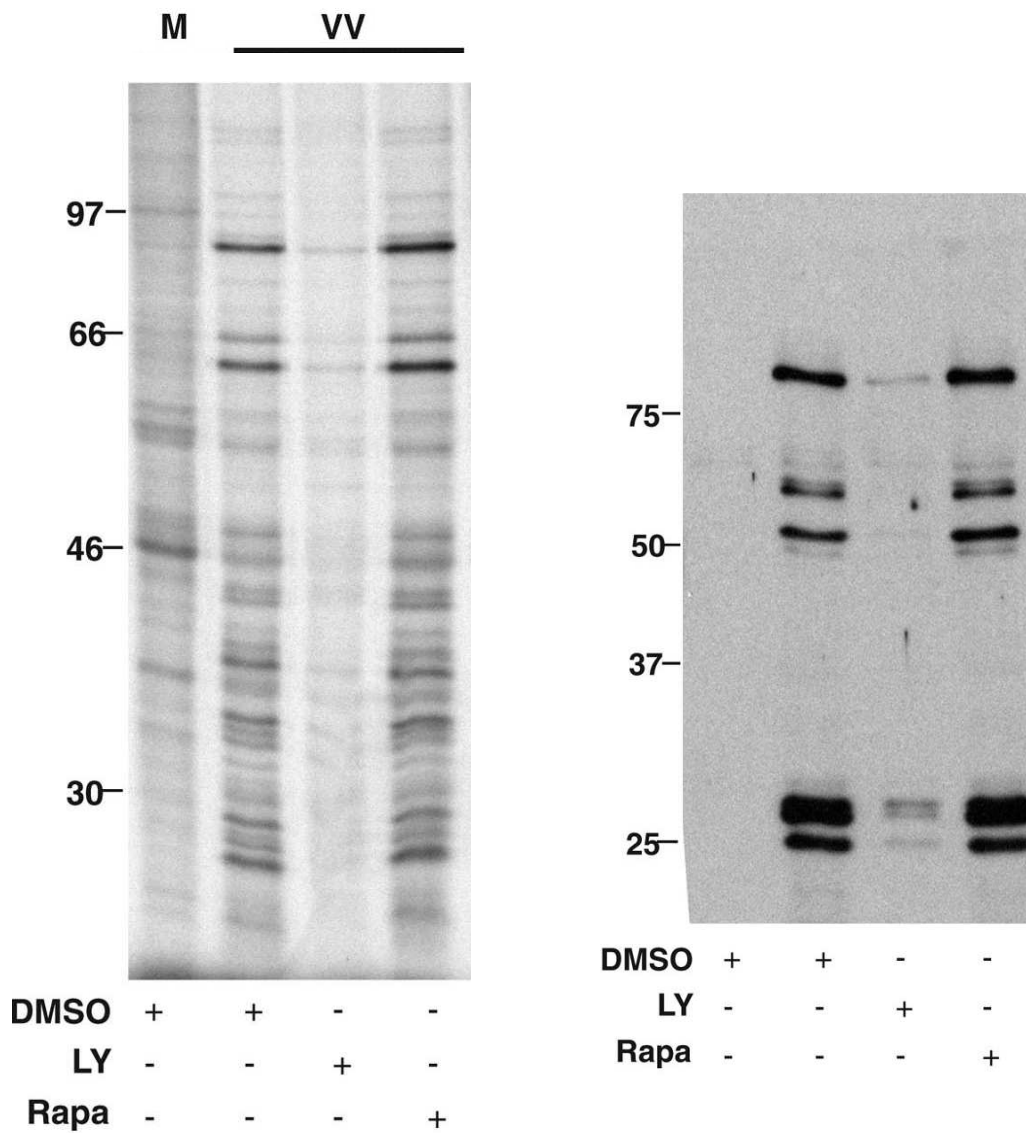
Figure 3.2.11 The effect of LY294002 and rapamycin on VacV translational rates. Growth-arrested NHDFs were mock or VacV-infected in the presence of DMSO, LY294002 or rapamycin. Cells were metabolically labeled with [^{35}S]methionine-cysteine, then samples were resolved by SDS-PAGE and exposed to x-ray film (on the left) or analyzed by immunoblotting (on the right).

3.2.5 The LY294002 effect on the production of infectious virus

We then examined the production of infectious virus in cells treated with inhibitors. 6×10^5 NHDFs were infected with 10 PFU VacV per cell in the presence of DMSO, rapamycin or LY294002, and at 18 hpi the virus was harvested by repeated freeze/thaw cycles to disrupt cellular membranes and release the virus. Infectious virus was measured by diluting the lysates and infecting BSC40 cells. The virus titer was quantified by plaque assay and illustrated on the graph (Fig. 3.2.12). LY294002 clearly reduced the production of infectious virus up to 48-fold, which again confirmed the importance of PI3 kinase in VacV replication. Similar to the previous results, rapamycin did not affect VacV life cycle significantly, reducing viral titers by only 3-fold. The assay was repeated several times giving comparable results each time.
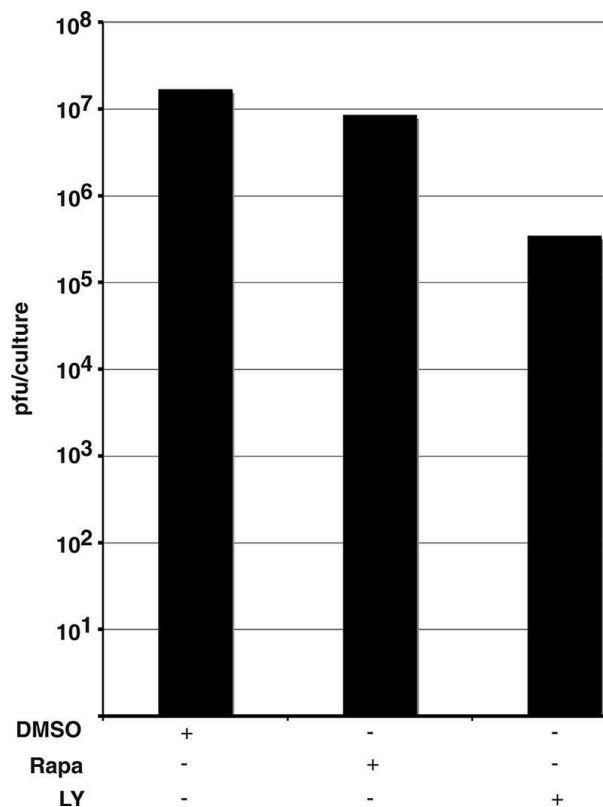

Figure 3.2.12 Titration of infectious virus production in the presence of DMSO, LY294002 (LY) or rapamycin (Rapa).

117

3.2.6   Investigation of apoptosis in LY294002-treated cells infected with VacV

After publishing the results described above (Zaborowska and Walsh, 2009), a subsequent paper showed apoptotic effects of LY294002 in mouse A31 cell line infected with vaccinia or cowpox virus (Soares *et al.*, 2009). As we had used serum-starved human cells, we then examined whether apoptosis occurred in other cell types treated with this PI3K inhibitor.

In our lab we had noticed before that the Akt inhibitor, Akt I, induces extensive apoptosis in human cells. This served as a control for detection of apoptosis in cells treated with LY294002. Three different cell lines including normal human cells (NHDFs), transformed human cells (HEK-293) and transformed monkey cells (BSC40s) were pretreated with DMSO, LY294002 or Akt inhibitor (Akti) for one hour, and then mock-infected or infected with VacV. The next day cells morphology was analyzed by phase microscopy and photographed (Fig. 3.2.13 a-c). Examination of the images clearly shows that cells treated with Akt inhibitor underwent apoptosis in all mock- and VacV-infected lines. In contrast, the PI3K inhibitor protected cells from morphological changes that suggested apoptotic death. The results were equal in all three analyzed cell lines, normal and transformed human cells and transformed monkey cells, suggesting that apoptosis caused by LY294002 in VacV-infected cells described by Soares *et al.* (2009) is specific only for certain cell types such as those derived from mice.
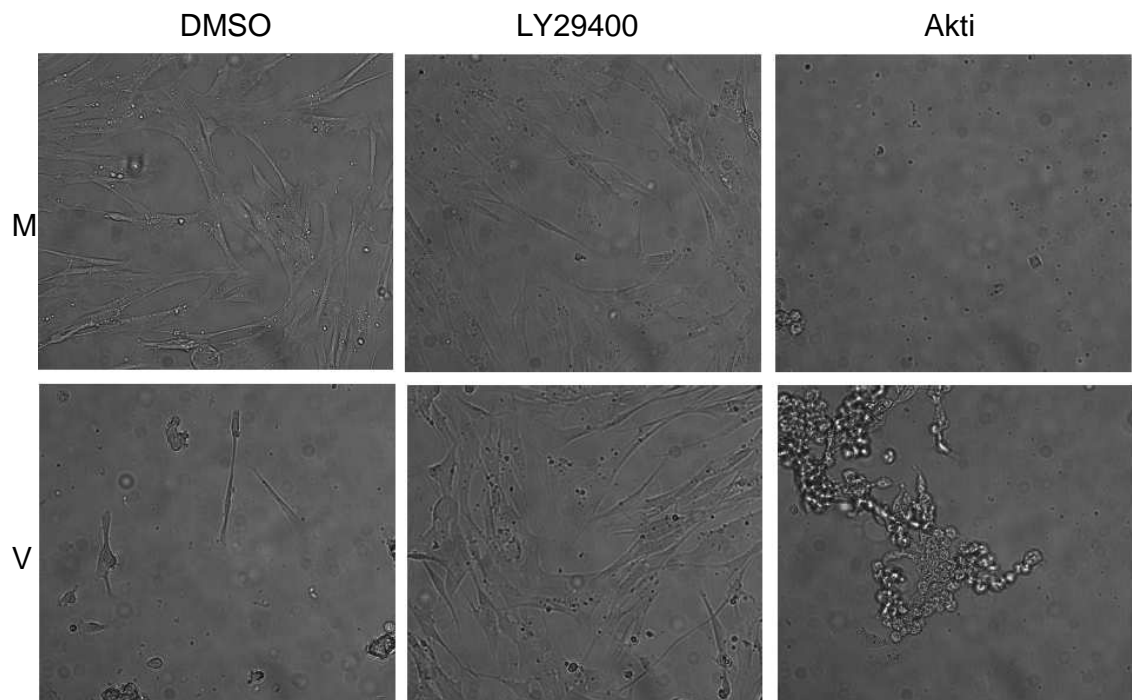
Figure 3.2.13 (a) Phase contrast microscopy photographs of mock (M) and VacV-infected (V) cycling NHDFs treated with DMSO, LY294002 and Akti.

|	DMSO	LY29400	Akti
M			
V			
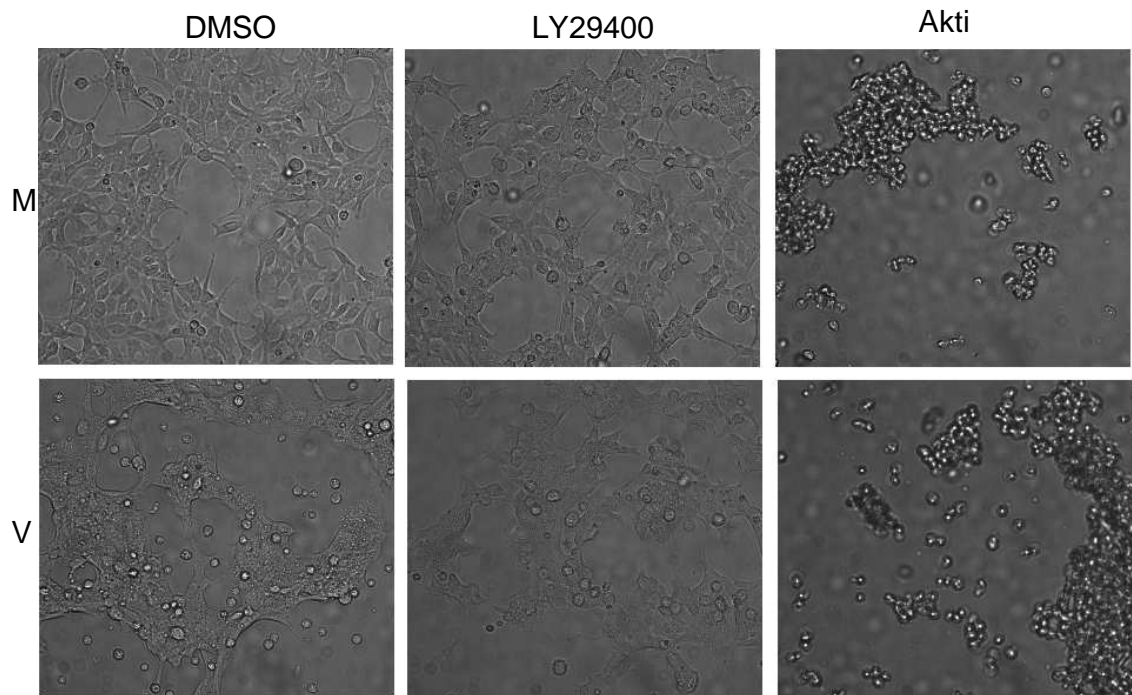
Figure 3.2.13 (b) Phase contrast microscopy photographs of mock (M) and VacV-infected (V) HEK-293 cells treated with DMSO, LY294002 and Akti.
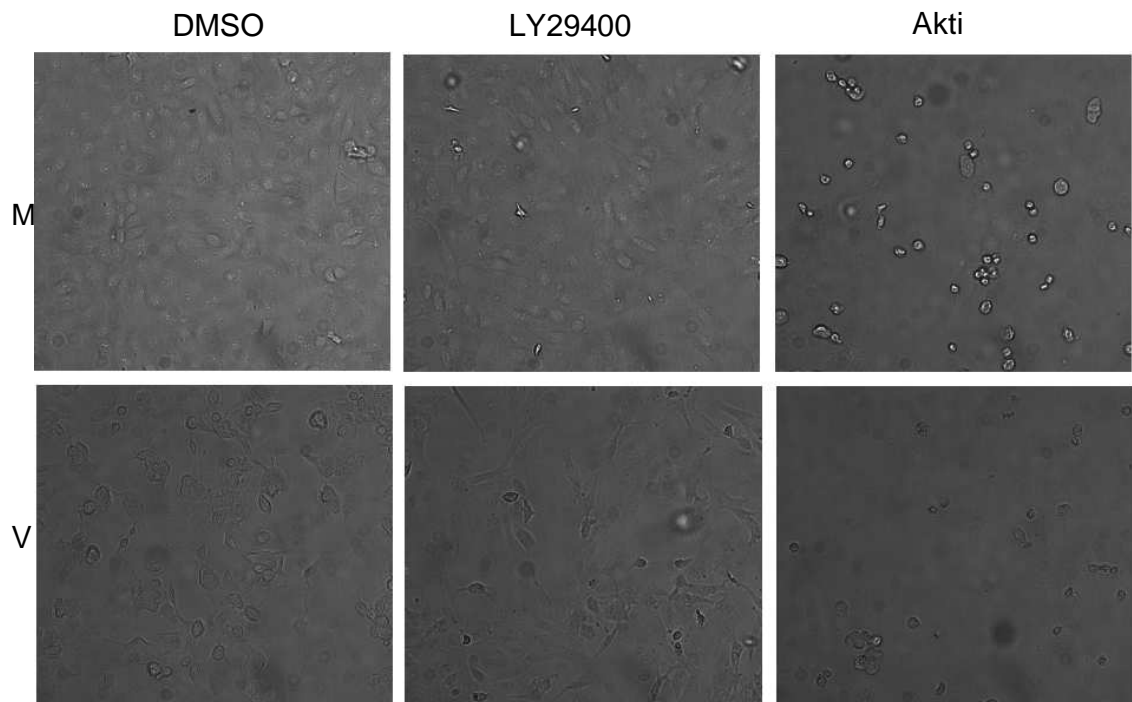
Figure 3.2.13 (c) Phase contrast microscopy photographs of mock (M) and VacV-infected (V) BSC40 cells treated with DMSO, LY294002 and Akti.

To examine the effect of the inhibitors, LY294002 and Akti on total VacV protein production, HEK-293 cells were pretreated with the inhibitors for 1 hour before infection with VacV. At 16 hpi cell lysates were fractionated on SDS-PAGE gel and probed for expression of viral genes by western blot analysis using antibodies against VacV proteins. As shown in Fig. 3.2.14, the VacV protein levels were reduced by LY294002, as observed in serum-starved NHDFs, while in the presence of Akti neither cellular nor viral proteins were detected suggesting that virus replication could not take place, most likely on account of the cells death. In addition, LY294002 blocked Akt phosphorylation demonstrating that the inhibitor was effective (Fig. 3.2.14).

Finally, the influence of LY294002 and Akti on PARP, an indicator of apoptosis, was examined. PARP (Poly [ADP-ribose] polymerase) is one of the targets for caspase-3 and caspase-7, the execution caspases that play essential roles in apoptosis. Once PARP and other substrates are cleaved by caspases, the cytoplasmic endonucleases are activated leading to degradation of nuclear material and cytoskeletal proteins (Elmore, 2007).

The samples described above were fractionated on SDS-PAGE gel and analyzed by immunoblotting against PARP and Caspase-7. As shown in figure 3.2.14, LY294002 did not cause PARP cleavage or caspase-7 processing in mock- or VacV-infected cells; while inhibition of Akt clearly resulted in PARP cleavage and apoptotic death of both mock-infected and VacV-infected cells.

These results demonstrated that inhibition of PI3K, as contrasted with the effects of Akti, does not cause apoptosis in a number of different cell types infected with vaccinia virus.
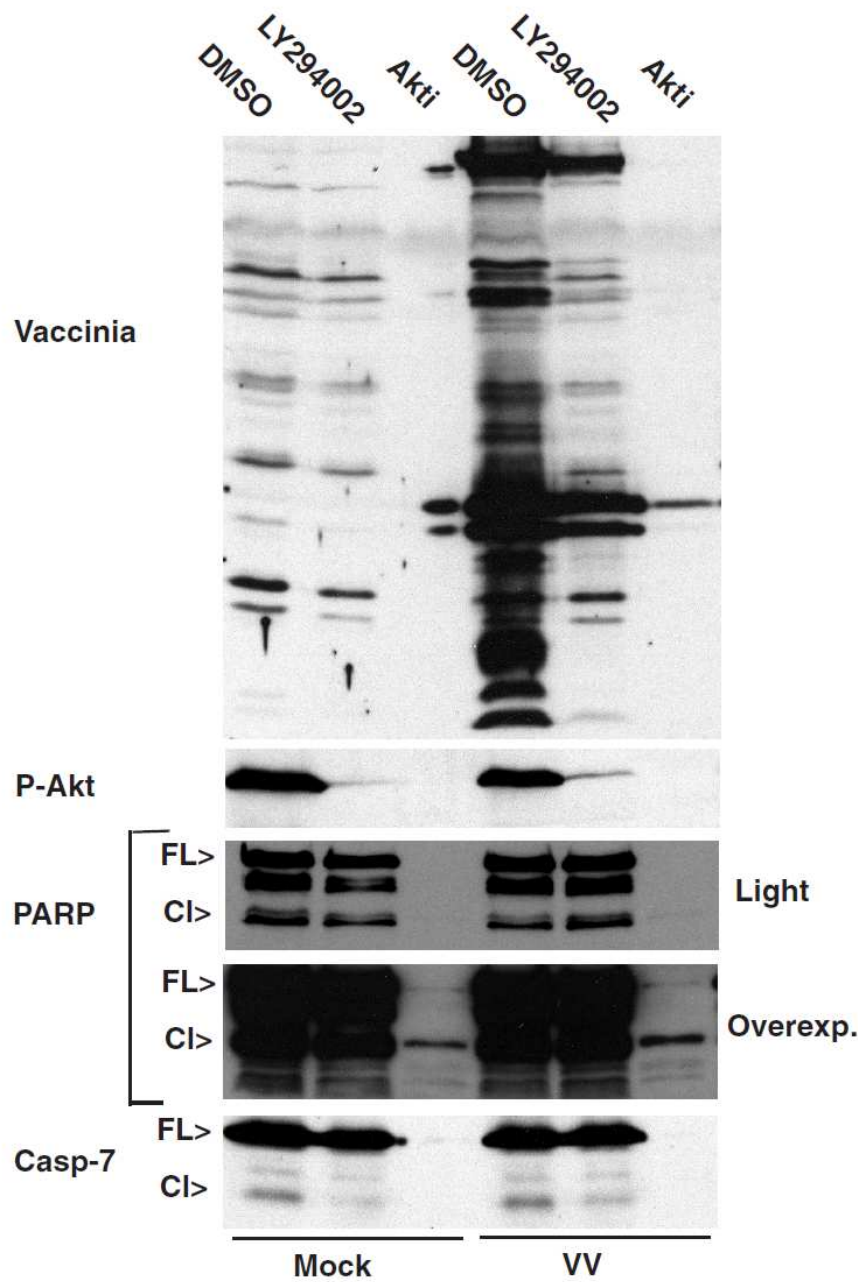
Figure 3.2.14 Immunoblots illustrating the effect of LY294002 and Akti on VacV protein levels (the upper part of image) and PARP cleavage and caspase-7 processing (lower part of image) in mock-infected (Mock) and VacV-infected (VV) HEK-293 cells.

3.2.7   The role of mTOR in VacV protein synthesis

As demonstrated before (sections 3.2.2.1, 3.2.2.2), the effect of LY294002 on 4E-BP1 and P-Akt was distinct from rapamycin; it caused a strong accumulation of 4E-BP1 and inhibited Akt phosphorylation in VacV-infected cells. This suggests that other unknown branches of the PI3K pathway may be involved in 4E-BP1 regulation and eIF4F formation. Notably, rapamycin only partially inhibits mTORC1 and does not affect mTORC2 complexes. In contrast to rapamycin, the recently discovered inhibitor Torin1 potently inhibits both mTORC1 (including rapamycin-sensitive and rapamycin-insensitive mTORC1) and mTORC2 complexes (Thoreen *et al.*, 2009). We therefore tested its influence on VacV infection in primary human cells. Figure 3.2.15 shows that Torin1 (50nM) blocked the phosphorylation of Akt and caused 4E-BP1 accumulation in VacV-infected cells. This was also observed in cells treated with two distinct inhibitors of PI3K, LY294002 (40 μM) and wortmannin (10 μM[5]) (Walker *et al.*, 2000).
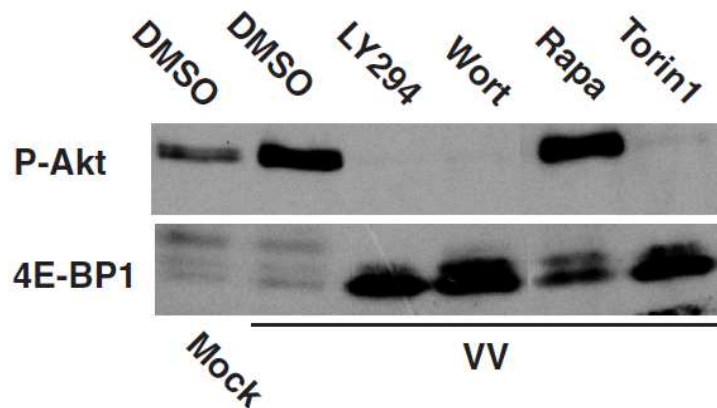
**Figure 3.2.15** Immunoblot illustrating the effect of Torin1 on Akt phosphorylation and 4E-BP1 phosphorylation and accumulation.

---

[5] 10μM wortmannin is considered a high concentration that inhibits PI3K class I, II and III, while low concentrations (250 nM) inhibit only class I of PI3K (Vlahos, 1994). However, for longer experiments higher concentrations are also necessary as wortmannin is unstable.

As Torin1 reproduced the effects of PI3K inhibitors on 4E-BP1 dephosphorylation and accumulation, 7-methyl GTP sepharose chromatography assay was carried out to look at the influence of Torin1 on eIF4F complex formation. Serum-starved NHDFs were pretreated with DMSO or 50 nM Torin1 for 1 hour, then mock-infected or infected with 10 PFU VacV per cell for 18 hours. Cap-binding eIF4E and levels of associated eIF4G were examined by western blotting. The results showed that, similarly to LY294002, Torin1 disrupted the eIF4F complex in both mock-infected and VacV-infected cells (Fig. 3.2.16).
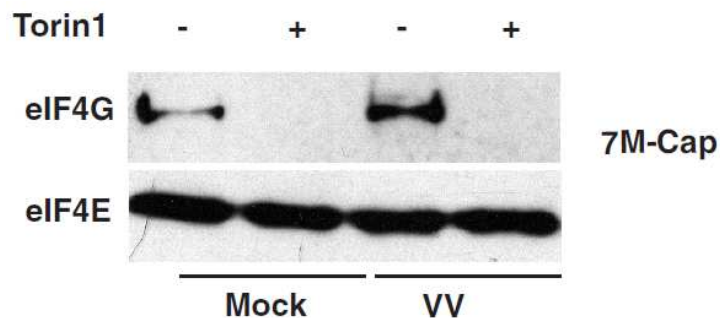
Figure 3.2.16 Immunoblot illustrating the effect of Torin1 on eIF4F complex formation in VacV-infected (VV) serum-starved NHDFs.

Examining rates of translation in VacV-infected serum-starved NHDFs at 18 hpi demonstrated that, although Torin1 reduced viral protein synthesis more efficiently than rapamycin, its effects were not as dramatic as might be expected, given the robust inhibition of eIF4F formation by Torin1 (Fig. 3.2.17 a).

In addition, viral protein accumulation at 18 hpi was not affected by Torin1 to the same extent as by LY294002 or wortmannin (Fig. 3.2.17 b). Two different concentrations of the PI3K inhibitors were used in this experiment. Two distinct concentrations of wortmannin (10 μM and 30 μM) reduced VacV protein synthesis to similar levels, and

similar to this, high concentration of LY294002 (40 µM), which inhibits both class I and class II of the PI3K (Vlahos, 1994), also reduced VacV protein levels. In contrast, low concentrations of LY294002 (2 µM), which did not completely block Akt or 4E-BP1 phosphorylation (not shown), were more similar to the effects of rapamycin. However, the effects of Torin1 were stronger compared to rapamycin demonstrating that eIF4F does play a role in the synthesis of VacV proteins, but that other functions of PI3K were also important in VacV replication.

Similar effects were obtained when performing titration of infectious virus production in the presence of inhibitors. 6×10^5 NHDFs were infected with 10 PFU VacV per cell in the presence of DMSO, 2 µM rapamycin, 50 nM Torin1 or 40 µM LY294002, and at 18 hpi the virus was harvested by repeated freeze/thaw cycles to disrupt cellular membranes and release the virus. Infectious virus was measured by diluting the lysates and infecting BSC40 cells. The virus titer was quantified by plaque assay and illustrated on the graph (Fig. 3.2.17 c), which clearly shows the increasing effect of each inhibitor on the production of infectious virus, in agreement with their effects on viral protein production.
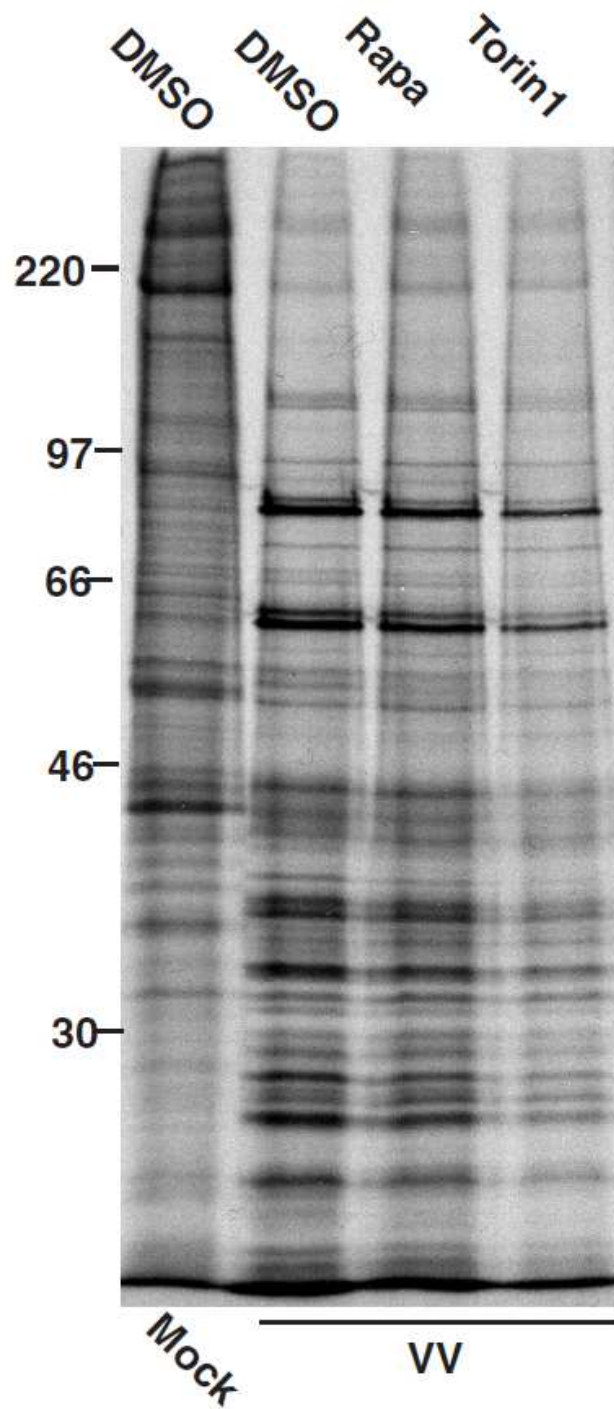
Figure 3.2.17 (a) Autoradiograph showing the effect of rapamycin and Torin1 on the total VacV protein synthesis. Cells metabolically labeled with [^{35}S]methionine-cysteine from 15-16 hpi. Molecular weight markers are indicated to the left.
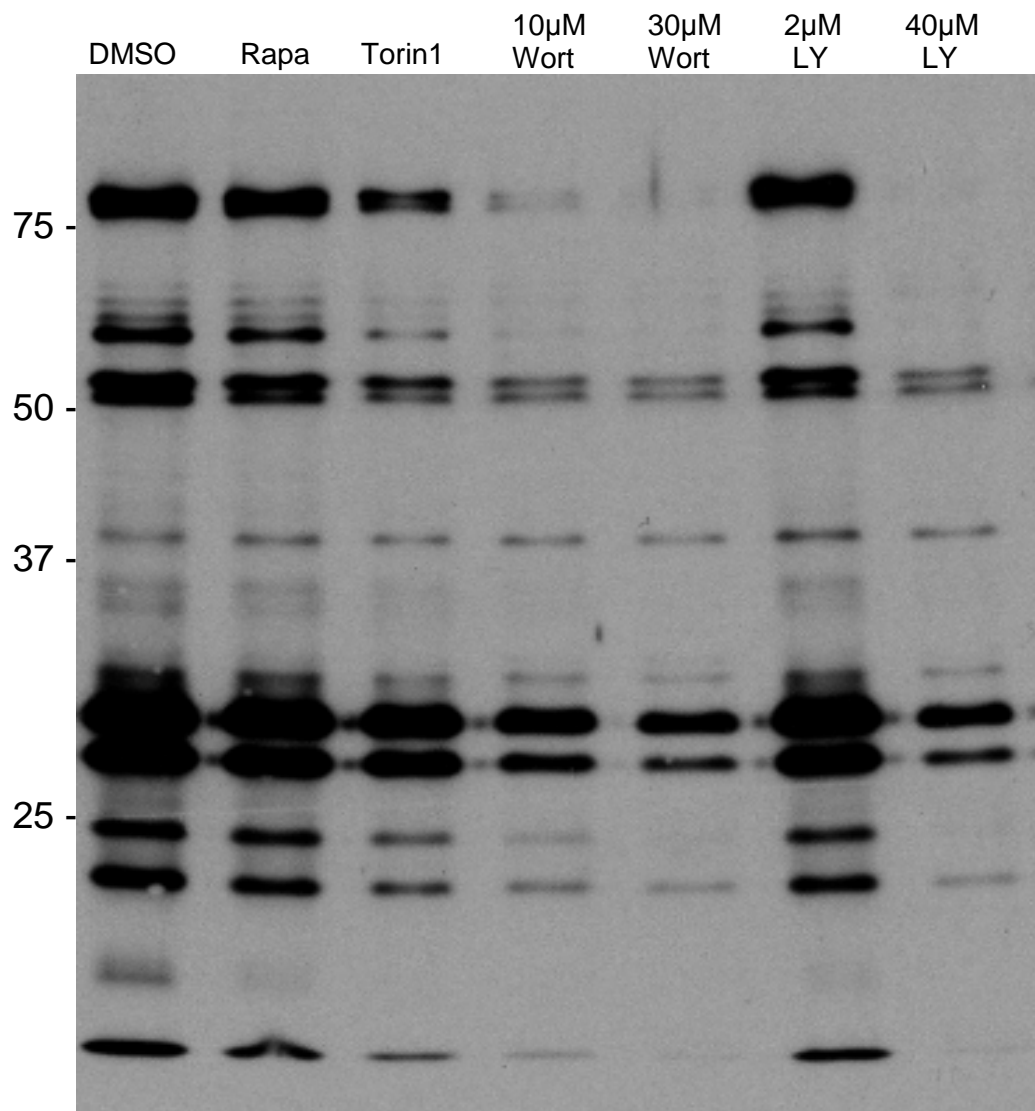
Figure 3.2.17 (b) Immunoblot comparison of the effect of Torin1, rapamycin, and PI3K inhibitors on the total VacV protein accumulation in serum-starved NHDFs at 18 hpi. Samples analyzed by western blotting using anti-VacV antiserum. (Rapa = rapamycin, Wort = wortmannin, LY = LY294002)
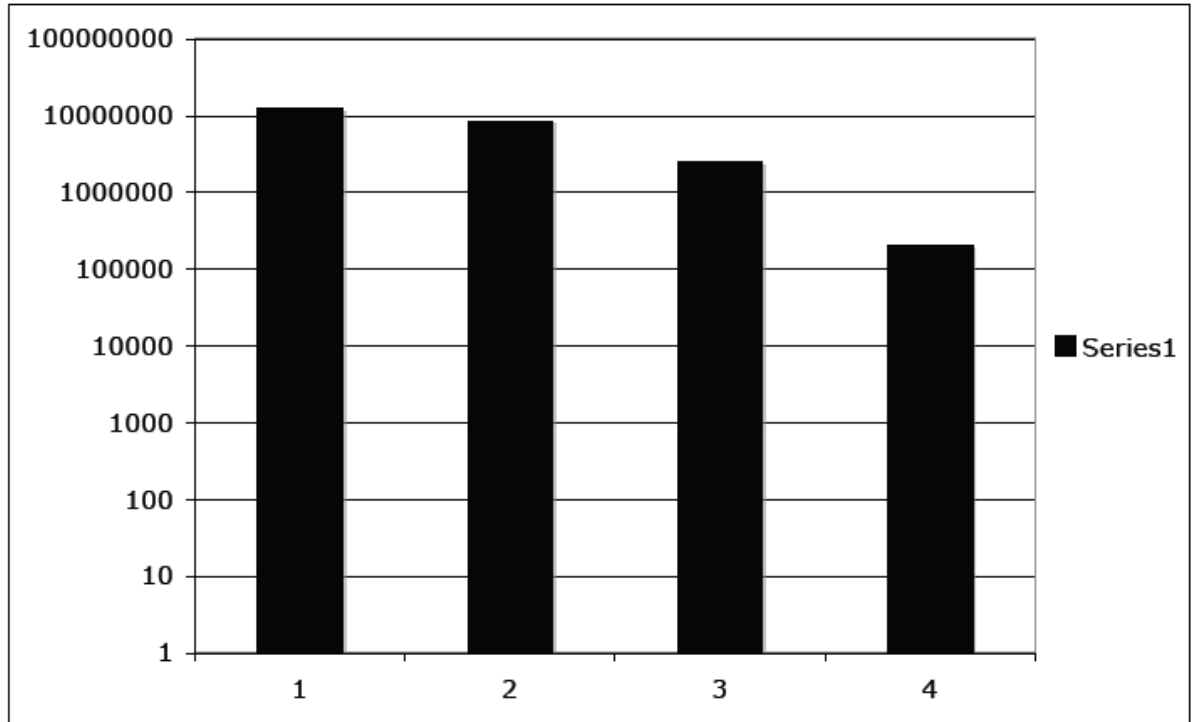
Figure 3.2.17 (c) Titration of infectious virus production in the presence of 1- DMSO, 2-rapamycin, 3- Torin1, and 4- LY294002.

3.3 Redistribution of translation factors during VacV infection

In the beginning of our investigation on redistribution of host translation factors caused by VacV, we speculated that a specific viral protein or cellular protein induced by the virus might associate with eIF4F and cause its rearrangement in infected cells. Therefore, we screened components of the eIF4F complex in VacV-infected cells to search for such a protein. This was done initially using serum-starved NHDFs infected for 16 hours to perform immunoprecipitation assays at the mid-phase of infection.

3.3.1 Identification of a viral protein associated with eIF4G in VacV-infected cells

The screening of translation factors was performed by metabolically labeling uninfected and VacV-infected cells from 15-16 hpi, and then immunoprecipitation of complexes from cell extracts using specific antibodies against eIF4G and PABP. Afterwards the immune complexes were resolved by SDS-PAGE and fixed, dried gels were exposed to x-ray film. Analysis of the detected proteins actively translated during labeling time in VacV-infected cells showed a 34-kDa protein associated with eIF4G that was not present in mock-infected cells (Fig. 3.3.1 a). In addition, immunoprecipitating eIF4G from cells infected for 24 hours demonstrated that the signal intensity from this polypeptide decreased significantly (Fig. 3.3.1 b), suggesting that it was no longer synthesized or no longer associated with eIF4G at this point.
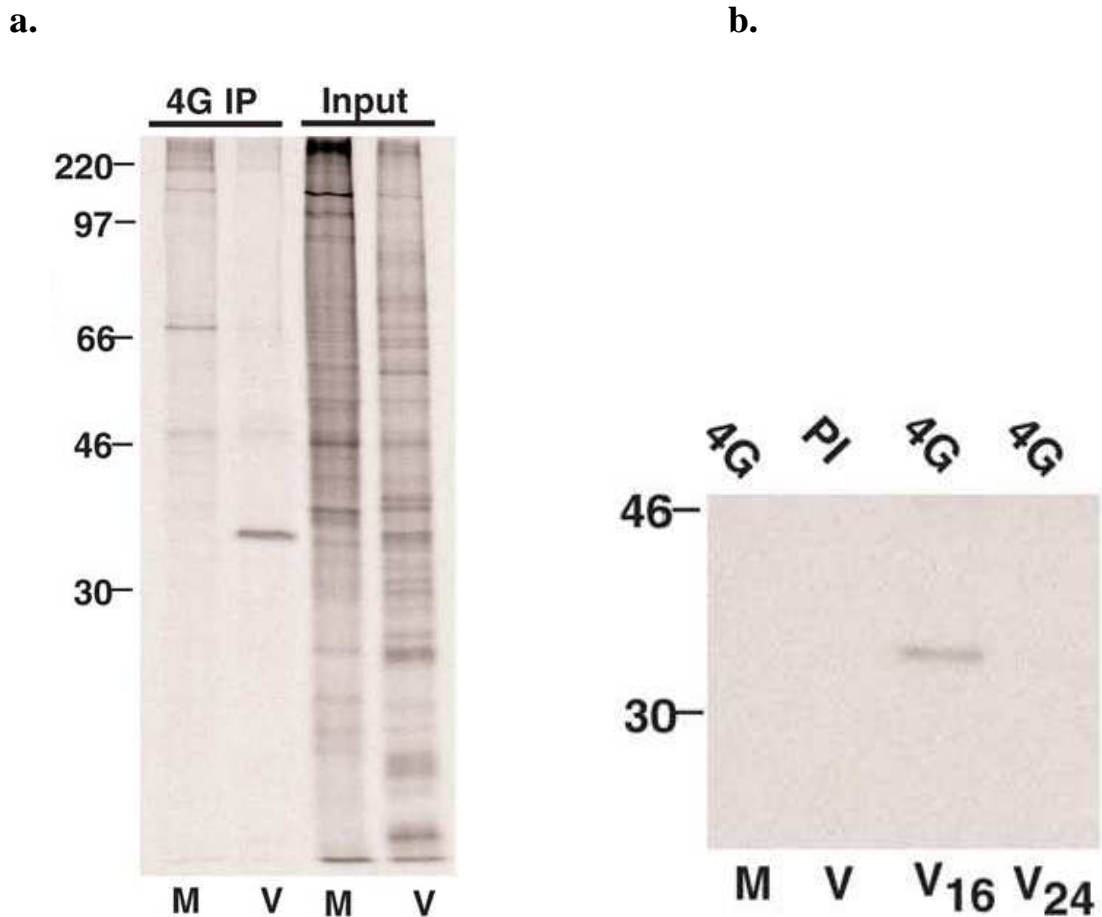
Figure 3.3.1 Autoradiographs of metabolically labeled starved NHDFs illustrating **(a)** an unknown 34-kDa protein associated with eIF4G at 16 hpi, and **(b)** its signal intensity at 16 and 24 hpi (to the right) Molecular weight markers are indicated to the left. (M = mock, V = VacV-infected, PI = pre-immune serum, 4G = anti-eIF4G IP, 16 = 16hpi, 24 = 24hpi)

We further examined whether this protein was present in anti-PABP immune complexes. PABP is an abundant RNA-binding protein involved in different cellular processes including translational control, but in VacV-infected cells the majority of PABP is distributed to different areas of the cell distinct from eIF4G (Mangus *et al*., 2003; Walsh *et al*., 2008). Immunoprecipitation of anti-eIF4G and anti-PABP immune complexes clearly demonstrated that the 34-kDa protein was only detected at significant

levels in anti-eIF4G immune complexes, and it did not visibly associate with anti-PABP immune complexes (Fig. 3.3.2).
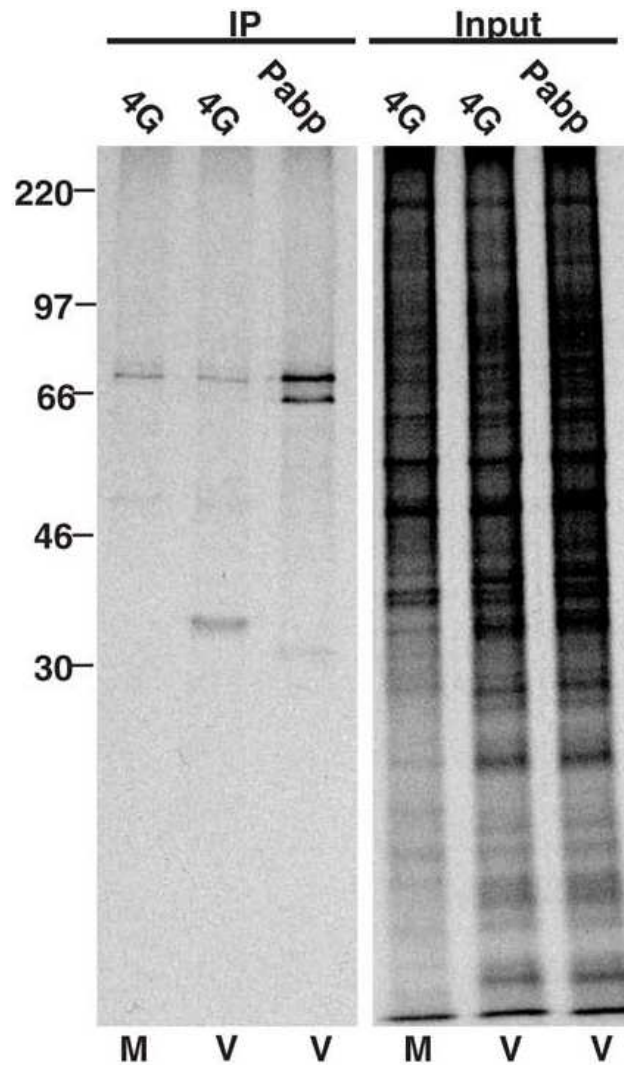
Figure 3.3.2 Autoradiograph illustrating metabolically labeled starved NHDFs and the specific association of the 34-kDa protein with eIF4G factor at 16 hpi (4G). (M = mock, V = VacV-infected)

Looking at eIF4E abundance by western blotting in immunoprecipitated eIF4G- and PABP-complexes in infected serum-starved NHDFs showed that this cap-binding protein was recovered with eIF4G in large amounts, but only very small amounts of

eIF4E were noticed in anti-PABP immune complexes, despite efficient antigen recovery (Fig. 3.3.3). This demonstrated that, of the total amount of this abundant multifunctional cellular protein, only small amounts of PABP were associated with eIF4F complexes in these cells. In the case of infected cells, PABP did not appear to associate with large amounts of either eIF4E or the 34-kDa protein found associated with eIF4G. Also, at 16 h point where eIF4F assembly begins an increase in eIF4E recovery is seen in both eIF4G and PABP immune complexes from infected cells.

.
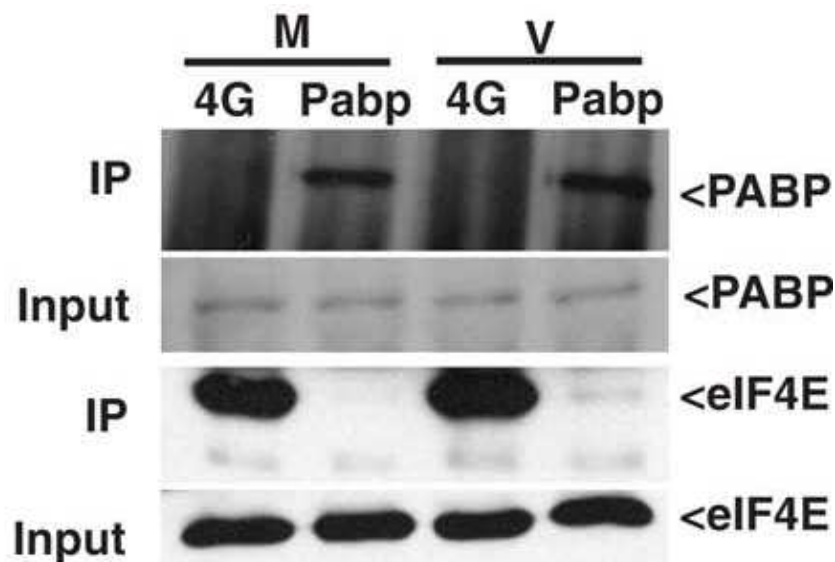
Figure 3.3.3 Immunoblot illustrating anti-eIF4G and anti-PABP complexes immunoprecipitated from infected serum-starved NHDFs. (M = mock, V = VacV-infected)

To identify the unknown 34-kDa protein, BSC40 cells were mock-infected or infected for 16 h. Nuclease-treated soluble cell extracts were prepared and immunoprecipitated with anti-eIF4G antiserum. Immune-complexes were resolved by SDS-PAGE, and the gels were silver-stained as described in section 2.2.12. A specific band present only in infected samples and migrating at 34-kDa was detected (Fig. 3.3.4 a). The band was cut out and analyzed by mass spectrometry. During the analysis in various independent

experiments an average of 4-6 peptides were identified, all of which corresponded to the VacV-encoded ssDNA-binding phosphoprotein I3 (GI no. 66275869), with sequence coverage ranging from 18.2-23 %. A sample MS/MS spectrum is shown in figure 3.3.4 b.

I3 protein is encoded by the VacV I3L gene, and has previously been shown to be an early-to-intermediate stage protein (Rochester and Traktman, 1998), which explains our observation that it is actively synthesized and detected in eIF4G immune complexes at intermediate, but not late stages of infection (Fig. 3.3.1 b).
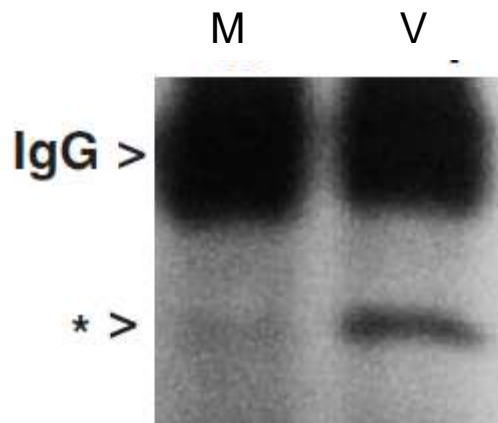
Figure 3.3.4 (a) Protein identification: representative image from silver-stained gel, with an asterix indicating the 34-kDa protein in question. (M = mock, V = VacV-infected)

MS/MS Spectra

Seq: R.EVVANVIGLSGDSER.V
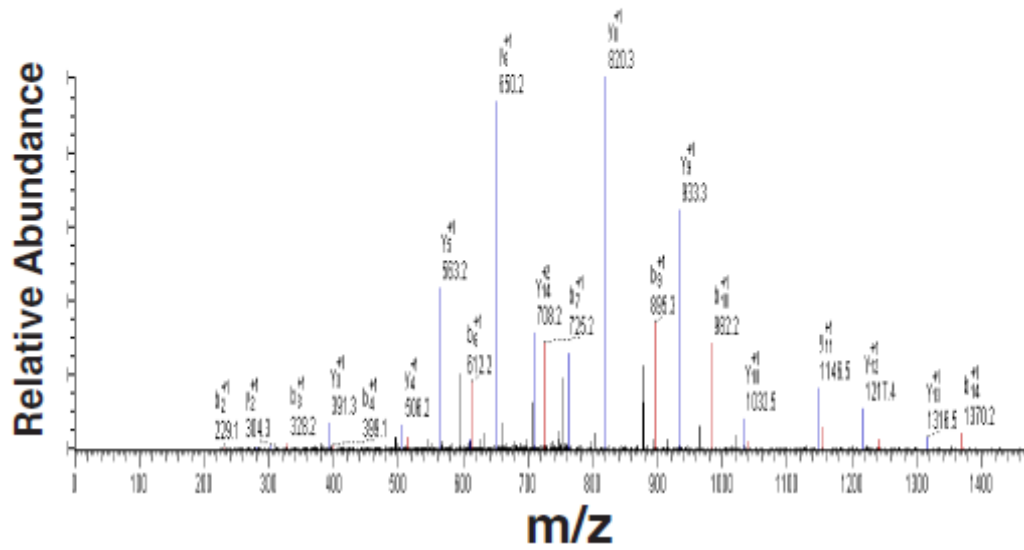
Figure 3.3.4 (b) Protein identification: a sample MS/MS spectra of a peptide from I3.

3.3.2   A non-immune based assay to examine I3 association

To verify the interaction of I3 with eIF4G by an alternative, non-immune-based assay, cell extracts were analyzed by 7-Methyl GTP-sepharose chromatography. In this experiment we used HEK-293 cells to examine a different cell type and where the infection reaches late stage by 16 hpi. This would tell us if I3 remained associated with eIF4G at late stages of infection, when its synthesis by the virus decreases, as shown in Fig. 3.3.1. HEK-293 cells were mock-infected or infected at moi 5 for 16 h, and then cap-binding eIF4F complexes were recovered from RNAse-treated soluble cell extracts on 7-Methyl GTP-sepharose.

Analysis of these complexes by western blotting clearly showed that I3 associated with eIF4F complexes purified from VacV-infected cells; furthermore, after addition of 3 mM free 7-Methyl GTP - which competes with the cap-sepharose for binding to eIF4F complex - to the extracts, I3 binding together with the eIF4F components eIF4E and eIF4G was strongly inhibited (Fig 3.3.5). All images were from the same blots and exposures, cropped to remove replicate experiments. A slower-migrating non-specific band noticed in all cap-bound samples probed with anti-I3 antiserum is indicated with an asterix, and is not I3 protein.

	7M-Cap			Input		
	M	VV	VV	M	VV	VV
eIF4G						
I3 →						
eIF4E						
7M-GTP	-	-	+	-	-	+
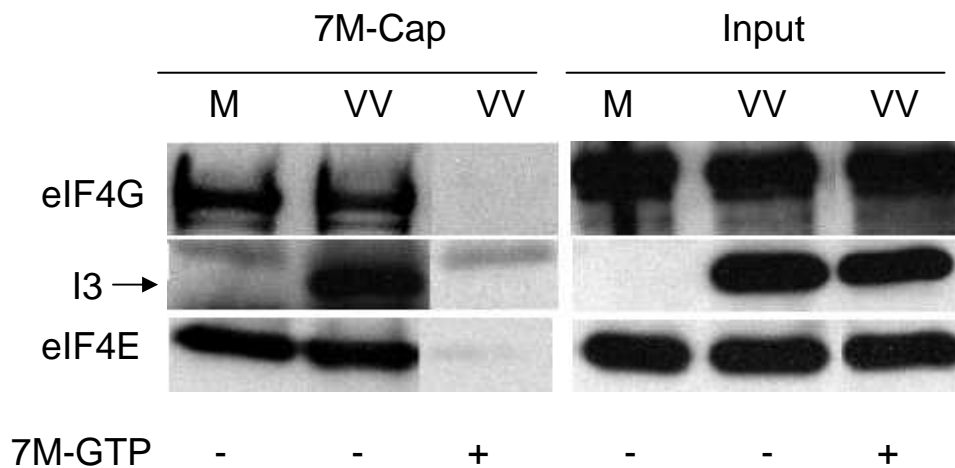
Figure 3.3.5 Immunoblot illustrating cap-bound complexes in mock (M) and VacV-infected (VV) HEK-293 cells. (+/-) indicate the presence/absence of free 7-Methyl GTP. Asterix indicates non-specific band.

3.3.3 Localization of I3 protein in infected cells

It has been shown recently that cellular translational factors such as eIF4G and PABP are redistributed during VacV infection to viral factories by an unknown mechanism (Katsafanas and Moss, 2007; Walsh *et al*., 2008). Having identified I3 as a viral protein associating with eIF4G, the subcellular localization of I3 and eIF4G in VacV-infected cells was examined by immunofluorescence assay. To do this we GFP-tagged the I3L gene and transfected cells, then infected the cells and analyzed the subcellular localization of I3 together with its binding partner eIF4G.

First of all, the I3L gene was PCR-amplified from VacV genomic DNA isolated from infected BSC40 cells using the primers containing EcoR1 and Kpn1 restriction sites (for details see section 2.2.13). DNA from uninfected cells was used as a control for specificity of the PCR reaction. The amplified PCR product was analyzed by agarose gel electrophoresis, which confirmed the presence of the amplified gene of expected size (Fig. 3.3.6). The PCR product was then purified, digested with EcoR1 and Kpn1

enzymes, then ligated into the EcoR1-Kpn1 cloning site of the mammalian expression plasmid pGFP-N which carried kanamycin resistance, to generate a C-terminally GFP-tagged form of I3 protein. pGFP plasmid contains an enhanced GFP mutant which allows the expression of GFP to be visualized with UV light.
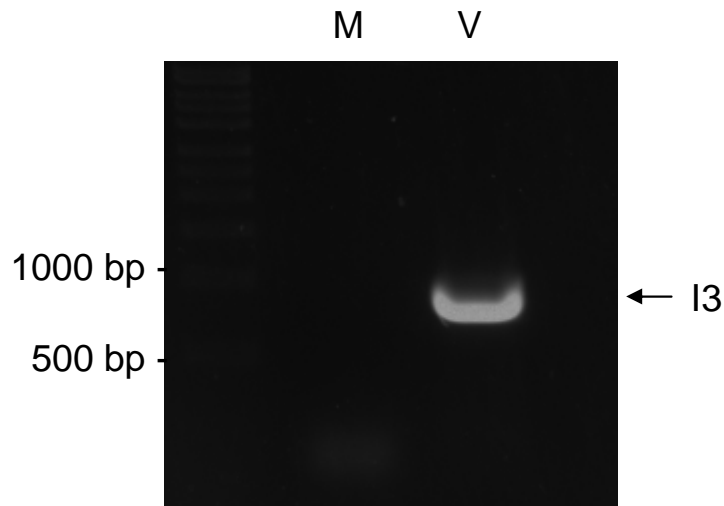
Figure 3.3.6 Gel electrophoresis analysis of PCR-amplified pGFP-I3L. (M = mock, V = VacV-infected)

HEK-293 cells were transfected with empty plasmid or 0.5 µg pGFP-I3L. To confirm the functionality of the fusion protein, at 24 hours post transfection cells were lysed in NP-40 Lysis Buffer, treated with nuclease and analyzed by 7-Methyl GTP-sepharose chromatography. Western blotting of the samples demonstrated that GFP-I3 was recovered in cap-complexes together with eIF4G and eIF4E, although at low levels - most likely because of low efficiency of the transient transfection (Fig. 3.3.7).

eIF4G

GFP-I3

eIF4E
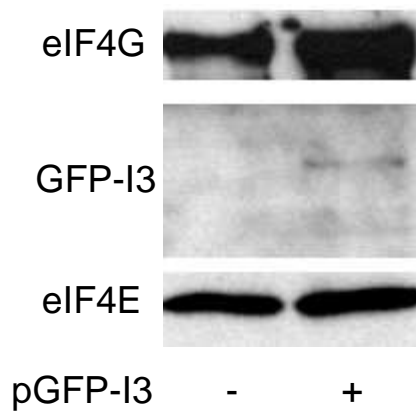
pGFP-I3   -   +

Figure 3.3.7 Immunoblot illustrating 7-Methyl GTP-sepharose chromatography of HEK-293 cells transfected with the control DNA (-) or pGFP-I3 (+).

To perform the immunofluorescence assay, transfected cells were VacV-infected at moi 5 for 16 hours. Cells were fixed in formaldehyde and probed with anti-eIF4G antiserum, which was detected with TRITC-conjugated anti-rabbit secondary. Cellular DNA in the nucleus and viral DNA in the factories were visualized using Hoescht, and cells were analyzed under a fluorescence microscope. As shown in figure 3.3.8, numerous viral factories formed nearby the nuclei, some of them larger than others and diffusely stained. eIF4G, normally dispersed in the nucleus and the cytoplasm of uninfected cells, relocalized to the viral replication compartments, as reported previously (Katsafanas and Moss, 2007; Walsh *et al.*, 2008). Interestingly, GFP-tagged I3 colocalized with eIF4G within the same distinct areas of viral factories, as can be seen in merged image (Fig. 3.3.8). Colocalization could be observed in over 80 % of the cells that expressed the plasmid at low levels, whereas high expression levels resulted in saturation of cells with GFP-I3, and difficulties to distinguish colocalization.
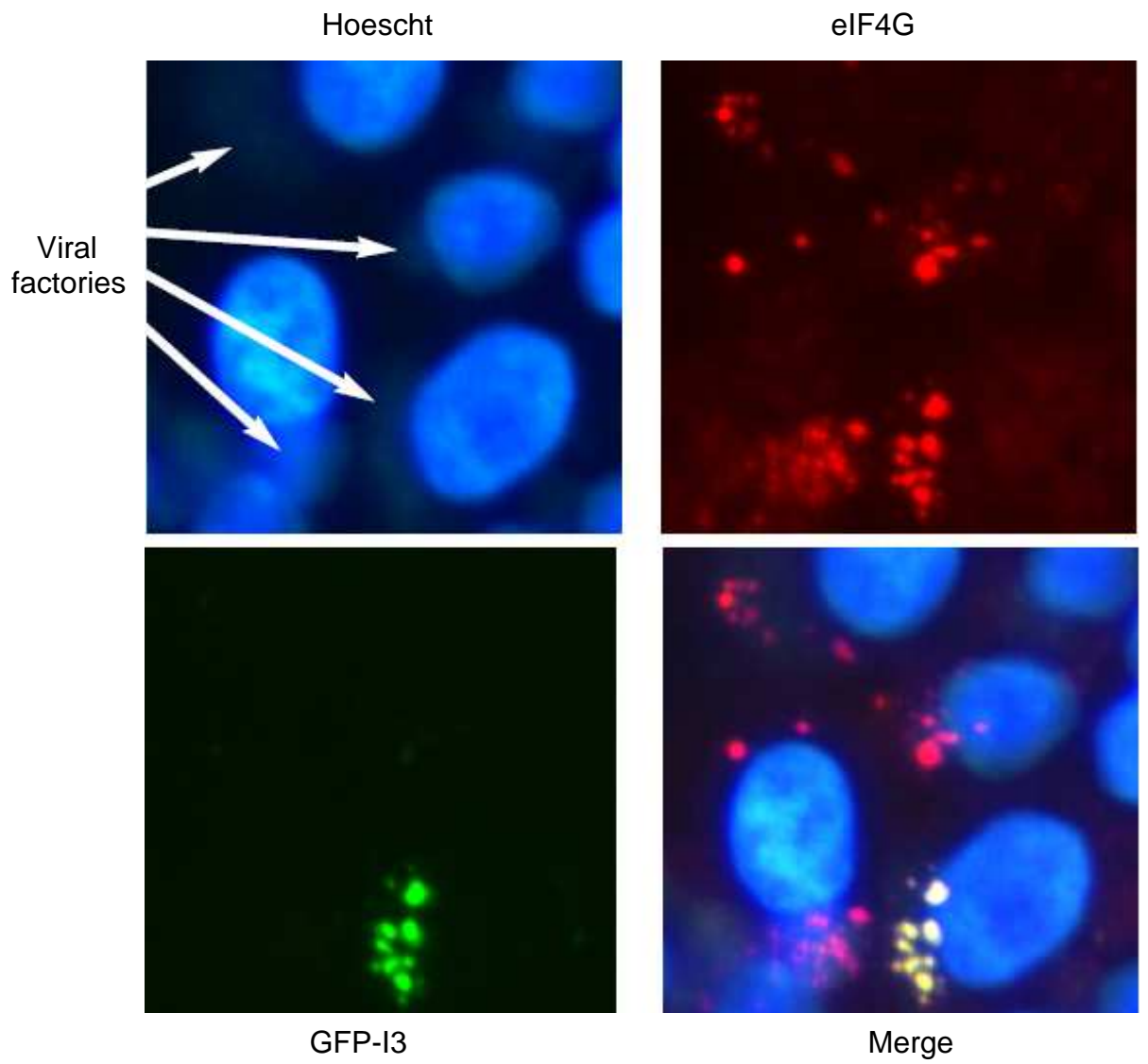
Figure 3.3.8 Immunofluorescence images illustrating accumulation of eIF4G and GFP-I3 in viral factories in VacV-infected HEK-293 cells.

3.3.4 Investigation of I3-eIF4F interaction in uninfected cells

The previous experiments showed that I3 associates with eIF4F complexes in infected cells. To examine the binding ability of I3 to eIF4F in the absence of other viral proteins, experiments with uninfected cells expressing I3L gene were carried out.

3.3.4.1 Expression of his-I3 in HEK-293 cells

To examine the ability of I3 to associate with eIF4F in uninfected cells, first of all I3L gene needed to be cloned and expressed in the cells. The I3L gene was PCR-amplified from VacV genomic DNA isolated from uninfected or infected BSC40 cells using the primers containing EcoR1 and Sal1 restriction sites, as well as N-terminal 6 x His sequence (for details see Section 2). The amplified PCR product was analyzed by agarose gel electrophoresis, which confirmed the presence of the amplified gene (Fig. 3.3.9).
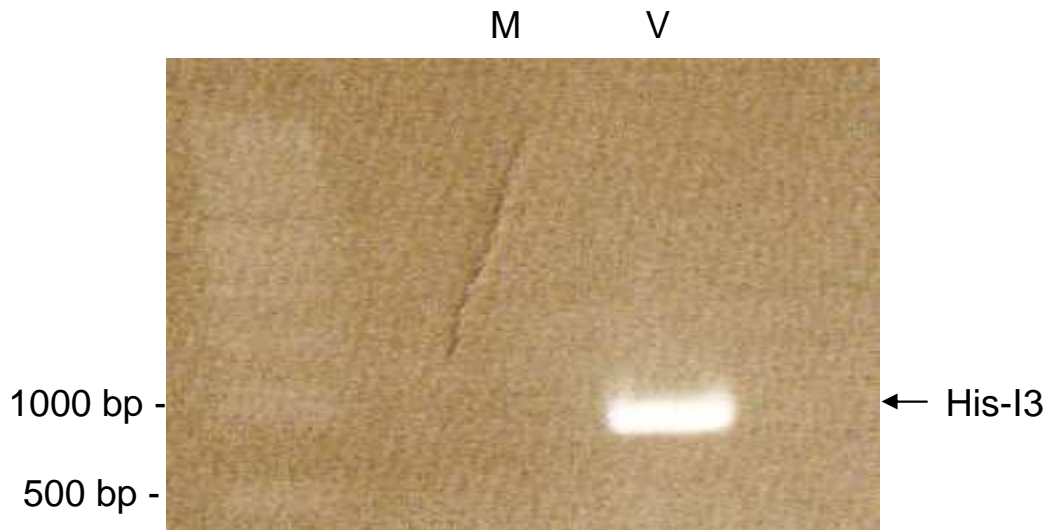
Figure 3.3.9 Gel electrophoresis analysis of PCR-amplified his-I3L. (M = mock, V = VacV-infected)

The amplified gene was purified, digested with EcoR1 and Sal1, then ligated into the EcoR1-Sal1 cloning site of the mammalian expression plasmid pCl-Neo which carried ampicillin resistance, to generate N-terminally his-tagged form of I3 protein. After transformation of pCI-His-I3L in DH5*alpha* cells, eight separated colonies (labeled A-H) were chosen to isolate the plasmids. DNA sequencing of those plasmids showed no mutations, and plasmid G was chosen to perform further experiments.

Two sets of HEK-293 cells, which were 45 % and 90 % confluent, were transfected with empty plasmid or 200 ng pCl-His-I3L. To confirm the presence of the fusion protein, 24 and 48 hours post transfection (hpt) cells were lysed and analyzed by western blotting using mouse anti-his antiserum. Figure 3.3.10 illustrates the expression of his-I3L plasmid 24 hpt, and shows the increased expression in the sample containing double amount of the cells. The expression of the plasmid significantly decreased at 48 hpt (data not shown), thus the analysis of transfected cells in further experiments was performed at 24 hpt.
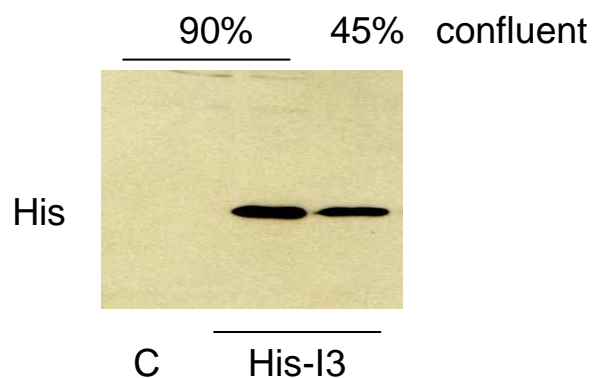
Figure 3.3.10 Immunoblot illustrating his-I3 expression in HEK-293 cells. (C = control sample transfected with empty plasmid)

3.3.4.2 His-I3 interaction with anti-eIF4G immune complexes in transfected cells

The I3-eIF4G interaction in HEK-293 cells was tested by recovering anti-his immune complexes from cell extracts. As I3 is an ss-DNA binding protein, to examine if exogenous ssDNA molecules could enhance I3-eIF4G association *in vitro*, 7.5 µg ssDNA was added to the cell extracts.

As shown in figure 3.3.11, his-tagged I3 was recovered efficiently from the cells expressing this protein, while no his-reactive bands were noticed in the control sample that did not contain I3. In contrast, eIF4G was recovered not only in the samples containing his-I3, but also in control samples lacking I3, suggesting the unspecific binding between anti-his antibody and eIF4G. For that reason we decided to repeat the cloning procedure and tag I3 with different sequences to avoid the unspecific binding.
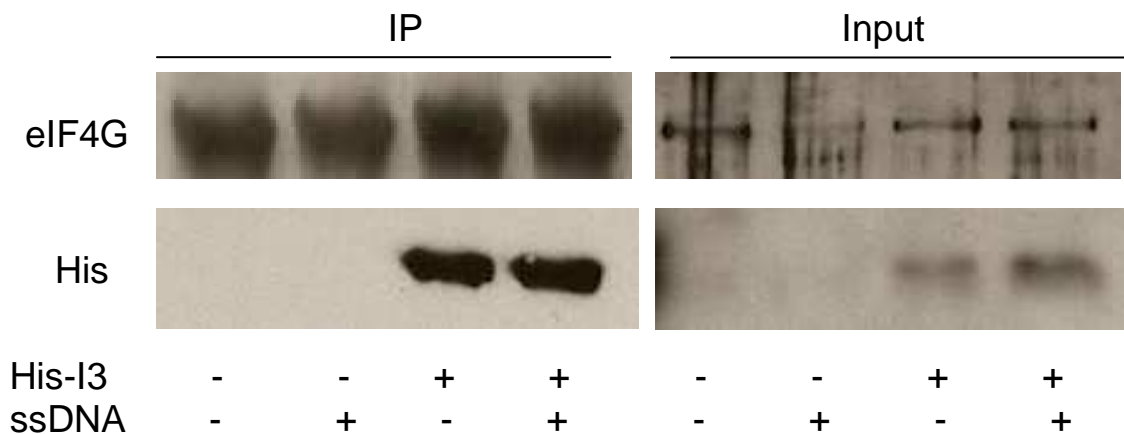
Figure 3.3.11 Immunoblot illustrating anti-his immune complexes immunoprecipitated from HEK-293 cells.

3.3.4.3 Expression of FLAG-I3 in uninfected cells

The FLAG-tag sequence was fused to either C- or N-terminal of I3L during PCR amplification, and the cloning procedure of FLAG-tagged I3 was carried out as described in Section 3.2.8.1. HEK-293 cells have been chosen again to examine the expression of C- and N-FLAG-tagged I3. Analysis of transfected cell extracts by western blotting demonstrated that C-FLAG-tagged I3 expressed more efficiently than N-FLAG-I3 (not shown), thus the C-FLAG-I3 plasmid was used to perform further experiments.

3.3.4.4 FLAG-I3 interaction with anti-eIF4G immune complexes in transfected cells

The FLAG-I3 interaction with eIF4G in HEK-293 cells was tested by recovering anti-FLAG immune complexes from uninfected cell extracts. As shown in figure 3.3.12, FLAG-tagged I3 has been efficiently recovered from the cells expressing this protein, although it was not detected in input samples. eIF4G was not recovered with FLAG-I3, most likely because of the low FLAG-I3 abundance in analyzed samples. However, eIF4G was not detected in the samples lacking FLAG-I3 (not shown), which indicates that no unspecific binding between anti-FLAG antibody and eIF4G protein occurs.

	IP		Input	
I3				
FLAG-I3	-	+	-	+
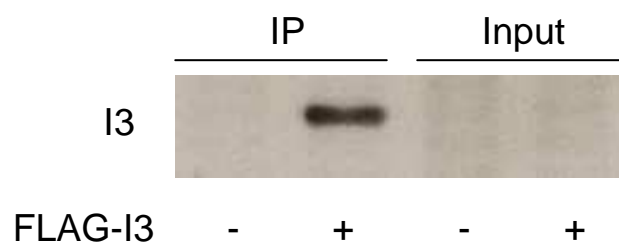
Figure 3.3.12 Immunoblot illustrating anti-FLAG immune complexes immunoprecipitated from HEK-293 cells.

3.3.4.5 Making stable cell lines

Because of the low expression levels of I3 in transiently transfected cells, we decided to create stable HEK-293 cell line over-expressing high levels of FLAG-I3. Having stable cell line highly expressing FLAG-I3 would provide consistency in performing experiments using always the same cells, instead of performing transient transfection for each experiment.

The following steps needed to be performed in order to establish a new stable cell line:

Transfection with the construct

⬇

Selection of cells expressing the construct

⬇

Clonal expansion of single cells in 96-well plate

⬇

Screening for expressing clones

⬇

Expanding and developing cell lines
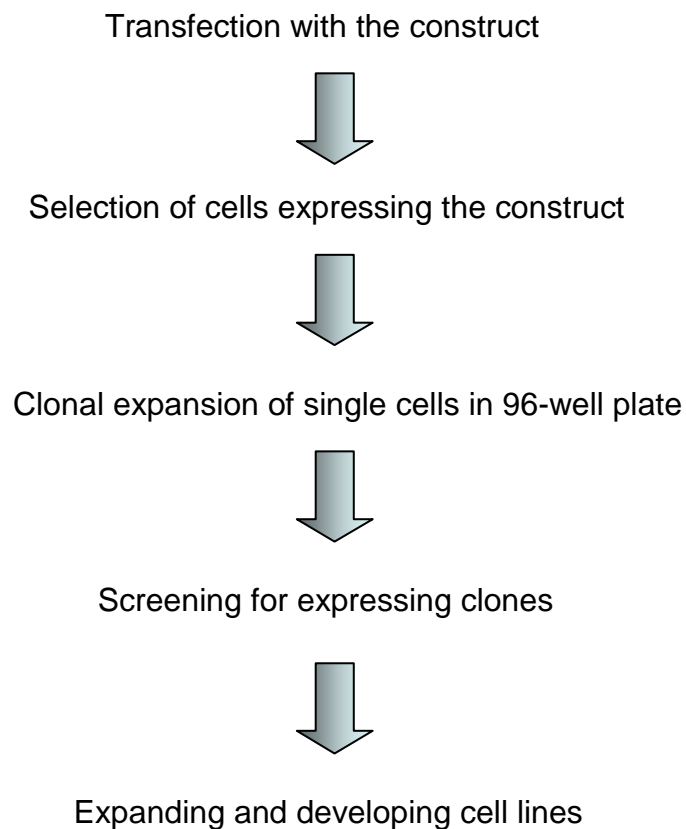
3.3.4.5.1 Cloning FLAG-tagged actin

To provide the control for I3-expressing cells, stable cell lines over-expressing FLAG-tagged actin and FLAG-tagged empty vector have been also established. Actin is the most abundant protein in eukaryotic cells and of similar size to I3 thus is thought to make a good control for over-expressing genes.

C-FLAG-actin was amplified from cDNA prepared from RNA isolated from human cells, and cloned as described in Section 3.2.8.1.

3.3.4.5.2 Selection of transfected cells

HEK-293 cells were transfected with 200 ng FLAG-I3, FLAG-actin or FLAG-empty vector. The following day cells expressing recombinant genes were selected by adding geneticin.

Geneticin (G418) is an aminoglycoside antibiotic that inhibits prokaryotic and eukaryotic protein synthesis, thus is toxic for mammalian cells. G418 is commonly used as a selective agent for the bacterial *neo* and *kan* genes. The product of these genes, aminoglycoside 3'-phosphotransferase (neomycin phosphotransferase) inactivates G418, neomycin, and kanamycin by phosphorylation. Therefore, introduction of any of these genes into cells results in their resistance to G418.

Recombinant genes used in this study have been ligated into pCI-neo plasmid which carries G418 resistance. The amount of G418 needed to eliminate the cells not expressing the constructs was titrated using HEK-293 cells (not shown).

At 24 hpt of cells with 0.5 μg of plasmid, the standard media were replaced with media containing G418 in a concentration of 1.5 mg/ml to initially select the cells that have

stably incorporated the plasmid. Selection was carried out for seven days, within which most of the cells that did not express the incorporated plasmid efficiently died. This was in line with the low transfection efficiency we were achieving with transient transfection experiments. The remaining cells were seeded on 96-well plates using medium containing reduced concentration of G418, in order to grow the colonies from single cells. Plates were viewed to identify wells containing single cells, which were marked, and plates were incubated at 37° C. When confluent, clones from 12-14 wells were trypsinized. Half of the cells was seeded into 24-well plates to continue the culture, while the other half was re-seeded into 96-well plates. The next day, when the cells on 96-well plate were confluent, they were lysed in Laemmli buffer and screened by western blotting using anti-FLAG or anti-I3 antiserum to examine the expression of recombinant genes (Fig. 3.3.13 a, b).
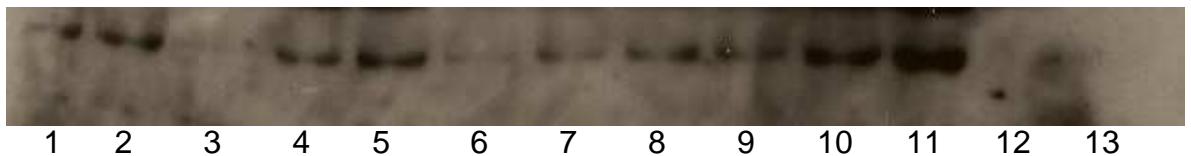
Figure 3.3.13 (a) Immunoblot illustrating the expression of FLAG-actin in selected HEK-293 cells. (1-13 indicate numerical order of the wells from which cells expressing FLAG-actin were lysed)
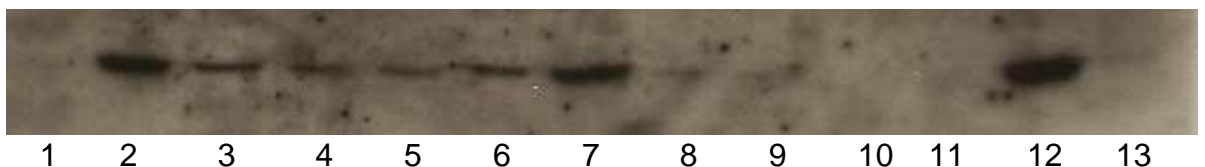
Figure 3.3.13 (b) Immunoblot illustrating the expression of FLAG-I3 in selected HEK-293 cells. (1-13 indicate numerical order of the wells from which cells expressing FLAG-I3 were lysed)

The clones with the highest expression of recombinant genes (no. 11 for FLAG-actin, no. 12 for FLAG-I3) were selected to perform further experiments.

3.3.4.6 FLAG-I3 interaction with anti-eIF4G immune complexes

A stable HEK-293 cell line over-expressing recombinant FLAG-tagged I3 was then used to examine I3 interaction with eIF4G by recovering anti-FLAG immune complexes from uninfected and infected cell extracts. Infecting the cells was performed in order to compare the efficiency of recovering I3 in the presence and absence of the other viral components. Immunoprecipitated complexes were analyzed by western blotting using anti-eIF4G and anti-FLAG/I3 antisera.

As shown in figure 3.3.14, eIF4G clearly associated with I3 in uninfected cells overexpressing FLAG-I3, although a faint band of eIF4G was noticed in the sample lacking the recombinant I3 (first lane); however, the higher position of that band suggests that it could be unspecific. Surprisingly, VacV-infection reduced eIF4G binding, most likely as a result of a competition between viral and recombinant I3 for binding to eIF4G. Since virus produces much greater amounts of I3 during replication (see input samples), it competed away FLAG-I3 from eIF4G.

Probing with anti-FLAG or anti-I3 antibodies revealed equal amounts of FLAG-I3 in both mock and infected samples. Moreover, no I3 has been detected in infected sample lacking FLAG-I3, indicating the specificity of recovering anti-FLAG immune complexes from cell extracts.
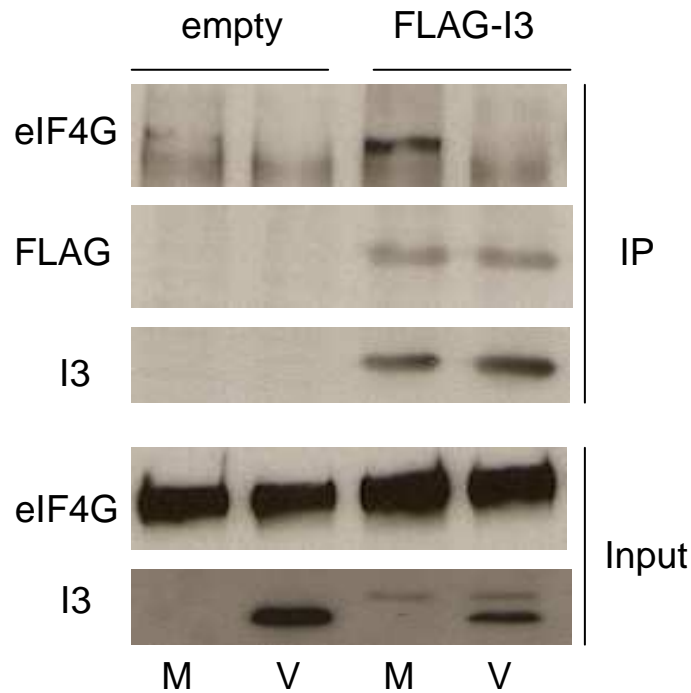
Figure 3.3.14 Immunoblot illustrating anti-FLAG immune complexes immunoprecipitated from HEK-293 cells. (M = mock, V = VacV-infected, empty = empty vector)

Looking at the input samples demonstrated similar amounts of eIF4G accumulated in all samples. Interestingly, anti-I3 antibody detected both FLAG-tagged (upper band) and viral I3, showing the differences in expression of the recombinant and viral I3.

3.3.4.7 Studies of FLAG-I3 binding to eIF4F by 7M GTP-sepharose 4B chromatography

The stable HEK-293 cell line expressing recombinant FLAG-tagged I3 was then used to examine I3 association with cap complexes in uninfected cells. Soluble cell extracts were prepared from HEK-293 cells expressing empty-vector and FLAG-I3, and treated with RNAseA. 7-Methyl GTP-sepharose 4B chromatography assay was performed, and samples were analyzed by western blotting using antisera against eIF4G, eIF4E and FLAG. As shown in figure 3.3.15, I3 was clearly detectable on 7-Methyl GTP-

sepharose, together with other components of the eIF4F complex. A non-specific band located just below I3 in input samples was also detected by anti-FLAG antiserum, but it was not detected in 7M-Cap samples. In contrast, I3 was not detected on sepharose resin alone, which was used as the control for the I3 binding (not shown). This experiment confirmed that other viral gene products are not required for the interaction of I3 with eIF4F.
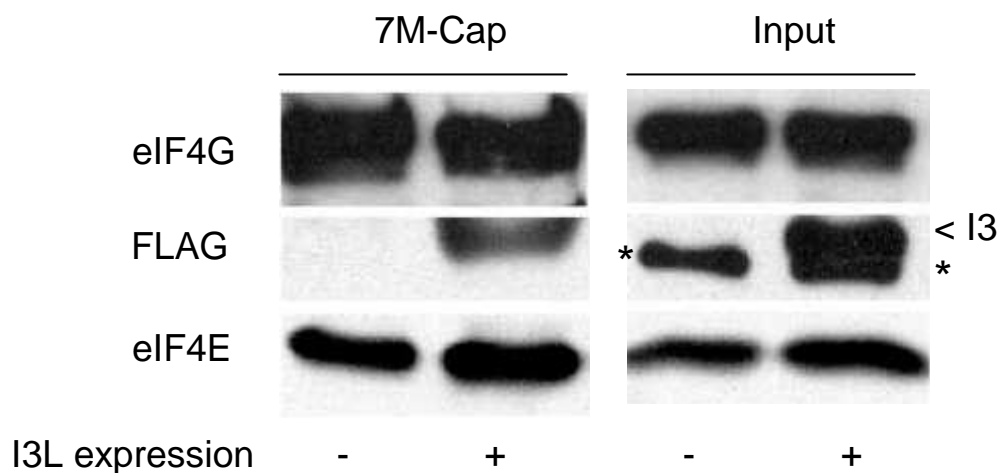
Figure 3.3.15 Immunoblot illustrating cap-bound complexes in HEK-293 cells expressing FLAG-I3. Migration of I3 detected with anti-FLAG antiserum is indicated with the arrow (<). A non-specific band detected by this antiserum in input samples is indicated by the asterix.

3.3.5 Investigation of I3-eIF4F interaction *in vitro*

To determine whether I3 interacts with eIF4G directly or whether it involves additional factors, we performed *in vitro* binding assays using purified I3 and eIF4G proteins. First of all, I3 was cloned and ligated into the bacterial expression plasmid pET-15b, which contains an N-terminal His-sequence tag, and then cloned into BL21 cells. Overnight seed cultures were used to inoculate 500 ml, which was induced to express His-I3 using IPTG for 1 h. The protein was then purified by running benzonase-treated cell lysates over His-TALON columns, followed by dialysis, and the presence of I3 was confirmed

by gel electrophoresis and western blotting. Due to low yields I3 could not be visualized well by coomassie staining (not shown).

To examine the binding, 200 ng his-I3 was incubated for 1 hour with 7-Methyl GTP-sepharose 4B alone or 7-Methyl GTP-sepharose 4B that had been preincubated with nuclease treated HEK-293 cell extracts containing eIF4F complexes. As an additional control, his-I3 was also incubated with sepharose 4B only, that had also been preincubated with HEK-293 cell extracts. After 1 h incubation all beads were extensively washed to remove unbound complexes, and samples were analyzed by western blotting. As shown in figure 3.3.16, recombinant I3 specifically associated with eIF4F purified from cell extracts, and did not interact with the control sepharose 4B beads. In addition, the association with 7-Methyl GTP-sepharose 4B did not occur in the absence of eIF4F, indicating the specificity of I3 binding to that complex.
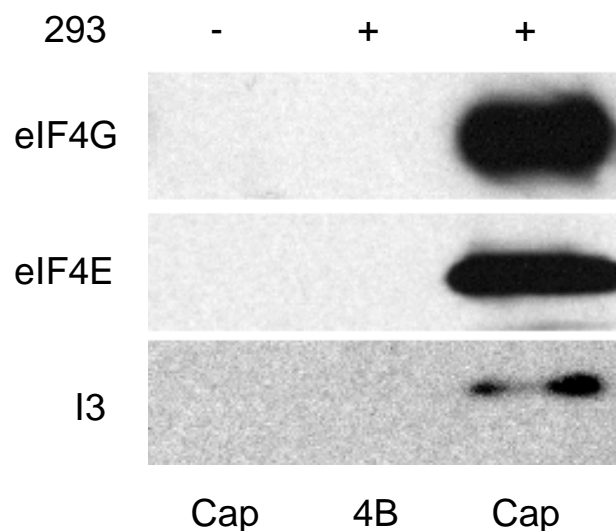
Figure 3.3.16 Immunoblot illustrating cap-bound complexes isolated from HEK-293 cell extracts and incubated with his-I3. (Cap = 7-Methyl GTP-sepharose 4B; 4B = sepharose 4B)

3.3.6 Investigation of I3-eIF4G interaction by *in vitro* binding assays

The previous experiments demonstrated that I3 interacts with eIF4F complexes in infected or uninfected cells, while purified his-I3 interacted with eIF4F from uninfected cell extracts. To examine whether I3 binds to eIF4G directly or whether it involves other factors that mediate indirect I3-eIF4G interaction, *in vitro* binding reactions were carried out. Three different fragments of GST-eIF4G were used in this experiment to define regions of binding, and because full length eIF4G is difficult to purify.

Three GST-tagged fragments of eIF4G: N-(aa157-626), M-(aa627-1045) and C-(aa1045-1560) terminal, were used in the assay (Cuesta *et al.*, 2000). Schematic representation of the regions is shown in figure 3.3.17, which also indicates the binding domains for PABP, eIF4E and RNA. To perform the assay, each of the fragments was isolated from benzonase – treated BL21 cells, and purified with glutathione-sepharose 4B. The presence of the proteins was then confirmed by performing gel electrophoresis and coomassie brilliant blue staining (not shown).
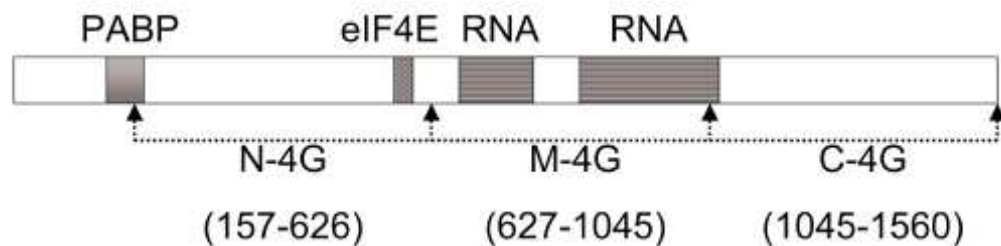
Figure 3.3.17 Schematic representation of the GST-tagged N-, M- and C-terminal regions of eIF4G. (The corresponding amino acid numbers of each fragment are indicated in brackets).

3.3.6.1 *In vitro* binding reactions with eIF4G fragments

To perform the binding assay purified proteins were incubated together with glutathione-sepharose which recovers GST-tagged complexes from the reaction buffer. 200 ng his-I3 was incubated for 2 hours with either dialysis buffer alone, to provide a control for the samples containing eIF4G, or together with 1 µg of each GST-tagged eIF4G fragment. The resin-bound complexes were then washed and analyzed by western blotting.

As illustrated in figure 3.3.18, each of the eIF4G fragments was evidently recovered from the reaction buffer with similar efficiency. However, while I3 was present at identical levels in input samples, it was found to bind specifically to the C-terminal fragment of eIF4G in Glutathione-sepharose samples.
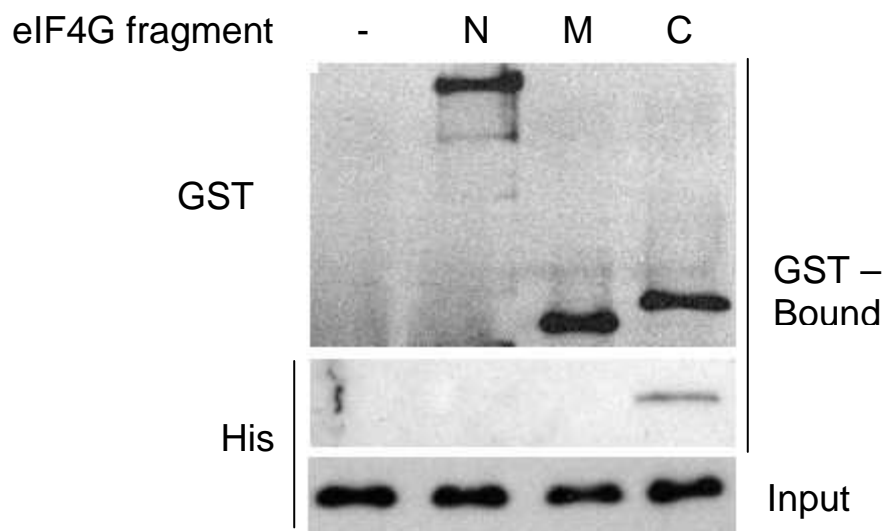
Figure 3.3.18 Immunoblot illustrating association of his-I3 with N-, M- and C-terminal fragments of eIF4G. Samples were probd with anti-GST (GST) or anti-His (His) antibodies.

This result clearly demonstrates that viral I3 associates with eIF4G protein through direct interaction. Moreover, it indicates that the location of I3-binding site on eIF4G

differs not only from PABP- and eIF4E-binding domains which are located on the N-terminal fragment of eIF4G, but also from binding domains for RNA situated largely in the M-fragment, demonstrating that I3 association did not involve the nucleic acid-binding regions of eIF4G.

3.3.7 *In vitro* binding reactions with I3 fragments

3.3.7.1 Generation of I3-fragments

To identify the region of I3 involved in its association with C-terminal fragment of eIF4G, binding reactions were performed using five different fragments of I3, that was serially deleted in its C-terminal region by approximately 50 amino acids each time (Fragments 1-4) or deleted in its N-terminus by 59 amino acids (Fragment 5) (Fig. 3.3.19) during PCR amplification. The PCR products were confirmed by agarose gel electrophoresis (Fig. 3.3.20). The sizes of the newly amplified I3 fragments are indicated in table 3.3.1. Each fragment was purified, digested and his-tagged by ligation into pET-15b plasmid. The plasmids were then transformed into BL21 cells, and proteins purified as described in Section 3.2.7.1.
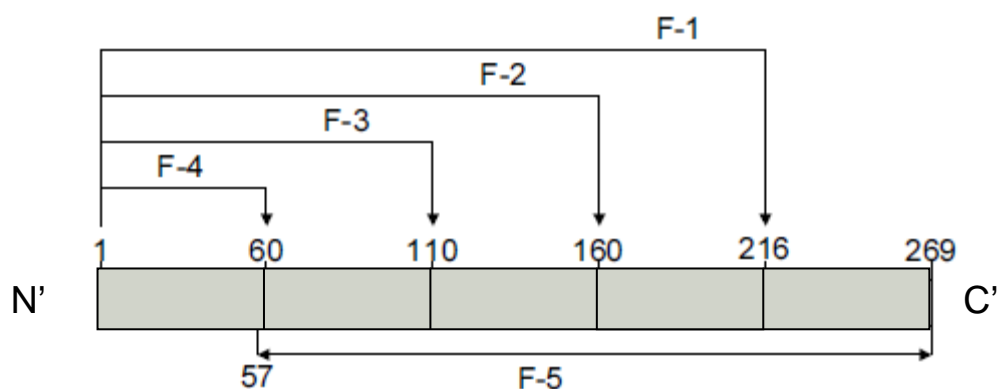
Figure 3.3.19 Schematic representation of the full-length I3 and its corresponding fragments together with their amino acids.

Table 3.3.1 The sizes (in base pairs [bp]) of full length (FL) I3 and its fragments (F1-F5)

I3 fragment	Size [bp]
FL	807
F1	648
F2	480
F3	330
F4	180
F5	636
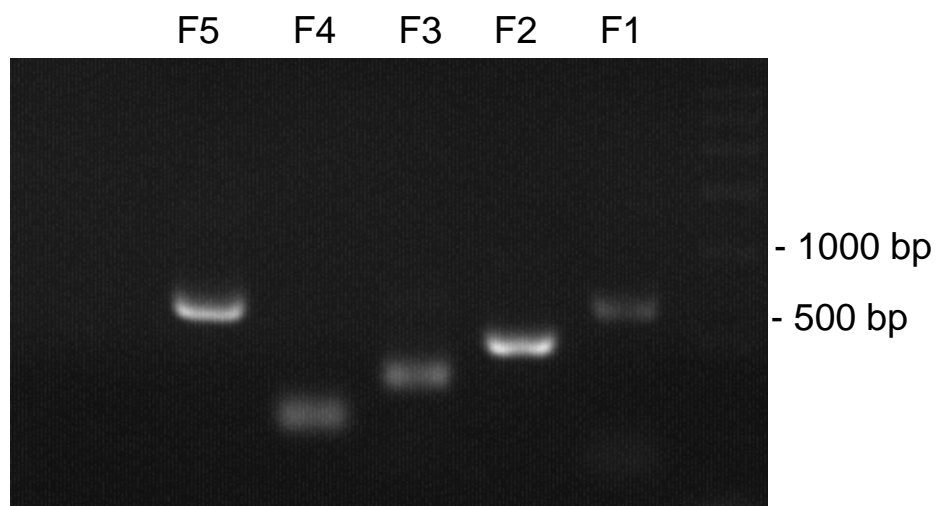
Figure 3.3.20 Gel electrophoresis image showing PCR-amplified I3 fragments F1-F5.

3.3.7.2 *In vitro* binding reactions

To examine which fragment(s) of his-I3 interacts with eIF4G, glutathione-sepharose and GST-tagged C-terminal eIF4G (C-4G) were incubated together with dialysis buffer alone, to provide the control sample, or containing full-length or truncated his-I3. Two independent preparations of full-length I3 were used in this assay (#1 and #2). The results from sample analysis by western blotting, using anti-his and anti-GST antibodies to detect I3 fragments and C-4G, are illustrated in figure 3.3.21. As can be seen on the immunoblots, C-4G was efficiently recovered on glutathione-sepharose in each sample. Both full-length I3 fragments were also recovered with C-4G, although differences in their abundance were noticed, more clearly illustrated in the lighter exposure of the input samples (lower panel). Furthermore, one of the I3 fragments labeled F1 (aa1-216) also bound to C-4G. Despite its low abundance compared to other fragments and seen in input samples, F1 clearly bound to C-4G suggesting that I3 associates with eIF4G by its C-terminal 160-216 fragment (Fig. 3.3.22). However, binding was not restored in F5, which contains that 160-216 domain. Possible reasons for this finding are discussed in Section 4.
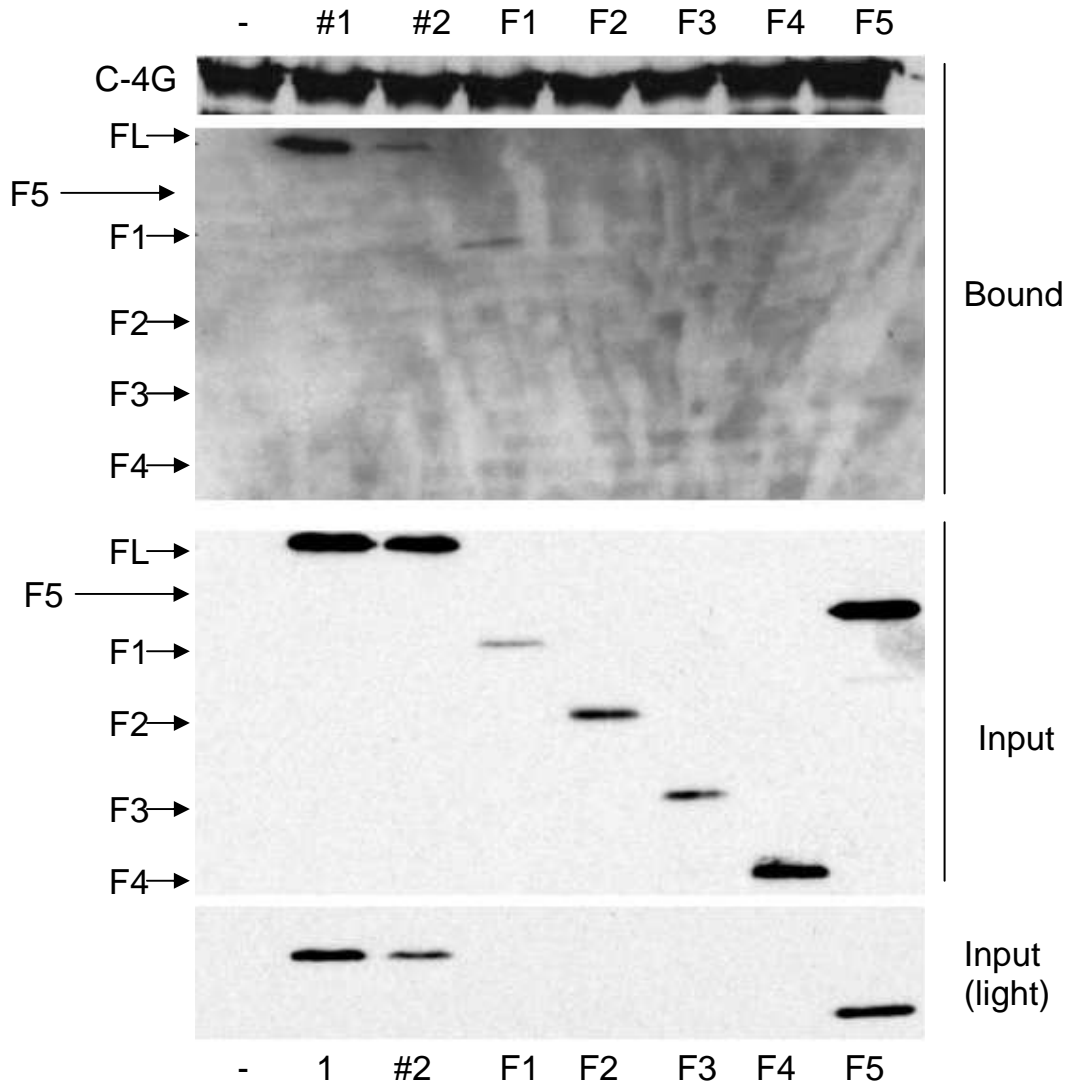
Figure 3.3.21 Immunoblot illustrating the binding reactions of I3 Fragments 1-5 with C-terminal eIF4G. (#1, #2 – full-length (FL) I3 from two independent preparations; F1-F5 – I3 fragments)
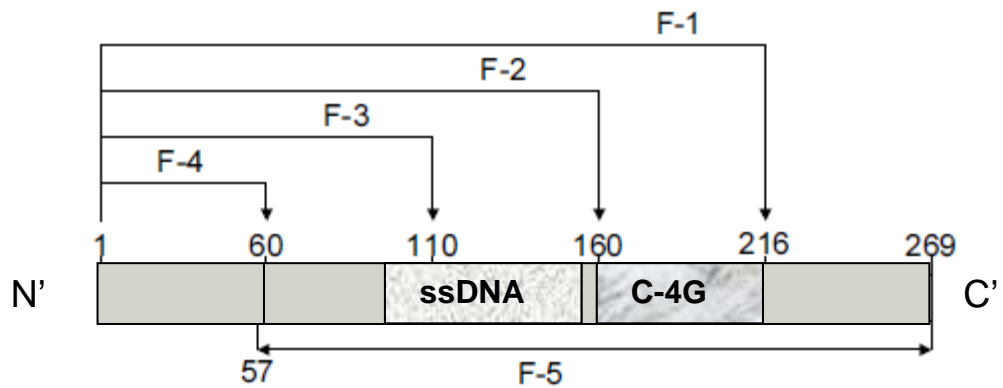
Figure 3.3.22 Schematic representation of the full-length I3 and its corresponding fragments indicating I3 binding site for eIF4G and ssDNA.

3.3.8 The role of mTORC1 in I3 binding to eIF4F

As mentioned before, mTORC1 is a complex regulating eIF4G phosphorylation as well as the activity of the translational repressor 4E-BP1. Furthermore, mTORC1 controls eIF4F complex formation by indirect regulation of eIF4E availability through 4E-BP1. Thus, its role in mediating the binding of viral I3 to cellular eIF4G/eIF4F was examined by treating the cells with rapamycin, the mTORC1 inhibitor. Binding was studied by 7-Methyl GTP-sepharose chromatography and immunoprecipitation assays.

3.3.8.1 Rapamycin effect on I3-eIF4F interaction

HEK-293 cells were infected overnight in the presence of 2 µM rapamycin or DMSO solvent control, then 7-Methyl GTP-bound complexes were recovered from RNAseA-treated soluble cell extracts, and associated proteins were analyzed by western blotting using antisera against eIF4G, eIF4E and I3. HEK-293 cells were used because viral infection has little effect on eIF4F levels in many actively cycling transformed cell lines where-in initiation complexes are largely pre-assembled (Walsh and Mohr, 2004), eliminating the complexity of analyzing potential differences in I3 binding under conditions where eIF4F levels were also significantly altered.

As shown before (see section 3.2.2), rapamycin treatment effectively prevented 4E-BP1 phosphorylation and release stimulated by VacV infection in both cap-bound and input samples (Fig. 3.3.23), but had no significant effect on eIF4F complex levels and the accumulation of I3 in infected cell extracts. In contrast, eIF4F-bound I3 was reduced approximately 3-fold in rapamycin-treated cultures. These findings demonstrated that maximal I3 binding to the eIF4F complex required cellular mTORC1 activity, although significant amounts of I3 remained associated with eIF4F in the presence of rapamycin.

Increasing volumes (1x and 2.5x) of input samples, shown in Fig. 3.3.23, were probed with anti-I3 antiserum to confirm quantitative antigen detection on blots, and minimal effects of rapamycin on I3 accumulation compared to its effects on association with eIF4F.
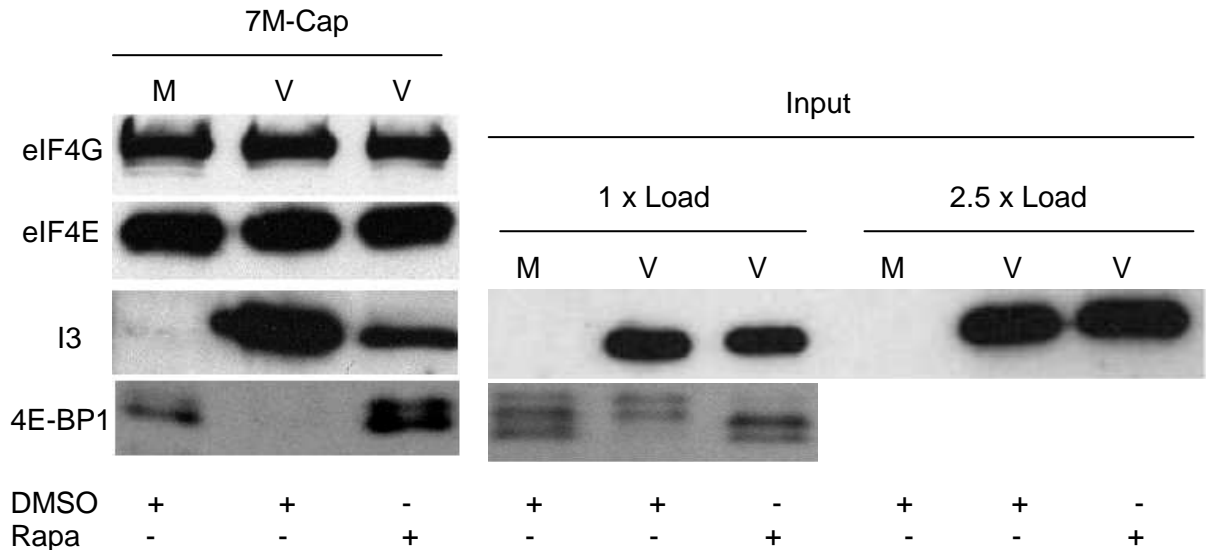
Figure 3.3.23 Immunoblot illustrating the influence of rapamycin on I3 binding to eIF4F complex. (M = mock, V = VacV-infected, Rapa = rapamycin)

To investigate this further, the effect of rapamycin on I3-eIF4F interaction was examined by binding assay using uninfected cell extracts. As demonstrated before, recombinant I3 interacts with eIF4F complexes purified from HEK-293 cell extracts using 7-Methyl GTP-sepharose 4B. To examine if mTORC1 inhibition affects this interaction, the same binding assay was performed using extracts prepared from HEK-293 cells treated with DMSO solvent control or 2μM rapamycin overnight, and the samples were analyzed by western blotting. As shown in figure 3.3.24, mTORC1 inhibitor reduced the efficiency of I3 binding. Notably, the effects on I3 binding and changes in 4E-BP1 association mediated by rapamycin were smaller than that in

infected cells. This result confirmed that the effect of rapamycin on the association of I3 with 7-Methyl GTP-bound complexes was not limited to the context of infection.
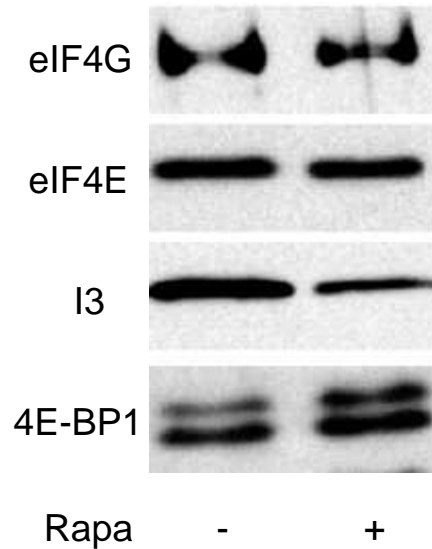
Figure 3.3.24 Immunoblot illustrating the effect of 2 µM rapamycin on I3-eIF4F interaction in HEK-293 cell extracts. (Rapa = rapamycin)

3.3.8.2 Rapamycin effect on I3-eIF4G association

To examine if inhibition of mTORC1 affects the association of I3 with eIF4G during VacV infection, the immunoprecipitation of anti-eIF4G and anti-I3 bound complexes from cell extracts was carried out. To avoid background noticed on western blots after probing for I3 in eIF4G immune complexes (data not shown), the association of these two proteins was determined by metabolic labeling of the cells, as described in section 3.3.1.

HEK-293 cells were mock or VacV-infected at moi 5 in the presence of DMSO solvent control or 2 µM rapamycin, then labeled with [^{35}S]methionine-cysteine for 1 h before making cell extracts. VacV replicates relatively fast in those actively dividing cells, thus

the infection was ended after 8 hours, when I3 was still actively synthesized and readily

detectable (see timecourse in section 3.1). Cells were lysed in NP-40 Buffer, nuclease

treated and precleared with normal rabbit serum. After that samples were divided in two

and immunoprecipitated with either anti-eIF4G or anti-I3 antiserum. The levels of

eIF4G and eIF4F were analyzed by western blotting, while I3 levels were examined by

exposing fixed and dried gel on X-ray film.
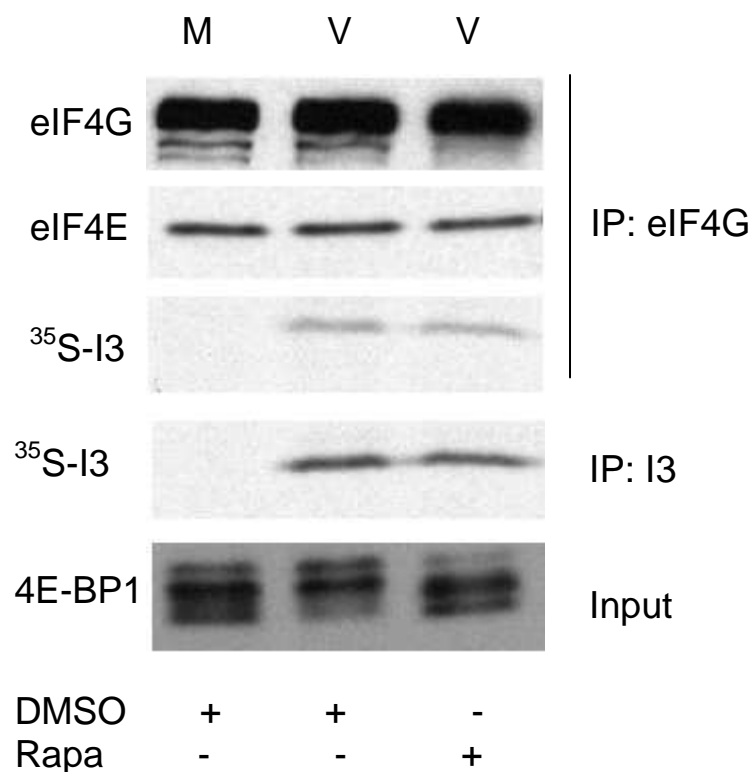
Figure 3.3.25 Immunoblot illustrating the influence of rapamycin on I3 association with eIF4G complex. (M = mock, V = VacV-infected, Rapa = rapamycin)

As demonstrated in Fig. 3.3.25, the same amounts of eIF4G were recovered with anti-

eIF4G bound complexes, and rapamycin did not affect the levels of eIF4E associated

with eIF4G in infected cells, in agreement with our previous findings that eIF4F levels

were not affected by rapamycin treatment in HEK-293 cells in cap-bound complexes

(Fig. 3.3.23). However, rapamycin did not affect I3-eIF4G binding in recovered anti-eIF4G complexes (Fig. 3.3.25), whereas it did decrease the amounts of I3 bound to eIF4F in 7M GTP-sepharose assay (Fig. 3.3.23). In addition, intensity of I3 signal remained unchanged also in anti-I3-immunoprecipitated samples (Fig. 3.3.25), indicating that there were no differences in the rates of I3 synthesis that could influence the interpretation of the I3-eIF4G binding assay. Failure of rapamycin to inhibit mTORC1 in this particular experiment was also excluded as analysis of the input samples by western blotting demonstrated that rapamycin effectively blocked 4E-BP1 phosphorylation (Fig. 3.3.23).

3.3.9   Investigation of possible I3-eIF4E interaction

The previous experiments demonstrated that I3 binding to eIF4F, but not accumulation was reduced by approximately 3-fold in rapamycin-treated cultures (Fig. 3.3.11), and that the association of I3 with 7-Methyl GTP-bound complexes was not limited to the context of infection (Fig. 3.3.12). In addition, in both cases the effects of rapamycin on I3 binding were proportional to the changes in 4E-BP1 binding to the cap, while no changes in eIF4G binding were observed. Therefore, the association of I3 with the 4E-BP1 binding partner - eIF4E, was considered and investigated in the following experiment.

First of all, eIF4E was batch-purified from BL21 cells on 7-Methyl GTP as described in Section 2. Then purified eIF4E was incubated for 1h with 200 ng his-I3, and the samples were analyzed by western blotting using anti-eIF4E and anti-I3 antisera. Figure 3.3.26 shows that while I3 did not associate with 7-Methyl GTP resin alone, it was recovered with the cap in the presence of eIF4E suggesting an I3-eIF4E interaction.

Subsequently, the ability of I3 to associate with eIF4E in the presence of eIF4G was examined. Since eIF4E interacts with the N-terminal fragment of eIF4G, the N-4G (aa157-626) used in the previous experiments was used to test the binding. Increasing amounts of a GST-fused N-4G was added into the binding reactions containing 7-Methyl GTP-associated eIF4E and his-I3, and samples were analyzed by immunoblotting using anti-GST and anti-His antisera. As can be seen in figure 3.3.26, inclusion of N-4G did not affect the I3 binding to cap complexes, suggesting that I3 association with eIF4E was not competitive at least for the large N-terminal fragment of eIF4G containing the eIF4E binding site.
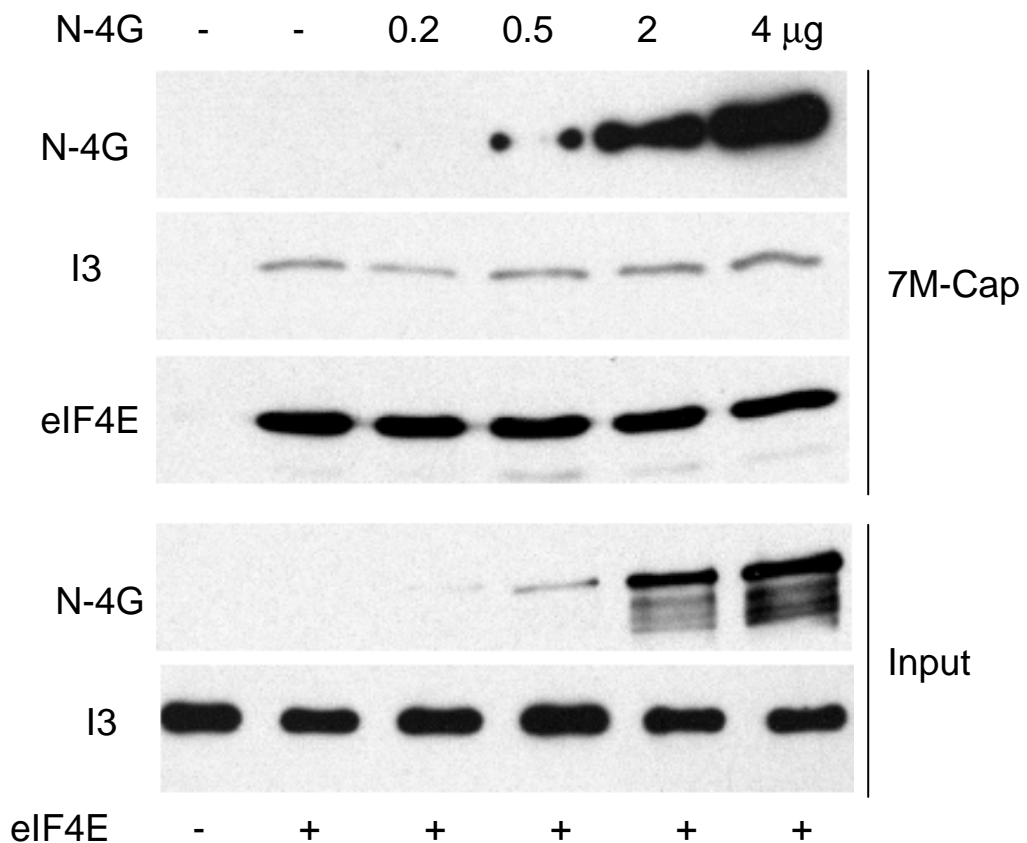
Figure 3.3.26 Immunoblot illustrating the I3 association with eIF4E in HEK-293 cells. N-4G was detected with anti-GST antibody, I3 was detected with anti-His antibody, eIF4E was detected with anti-eIF4E antibody. 7M GTP Sepharose alone (-) or batch absorbed with eIF4E (+) is indicated at the bottom of the panel.

3.3.10 Inhibition of viral DNA polymerase by PAA and its influence on translation

Our findings to date suggested that mTORC1 was activated by VacV and the viral protein I3 binds eIF4G and possibly eIF4E, also. We then examined the stage of viral infection at which these events occur by using PAA.

Phosphonoacetic acid (PAA) is an organophosphorus compound that inhibits DNA polymerase. PAA preferentially inhibits viral but not essential eukaryotic DNA polymerases, which is the basis for the therapeutic use of this drug as an antiviral agent. There are many antibiotics and synthetic compounds that inhibit synthesis of DNA, such as oligomycin and chromomycin (Ward *et al.*, 1965). However, these inhibitors interfere with DNA synthesis by forming a complex with template DNA. This type of interaction lacks specificity and results in inhibition of all DNA-primed enzymes. In contrast, PAA was shown not to interact with template DNA (Mao *et al.*, 1975). The mechanism of blocking DNA synthesis appears to be similar in all types of viruses. PAA binds to the pyrophosphate exchange site of DNA polymerase and blocks formation of the 3'-5'-phosphodiester linkage, which prevents further elongation of viral DNA (Leinbach *et al.*, 1976).

PAA was found to inhibit the replication of a variety of animal viruses such as herpes simplex virus (Shipkowitz *et al.*, 1973), cytomegalovirus (Huang, 1975), vaccinia virus (Bolden *et al.*, 1975), Marek's disease virus (Leinbach *et al.*, 1976), Epstein-Barr virus (Nyormoi *et al.*, 1976), and African swine fever virus (Moreno *et al.*, 1978). In addition, Overby *et al.* (1977) noted that this drug reduced VacV plaque formation, although the level of inhibition was lower than that observed with herpesviruses. PAA was also shown to block the formation of viral factories, the distinct compartments of VacV replication, and to reduce 4E-BP1 phosphorylation during VacV infection, leading to

the suggestion that late gene products or viral factory formation may be involved (Walsh *et al.*, 2008). However, the full effect of this inhibitor on eIF4F complex formation has not been explored so far.

3.3.10.1 The effect of PAA on eIF4F complex formation

To examine the effect of PAA on eIF4F complex formation in more detail, 7-Methyl GTP-sepharose chromatography assay was performed. Serum-starved NHDFs, cells in which assembly of eIF4F during VacV infection is readily detected, were mock-infected or infected with VacV in the presence or absence of PAA, and the levels of eIF4E-bound eIF4G and 4E-BP1 were examined as described before (Section 3.3.3).

As reported previously, VacV infection stimulated 4E-BP1 phosphorylation and release from eIF4E, and increased the binding of eIF4G to eIF4E. In contrast, PAA did not significantly alter the ability of VacV to release 4E-BP1 from eIF4E, although it did affect the mobility of 4E-BP1 in input samples (Fig. 3.3.27). This suggested that the turnover or rate of 4E-BP1 phosphorylation was affected by PAA, but not enough to affect release from eIF4E. In agreement, PAA only partly reduced the phosphorylation of Akt at either T308 or S473 (Fig. 3.3.28). However, PAA significantly reduced VacV-induced enhancement of eIF4G binding to eIF4E, demonstrating that eIF4F complex formation was stimulated at late stages of infection in conjunction with DNA replication and viral factory formation.
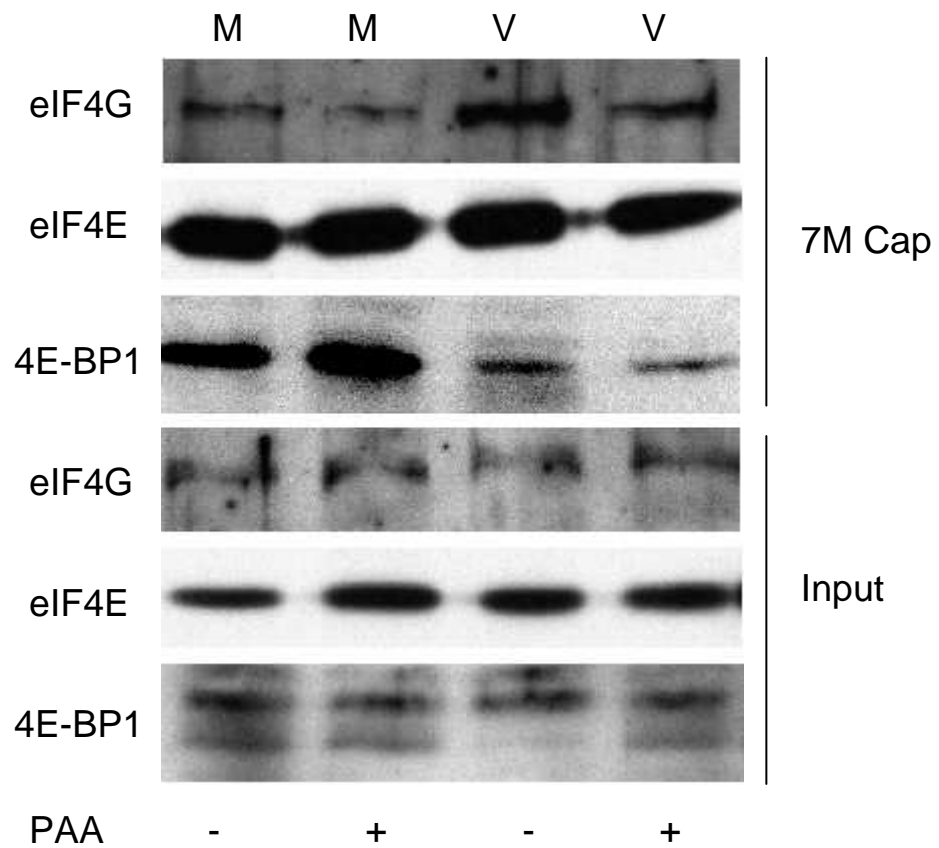
Figure 3.3.27 Immunoblot illustrating the effect of PAA on eIF4F complex formation in mock and VacV-infected serum-starved NHDFs. (M = mock, V = VacV-infected)
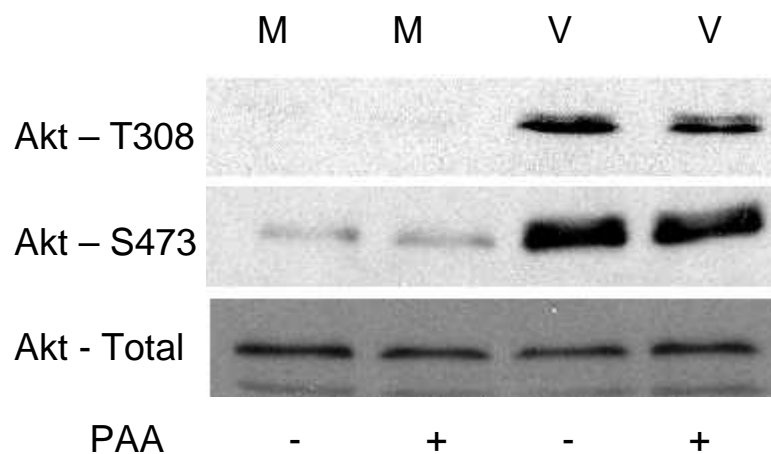
Figure 3.3.28 Immunoblot illustrating the effect of PAA on Akt phosphorylation in mock and VacV-infected NHDFs. (M = mock, V = VacV-infected)

3.3.10.2 The effect of PAA on I3 binding

We then examined whether PAA affected I3 binding to eIF4F complexes. HEK-293 cells were used in this experiment as infecting NHDFs in the presence of PAA caused changes in eIF4F levels that would complicate the interpretation of binding results. HEK-293 cells were pretreated with PAA and mock-infected or infected with VacV for 16 hours. Soluble cell extracts were treated with RNAse and a cap-pulldown assay was performed. Input and cap-bound samples were analyzed by western blotting (Fig 3.3.29 a). I3 binding to eIF4F was not affected by PAA, demonstrating that it was bound to eIF4F early in infection. Western blotting of input samples against VacV proteins demonstrated that PAA had worked to block late stages of VacV infection (Fig. 3.3.29 b). This suggested that I3 bound to eIF4F early in infection but that eIF4F assembly in NHDFs required late stage events.
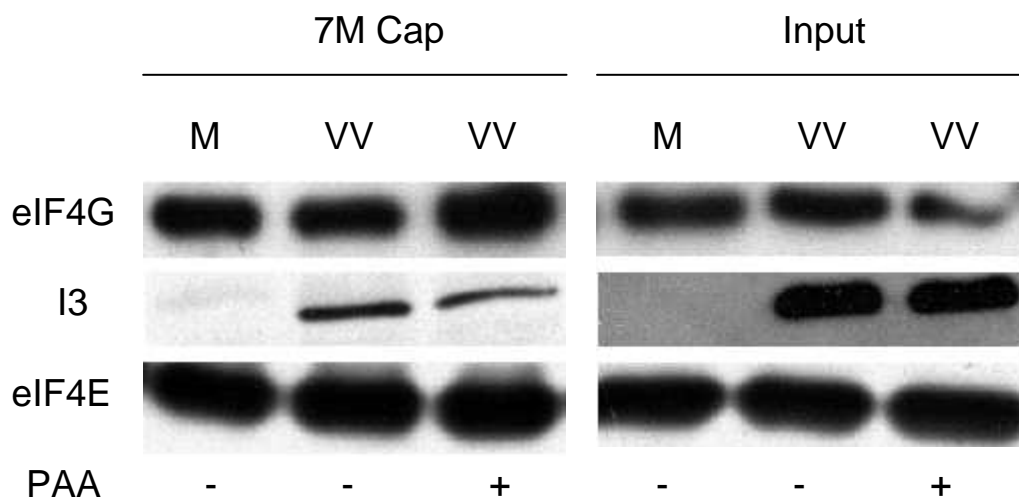
Figure 3.3.29 (a) Immunoblot illustrating the effect of PAA on I3 binding to eIF4F in VacV-infected HEK-293 cells.
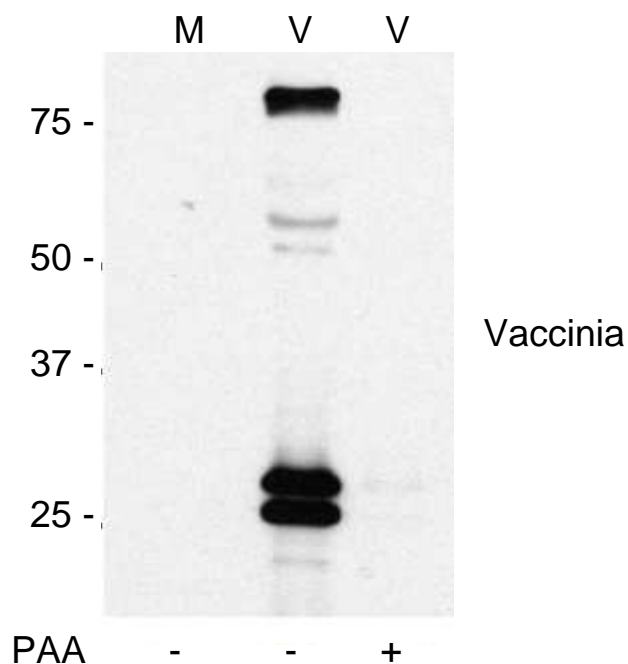
Figure 3.3.29 (b) Immunoblot illustrating the effect of PAA on the total VacV protein accumulation. (M = mock, V = VacV-infected)

3.3.10.3 The effect of PAA on VacV protein synthesis

Next, the synthesis of VacV proteins in the presence of PAA was examined. Serum-starved NHDFs were pre-treated for 1 h with PAA, then infected at moi 10 and metabolically labeled at 18-19 hpi followed by lysing in Laemmli buffer. The cell extracts were resolved by SDS-PAGE and fixed, dried gels were exposed to x-ray film.

Analysis of the proteins actively translated during the labeling time showed that although PAA notably decreased cellular protein production, it effectively blocked the synthesis of viral proteins, as illustrated in figure 3.3.30. This result indicates the significance of DNA synthesis in VacV replication and protein synthesis.

PAA treated samples showed that some viral proteins were actively translated while the virus failed to completely shut down host translation. It is possible that more complete

host shut-off needs the formation of viral factories where translation factors are sequestered.
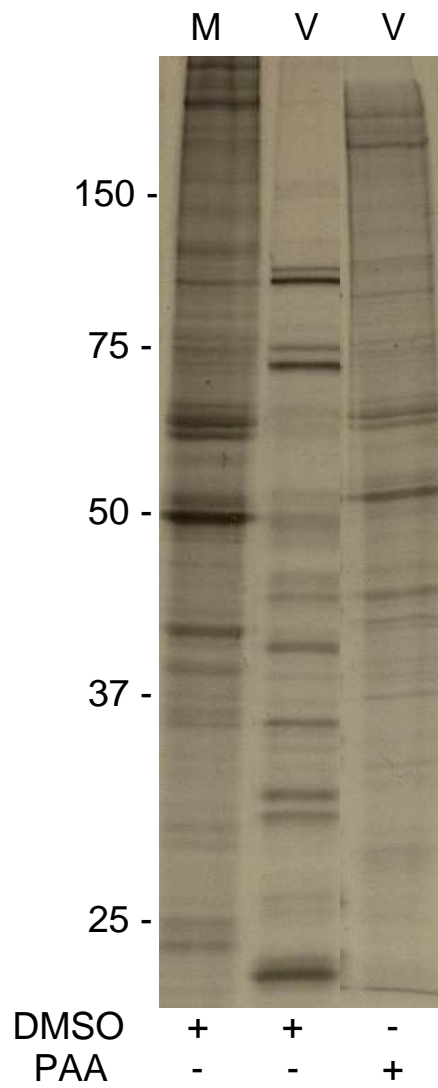
Figure 3.3.30 Autoradiograph illustrating the PAA effect on the total rates of VacV protein synthesis. (M = mock, V = VacV-infected)

3.3.11 The effect of I3 on cellular translational rates

To determine if I3 affected cellular translational rates, the control HEK-293 cells and cells expressing recombinant I3 (FLAG-I3) were metabolically labeled for 1 h and analyzed by SDS-PAGE. Figure 3.3.31 demonstrates that no significant differences in the pattern or rates of cellular protein synthesis were observed.
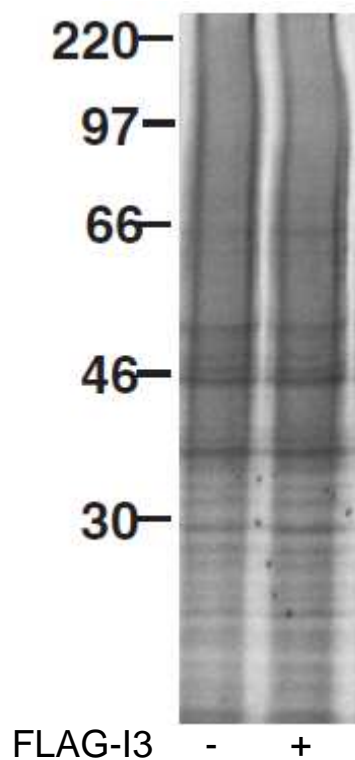
FLAG-I3   -   +

Figure 3.3.31 Autoradiograph illustrating the I3 effect on cellular protein synthesis in metabolically labeled empty vector control (-) and FLAG-I3 (+) HEK-293 cells. Migration of molecular weight standards (in kDa) is indicated to the left.

3.3.12 The effect of I3 on translation of viral RNA *in vitro*

To examine the effect of I3 on viral translation, initially RNA was isolated from VacV-infected HEK-293 cells. Next, rabbit reticulocyte lysates containing ^{35}S-Methionine were programmed with 10 μg of total RNA isolated from infected cells in the presence of dialysis buffer alone or 200 ng purified his-I3, and the reactions were incubated at 30^0C for 1h. After that the samples were boiled with equal volumes of 2x Laemmli buffer (the experiment to this stage was performed by Dr. Derek Walsh) and resolved by SDS-PAGE. The gels were fixed, dried and exposed to x-ray film. As shown in figure 3.3.32, the presence of I3 in *in vitro* translation reactions did not significantly affect the rates or patterns of viral protein synthesis.
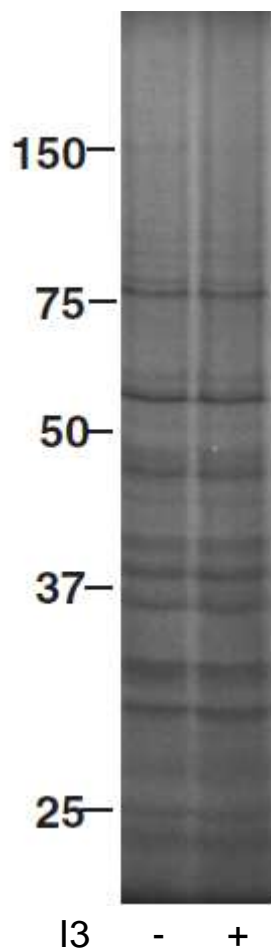
Figure 3.3.32 Autoradiograph illustrating the effect of recombinant I3 on translation of VacV RNA. Migration of molecular weight standards (in kDa) is indicated to the left.

3.3.13 Recruitment of translational factors to ssDNA

We have shown that VacV-encoded I3 binds eIF4F in a PAA-insensitive manner yet eIF4G assembly and host shut-off were sensitive to PAA. It has been shown previously that eIF4G and eIF4E (Walsh *et al.*, 2008) as well as I3 (Rochester and Traktman, 1998) redistribution are sensitive to inhibitors of DNA replication, which prevent viral factoy formation. Indeed, we demonstrated that eIF4G and I3 co-localize within factories. These findings suggest that I3 may not directly stimulate eIF4F formation but may act to retain eIF4F in factories once they form.

As demonstrated earlier in this study, exogenously-expressed I3 associates with eIF4F in uninfected cells. Accumulation of I3 in factories is thought to be due to its binding to ssDNA, retaining it there. Thus, the possibility that I3 can mediate the recruitment of translation initiation factors to ssDNA *in vitro* was examined, mimicking what might happen in viral factories.

Soluble cell extracts were prepared from FLAG-Actin- and FLAG-I3-expressing HEK-293 cells, and a binding assay with recovering DNA on anti-biotin antibody-conjugated sepharose was carried out, as described in Section 2. The samples were then analyzed by immunoblotting using anti-eIF4G, anti-PABP, and anti-I3 antibodies. The results illustrated a low level of eIF4G bound to ssDNA in control extracts with FLAG-actin (Fig. 3.3.32). However, in the presence of I3 large amounts of eIF4G were recovered. Similarly to eIF4G, significantly greater amounts of PABP were also bound to the beads in the presence of I3.

To verify the specificity of translation factor recruitment by I3 the association of RBM3 was examined in the same samples. RBM3 is a cellular protein with both RNA and ssDNA binding properties that has been shown to potentially interact with VacV A2

protein, but not I3 (Derry *et al*., 1995; Dellis *et al*., 2004). While RBM3 was found

associated with ssDNA in both extracts its association was modestly reduced in I3

samples comparing to control extracts (Fig. 3.3.33), probably as a result of competition

for binding from I3 itself.
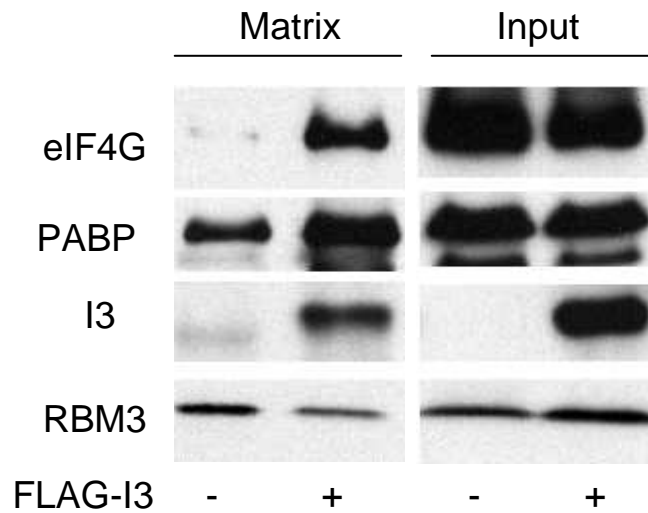
Figure 3.3.33 Immunoblot illustrating recruitment of translation factors to ssDNA by I3.

These results suggested that I3 did not directly influence translation of cellular or viral

mRNAs but is likely to play a role in the redistribution of factors to viral factories

during infection.

3.3.14 Creating a VacV mutant lacking the I3L gene

As a final point of this study we aimed to determine a role for I3 in regulating translation and manipulation of the eIF4F complex during infection. Previous attempts to generate I3L mutants by recombination were unsuccessful (Rochester and Traktman, 1998). We attempted to create a viral mutant lacking the I3L gene using a novel DH10B/Vac-Bac/λ system established by Domi and Moss (2005). The DH10B/Vac-Bac/λ system is a bacterial artificial chromosome (BAC) containing the entire VacV genome engineered in *Escherichia coli* by homologous recombination, using bacteriophage λ-encoded enzymes that mediate recombination process. This system uses recombinogenic engineering technology, which avoids the use of restriction enzymes or ligases and allows efficient recombination of BACs maintained in *E. coli* (Copeland *et al.*, 2001; Britt *et al.*, 2004). The system contains a mini-λ prophage encoding the *red* recombination system composed of 5' to 3' exonuclease (Exo), a single-strand DNA binding protein (Bet) and a nuclease inhibitor (Gam), under the control of the temperature-sensitive λ *c*I857 repressor (Yu *et al.*, 2000; Court *et al.*, 2002).

3.3.14.1 Deletion of the I3L ORF

The I3L ORF was deleted from the VAC-BAC plasmid in two steps. In the first step I3L ORF in the VAC-BAC plasmid was replaced with the ampicillin (Amp) resistance gene by recombination in *Escherichia coli*. The Amp gene was amplified from pET plasmid by PCR using primers containing approximately 18 bp of the 5' and 3'end of the Amp gene and 50 bp of homologous sequences flanking the region where I3L overlaps the adjacent I2L or I4L genes. Analysis of the PCR product by agarose gel

electrophoresis confirmed the amplification of the Amp gene with the expected size of
approximate 700 bp (Fig. 3.3.34).
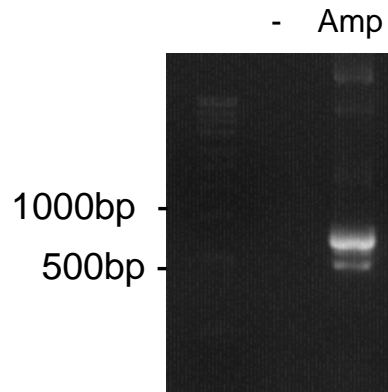
Figure 3.3.34 Gel electrophoresis image showing PCR-amplified Amp gene containing the
homologous sequences flanking the region where I3 overlaps with the adjacent I2 and I4 gene.
(Amp = PCR amplified ampicillin)

The PCR product was then gel purified and used to transform competent *E.coli* cells
harboring VAC-BAC plasmid/λ (cells preparation described in Section 2) through
electroporation, and ampicillin-resistant colonies were selected to isolate recombinant
VAC-BAC that had taken up the Amp gene in place of I3.

To confirm the presence of Amp insert in the VAC-BAC plasmid, the PCR using the
Amp primers used for its amplification was performed (not shown). To confirm that the
Amp gene replaced the I3L ORF, PCR was performed on wildtype (WT) and
recombinant (ΔI3L) VAC-BAC DNA using primers flanking the I3 gene in VacV. As
can be seen in figure 3.3.35, the Amp ORF successfully replaced I3L ORF. The
difference in sizes of the products results from the fact that the Amp gene is larger than
I3L.
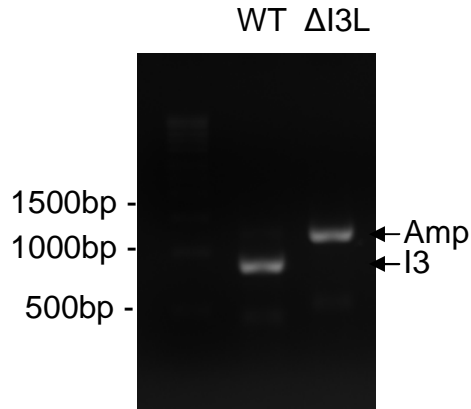
Figure 3.3.35 Gel electrophoresis image showing PCR-amplified sequences using primers in the adjacent I2 and I4 gene of VacV. (WT = wildtype VAC-BAC containing I3L gene, ΔI3L = recombinant VAC-BAC containing Amp gene in the place of I3L)

3.3.14.2 Attempting to recover ΔI3L mutant virus

The final step was to recover the infectious recombinant virus by transfecting BSC40 cells with the VAC-BAC-ΔI3L plasmid in a presence of 0.1 PFU per cell helper fowlpox virus (FPV). Because VAC-BAC plasmid does not contain viral enzymes needed to initiate replication, the fowlpox virus was used to provide the enzyme functions necessary. FPV is an avian poxvirus that does not replicate in mammalian cells and no recombination with the VacV genome was detected (Scheiflinger *et al.*, 1992). At 2 hpi cells were transfected with 1μg of the VAC-BAC or VAC-BAC-ΔI3L. Transfected cells were incubated at 37° C for several days. During that time, viral plaque formation was expected to be seen in the transfects.

After 5 days cytopathic effect and plaque formation were observed in cells transfected with wildtype VAC-BAC (two plaques can be seen in Fig. 3.3.36 a), but no cytopathic effect was seen either in the control well transfected with no DNA or in the cells containing VAC-BAC-ΔI3L up to 10 days post-transfection (Fig. 3.3.36 b). To test if

exogenously added I3 could rescue the VacV-ΔI3L mutant, cells were transfected with 1μg of VAC-BAC-ΔI3L and 1μg of his-tagged pCI-I3, but no cytopathic effect was observed up to 10 days post-transfection (Fig. 3.3.36 c). As can be seen in figures 3.37 a-c, extending incubation time up to 17 days resulted in increased cytopathic effect in cells containing wildtype VAC-BAC, demonstrating the production of infectious, replicating virus (Fig. 3.3.37 a), while still no signs of virus replication were noticed in the presence of ΔI3L mutant (Fig. 3.3.37 b-c). These results suggest the inability of VacV replication in the absence of I3L.

The experiment described above was carried out in two different types of cells (BSC40 and HEK-293) and with the use of two independent preparations of VAC-BAC and VAC-BAC-ΔI3L. Furthermore, three unsuccessful attempts of generation the VacV-ΔI3L mutant were carried out, but the virus lacking I3L gene did not replicate in the cells. Thus, our study confirmed the previous assumptions (Rochester and Traktman, 1998) that I3L is an essential poxvirus gene. However, it is possible that I3 contains unknown promoters that regulate I2 expression that are lost when I3 is replaced by the Amp gene. This is something we need to investigate further before dismissing this approach.

Furthermore, three independent siRNAs targeting the I3 mRNA failed to affect I3 accumulation in HEK-293 or HeLa cells (not shown). Thus, further analysis of the role of I3 in regulating translation in infected cells will require more competent methods to affect I3 expression during infection or the generation of partial deletions in I3L that might allow virus to be recovered.
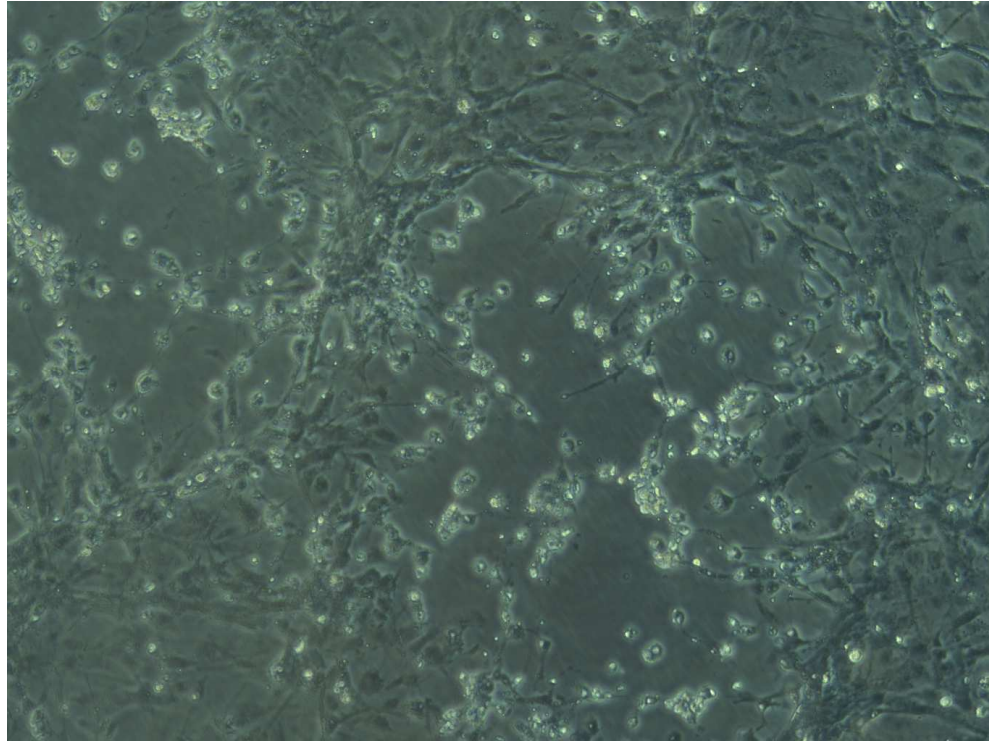
Figure 3.3.36 (a) Photograph of BCS40 cells transfected with VAC-BAC. Image was taken 10 days post-transfection by phase contrast microscopy.
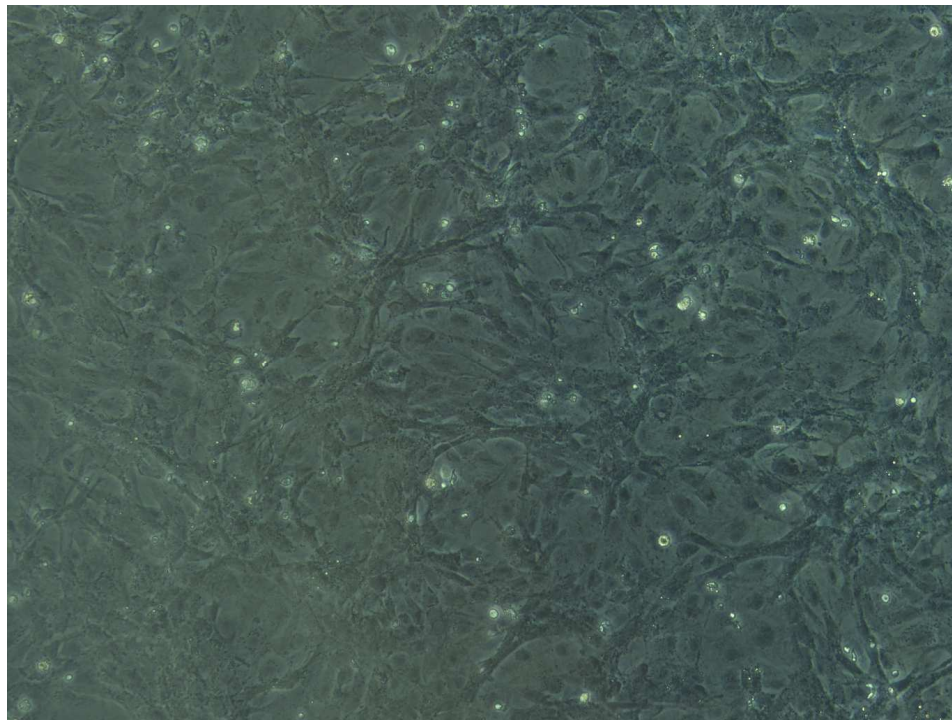
Figure 3.3.36 (b) Photograph of BCS40 cells transfected with VAC-BAC-ΔI3L. Image was taken 10 days post-transfection by phase contrast microscopy.
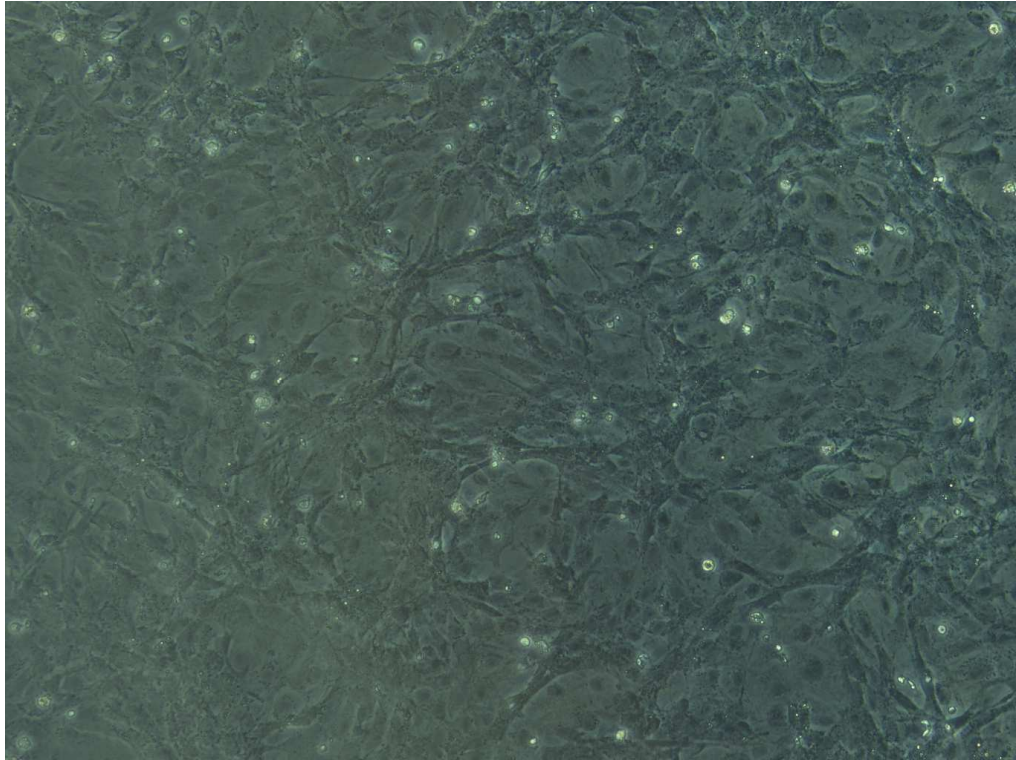
Figure 3.3.36 (c) Photograph of BCS40 cells transfected with VAC-BAC-ΔI3L and pCI-I3. Image was taken 10 days post-transfection by phase contrast microscopy.
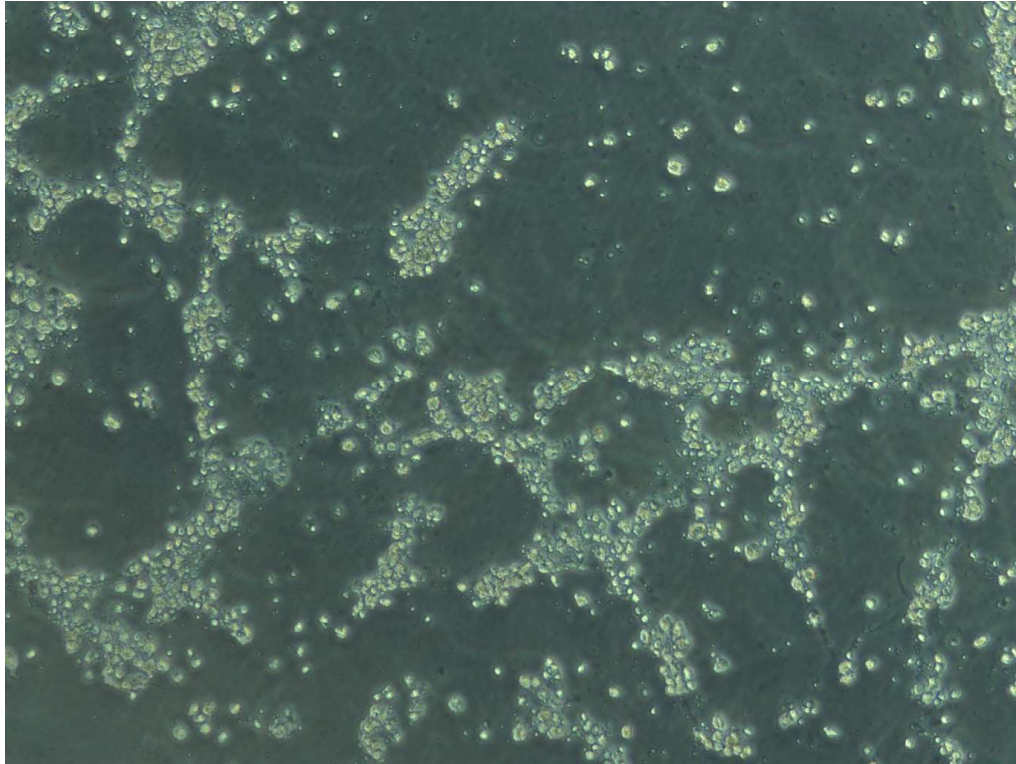
Figure 3.3.37 (a) Photograph of BCS40 cells transfected with VAC-BAC. Image was taken 17 days post-transfection by phase contrast microscopy.
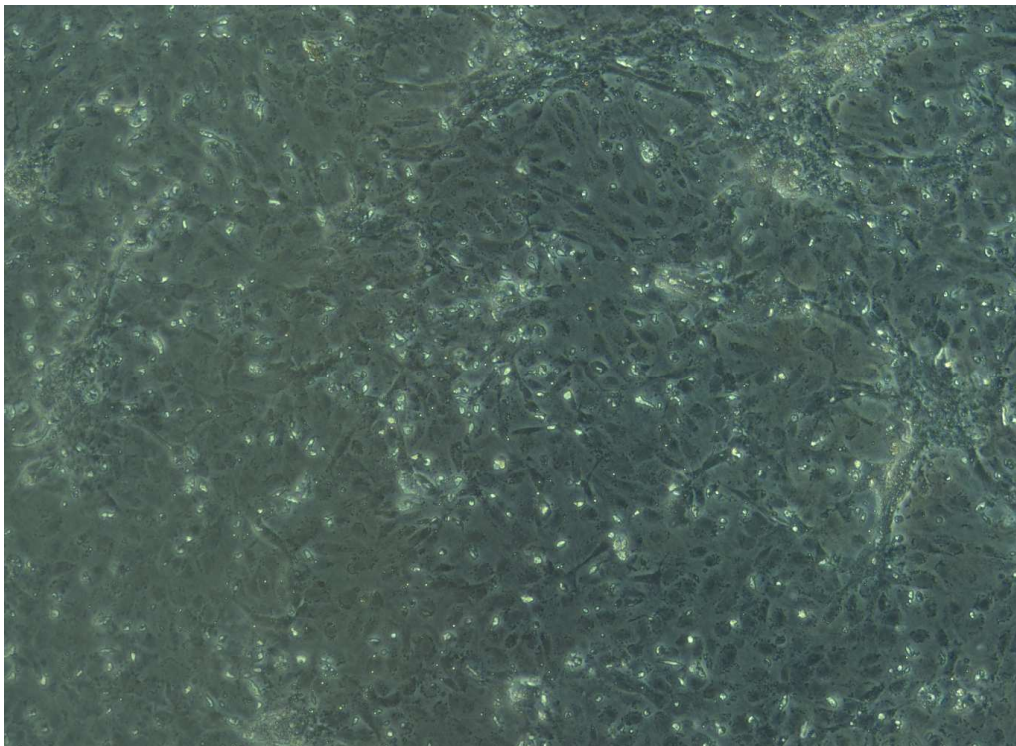
Figure 3.3.37 (b) Photograph of BCS40 cells transfected with VAC-BAC-ΔI3L. Image was taken 17 days post-transfection by phase contrast microscopy.
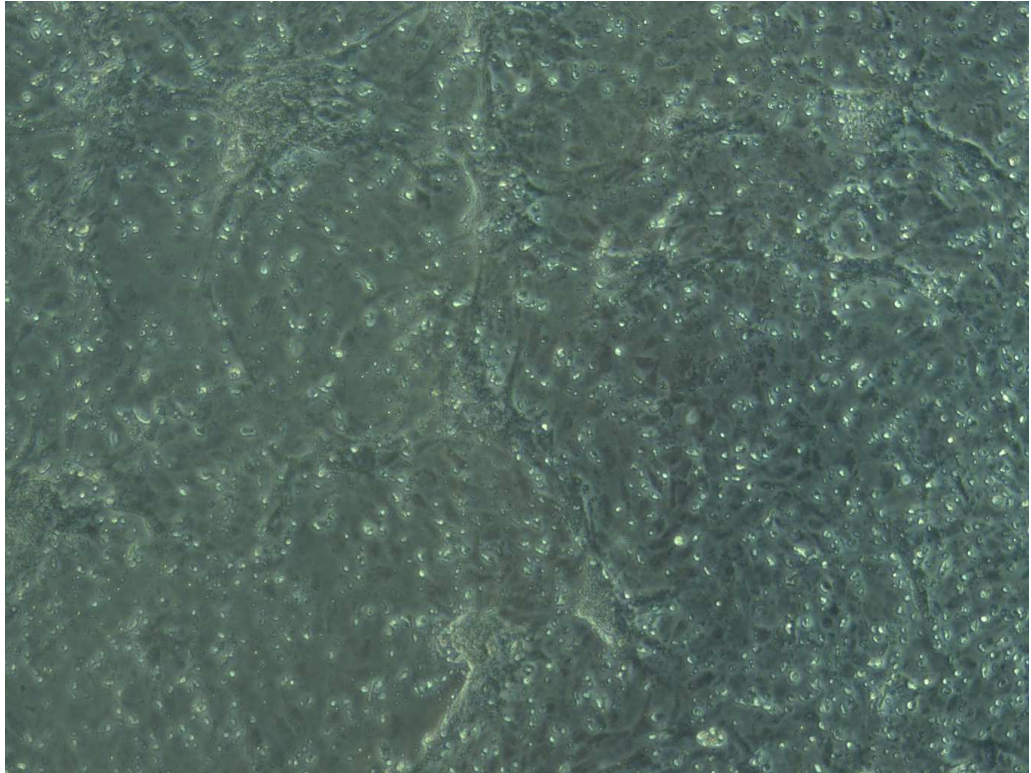
Figure 3.3.37 (c) Photograph of BCS40 cells transfected with VAC-BAC-ΔI3L and pCI-I3. Image was taken 17 days post-transfection by phase contrast microscopy.

Section 4.0

Discussion

4.1 General overview

Even the largest and most complex known viruses encoding hundreds of proteins remain dependent upon the host translational machinery. The reason is that viral genomes are not large enough to encode all of the factors necessary for translation, and viruses do not harbor functional ribosomes in their virions. Therefore, successful amplification of the viral genome requires competition between viral and cellular mRNAs for the host cell translation apparatus. As a result both RNA and DNA viruses developed a variety of sophisticated strategies to usurp host ribosomes.

A major target for all RNA and DNA viruses is eIF4F, a key translation initiation complex (Schneider and Mohr, 2003; Mohr *et al*., 2007). Depending on the strategy used by a particular virus, eIF4F can be completely inactivated or actively stimulated by viral factors. As such, in addition to modulating cellular signaling pathways that regulate host translation factor activity, a growing number of viruses are being found to encode proteins that directly interact with the eIF4F complex. Furthermore, a number of viruses have been shown to generate substitutes for particular translation initiation factors (Groft and Burley, 2002; Burgui *et al.*, 2007; Mir and Panganiban, 2008).

VacV was previously shown to dynamically stimulate the activity of the eIF4F complex to promote viral translation. VacV infection results in inactivation of the translational repressor 4E-BP1 and stimulation of eIF4E assembly into an active eIF4F complex. VacV was also found to stimulate the eIF4G-associated kinase Mnk1 to promote eIF4E phosphorylation and enhance viral protein synthesis and replication (Walsh *et al.*, 2008). Moreover, VacV infection causes redistribution of cellular translational factors to the viral replication sites (Katsafanas and Moss, 2007; Walsh *et al.*, 2008). However,

the strategies used by VacV to manipulate the eIF4F complex have not been established so far.

In this study we evaluated the signaling pathways that regulate assembly of eIF4F complexes in VacV-infected cells. Furthermore, we propose that VacV-encoded I3 protein plays a significant role in usurping cellular translational factors and their redistribution by VacV.

4.2 Signaling pathways regulating eIF4F complex assembly in VacV-infected cells

Manipulation of intracellular signaling pathways is important for successful viral replication. In the case of poxviruses, regulation of signaling pathways has been shown to play a pivotal role in the biology of these pathogens (de Magalhaes *et al.*, 2001; McFadden, 2005; Werden and McFadden, 2008). In addition, the strategies of altering signaling pathways appear to be virus specific and can differ within a virus family. For example, while both VacV and cowpox virus (CPXV) stimulate the MEK/extracellular signal-regulated kinase (ERK)/EGR-1 pathway, inhibition of this pathway affected VacV, but not CPXV replication (Silva *et al.*, 2006).

One of the key cellular signaling pathways that regulate the assembly of eIF4F complexes is phosphatidylinositol 3'-kinase–Akt–mammalian target of rapamycin (PI3K–Akt–mTOR). Mammalian DNA viruses have evolved a range of mechanisms to obtain the benefits from activating this pathway, including regulation of translation through the activation of mTOR. mTOR kinase has been found to associate with two functionally varying complexes named mTORC1 and mTORC2 (Sarbassov *et al.*, 2004). Vaccinia virus has recently been shown to stimulate mTORC1 and phosphorylate the translational repressor 4E-BP1 in a rapamycin-sensitive manner (Walsh *et al.*, 2008). However, whether VacV activates mTORC1 directly or involves kinases regulating mTOR remained unknown so far. In this study, we aimed to determine if stimulation of mTOR by VacV involves activation of the host PI3 kinase, and investigate its impact on virus replication in various cell lines.

4.2.1 Role of PI3K signaling in poxvirus protein synthesis

The PI3K pathway is the major pathway that controls mRNA translation, hence it is a significant target for many viruses trying to take control of the cell (Rahaus *et al*., 2006; Hale and Randall, 2007). However, a number of viruses such as measles virus and vesicular stomatitis virus do not require activation of PI3 kinase to replicate, stimulating rather its downstream substrates (Avota *et al.*, 2001; Gruenberg *et al.*, 2006; Dunn *et al.*, 2009). Previous studies of poxvirus signaling have demonstrated that myxoma virus, a rabbit-specific poxvirus, stimulates Akt directly by the host range protein MT-5, without involving its upstream regulator PI3K (Wang and Zal, 2006; Stanford *et al*., 2007; Werden *et al*., 2007). Importantly, this was insensitive to even high concentrations of the PI3K inhibitor, LY294002. Here, we showed that VacV activates upstream PI3K/Akt signaling to activate mTOR. The role of PI3K in regulating VacV translation was examined by using specific inhibitors of PI3K, LY294002 and Wortmannin (Povis *et al.*, 1994; Vlahos *et al.*, 1994).

Looking at the kinases and substrates downstream of PI3K in infected cells demonstrated that LY294002 dramatically reduced phosphorylation of the crucial factors regulating translation such as Akt and the substrates of mTORC1: 4E-BP1 and p70S6 kinase (p70S6K) (Fig. 3.2.1, 3.2.3). Similarly, inhibition of mTORC1 activity by rapamycin resulted in blocked VacV-mediated phosphorylation of 4E-BP1, as expected and reported previously (Walsh *et al.*, 2008), and prevented phosphorylation of p70S6K. However, in contrast to LY294002, rapamycin did not block phosphorylation of Akt, the upstream target of mTORC1 (Fig. 3.2.1); instead, rapamycin caused a modest increase in phosphorylation of this kinase. This increase might be due to the feedback mechanisms where mTORC1 inhibits Akt indirectly through mTORC2 (Julien

et al., 2010). These findings clearly demonstrate that VacV, unlike myxoma virus, does require the host PI3 kinase to stimulate downstream signaling to mTORC1.

Inhibition of PI3K also significantly affected the formation of eIF4F complexes by preventing VacV-stimulated phosphorylation of translational repressor 4E-BP1 (Fig. 3.2.5). Indeed, PI3K inhibition resulted in robust recruitment of 4E-BP1 to eIF4E exceeding the levels observed in the cells either uninfected or infected in the presence of rapamycin, and caused a corresponding strong reduction in the amount of eIF4G bound to eIF4E. In contrast, rapamycin treatment only modestly reduced the amounts of eIF4G bound to eIF4E, and did not stop the virus from increasing eIF4F levels above those in infected cells. Inhibition of VacV-induced phosphorylation of 4E-BP1 in the presence of rapamycin, and more complete hypophosphorylation caused by LY294002 was also observed in input samples. Although both drugs prevented VacV-induced phosphorylation of 4E-BP1 with similar efficiency, maintaining it at the levels observed in uninfected cells or below, looking at the total abundance of 4E-BP1 in low percentage gel demonstrated that rapamycin prevented its degradation in infected cells, as reported previously (Walsh *et al.*, 2008), but accumulation of hypophosphorylated 4E-BP1 occurred to a much greater extent in the presence of LY294002 (Fig. 3.2.6), despite the fact that both inhibitors blocked phosphorylation of p70S6K equally (Fig. 3.2.3). This suggests that rapamycin prevents the virus-stimulated phosphorylation of 4E-BP1, but LY294002 reduces this phosphorylation below the levels observed in uninfected cells. Recent data demonstrated that phosphorylation of 4E-BP1 leads to ubiquitination and degradation of this protein (Elia *et al.*, 2008), which results in enhanced protein synthesis. In contrast, dephosphorylation of 4E-BP1 was shown to increase its stability (Schneider *et al.*, 2005; Le Bouffant *et al.*, 2006), which leads to inhibition of translational rates. This may explain the increased levels of

hypophosphorylated 4E-BP1 in LY294002-treated cells accompanied by dramatically reduced translational rates caused by this drug. In addition, phosphorylation of eIF4E, known to enhance VacV replication (Walsh *et al.*, 2008), was also suppressed in LY294002-treated cultures (Fig. 3.2.7), most likely due to the collapse of eIF4F complexes, which prevents proper positioning of the eIF4G-bound kinase Mnk1 in proximity to its substrate, eIF4E, similar to previous reports (Tuazon *et al,*, 1990; Pyronnet *et al.*, 1999; Walsh and Mohr, 2006). Furthermore, we demonstrated that LY294002 did not cause significant changes in eIF4G phosphorylation, which is partially regulated by mTORC1 (Fig. 3.2.8). Thus, dramatic loss of phosphorylated forms of this scaffold protein is unlikely to contribute to the collapse of eIF4F.

To this point, the VacV strategies to commandeer the host translation machinery were examined in rapamycin-sensitive way, showing the importance of the mammalian target of rapamycin (mTOR) in stimulation of 4E-BP1 phosphorylation (Walsh *et al*., 2008). A number of research teams noticed the stimulation of mTOR by numerous groups of viruses (Feigenblum and Schneider, 1996; Gingras and Sonenberg, 1997; Kudchodkar *et al*., 2004; Walsh and Mohr, 2004; Moody *et al*., 2005; Oh *et al*., 2006; Castello *et al.*, 2009). However, rapamycin treatment usually does not significantly affect virus replication or protein synthesis. Kudchodkar *et al.* (2004) showed that in cells infected with human cytomegalovirus (HCMV), rapamycin only partially affects 4E-BP1 phosphorylation, and distorted composition of both mTORC1 and mTORC2 complexes in infected cells may explain this effect (Kudchodkar *et al.*, 2004). In contrast, in cells infected with herpes simplex virus type 1 (HSV-1), rapamycin completely blocks phosphorylation and release of 4E-BP1, and has a modest effect on eIF4F formation and virus replication (Walsh and Mohr, 2004). The effects of rapamycin observed in this research are very similar, and suggest that 4E-BP1 abundance may be insufficient in

regulating virus replication, at least in NHDFs used in this study. In addition, the effects of LY294002 illustrate that rapamycin-insensitive signaling pathway controls both 4E-BP1 phosphorylation and accumulation to suppress eIF4F formation in VacV-infected cells by an unknown mechanism that may involve mTORC2 kinase.

Given their effects on eIF4F formation, the effect of LY294002 and rapamycin on total VacV translational rates, CPE and virus replication was examined. The role of PI3K in the VacV life cycle was evident in various experiments carried out in this study. Looking at the morphology of the cells treated with PI3K inhibitor before and during infection, and comparing them with infected cells treated with DMSO, clearly showed that cells were indeed infected in the presence of LY294002, but a reduced cytopathic effect suggested that VacV replication was strongly inhibited by this drug, but not by rapamycin (Fig. 3.2.10). These observations suggested that PI3 kinase, in contrast to rapamycin-sensitive mTORC1, is crucial for effective replication of VacV.

While rapamycin did not affect viral protein synthesis, LY294002 robustly suppressed translational rates, even at high input doses of virus (Fig. 3.2.11). The effects on translation rates were also reflected in the abundance of late viral proteins and viral titers, which were dramatically reduced in LY294002-treated cells, but not in those treated with rapamycin. Low levels of translation observed in those samples, despite disruption and dramatically reduced levels of eIF4F complexes, may reflect suggestions that although VacV mRNAs require eIF4F for efficient protein synthesis, translational processes can still be carried out in infected cells in the absence of those complexes (Aldabe *et al.*, 1995; Mulder *et al.*, 1998; Shirokikh and Spirin, 2008).

Stimulation of other kinases activated by VacV but occurring outside of the PI3K pathway, such as extracellular signal regulated kinase (Erk) (de Magalhaes *et al.*, 2001),

was only slightly affected by PI3K inhibition (Fig. 3.2.4), proving that the inhibitors worked only for the specific proteins. The modest effect on Erk was likely due to effects on virus replication rather than off-target effects of the inhibitors. Indeed, the inhibitors were used at a lower concentration than those used by Wang and Zal (2006), Stanford *et al.* (2007) and Werden *et al.* (2007), and to which myxoma virus is resistant. As such, VacV and myxoma virus activate Akt by distinct mechanisms.

4.2.2 Investigation of cellular stress response and apoptosis in LY294002-treated cells infected with VacV

The PI3K/Akt/mTORC1 pathway regulates cellular processes such as cell growth, proliferation, protein synthesis and apoptosis (Lawlor and Alessi, 2001) that are important for viral replication. Therefore, manipulation of this pathway appears to be a common strategy used by many viruses to control protein synthesis and cell survival. This pathway would be particularly important for DNA viruses whose translation is cap dependent. However, the Akt signaling can also negatively affect viral replication. For example, activation of some kinases downstream of Akt signaling results in cellular stress responses that can inhibit mTORC1 (Lee and Esteban, 1994; Avruch *et al.*, 2006).

Here, we examined if inhibition of PI3K by LY294002 causes cellular stress response in VacV-infected cells. As mentioned previously (Section 3.2.3), increased phosphorylation of eIF2α can be caused by physiological stress and lead to disruption in translation or cell death. Therefore it is one of the widely used indicators of cellular stress responses and apoptosis (Clemens, 2001). However, the levels of phosphorylated forms of eIF2α in VacV-infected cells treated with DMSO solvent control, rapamycin or LY294002 showed no noticeable differences in those samples (Fig. 3.2.9). Furthermore,

no changes in eIF4G abundance, a factor that is cleaved during apoptosis (Clemens *et al.*, 1998), were noticed in those samples suggesting that cellular stress responses were not involved in inhibition of viral replication caused by this drug. Furthermore, studying the morphology of the cells showed no signs of apoptotic death and demonstrated that LY294002 actually protected the cells from morphological changes caused by the virus, suggesting that VacV replication cycle was robustly inhibited by this drug, while rapamycin did not seem to reduce virus replication (Fig. 3.2.10).

Interestingly, shortly after publishing our findings (Zaborowska and Walsh, 2009), Soares *et al.* (2009) demonstrated that LY294002 caused apoptosis in mouse A31 cells infected with vaccinia or cowpox virus (CPXV). This group showed that inhibition of PI3 kinase by LY294002 during either VacV or CPXV infection increased the cleavage of proteins associated with the induction of apoptosis, such as the executioner caspase-3 and PARP. Furthermore, inhibition of proapoptotic signals by zVAD.fmk prevented the cleavage of caspase-3 and increased viral replication. It was suggested that increased cytopathic effect in VacV- and CPXV-infected A31 cells treated with LY294002 was due to pharmacological inhibition of the antiapoptotic activity mediated by the PI3K/Akt pathway. However, our investigation of apoptosis in various human and monkey cell lines did not show any significant apoptotic effects of LY294002 (Fig. 3.2.14). Our findings demonstrate that treating the cells with LY294002 did not result in the cleavage of caspase-7 or PARP, observed in the control cells treated with Akt inhibitor I (Akti)[6]. In addition, no changes in cell morphology were observed in cultures infected in the presence of LY294002 suggesting that cells did not undergo apoptosis, in contrast to the cells treated with Akti (Fig. 3.2.13 a-c). Similarly, other groups investigating LY294002's effect on VacV-infected human and monkey cells did

---

[6] Apoptotic death of the cells treated with Akti may be off-target effect of the drug or could be caused by Akt inhibition while PI3K is still active. However, here Akti served as a control for apoptosis.

not notice apoptotic death caused by this inhibitor (Dunn *et al*., 2009, Hu *et al*. 2009; McNulty *et al.*, 2010). Therefore, apoptosis caused by LY294002 in VacV-infected cells appears to be specific only for certain mouse cell line(s).

4.2.3   The role of mTOR in VacV protein synthesis

At the time our results were being published, Thoreen and colleagues (2009) identified a new mTOR inhibitor named Torin1, a member of the pyridinonequinoline class of kinase inhibitors, which acts as a highly potent and selective inhibitor that suppresses both mTORC1 and mTORC2 complexes with IC_{50} values between 2 and 10nM through an ATP-competitive mechanism. Interestingly, this group demonstrated that the effects of Torin1 were independent of mTORC2 inhibition and were instead caused by suppression of rapamycin-resistant functions of mTORC1 that are crucial for cap-dependent translation. Furthermore, the effects of Torin1 were at least partially mediated by mTORC1-dependent and rapamycin-resistant phosphorylation of 4E-BP1.

We therefore tested whether Torin1 affected VacV infection of NHDFs as described in section 3.1.6. We showed that inhibition of mTORC1 and mTORC2 using Torin1 completely disrupted eIF4F complexes both in infected and uninfected cells, demonstrating that PI3K activation of mTOR signaling was involved in the formation of eIF4F during VacV infection, and confirming that the effects of LY294002 were specific to this signaling pathway. In addition, Torin1 blocked phosphorylation of Akt and prevented VacV-induced phosphorylation of 4E-BP1 causing its accumulation at similar levels as LY294002 (Fig. 3.2.15) indicating that phosphorylation and accumulation of this translational repressor is regulated in rapamycin-insensitive manner. These findings demonstrate that treating VacV-infected cells with either Torin1

or LY294002 results in similar impact on the main signaling pathway regulating protein synthesis and leads to disruption of eIF4F. However, Torin1 did not significantly affect VacV protein synthesis (it affected translation better than rapamycin, but not as drastically as LY294002 or wortmannin) despite the fact that eIF4F was disrupted in the presence of this inhibitor, with the translational rates of VacV proteins only partly reduced (Fig. 3.2.17 a-b). This suggests that mTOR inactivation and eIF4F disruption contribute to the effects of LY294002 on VacV replication but that other PI3K-dependent processes are involved in the effects of this inhibitor on virus replication. In terms of mTORC1 and mTORC2, Moorman and Shenk (2010) recently showed that Torin1, but not rapamycin, blocks mTOR signaling, disrupts assembly of eIF4F, and significantly decreases accumulation of viral proteins in human cytomegalovirus- and HSV-infected cells. However, these experiments were performed at moi 0.05 for three days, which amplifies small defects in virus replication. As such, the effects of mTOR inhibition in herpesvirus-infected cells appear to be similar to the effects in VacV-infected cells. Our results suggest that VacV has a specifically low requirement for eIF4F to translate its mRNAs. This is in agreement with previous studies in transformed cell lines (Aldabe *et al*., 1995; Mulder *et al*., 1998) and a recent in vitro analysis that suggested that the unusual polyA-tract in the 5'UTR of VacV mRNAs may reduce their dependence on normal cap-dependent translation initiation processes (Shirokikh and Spirin, 2008). However, their seemingly low dependence on eIF4F may simply be similar to abundant, unstructured "housekeeping" mRNAs.

Our findings do demonstrate that eIF4F activity enhances viral protein synthesis and is beneficial for virus replication, even if the effect of disrupting this critical complex is not as dramatic as might be expected.

4.3 Direct manipulation of the eIF4F complex by vaccinia virus

Given the importance of the eIF4F complex in regulating translation, a number of viruses encode proteins that directly interact with eIF4F to manipulate its function. Among RNA viruses, rotavirus-encoded protein NSP3 binds specifically to the conserved 3'end of viral mRNA and to the translation initiation protein eIF4G (Piron *et al.*, 1998; Vende *et al.*, 2000). In addition, eIF4G displays higher affinity for NSP3 than for PABP and as a consequence the interaction between eIF4G and PABP is disrupted in rotavirus-infected cells (Groft and Burley, 2002), which results in reduced efficiency of host mRNA translation and circularization-mediated enhancement of viral protein synthesis. Similarly, the expression of influenza virus NS1 protein has been shown to promote translation of viral but not cellular mRNAs by association with eIF4G (Aragon *et al.*, 2000; Burgui *et al.*, 2003). NS1 was found to recruit eIF4G to the 5'UTR of the viral mRNA, allowing the preferential translation of the influenza virus messengers. Further study demonstrated that influenza virus-encoded polymerase competes with eIF4E to bind to the cellular cap structures and eIF4G, and suggested the role of viral polymerase as a substitute for the eIF4E factor with the aim to promote viral mRNA translation (Burgui *et al.*, 2007). Hantavirus in turn took this approach even further and has been recently shown to replace the entire cellular eIF4F complex with the viral nucleocapsid protein (N) (Mir and Panganiban, 2008). N protein was shown to directly interact with 5'mRNA cap replacing eIF4E function, and with 43S pre-initiation complex functionally replacing eIF4G activity. N was also able to substitute as an RNA helicase in rabbit reticulocyte lysates, functionally replacing eIF4A activity. Thus N protein acts as a viral translation initiation factor with all of the properties of the eIF4F complex. N-mediated translation initiation is a viral strategy comparable to IRES. While

IRES is a *cis*-acting element that functionally supplants the requirement for cap-dependent translation, N is a *trans*-acting element that replaces eIF4F.

In the case of DNA viruses, adenovirus-encoded 100k protein was shown to inhibit phosphorylation of eIF4E at Ser209 and block cellular protein synthesis during the late phase of infection by preventing the association of the eIF4E kinase Mnk1 with the scaffold protein eIF4G (Cuesta *et al*, 2000). In addition, Xi *et al.* (2004) demonstrated that 100k binds to eIF4G to promote translation of viral mRNAs via ribosome shunting, whereby the ribosomes jump to the start codon rather than scanning the mRNA. Another example is ICP6 protein encoded by HSV-1 virus (Walsh and Mohr, 2006), which has homology to the cellular chaperone Hsp27 that regulates eIF4F levels during stress (Cuesta *et al.*, 2000). ICP6 was shown to promote the assembly of eIF4F complexes and is thought to directly promote the association of eIF4E with the N terminus of eIF4G without involving other cellular or viral components (Walsh and Mohr, 2006).

Looking at the growing number of viruses encoding factors that interact with the scaffold protein eIF4G suggests that it is a common strategy used by both RNA and DNA viruses to directly manipulate the key translation initiation complex eIF4F. How vaccinia virus, the prototypical poxvirus, controls the host translational apparatus remained unknown so far. Our findings demonstrated that, in addition to activating the signal pathways that regulate eIF4F, VacV also encodes a protein that directly interacts with this complex.

4.3.1 Redistribution of selected proteins during VacV infection

An unusual feature of VacV is that, although it is a DNA virus, it replicates exclusively in the cytoplasm of the infected cell. During VacV infection a number of selected cellular proteins such as molecular chaperone Hsp90 (Hung *et al.*, 2002), Cyclophilin A (Castro *et al.*, 2003), G3BP/Caprin-1 (p137) heterodimer (Katsafanas and Moss, 2007), Topoisomerase II (Lin *et al.*, 2008), and DNA Ligase I (Paran *et al.*, 2009) have been shown to redistribute to viral factories suggesting their importance in VacV replication. Amongst cellular translational factors, the components of eIF4F complex, eIF4G and eIF4E were found to be dramatically redistributed and accumulated within the viral factories, while the poly(A)-binding protein (PABP) and ribosomal proteins appear to accumulate mostly around the factories (Katsafanas and Moss, 2007; Walsh *et al.*, 2008). In contrast, a number of other RNA-binding proteins do not redistribute during infection. Therefore, rearrangement of cellular proteins during VacV infection appears to be selective and most likely mediated by specific functions, like in the case of the recruitment of cellular topoisomerase II by viral DNA ligase described by Lin *et al.* (2008).

Apart from VacV, African swine fever virus (ASFV) is the only other DNA virus that replicates exclusively in the cytoplasm and it also causes relocalization of both eIF4G and eIF4E to viral factories (Castello *et al.*, 2009). In addition, immunofluorescence technique revealed redistribution of other initiation and elongation factors such as eIF3, eIF2, eEF2 and ribosomes, and their accumulation within and around the virosomes, suggesting that viral replication, transcription, translation and morphogenesis occur in close proximity in ASFV virosomes. Consequently, all these processes appear to be tightly coupled, taking place in discrete cytoplasmic areas to maximize their efficiency.

The same group investigated redistribution of the mitochondrial network during ASFV infection using MitoTracker probes, which are a series of mitochondrion-selective dyes that are retained during cell fixation. While mitochondria appeared uniformly distributed in the cytoplasm of uninfected cells, their accumulation at the periphery of ASFV factories was evident at 16 hpi, suggesting that ATP synthesis is also coupled with viral replication and protein synthesis (Castello *et al.*, 2009).

VacV proteins also accumulate in the sites of replication. For instance, VacV-encoded E3, a double-stranded RNA-binding protein that prevents activation of PKR and RNase L innate immune defenses (Chang *et al.*, 1992; Rivas *et al.*, 1998), was found to associate with factories. In addition, the fact that viral-encoded transcription factors also accumulate within the virosomes led to the suggestion that poxvirus transcription and translation are linked, but probably not directly coupled as in bacteria (Katsafanas and Moss, 2007). Several other VacV early proteins encoded by genes B1R, H5R (Beaud and Beaud, 1997) and early/intermediate protein encoded by I3L (Rochester and Traktman, 1998) were also found to associate with the factories; moreover, it was suggested that those proteins are simultaneously the precursors of sites of viral DNA synthesis, since the factories incorporated BrdU upon washout of a viral DNA replication inhibitor (Domi and Beaud, 2000). One or more of these proteins may play a role in redistribution of host factors to viral factories.

4.3.2   Discovery of a VacV protein that associates with eIF4F

In the beginning of the investigation of redistribution of translation factors caused by VacV we speculated that a specific viral protein or cellular protein induced by the virus

might interact with eIF4F and/or other factors involved in protein synthesis and trigger their relocation in infected cells. Screening the components of the eIF4F complex in VacV-infected normal human diploid fibroblasts (NHDFs) resulted in discovery of a 34-kDa protein actively translated and associated with anti-eIF4G immune complexes at 16 but not 24 hpi (Fig. 3.3.1 a-b), which suggested that it is either no longer synthesized or no longer associated with eIF4G at late stages of infection. In contrast, the 34-kDa protein did not associate with anti-PABP immune complexes immunoprecipitated from the cell extracts (Fig. 3.3.2). The 34-kDa protein was then identified by mass spectrometry as an ssDNA-binding phosphoprotein (I3) encoded by VacV I3L ORF (Fig. 3.3.4 b).

I3 has been shown previously to be an early-to-intermediate stage protein (Rochester and Traktman, 1998), which agrees with the idea that it is not actively synthesized at late stages of infection (Fig. 3.3.1 b). Furthermore, I3 shows strong affinity for ssDNA and was revealed to associate with ribonucleotide reductase, suggesting an interaction with the nucleotide synthetic machinery at the replication fork and its potential role in DNA replication and/or repair (Davis and Mathews, 1993; Rochester and Traktman, 1998; Domi and Beaud, 2000; Welsch *et al.*, 2003). In addition, I3 phosphorylation on serine residues does not alter its binding properties for ssDNA (Rochester and Traktman, 1998). The function of I3 is poorly understood, although previous observations lead to the suggestion that I3 plays an essential role in the vaccinia virus infectious cycle, most likely as a viral SSB (Rochester and Traktman, 1998), but other functions of I3 can not be excluded.

The interaction between I3 and eIF4G was verified by performing the reverse immunoprecipitation using anti-I3 antiserum. At first, eIF4G was not recovered with anti-I3 immune complexes, most likely because the antibody epitope and eIF4G binding

site are the same region, or because direct binding of an antibody to I3 alters its structure causing release of bound factors, such as eIF4G. Generating a stable cell line over-expressing FLAG-tagged I3 allowed us to immunoprecipitate anti-FLAG immune complexes from infected and uninfected cells expressing FLAG-I3, together with associated eIF4G. As shown in figure 3.3.14, FLAG-I3 clearly bound to eIF4G in uninfected cells. In addition, viral I3 competed away the recombinant I3 from binding to eIF4G, which resulted in the loss of eIF4G association with FLAG-immune complexes in infected cells. This could be the effect of much lower expression of recombinant versus viral I3 detected by anti-I3 antiserum in input samples. However, the fact that eIF4G can be recovered together with FLAG-I3 complexes suggests an interaction between those two proteins that does not require other viral factors.

Our discovery that I3 interacts with eIF4G was verified by an alternative, non-immune based assay. eIF4F complexes were recovered from infected HEK-293 cells by 7-Methyl GTP-sepharose 4B chromatography and the samples were then analyzed by immunoblotting. As shown in figure 3.3.5, while no I3 was detected in mock-infected sample, it clearly associated with eIF4F complexes in infected cells. In addition, the binding of I3 was competitively inhibited by the addition of free 7-Methyl GTP to the extracts. The fact that I3 was bound to eIF4F in HEK-293 cells at this time point suggested that I3 did remain associated with eIF4F at the late stages of infection reached by 16 h in HEK-293 cells. This further supported the idea that the lack of ^{35}S-labelled I3 in eIF4G immune complexes at 24 hpi in serum-starved NHDFs simply reflected the fact that its synthesis declined at late stages.

Furthermore, recovering cap-bound complexes from uninfected HEK-293 cells over-expressing I3 by performing 7-Methyl GTP-sepharose 4B chromatography

demonstrated that I3 was able to bind to eIF4F on its own, in the absence of other viral proteins and enzymes (Fig. 3.3.15). Direct interaction of I3 with cap complexes was also verified by adding purified I3 to HEK-293 cell extracts (Fig. 3.3.16). These results strongly confirmed the specificity of I3-eIF4F interaction. The ability of I3 to directly interact with eIF4G was investigated further by performing *in vitro* binding assays.

4.3.3   Identification of I3- and eIF4G-binding domains

Having identified I3 as a viral protein associating with translational factor eIF4G we then precisely investigated this interaction. By a series of experiments using purified proteins we demonstrated that I3 binds to eIF4G by direct interaction, moreover, this binding occurred in the absence of other viral proteins.

As demonstrated in Section 3.3.5, recovering cap complexes from uninfected HEK-293 cell extracts confirmed the ability of purified, his-tagged I3 to associate with eIF4F *in vitro* (Fig. 3.3.16). Therefore, a binding assay with eIF4G fragments could be carried out with the aim to determine whether I3 associates with eIF4G directly or whether it involves other factors that mediate that reaction. The binding assays were performed using his-I3 and three GST-tagged fragments of eIF4G: N-(aa157-626), M-(aa627-1045), and C-(aa1045-1560) terminal, and GST-bound complexes were recovered by glutathione-sepharose 4B. Analysis of the samples by immunoblotting suggested that the I3-binding site is localized on the C-terminal fragment of eIF4G. It is worth to mention that RNA-binding domains of eIF4G are located mostly in the M-fragment, while the direct interaction with I3 occurred with the C-terminal part of the gene, indicating that this interaction did not involve the nucleic acid-binding regions of eIF4G. Moreover, I3 does not appear to compete with either eIF4E or PABP for the

binding site of eIF4G, as their domains are situated within the N-terminal fragment. C-terminal part of eIF4G contains, however, the Mnk1/2 binding domains, and Ad 100k protein also binds the C-terminus to evict Mnk1/2 and inhibit translation (Cuesta *et al.*, 2000). However, the competition between Mnk1/2 and I3 can be excluded on account of the fact that VacV was shown to stimulate the eIF4E kinase during infection to promote eIF4E phosphorylation (Walsh *et al.*, 2008). This suggests that I3 seems to bind a region of C-4G distinct from that of Mnk1/2 and Ad 100k.

Identification of the region of I3 involved in its association with eIF4G was then performed by the same binding assay, using five his-tagged deletion fragments of I3 as described in Section 3.3.7, and GST-tagged C-terminal fragment of eIF4G (C-4G). Sample analysis by immunoblotting using anti-his and anti-GST antisera demonstrated that only the fragment labeled F1 (aa1-216) and deleted within the C-terminal region of I3 was found to associate with C-4G *in vitro*, despite its low abundance in the reaction observed in input samples (Fig. 3.3.21). Noteworthy is the fact that the predicted nucleic acid-binding domain of I3 is located within amino acids 91-154 (Rochester and Traktman, 1998), which is a part of the fragment F2 and distinct from the region required for binding to C-4G (Fig. 3.3.22). Moreover, the C-terminus of I3 containing the putative eIF4G binding site has been shown to be highly acidic (Davis and Mathews, 1993), similar to other ssDNA-binding proteins such as bacteriophage T4 gene 32 protein, where a role in replication has been demonstrated (Chase and Williams, 1986). In addition, this region of the gene 32 protein was also shown to mediate interactions with other proteins (Krassa *et al.*, 1991), suggesting that it shares similar features with VacV I3.

Surprisingly, the large fragment F5 deleted in its N-terminal domain but containing amino acid sequences from region 160-216 failed to restore binding to C-4G. The possible reason is that the loss of N-terminal region resulted in changing the protein structure that is no longer able to interact with eIF4G, or it could be that both domains are involved in binding. Although the binding assay still needs to be optimized, finding the region of I3 responsible for its interaction with eIF4G provides an important issue for future study.

Study of I3 interactions demonstrated that this protein directly associates with the key cellular translational factor eIF4G and with cap complexes, suggesting its role as an important tool used by the virus to commandeer crucial components of the host translational apparatus.

4.4 Inhibition of host mTORC1 activity and its influence on I3-eIF4F interaction

It was shown previously that VacV infection stimulates the activity of mTORC1 complex which results in inactivation of the translational repressor 4E-BP1 by phosphorylation leading to stimulation of eIF4F complex formation (Walsh *et al.*, 2008). Treating cells with the mTORC1 inhibitor - rapamycin - effectively prevented inactivation of 4E-BP1 and partially reduced the production of infectious virus, as can be seen in figure 3.2.12. Here, we established that inhibition of mTORC1 also affects the interaction between I3 and eIF4F complexes.

4.4.1   Effect of rapamycin on I3 association with eIF4F complexes

To examine I3-eIF4F interaction in the presence of rapamycin, 7-Methyl GTP-bound complexes were recovered from infected HEK-293 cells, and associated proteins were

analyzed by western blotting. As shown previously, rapamycin effectively prevented phosphorylation of 4E-BP1 mediated by VacV but did not alter the levels of eIF4F complexes and had no significant effect on the accumulation of I3 in infected cell extracts (Fig. 3.3.23). However, rapamycin did reduce the levels of I3 bound to eIF4F approximately 3-fold, although significant amounts of I3 remained associated with eIF4F, which was not disrupted by rapamycin. Similarly, binding of recombinant, his-tagged I3 to eIF4F was partially reduced when cap complexes were recovered from uninfected cell extracts treated with rapamycin (Fig. 3.3.24), demonstrating that the effect of rapamycin is not limited to the context of infection. These results indicate that I3 continues to associate with the major initiation complex in the presence of rapamycin, which would explain why this inhibitor did not affect the total VacV translational rates or total levels of I3, as illustrated in figure 3.2.11. Furthermore, our results do demonstrate that although rapamycin did not drastically affect interaction between I3 and cap complexes, maximal I3 binding required the activity of cellular mTORC1.

4.4.2 Effect of rapamycin on I3 association with eIF4G

We then examined whether the same effects were observed when the association of I3 with eIF4F complexes was performed by immunoprecipitation of eIF4G from infected cells. Western blot analysis demonstrated that eIF4G and eIF4E levels remained unaltered in infected cells with or without the presence of rapamycin (Fig. 3.3.25), indicating that eIF4F complex is not disrupted by rapamycin in HEK-293 cells. Surprisingly, in contrast to findings with 7-Methyl GTP-sepharose, rapamycin did not affect the levels of ^{35}S-labeled I3 associated with eIF4G indicating that I3 association

with the scaffold protein in infected cells is not regulated by mTORC1 complexes. This outcome could explain our previous findings that rapamycin, in contrast to LY294002, does not affect VacV protein synthesis or accumulation of viral proteins (Fig. 3.2.11).

The fact that inhibition of mTORC1 results in reduction of I3 levels associated with 7-Methyl GTP cap complexes, but not with eIF4G itself, could reflect differences in the sensitivity of assays used in those experiments. However, each assay was directly recovering different components of the eIF4F complex, namely eIF4E and eIF4G, which suggests the possibility of I3 interaction with other factors bound to the cap. Taking into consideration that during VacV infection viral I3, as well as cellular eIF4G and eIF4E were shown to accumulate within the sites of viral replication (Rochester and Traktman, 1998; Katsafanas and Moss, 2007; Walsh *et al.*, 2008), we tested whether I3 might also associate with the cap-binding protein eIF4E.

4.4.3   Investigation of possible I3-eIF4E interaction

To test if I3 could bind to eIF4E, a binding assay using his-I3 and batch-purified eIF4E was carried out. As demonstrated in figure 3.3.26, I3 did associate with the 7-Methyl GTP cap complexes in the presence of eIF4E, and in the absence of the remaining eIF4F components. This result suggests that I3 might have the ability to associate with both eIF4G and eIF4E factors, although this implication needs to be verified by performing *in vitro* binding assays using purified eIF4E protein and I3 fragments.

On the assumption that I3 does interact with eIF4E, we examined whether the efficiency of this binding is affected by the presence of eIF4G. To do this, increasing amounts of a GST-tagged N-terminal fragment of eIF4G (N-4G) containing the eIF4E binding site, but bereft of the binding site for I3, was added to the binding reactions. Western blotting

analysis of the samples demonstrated that inclusion of N-4G did not change the levels of I3 bound to the cap complexes (Fig. 3.3.26). I3 binding did not increase as I3 binds the C-terminal domain of eIF4G. This experiment demonstrated that association of I3 with eIF4E was not competitive at least for the N-terminal fragment of eIF4G, and suggested that I3 can interact with both free and eIF4G-associated eIF4E.

Those results suggest that most likely the interaction between I3 and eIF4E does occur. Moreover, our observations imply that the effect of rapamycin on association between I3 and cap-complexes might reflect competition between I3 and 4E-BP1 for binding to free eIF4E that is not a part of eIF4F complex. This would explain why inhibition of mTORC1 did not affect I3 binding to eIF4G but it did reduce the I3 association with cap-complexes. Furthermore, it was suggested that eIF4E has a larger footprint for 4E-BP1 than that of eIF4G, which partially overlaps the eIF4G-binding domain (Matsuo *et al.*, 1997; Tomoo *et al.*, 2006; Moerke *et al.*, 2007). If that is the case, with its larger footprint on eIF4E, 4E-BP1 could potentially affect the association of proteins with eIF4E that are not affected by binding of eIF4G.

4.5 Regulation of PABP in VacV-infected cells

In addition to enhancing the levels of eIF4F, VacV also stimulates the recruitment of PABP to eIF4F complexes in infected cells (Walsh *et al.*, 2008). As reported previously, in contrast to eIF4G and eIF4E proteins that accumulate inside the factories (Rochester and Traktman, 1998; Katsafanas and Moss, 2007; Walsh *et al.*, 2008), only small amounts of PABP are recruited into these sites of viral replication (Walsh *et al.* 2008). However, the redistribution and localization of large pools of PABP near the factories suggest that PABP might play a role in VacV protein synthesis. Our findings imply that

low abundance of PABP found in the factories might be the result of its interaction with eIF4F complexes bound to I3 protein.

As demonstrated previously by performing cap-assays, VacV infection causes increased formation of eIF4F complexes and recruitment of PABP, while the overall abundances of eIF4F components as well as PABP remain constant in infected and uninfected cells (Walsh *et al.*, 2008). This study confirmed the increased formation of eIF4F complexes and recruitment of PABP by immunoprecipitation, demonstrating increased recovery of eIF4E in eIF4G and PABP immune complexes recovered from infected cells. In addition, only low levels of eIF4E were detected in PABP immune complexes recovered from both mock and infected cells (Fig. 3.3.3), suggesting that only small amounts of the total cellular pool of PABP were in fact associated with eIF4F complexes, at least in NHDFs. This would explain the fact that only very little of PABP was found accumulated within viral factories, most likely as a result of its association with I3-bound eIF4F complexes. Similarly, it is possible that PABP complexes contain small amounts of I3 as part of the eIF4F-associated portion of PABP that was not detected by the assay. The fact that I3 was able to mediate the recruitment of eIF4G-bound PABP to ssDNA *in vitro* (Fig. 3.3.33) appears to confirm that assumption. Therefore, this study demonstrates that although I3 was not able to directly associate with PABP, it could effectively recruit eIF4F complexes associated with PABP. Indeed, our findings demonstrate that binding domains for I3 and PABP are located on different termini of eIF4G, suggesting that those two proteins are likely to be able to interact with the scaffold protein simultaneously.

4.6 Function of I3 in regulating translation

The precise function(s) of I3 remain poorly understood. Rochester and Traktman (1998) identified I3 as a viral single-stranded DNA (ssDNA) binding protein (SSB), and its role as a viral SSB has been considered. The fact that I3 is intensively synthesized before and during DNA replication, its accumulation in the sites of viral DNA replication and high-affinity binding to ssDNA makes it an ideal candidate for a viral SSB.

Single-stranded DNA-binding proteins (SSBs) are crucial elements in cells of all living organisms. SSB proteins associate with ssDNA in a sequence independent manner, preventing ssDNA from forming secondary structures and from degradation by nucleases (Greipel *et al.*, 1989). As such, SSBs participate in all processes involving ssDNA, such as replication, repair and recombination, playing a role of a multifunctional protein (Greipel *et al.*, 1989; Meyer and Laine, 1990; Moore *et al.*, 1991; Alani *et al.*, 1992). SSB proteins occur in prokaryotes and eukaryotes and share sequences as well as biochemical and structural characteristics.

During their investigation of the potential role of I3 as an SSB carried out by Rochester and Traktman (1998), the analogy of I3 to the cellular Replication Protein A (RPA), which acts as a human SSB, has been considered. RPA is a heterotrimeric single-stranded DNA-binding protein (SSB) that is highly conserved in eukaryotes and plays a critical role in many aspects of nucleic acid metabolism. RPA homologues have been identified in all eukaryotic organisms examined and interact with and/or modify the activities of multiple proteins (Wold MS, 1997), such as the components of the repair machinery as well as the replication machinery (He *et al.*, 1995; Li *et al.*, 1995; Nagelhus *et al.*, 1997). Similarly, I3 might associate with such viral enzymes as the

uracil DNA glycosylase (UDG). Verification of such an interaction would clarify the fact that UDG, similarly to I3, was shown to be essential for DNA replication (Stuart *et al.*, 1993; Millns *et al.*, 1994).

Furthermore, earlier studies showed the interaction between I3 and VacV ribonucleotide reductase, suggesting that I3 may interact with the nucleotide synthetic machinery at the replication fork. It was also considered whether I3 is involved in promoting poxviral recombination (Tseng *et al*., 1999). Furthermore, David and Mathews (1993) observed that I3, similarly to SSB of bacteriophage T4 (gene 32 protein), has a highly acidic C-terminus. This fragment of gene 32 protein is responsible for mediating interactions with other proteins. Similarly, we demonstrated that the C-terminal region of I3 interacts with the scaffold protein eIF4G.

Studies to date of the function of I3 in VacV life cycle were limited to its role in viral replication as a viral SSB protein. The results described in our study provide the first evidence of I3's interaction with key cellular proteins mediating protein synthesis.

4.6.1   Role of I3 in stimulating translation

This study demonstrated that I3 associated with the eIF4F complex at early-to-intermediate stages of infection (Fig. 3.3.1, 3.3.2), when the majority of viral proteins are synthesized, and was not affected by PAA (Fig. 3.3.29). However, PAA did affect eIF4F formation in infected cells (Fig. 3.3.27), suggesting that I3 was not capable of directly stimulating the formation of eIF4F complexes. In addition, looking at the translational rates of control HEK-293 cells and cells expressing recombinant I3 demonstrated that no significant changes in rates or patterns of cellular protein synthesis were observed in the presence of I3 (Fig. 3.3.33). We also examined whether I3 affects

translation of RNA isolated from VacV-infected cells *in vitro* using rabbit reticulocyte lysates programmed with RNA isolated from infected HEK-293 cells. As illustrated in figure 3.3.34, similarly to the effects of I3 on host protein synthesis, the presence of I3 did not significantly influence the rates or patterns of viral protein synthesis. As such, I3 does not appear to have any significant direct effect on the translation of either host or viral messages.

4.6.2   Role of I3 in recruitment of translational factors to the factories

Although I3 did not influence translation directly, our findings demonstrate that it is likely to be involved in indirect regulation of translation by associating with translational factors and retaining them within viral factories. While redistribution of translational factors eIF4G, eIF4E and PABP caused by VacV has been previously described (Katsafanas and Moss, 2007; Walsh *et al.*, 2008), the mechanism of this movement remained unknown so far. By performing immunofluorescence assay using VacV-infected cells expressing GFP-tagged I3 we demonstrated that it colocalized within viral factories together with the scaffold protein eIF4G (Fig. 3.3.8), suggesting direct involvement of I3 in redistribution of eIF4G, and most likely eIF4E shown to colocalize with eIF4G within the virosomes (Walsh *et al.*, 2008). We examined the role of ssDNA in the ability of I3 to associate with translational factors and their relocalization to the factories.

I3 was shown to have high affinity for ssDNA, which appears to explain its retention in viral factories (Rochester and Traktman, 1998; Tseng *et al.*, 1999; Domi and Beaud, 2000). By performing binding assay using exogenously added ssDNA we demonstrated that I3 is able to selectively recruit host translation initiation factors to ssDNA *in vitro*

(Fig. 3.3.32). Specificity of recruitment of translational factors by I3 was verified by looking at the association of RBM3, the cellular protein interacting with both RNA and ssDNA, in the same samples. As illustrated in figure 3.3.32, binding of RBM3 to ssDNA was visibly reduced in the presence of I3, most likely as a consequence of competition from I3 for binding to ssDNA. In addition to confirming the specificity of I3 function in recruiting translation factors, this also demonstrated that I3 was not simply stabilizing the input ssDNA in extracts and, thereby, non-specifically mediating the increased recovery of nucleotide-binding proteins in general. The fact that I3 possessed the ability to directly bind and recruit specific factors to ssDNA and co-localize with them to distinct sites of viral replication suggests a novel approach adopted by a DNA virus to manipulate the translation initiation complex eIF4F.

4.6.2.1 Effect of PAA on eIF4F complex formation

Recently a number of viruses have been shown to increase the levels of eIF4F to promote viral protein synthesis. Although many DNA viruses are now known to inactivate 4E-BP1, several DNA viruses including HSV-1, HCMV, and VacV are able to mediate eIF4F complex formation through additional, rapamycin-insensitive mechanisms due to enhancement of eIF4G binding to eIF4E, which can occur in the absence of significant release of the repressor 4E-BP1 (Kudchodkar *et al*., 2004; Walsh and Mohr, 2004; Walsh *et al*., 2005; Zaborowska and Walsh, 2009). Interestingly, in HSV-1-infected cells the release of 4E-BP1 alone does not appear to be sufficient to promote eIF4F complex formation in the absence of the viral eIF4F chaperone ICP6 (Walsh and Mohr, 2006). Similarly, we show that stimulation of eIF4F complex formation in VacV-infected cells was reduced in the presence of PAA in spite of

efficient release of 4E-BP1 from eIF4E (Fig. 3.3.27). In addition, PAA did not significantly affect the ability of I3 to interact with eIF4F (Fig. 3.3.29) suggesting that, in contrast to HSV-1-encoded ICP6 protein, I3 binding alone is not sufficient to promote initiation complex formation. PAA blocks viral factory formation and redistribution of eIF4G (Walsh *et al.*, 2008) suggesting that I3 might increase the formation of eIF4F complexes in cell types where the rates of complex formation are low by concentrating host translation factors within viral factories to enhance the efficiency of viral protein synthesis. Similar process of eIF4F assembly was also observed in serum-starved NHDFs infected with human cytomegalovirus (HCMV) (Walsh *et al.*, 2005). HCMV induces an increase in the overall abundance of eIF4F components and promotes assembly of eIF4F complexes. However, in contrast to HSV-1, HCMV does not appear to encode any protein involved in promoting the formation of eIF4F and, in contrast to VacV, does not redistribute host translation factors.

It is likely that increased levels of eIF4F complexes observed in VacV-infected serum-starved NHDFs, which contain low levels of translation factors (Arias *et al.*, 2009), are caused by changes in the on-off rates of eIF4E:eIF4G interaction under more concentrated conditions within viral factories. I3 is unlikely to affect on-off rates of eIF4E:eIF4G interaction directly and in the presence of PAA, when no viral factories are formed to accumulate the factors, thus the levels of eIF4F complexes remain unaltered compared to those in uninfected cells.

4.6.3   VacV ΔI3L mutant

The literature to date, as well as the results obtained in this study, indicate the importance of I3 protein in VacV replication and protein synthesis. The attempt to generate a VacV mutant lacking I3L gene by recombination, carried out in P. Traktman's laboratory (Rochester and Traktman, 1998), was unsuccessful. Similarly, this study shows that using a Vac-Bac/λ system developed by Domi and Moss (2005) also failed to recover ΔI3L mutant virus, although it was possible to replace I3L ORF with the gene encoding ampicillin (Fig. 3.3.35), and recover wild-type virus from the BAC system (Fig. 3.36-a, 3.37-a). Furthermore, several different siRNAs targeting the I3 mRNA failed to affect I3 accumulation in HEK-293 or HeLa cells (not shown). These outcomes suggest that the I3L gene product is essential during the vaccinia virus infectious cycle. However, despite the fact that the assay was performed in three repeats, it is possible that inability to recover ΔI3L mutant was caused by spontaneous mutation within the viral genome. Unfortunately, because of time limitation more thorough analysis of VacV ΔI3L mutants could not be performed. However, further investigation of I3 function based on Vac-Bac/λ system would be highly recommended. Furthermore, due to incredibly fast headway in developing new techniques in molecular biology, it may be possible to develop new techniques of creating viral mutants that would allow efficient studies of the role of this multifunctional protein in VacV life cycle.

Section 5.0

Conclusion and future work

5.1 Conclusion

In this study we demonstrate that PI 3-kinase plays a critical role in regulating protein production during VacV infection, at least in part by controlling the abundance and activity of 4E-BP1, the translational repressor. We also show that 4E-BP1 phosphorylation and abundance is regulated by unknown rapamycin-insensitive mechanism regulated by PI3K, inhibition of which results in dramatic suppression of both the eIF4F complex formation and the total translational rates in VacV-infected cells.

Inhibition of both mTORC1 and mTORC2 complexes using a novel inhibitor Torin1 resulted in suppression of eIF4F formation but did not dramatically affect VacV protein synthesis, suggesting VacV has a low requirement for eIF4F to translate its mRNAs, as reported previously. However, we show that eIF4F activity enhances viral protein synthesis and is beneficial to virus replication.

Moreover, we provide the first evidence of interaction between VacV-encoded protein I3 and cellular translational factors. This study shows that I3 binds to eIF4G by direct interaction with its C-terminal region, and likely interacts with eIF4E as well. We demonstrate that I3 is capable of specifically recruiting initiation factors eIF4G and PABP to ssDNA and co-localizes with eIF4G within viral factories. In addition PAA, a DNA polymerase inhibitor, did not significantly affect the ability of I3 to interact with eIF4F but it did suppress viral factory formation and eIF4F complex formation, suggesting that I3 binding alone is not sufficient to promote complex assembly. I3 did not appear to affect host or viral mRNA translation. As such, we propose that I3 regulates translation factor redistribution to viral factories during infection.

Furthermore, mTORC1 inhibition by rapamycin only modestly affected VacV translation and the association of I3 with eIF4F, while it did prevent VacV-induced phosphorylation of 4E-BP1. However, our results indicate that maximal efficiency of VacV protein synthesis and I3 binding required the activity of cellular mTORC1.

Our attempts to recover a VacV mutant lacking the I3L gene using Vac-Bac/λ system were unsuccessful, although we did replace I3L ORF with the gene encoding ampicillin. In addition, siRNA targeting I3 mRNA did not affect I3 accumulation. These findings indicate that I3L is an essential gene in VacV replication, in agreement with the previous reports.

In overall conclusion, this study proposes a novel function of VacV-encoded protein I3 in translation and therefore suggests a novel approach adopted by a DNA virus to manipulate the translation initiation complex eIF4F. However, the exact mechanism of this process remains to be investigated further.

5.2 Future directions

➢ In the case of signaling, more extensive investigation of Torin1 effect on PI3K signaling pathway during VacV infection should be carried out.

➢ Study the mechanism of the PI3K activation by VacV.

➢ It would be recommended to investigate the possible interaction between I3 and eIF4E by performing the binding assays with purified proteins.

➢ It is possible that I3 binds also the other host cell factors, in addition to translation factors. Analysis of anti-I3 immune complexes recovered from infected cells would be interesting.

➢ Further studies of the exact mechanism by which cellular translational factors are redistributed during VacV infection and the role of ssDNA in this mechanism would be highly recommended.

➢ It would be also interesting to study the possible interaction between I3 and microtubules responsible for intracellular transport.

➢ Further research based on the Vac-Bac/λ system using multiple repeats of VacV ΔI3L mutant preparation could result in recovering the mutant virus and allow to study the function of I3 in VacV protein synthesis.

➢ Finally, it would be recommended to study the role of PABP in VacV infectious cycle, starting from identifying the unknown protein associated with anti-PABP immune complexes in infected cells, noticed in figure 3.3.2.

Section 6.0

Bibliography

Adhikary S, Eilers M (2005) Transcriptional regulation and transformation by Myc proteins. *Nat Rev Mol Cell Biol* 6: 635-645.

Alani E, Thresher R, Griffith JD, Kolodner RD (1992) Characterization of DNA-binding and strand-exchange stimulation properties of y-RPA, a yeast single-strand-DNA-binding protein. *J Mol Biol* 227: 54-71.

Aldabe R, Feduchi E, Novoa I, Carrasco L (1995) Efficient cleavage of p220 by poliovirus 2Apro expression in mammalian cells: effects on vaccinia virus. *Biochem Biophys Res Commun* 215: 928-36.

Alessi DR, Andjelkovic M, Caudwell B, Cron P, Morrice N, Cohen P, Hemmings BA (1996) Mechanism of activation of protein kinase B by insulin and IGF-1. *EMBO J* 15: 6541–6551.

Ali IK, McKendrick L, Morley SJ, Jackson RJ (2001) Truncated initiation factor eIF4G lacking an eIF4E binding site can support capped mRNA translation. *Embo J* 20: 4233-4242.

Andrade MA, Bork P (1995) HEAT repeats in the Huntington's disease protein. *Nat Genet* 11: 115-116.

Aragón T, de la Luna S, Novoa I, Carrasco L, Ortín J, *et al.* (2000) Eukaryotic translation initiation factor 4GI is a cellular target for NS1 protein, a translational activator of influenza virus. *Mol Cell Biol* 20: 6259-6268.

Arcaro A, Zvelebil MJ, Wallasch C, Ullrich A, Waterfield MD, Domin J (2000) Class II phosphoinositide 3-kinases are downstream targets of activated polypeptide growth factor receptors. *Mol Cell Biol* 20: 3817-30.

Arias C, Walsh D, Harbell J, Wilson AC, Mohr I (2009) Activation of host translational control pathways by a viral developmental switch. *PLoS Pathogens* 5: e1000334.

Avota E, Avots A, *et al.* (2001) Disruption of Akt kinase activation is important for immunosuppression induced by measles virus. *Nat Med* 7: 725-731.

Avruch J, Hara K, Lin Y, Liu M, Long X, Ortiz-Vega S, Yonezawa K (2006) Insulin and amino-acid regulation of mTOR signaling and kinase activity through the Rheb GTPase. *Oncogene* 25: 6361–6372.

Bader AG, Kang S, Zhao L, Vogt PK (2005) Oncogenic PI3K deregulates transcription and translation. *Nat Rev Cancer* 5: 921-929.

Baldo P, Cecco S, *et al.* (2008) mTOR pathway and mTOR inhibitors as agents for cancer therapy. *Curr Cancer Drug Targets* 8: 647–665.

Balvay L, Lopez Lastra M, Sargueil B, Darlix JL, Ohlmann T (2007) Translational control of retroviruses. *Nat Rev Microbiol* 5(2): 128-140.

Baroudy BM, Venkatesan S, Moss B (1982) Incompletely base-paired flip-flop terminal loops link the two DNA strands of the vaccinia virus genome into one uninterrupted polynucleotide chain. *Cell* 28(2): 315-324.

Beaud G, Beaud R (1997) Preferential virosomal location of underphosphorylated H5R protein synthesized in vaccinia virus-infected cells. *J Gen Virol* 78: 3297-3302.

Bedson HS, Dumbell KR (1964) Hybrids derived from the viruses of variola major and cowpox. *J Hyg* 62: 147-158.

Bolden A., Aucker J., Weissbach A (I975) Synthesis of herpes simplex virus, vaccinia virus and adenovirus DNA in isolated HeLa cell nuclei. I. Effect of viral-specific antisera and phosphonoacetic acid. *J Virol* 16: I584-I592.

Bonneau AM, Sonenberg N (1987) Involvement of the 24-kDa cap-binding protein in the regulation of protein synthesis in mitosis. *J. Biol. Chem* 262: 11134–11139.

Bradford MM (1976) A rapid and sensitive method for quantitation of microgram quantities of protein utilizing the principle of protein-dye-binding. *Anal Biochem* 72: 248-254.

Britt WJ, Jarvis M, Seo JY, Drummond D, Nelson J (2004) Rapid Genetic Engineering of Human Cytomegalovirus by Using a Lambda Phage Linear Recombination System: Demonstration that pp28 (UL99) Is Essential for Production of Infectious Virus. *J Virol* 78: 539-543.

Brema JG, Kalisa-Ruti, Steniowski MV, Zanotto E, Gromko AI, Arita I (1980) Human monkeypox. 1970-79. *Bull WHO* 58: 165-182.

Brockman WW, Nathans D (1974) The isolation of simian virus 40 variants with specifically altered genomes. *PNAS* 71: 942-946.

Brown RA, Domin J, Arcaro A, Waterfield MD, Shepherd PR (1999) Insulin activates the alpha isoform of class II phosphoinositide 3-kinase. *J Biol Chem* 274: 14529-32.

Bu X, Haas DW, Hagedorn CH (1993) Novel phosphorylation sites of eukaryotic initiation factor-4F and evidence that phosphorylation stabilizes interactions of the p25 and p220 subunits. *J Biol Chem* 268: 4975–4978.

Burgui I, Aragón T, Ortín J, Nieto A (2003) PABP1 and eIF4GI associate with influenza virus NS1 protein in viral mRNA translation initiation complexes. *J Gen Virol* 84: 3263-3274.

Burgui I, Yángüez E, Sonenberg N, Nieto A (2007) Influenza virus mRNA translation revisited: is the eIF4E cap-binding factor required for viral mRNA translation? *J Virol* 81: 12427-12438.

Cao Q, Richter JD (2002) Dissolution of the maskin–eIF4E complex by cytoplasmic polyadenylation and poly(A)-binding protein controls cyclin B1 mRNA translation and oocyte maturation. *EMBO J* 21: 3852–3862.

Cardone MH, Roy N, Stennicke HR, Salvesen GS, Franke TF, Stanbridge E, Frisch S, Reed JC (1998) Regulation of cell death protease caspase-9 by phosphorylation. *Science* 282: 1318–1321.

Carmichael AG, Silverstein AM (1987) Smallpox in Europe before the seventeenth century: Virulent killer or benign disease? *J Hist Med Allied Sci* 42: 147-168.

Carter MS, Kuhn KM, Sarnow P (2000) Cellular internal ribosome entry site elements and the use of cDNA microarrays in their investigation. In Sonenberg N, Hershey JWB & Mathews MB (eds). *Translational Control of Gene Expression*. Cold Spring Harbor, NY: Cold Spring Harbor Laboratory. Pp. 615-636.

Castelló A, Quintas A, Sánchez EG, Sabina P, Nogal M *et al.* (2009) Regulation of host translational machinery by african Swine Fever virus. *PLoS Pathogens* 5: e1000562.

Castro AP, Carvalho TM, Moussatché N, Damaso CR (2003) Redistribution of cyclophilin A to viral factories during vaccinia virus infection and its incorporation into mature particles. *J Virol* 77: 9052-9068.

Chang HW, Watson JC, Jacobs BL (1992) The E3L gene of vaccinia virus encodes an inhibitor of the interferon-induced, doublestranded RNA-dependent protein kinase. *PNAS* 89: 4825–4829.

Chase JW, Williams KR (1986) Single-Stranded DNA Binding Proteins Required for DNA Replication. *Annu Rev Biochem* 55: 103-136.

Chiang GG, Abraham RT (2007) Targeting the mTOR signaling network in cancer. *Trends Mol Med* 13: 433–442.

Clemens MJ, Bushell M, Morley SJ (1998) Degradation of eukaryotic polypeptide chain initiation factor (eIF) 4G in response to induction of apoptosis in human lymphoma cell lines. *Nature* 17(22): 2921-2931.

Clemens MJ (2001) Initiation factor eIF2α phosphorylation in stress responses and apoptosis. In: RE Rhoads (ed). *Signaling pathways for translation. Stress, calcium, and rapamycin*. Heidelberg, Germany: Springer. Pp. 57-89

Clemens MJ (2004) Targets and mechanisms for the regulation of translation in malignant transformation. *Oncogene* 23(18): 3180-3188.

Cohen N, Sharma M, Kentsis A, Perez JM, Strudwick S, Borden KL (2001) PML RING suppresses oncogenic transformation by reducing the affinity of eIF4E for mRNA. *EMBO J* 20: 4547-59.

Condit RC, Moussatche N, Traktman P (1996) In a nutshell: Structure and assembly of the vaccinia virion. *Advances in Virus Research* vol.66: 31-124.

Copeland NG, Jenkins NA, Court DL (2001) Recombineering: a powerful new tool for mouse functional genomics. *Nat Rev Genet* 2: 769-779.

Court DL, Sawitzke JA, Thomason LC (2002) Genetic engineering using homologous recombination. *Annu Rev Genet* 36: 361-388.

Cowling VH (2010) Regulation of mRNA cap methylation. *Biochem J* 425: 295-302.

Cuesta R, Xi, Q, Schneider RJ (2000) Adenovirus-specific translation by displacement of kinase Mnk1 from cap-initiation complex eIF4F. *EMBO J* 19: 3465-3474.

Cuesta R, Laroia G, Schneider RJ (2000) Chaperone hsp27 inhibits translation during heat shock by binding eIF4G and facilitating dissociation of cap-initiation complexes. *Genes & Dev* 14: 1460–1470.

Cuesta R, Xi Q, Schneider RJ (2004) Structural basis for competitive inhibition of eIF4G-Mnk1 interaction by the adenovirus 100-kilodalton protein. *J Virol* 78: 7707-7716.

Culjkovic B, Topisirovic I, Borden KLB (2007) Controlling gene expression through RNA regulons. *Cell Cycle* 6: 65– 69.

Cyrklaff M, Risco C, Fernandez JJ, Jimenez MV, Esteban M, Baumeister W, Carrascosa JL (2005) Cryo-electron tomography of vaccinia virus. *PNAS* 102: 2772-2777.

Damaso CR, Esposito JJ, Condit RC, Moussatche N (2000) An emergent poxvirus from humans and cattle in Rio de Janeiro state: Cantagalo virus may derive from Brazilian smallpox vaccine. *Virology* 277: 439-449.

Damon IK (2007) Poxviruses. In: Howley DMKaPM (ed). *Fields virology*. Philadelphia, PA: Lippincott Williams & Wilkins. Pp. 2947-2975.

Datta SR, Dudek H, Tao X, Masters S, Fu H, Gotoh Y, Greenberg ME (1997) Akt phosphorylation of BAD couples survival signals to the cell-intrinsic death machinery. *Cell* 91: 231–241.

Davis RE, Mathews CK (1993) Acidic C terminus of vaccinia virus DNA-binding protein interacts with ribonucleotide reductase. *Proc Natl Acad Sci* USA 90: 745-749.

de Benedetti A, Harris AL (1999) eIF4E expression in tumors: its possible role in progression of malignancies. *Int J Biochem Cell Biol* 31(1): 59-72.

de Benedetti A, Graff JR (2004) eIF-4E expression and its role in malignancies and metastases. O*ncogene* 23(18): 3189-3199.

de los Rios JEG, Jimenez-Gomez JA (2007) Smallpox: an old disease but still a threat in the XXI century. In: A. Mendez-Vilaz (ed). *Communicating Current Research and Educational Topics and Trends in Applied Microbiology*. Badajoz, Spain: Formatex. Pp. 657-667.

de Magalhaes JC, Andrade AA, *et al*. (2001) A mitogenic signal triggered at an early stage of vaccinia virus infection: implication of MEK/ERK and protein kinase A in virus multiplication. *J Biol Chem* 276: 38353–38360.

de Moor CH, Richter JD (1999) Cytoplasmic polyadenylation elements mediate masking and unmasking of cyclin B1 mRNA. *EMBO J* 18: 2294–2303.

DeLange AM, McFadden G (1987) Efficient resolution of replicated poxvirus telomeres to native hairpin structures requires two inverted symmetrical copies of a core target DNA sequence. *J Virol* 61: 1957-1963.

Dellis S, Strickland KC, McCrary WJ, Patel A, Stocum E, *et al*. (2004) Protein interactions among the vaccinia virus late transcription factors. *Virology* 329: 328-336.

Derry JM, Kerns JA, Francke U (1995) RBM3, a novel human gene in Xp11.23 with a putative RNA-binding domain. *Hum Mol Genet* 4: 2307-2311.

Dimmock NJ, Easton AJ, Leppard KN (2007) *Introduction to modern virology*. Vaccines and antivirals: the prevention and treatment of virus diseases. Singapore: Blackwell Publishing Ltd.

Domi A, Beaud G (2000) The punctuate sites of vaccinia virus early proteins are precursors of sites of viral DNA synthesis. *J Gen Virol* 81: 1231-1235.

Domi A, Moss B (2002) Cloning the vaccinia virus genome as a bacterial artificial chromosome in *Escherichia coli* and recovery of infectious virus in mammalian cells. *PNAS* 99: 12415-12420.

Domi A, Moss B (2005) Engineering of a vaccinia virus bacterial artificial chromosome in *Escherichia coli* by bacteriophage λ −based recombination. *Nature methods* 2: 95-97.

Dostie J, Ferraiuolo M, Pause A, Adam SA, Sonenberg N (2000) A novel shuttling protein, 4E-T, mediates the nuclear import of the mRNA $5^{\llcorner}$ cap-binding protein, eIF4E. *EMBO J* 19: 3142–3156.

Du S, Traktman P (1996) Vaccinia virus DNA replication: Two hundred base pairs of telomeric sequence confer optimal replication efficiency on minichromosome templates. *PNAS* 93: 9693-9698.

Duff RG, Overby LR (1975) In: Abstracts of the Annual Meeting of the American Society for Microbiology. Washington, D.C.: American Society for Microbiology. Pp.240.

Dunn EF, Fearns R, Connor JH (2009) Akt inhibitor Akt-IV blocks virus replication through an Akt-independent mechanism. *J Virol* 83: 11665-11672.

Dyer JR, Michel S, Lee W, Castellucci VF, Wayne NL, Sossin WS (2003) An activity-dependent switch to capindependent translation triggered by eIF4E dephosphorylation. *Nat Neurosci* 6: 219–220.

Elia A, Constantinou C, Clemens MJ (2008) Effects of protein phosphorylation on ubiquitination and stability of the translational inhibitor protein 4E-BP1. *Oncogene* 27: 811-822.

Elmore S (2007) Apoptosis: A review of programmed cell death. *Tox Pathol* 35: 495-516.

Engelma JA, Luo J, Cantley LC (2006) The evolution of phosphatidylinositol 3-kinases as regulators of growth and metabolism. *Nat Rev Genet* 7: 606–619.

Engelman JA (2009) Targeting PI3K signalling in cancer: opportunities, challenges and limitations. *Nat Rev Cancer* 9:550–562.

Fasolo A, Sessa C (2008) mTOR inhibitors in the treatment of cancer. *Expert Opin InvestiG Drugs* 17: 1717–1734.

Feigenblum D, Schneider RJ (1996) Cap-binding protein (eukaryotic initiation factor 4E) and 4E- inactivating protein BP-1 independently regulate cap-dependent translation. *Mol Cell Biol* 16: 5450-5457.

Fenner F, Henderson DA, Arita I, Jezek Z, Ladnyi ID (1988) Smallpox and ist eradication. World Health Organization. Geneva.

Flynn A, Proud G (1996) Insulin-stimulated phosphorylation of initiation factor 4E is mediated by the MAP kinase pathway. *FEBS Lett* 389: 162-166.

Frederickson RM, Montine KS, Sonenberg N (1991) Phosphorylation of eukaryotic translation initiation fac- tor 4E is increased in Src-transformed cell lines. *Mol Cell Biol* 11: 2896-2900.

Fruman DA, Meyers RE, Cantley LC (1998) Phosphoinositide kinases. *Annu Rev Biochem* 67: 481-507.

Furic L, Rong L, Larsson O, *et al.* (2010) eIF4E phosphorylation promotes tumorigenesis and is associated with prostate cancer progression. *PNAS* 107(32): 14134-14139.

Gale M. Jr, Tan S, Katze MG (2000) Translational control of viral gene expression in eukaryotes. *Microbiol Mol Biol Rev* 64: 239-280.

Garfin DE (2003) Gel electrophoresis of proteins. In: Davey J and Lord M (eds). *Essential Cell Biology*, Vol.1: Cell Structure, A Practical Approach. Oxford UK: Oxford University Press. Pp. 197-268.

Garon CF, Barbosa E, Moss B (1978) Visualization of an inverted terminal repetition in vaccinia virus DNA. *PNAS* 75: 4863-4867.

Gingras AC, Svitkin Y, Belsham GJ, Pause A, Sonenberg N (1996) Activation of the translational suppressor 4E-BP1 following infection with encephalomyocarditis virus and poliovirus. *PNAS* 93: 5578-5583.

Gingras AC, Sonenberg N (1997) Adenovirus infection inactivates the translational inhibitors 4E-BP1 and 4E-BP2. *Virology* 237**:**182–186.

Gingras AC, Raught B, Sonenberg N (1999) eIF4F initiation factors: effectors of mRNA recruitment to ribosomes and regulation of translation. *Annu Rev Biochem* 68: 913-963.

Gingras AC, Raught B, Sonenberg N (2001) Regulation of translation initiation by FRAP/mTOR. *Gen Dev* 15: 807-826.

Gingras AC, Raught B, Sonenberg N (2004) mTOR signaling to translation. *Curr Top Microbiol Immunol* 279: 169-197.

Gingras AC, Raught B, Sonenberg N (2007) Control of translation by the target of rapamycin proteins. In: Rhoads RE (ed). *Signaling pathways for translation. Stress, calcium, and rapamycin.* Heidelberg, Germany: Springer. Pp. 143-174.

Goodfellow IG, Chaudhry Y, Gioldasi I, Gerondopoulos A, Natoni A, Labrie L, Laliberte JF, Roberts L (2005) Calicivirus translation initiation requires an interaction between VPg and eIF4E. *EMBO Rep* 6: 968–972.

Goodfellow IG, Roberts LO (2008) Eukaryotiv initiation factor 4E. *Int J Bioch Cell Biol* 40: 2675-2680.

Graham FL, Smiley J, Russell WC, Nairn R (1977) Characteristics of a human cell line transformed by DNA from human adenovirus type 5. *J Gen Virol* 36: 59-72.

Greipel J, Urbanke C, Maass G (1989) The single-stranded DNA binding protein of Escherichia coli. Physicochemical properties and biological functions. In: Saenger W & Heinemann U (eds). *Protein–Nucleic Acid Interaction*. London: Macmillan. Pp. 61-86.

Griffiths G, Roos N, Schleich S, Locker JK (2001) Structure and assembly of intracellular mature vaccinia virus: thin-section analyses. *J Virol* 75: 11056-11070.

Groft CM, Burley SK (2002) Recognition of eIF4G by rotavirus NSP3 reveals a basis for mRNA circularization. *Mol Cell* 9(6): 1273–1283.

Gruenberg J, van der Goot FG (2001) Mechanisms of pathogen entry through the endosomal compartments. *Nat Rev Mol Biol Cell Biol* 7: 495-504.

Guertin DA, Sabatini DM (2007) Defining the role of mTOR in cancer. *Cancer Cell* 12: 9–22.

Guhaniyogi J, Brewer G (2001) Regulation of mRNA stability in mammalian cells. *Gene* 265: 11-23.

Haghighat A, Mader S, Pause A, Sonenberg N (1995) Repression of cap-dependent translation by 4E-binding protein 1: competition with p220 for binding to eukaryotic initiation factor-4E, *EMBO J* 14: 5701-5709.

Haghighat A, Sonenberg N (1997) eIF4G dramatically enhances the binding of eIF4E to the mRNA 5'-cap structure. *J Biol Chem* 272: 21677-21680.

Hale BG, Randall RE (2008) PI3K signalling during influenza A virus infections. *Biochem Soc Trans* 35: 186-188.

Hambidge S, Sarnow P (1992) Translational enhancement of the poliovirus 5' noncoding region mediated by virus-encoded polypeptide 2A. *PNAS* 89: 10272-10276.

Hara K, Maruki Y, Long X, Yoshino K, Oshiro N, Hidayat S, Tokunaga C, Avruch J, Yonezawa K (2002) Raptor, a binding partner of target of rapamycin (TOR), mediates TOR action. *Cell* 110(2):177-89.

Hay N, Sonenberg N (2004) Upstream and downstream of mTOR. *Gen Dev* 18: 1926-1945.

He Z, Henricksen LA, Wold MS, Ingles CJ (1995) RPA involvement in the damage-recognition and incision steps of nucleotide excision repair. *Nature* 374: 566–569.

Heitman J, Movva NR, Hall MN (1991) Targets for cell cycle arrest by the immunosuppressant rapamycin in yeast. *Science* 253: 905-909.

Hellen CU (2009) IRES-induced conformational changes in the ribosome and the mechanism of translation initiation by internal ribosomal entry. *Biochem Biophys Acta* 1789(9–10): 558–570.

Hellen CU, Sarnow P (2001) Internal ribosome entry sites in eukaryotic mRNA molecules. *Genes Dev* 15 (13): 1593–612.

Heuser J (2005) Deep-etch EM reveals that the early poxvirus envelope is a single membrane bilayer stabilized by a geodetic "honeycomb" surface coat. *J Cell Biol* 169: 269-283.

Hinnebusch AG (2006) eIF3: a versatile scaffold for translation initiation complexes. *Trends Biochem Sci* 31: 553-562.

Hinton TM, Coldwell MJ, Carpenter GA, Morley SJ, Pain VM (2007) Functional analysis if individual binding activities of the scaffold protein eIF4G. *J Biol Chem* 282: 1695-1708.

Hopkins DR (2002) *The greatest killer – Smallpox in history*. Chicago, Illinois: University of Chicago Press.

Hu N, Yu R, Shikuma C, Shiramizu B, Ostrwoski MA, Yu Q (2009) Role of cell signaling in poxvirus-mediated foreign gene expression in mammalian cells. *Vaccine* 27: 2994–3006.

Huang ES (1975) Human cytomegalovirus IV. Specific inhibition of virus-induced DNA polymerase activity and viral DNA replication by phosphonoacetic acid. *J Virol* 16: 1560-1565.

Hung JJ, Chung CS, Chang W (2002) Molecular chaperone Hsp90 is important for vaccinia virus growth in cells. *J Virol* 76: 1379-1390.

Iborra FJ, Jackson DA, Cook PR (2001) Coupled transcription and translation within nuclei of mammalian cells. *Science* 293: 1139–1142.

Iyer LM, Aravind L, Koonin EV (2001) Common origin of four diverse families of large eukaryotic DNA viruses. *J Virol* 75: 11720-11734.

Jang SK, Krausslich HG, Nicklin MJ, Duke GM, Palmenberg AC, Wimmer E (1988) A segment of the 5' nontranslated region of encephalomyocarditis virus RNA directs internal entry of ribosomes during in vitro translation. *J Virol* 62: 2636-2643.

Jones RM, Branda J, Johnston KA, Polymenis M, Gadd M, Rustgi A, Callanan L, Schmidt EV (1996) An essential E box in the promoter of the gene encoding the mRNA cap-binding protein (eukaryotic initiation factor 4E) is a target for activation by c-myc. *Mol Cell Biol* 16: 4754-4764.

Joshi B, Cai AL, Keiper BD, Minich WB, Mendez R, Beach CM, Stepinski J, Stolarski R, Darzynkiewicz E, Rhoads RE (1995) Phosphorylation of eukaryotic protein synthesis initiation factor 4E at Ser-209. *J Biol Chem* 270: 14597-14603.

Julien LA, Carriere A, Moreau J, Roux PP (2010) mTORC1-Activated S6K1 Phosphorylates Rictor on Threonine 1135 and Regulates mTORC2 Signaling. *Mol Cell Biol* 30: 908-921.

Jung MY, Lorenz L, Richter JD (2006) Translational Control by Neuroguidin, a Eukaryotic Initiation Factor 4E and CPEB Binding Protein. *Mol Cell Biol* 26: 4277-4287.

Kahvejian A, Svitkin YV, Sukarieh R, M'Boutchou MN, Sonenberg N (2005) Mammalian poly(A)-binding protein is a eukaryotic translation initiation factor, which acts via multiple mechanisms. *Genes Dev* 19: 104-113.

Kandel ES, Hay N (1999) The regulation and activities of the multifunctional serine/threonine kinase Akt/PKB. *Exp Cell Res* 253(1): 210-229.

Katsafanas GC, Moss B (2007) Colocalization of transcription and translation within cytoplasmic poxvirus factories coordinates viral expression and subjugates host functions. *Cell Host Microbe* 2: 221-228.

Katso R, Okkenhaug K, Ahmadi K, White S, Timms J, Waterfield MD (2001) Cellular function of phosphoinositide 3-kinases: Implications for development, homeostasis, and cancer. *Cell Dev Biol Ann Rev* 17: 615-75.

Keck JG, Baldick CJ, Moss B (1990) Role of DNA replication in vaccinia virus gene expression: A naked template is required for transcription of three late transactivator genes. *Cell* 61(5): 801-809.

Kennedy SG, Kandel ES, Cross TK, Hay N (1999) Akt/Protein kinase B inhibits cell death by preventing the release of cytochrome c from mitochondria. *Mol Cell Biol* 19: 5800-5810.

Kieft JS (2008) Viral IRES RNA structures and ribosome interactions. *Trends Biochem Sci* 33(6): 274–283.

Kim DH, Sarbassov DD, Ali SM, Latek RR, Guntur KV, Erdjument-Bromage H, Tempst P, Sabatini DM (2003) GbetaL, a positive regulator of the rapamycin-sensitive pathway required for the nutrient-sensitive interaction between raptor and mTOR. *Mol Cell* 11(4): 895-904.

Knauf U, Tschopp C, Gram H (2001) Negative regulation of protein translation by mitogen-activated protein kinase-interacting kinases 1 and 2. *Mol Cell Biol* 21: 5500–5511.

Kolhapure RM, Deolankar RP, Tupe CD, Raut CG, Basu A, Dama BM, Pawar SD, Joshi MV, Padbidri VS, Goverdhan MK, Banerjee K (1997) Investigation on buffalopox outbreaks in Maharashtra State during 1992-1996. *Indian J Med Res* 106: 441-446.

Koul D, Shen R, Kim YW (2010) Cellular and in vivo activity of a novel PI3K inhibitor, PX-866, against human glioblastoma. *Neuro Oncol* 12(6): 559-569.

Kovacs GR, Moss B (1996) The vaccinia virus H5R gene encodes late gene transcription factor 4: purification, cloning and overexpression. *J Virol* 70: 6796-6802.

Kozak M (1989) The scanning model for translation: an update. *J Cell Biol* 108: 229-241.

Krassa KB, Green LS, Gold L (1991) Protein-protein interactions with the acidic COOH terminus of the single-stranded DNA-binding protein of the bacteriophage T4. *PNAS* 88: 4010-4114.

Ktori CP, Shepherd R, O'Rourke L (2003) TNF-alpha and leptin activate the alpha-isoform of class II phosphoinositide 3-kinase. *Biochem Biophys Res Com* 306: 139-43.

Kudchodkar SB, Yu Y, *et al*. (2004) Human cytomegalovirus infection induces rapamycin-insensitive phosphorylation of downstream effectors of mTOR kinase. *J. Virol* 78:11030–11039.

Kunz J, Henriquez R, Schneider U, Deuter-Reinhard M, Movva NR, Hall MN (1993) Target of rapamycin in yeast, TOR2, is an essential phosphatidylinositol kinase homolog required for G1 progression. *Cell* 73: 585-596.

Lai HK, Borden KL (2000) The promyelocytic leukaemia (PML) protein suppresses cyclin D1 protein production by altering the nuclear cytoplasmic distribution of cyclin D1 mRNA. *Oncogene* 19: 1623–1634.

Lamphear BJ, Kirchweger R, Skern T, Rhoads RE (1995) Mapping of Functional Domains in Eukaryotic Protein Synthesis Initiation Factor 4G (eIF4G) with Picornaviral Proteases *J Biol Chem* 270: 21975–21983.

Lawlor MA, Alessi DR (2001) PKB/Akt: a key mediator of cell proliferation, survival and insulin responses? *J Cell Sci* 114: 2903-2910.

Le Bouffant R, Cormier P, Mulner-Lorillon O, Belle R (2006) Hypoxia and DNA-damaging agent bleomycin both increase the cellular level of the protein 4E-BP. *J Cell Biochem* 99: 126–132.

Lee SB, Esteban M (1994) The interferon-induced double-stranded RNA-activated protein kinase induces apoptosis. *Virology* 199: 491–496.

Lefkowitz EJ, Upton C, Changayil SS, Buck C, Traktman P, Buller RML (2005) Poxvirus bioinformatics resource center: A comprehensive *Poxviridae* informational and analytical resource. *Nucleic Acids Res* 33: 331-316.

Leinbach SS, Reno JM, Lee LF, Isbell AF, Boezi JA (1976) Mechanism of phosphonoacetate inhibition of herpesvirus-induced DNA polymerase. *Biochem* 15: 426-430.

Lemke LE, Paine-Murrieta GD, Taylor CW, Powis G (1999) Wortmannin inhibits the growth of mammary tumors despite the existence of a novel wortmannin-insensitive phosphatidylinositol-3-kinase. *Cancer Chem Pharm* 44(6): 491-497.

Lemon SM, Honda M (1997) Internal Ribosome Entry Sites within the RNA Genomes of Hepatitis C Virus and Other Flaviviruses. *Sem Virol* 8: 274-288.

Leonard S, Plante D, Wittmann S, Daigneault N, Fortin MG, Laliberte JF (2000) Complex Formation between Potyvirus VPg and Translation Eukaryotic Initiation Factor 4E Correlates with Virus Infectivity. *J Virol* 74: 7730–7737.

Li L, Lu X, Peterson CA, Legerski RJ (1995) An interaction between the DNA repair factor XPA and replication protein A appears essential for nucleotide excision repair. *Mol Cell Biol* 15: 5396–5402.

Li S, Sonenberg N, Gingras AC, Peterson M, Avdulov S, Polunovsky VA, *et al*. (2002) Translational control of cell fate: availability of phosphorylation sites on translational repressor 4E-BP1 governs its proapoptotic potency. *Mol Cell Biol* 22: 2853–2861.

Lin YC, Li J, Irwin CR, Jenkins H, DeLange L, *et al*. (2008) Vaccinia virus DNA ligase recruits cellular topoisomerase II to sites of viral replication and assembly. *J Virol* 82: 5922-5932.

Lin YC, Malina A, Pelletier J (2009) c-Myc and eIF4F Constitute a Feedforward Loop That Regulates Cell Growth: Implications for Anticancer Therapy. *Cancer Res* 69(19): 7491-7494.

Ling J, Morley SJ, Traugh JA (2005) Inhibition of cap-dependent translation via phosphorylation of eIF4G by protein kinase Pak2. *EMBO J* 24**:** 4094–4105.

Lopez-Lastra M, Rivas A, Barria MI (2005) Protein synthesis in eukaryotes: The growing biological relevance of cap-independent translation initiation. *Biol Res* 38: 121-146.

Low W, Harries M, Ye H, Du MQ, Boshoff C, Collins M (2001) Internal Ribosome Entry Site Regulates Translation of Kaposi's Sarcoma-Associated Herpesvirus FLICE Inhibitory Protein. *J Virol* 75: 2938-2945.

Macejak DG, Sarnow P (1991) Internal initiation of translation mediated by the 5' leader of a cellular mRNA. *Nature* 353: 90-94.

Mackett M (1979) Conservation and variation in orthopoxvirus genome structure. *J Gen Virol* 45: 683-701.

Mader S, Lee H, Pause A, Sonenberg N (1995) The translation initiation factor eIF-4E binds to a common motif shared by the translation factor eIF-4G and the translational repressors 4E-binding proteins. *Mol Cell Biol* 15: 4990-4997.

Mader S, Sonenberg N (1995) Cap binding complexes and cellular growth control. *Biochimie* 77: 40-44.

Maffucci T, Cooke FT, Foster FM, Traer CJ, Fry MJ, Falasca M (2005) Class II phosphoinositide 3-kinase defines a novel signaling pathway in cell migration. *J Cell Biol* 169: 789-99.

Maier U, Babich A, Nurnberg B (1999) Roles of non-catalytic subunits in G bg-induced activation of class I phosphoinositide 3-kinase isoforms b and g. *J Biol Chem* 274: 29311–29317.

Mallardo M, Schleich S, Krijnse Locker J (2001) Microtubule-dependent organization of vaccinia virus core-derived early mRNAs into distinct cytoplasmic structures. *Mol Biol Cell* 12: 3875-3891.

Mamane Y, Petroulakis E, Rong LW, Yoshida K, Ler LW, Sonenberg N (2004) eIF4E – from translation to transformation. *Oncogene* 23: 3172–3179.

Mangus DA, Evans MC, Jacobson A (2003) Poly(A)-binding proteins: multifunctional scaffolds for the post-transcriptional control of gene expression. *Genome Biol* 4: 223.

Mao JCH, Robishaw EE, Overby LR (1975) Inhibition of DNA polymerase from herpes simplex virus- infected Wi-38 cells by phosphonoacetic acid. *J Virol* 15: 1281-1283.

Marcotrigiano J, Gingras AC, Sonenberg N, Burley SK (1997) Cocrystal structure of the messenger RNA 5' cap-binding protein (eIF4E) bound to 7-methyl-GDP. *Cell* 89(6): 951-61.

Marcotrigiano J, Gingras AC, Sonenberg N, Burley SK (1999) Cap-dependent translation initiation in eukaryotes is regulated by a molecular mimic of eIF4G. *Mol. Cell* 3 (6): 707–16.

Marzluff WF (1992) Histone 3'ends: Essential and regulatory functions. *Gene Expr* 2(2): 93-97.

Mastrangelo MJ, Eisenlohr LC, Gomella L, Lattime EC (2000) Poxvirus vectors: orphaned and underappreciated. *J Clin Invest* 105: 1031-1034.

Mathews MB, Sonenberg N., Hershey JWB (2007) Origins and principles of translational control. In: M. B. Mathews NS, N. Sonenberg and J. W. B. Hershey, editor. Translational control in biology and medicine. Cold Spring Harbor, NY: Cold Spring Harbor Laboratory Press. pp. 1-40.

Matsuo H, Li H, McGuire AM, Fletcher CM, Gingras AC, Sonenberg N, Wagner G (1997) Structure of translation factor eIF4E bound to m7GDP and interaction with 4E-binding protein. *Nat Struct Biol* 4: 717–724.

Mbuy GN, Morris RE, Bubel HC (1982) Inhibition of cellular protein synthesis by vaccinia virus surface tubules. *Virology* 116(1): 137-147.

McFadden G (2005) Poxvirus tropism. *Nat Rev Microbiol* 3: 201-213.

McKendrick L, Pain VM, Morley SJ (1999) Translation initiation factor 4E. *Int J Biochem Cell Biol* 31(1): 31-5.

McKendrick L, Morley SJ, Pain VM, Jagus R, Joshi B (2001) Phosphorylation of eukaryotic initiation factor 4E (eIF4E) at Ser209 is not required for protein synthesis in vitro and in vivo. *Eu. J. Biochem* 268: 5375–5385.

McNulty S, Bornmann W, Schriewer J, Werner C, Smith SK, *et a*l. (2010) Multiple Phosphatidylinositol 3-Kinases Regulate Vaccinia Virus Morphogenesis. *PLoS ONE* 5(5): e10884.

Meyer RR, Laine PS (1990) The single-stranded DNA-binding protein of Escherichia coli. *Microbiol Rev* 54: 342-380.

Merchlinsky M (1990) Mutational analysis of the resolution sequence of vaccinia virus DNA: Essential sequence consists of two separate AT-rich regions highly conserved among poxviruses. *J Virol* 64: 5029-5035.

Millns AK, Carpenter MS, DeLange AM (1994) The vaccinia virus-encoded uracil DNA glycosylase has an essential role in viral DNA replication. *Virology* 198: 504–513.

Minich WB, Balasta ML, Goss DJ, Rhoads RE (1994) Chromatographic resolution of in vivo phosphorylated and nonphosphorylated eukaryotic translation initiation factor eIF-4E: increased cap affinity of the phosphorylated form. *PNAS* 91: 7668–7672.

Mir MA, Panganiban AT (2008) A protein that replaces the entire cellular eIF4F complex. *Embo J* 27: 3129-3139.

Moerke NJ, Aktas H, Chen H, Cantel S, Reibarkh MY, Fahmy A, Gross JD, Degterev A, Yuan J, Chorev M, Halperin JA, Wagner G (2007) Small-molecule inhibition of the interaction between the translation initiation factors eIF4E and eIF4G. *Cell* 128: 257-267.

Mohr IJ, Pe'ery T, Mathews MB (2007) Protein synthesis and translational control during viral infection. In: M. B. Mathews NS, N. Sonenberg and J. W. B. Hershey, editor. Translational control in biology and medicine. Cold Spring Harbor, NY: Cold Spring Harbor Laboratory Press. pp. 545-595.

Molecular biology of the cell (2002) Alberts B, Bray D, Lewis J, Raff M, Roberts K, Watson JD. New York: Garland Science.

Moody CA, Scott RS et al. (2005) Modulation of the cell growth regulator mTOR by Epstein-Barr virus-encoded LMP2A. *J Virol* 79**:** 5499–5506.

Moore SP, Erdile T, Kelly T, Fishel R (1991) The human homologous pairing protein HPP-1 is specifically stimulated by the cognate single-stranded binding protein hRP-A. *PNAS* 88: 9067-9071.

Moorman NJ, Shenk T (2010) Rapamycin-Resistant mTORC1 Activity is Required for Herpesvirus Replication. *J Virol* 84(10): 5260-5269.

Moreno MA, Carrascosa AL, Ortin J, Vinuela E (1978) Inhibition of African swine fever (ASF) virus replication by phosphonoacetic acid. *J Gen Virol* 93: 253-258.

Morley SJ, Rau M, Kay JE, Pain VM (1993). Increased phosphorylation of eukaryotic initiation factor 4 ⌐ during activation of T lymphocytes correlates with increased eIF-4F complex formation. *Eur J Biochem* 218: 39–48.

Morley S (1994) Signal transduction mechanisms in the regulation of protein synthesis. *Mol Biol Rep* 19: 221-231.

Morley SJ, McKendrick L (1997) Involvement of stress-activated protein kinase and p38/ERK mitogen-activated protein kinase signaling pathways in the enhanced phosphorylation of initiation factor 4E in NIH 3T3 cells *J Biol Chem* 272: 17887-17893.

Morley S (2001) The regulation of eIF4F during cell growth and cell death. In: RE Rhoads, editor. *Signaling pathways for translation. Stress, calcium, and rapamycin.* Heidelberg, Germany: Springer. pp. 1-37.

Morley SJ, Naegele S (2002) Phosphorylation of eukaryotic initiation factor (eIF) 4E is not required for de novo protein synthesis following recovery from hypertonic stress in human kidney cells. *J Biol Chem* 277: 32855–32859.

Morley SJ, Coldwell MJ, Clemens MJ (2005) Initiation factor modifications in the preapoptotic phase. *Cell Death Differ* 12: 571-84.

Moss B (1996) Genetically engineered poxviruses for recombinant gene expression, vaccination, and safety. *Proc Natl Acad Sci USA* 93: 11341-11348.

Moss B, Ward BM (2001) High-speed mass transit for poxviruses on microtubules. *Nat Cell Biol* 3(11): 245-246.

Moss B (2006) Poxvirus entry and membrane fusion. *Virology* 344: 48-54.

Moss B (2007) Poxviridae: the viruses and their replication. In: Howley DMKaPM, editor. *Fields virology*. Philadelphia, PA: Lippincott Williams & Wilkins. Pp. 2849-2883.

Mulder J, Robertson ME, Seamons RA, Belsham GJ (1998) Vaccinia virus protein synthesis has a low requirement for the intact translation initiation factor eIF4F, the cap-binding complex, within infected cells. *J Virol* 72**:** 8813-9.

Muller G, Williamson JD (1987) *Poxviridae*. In: Animal Virus Structure. Elsevier Science Publishers B.V. Amsterdam, Netherlands. Edited by Nermut MV and Steven AC. Pp. 421-434.

Munroe D, Jacobson A (1990) mRNA poly(A) tail, a 3' enhancer of translational initiation. *Mol Cell Biol* 10: 3441-3455.

Muthukrishnan S, Both GW, Furuichi Y, Shatkin AJ (1975) *Nature* 255: 33–7.

Nagelhus TA, Haug T, Singh KK, Keshav KF, Skorpen F, Otterlei M, Bharati S, Lindmo T, Benichou S, Benarous R, Krokan HE (1997) A sequence in the N-terminal region of human uracil-DNA glycosylase with homology to XPA interacts with the C-terminal part of the 34-kDa subunit of replication protein A. *J Biol Chem* 272: 6561–6566.

Nalefski EA, Falke JJ (1996) The C2 domain calcium-binding motif: Structural and functional diversity. *Prot Sci* 5(12): 2375-2390.

Nobukuni T, Joaquin M, Roccio M, Dann SG, Kim SY, Gulati P, Byfield MP, *et al*. (2005) Amino acids mediate mTOR/raptor signaling through activation of class 3 phosphatidylinositol 3OH-kinase. *PNAS* 102: 14238-43.

Nyormoi O, Thorley-Lawson DA, Elkington J, Strominger JL (1976) Differential effect of phosphonoacetic acid on the expression of Epstein-Barr viral antigens and virus production. *PNAS USA* 73: 1745-1748.

Oh KJ, Kalinina A, Park NH, Bagchi S (2006) Deregulation of eIF4E: 4E-BP1 in differentiated human papillomavirus-containing cells leads to high levels of expression of the E7 oncoprotein. *J Virol* 80**:** 7079–7088.

O'Shea C, Klupsch K, Choi S, Bagus B, Soria C, et al. (2005) Adenoviral proteins mimic nutrient/growth signals to activate the mTOR pathway for viral replication. *Embo J* 24: 1211-1221.

Overby LR, Duff RG, Mao JCH (1977) Antiviral potential of phosphonoacetic acid. *Ann NY Acad Sci* 284: 310-320.

Pain WM (1996) Initiation of protein synthesis in eukaryotic cells. *Eur J Biochem* 236: 747-771.

Pap M, Cooper GM (1998) Role of glycogen synthase kinase-3 in the phosphatidylinositol 3-kinase/Akt cell survival pathway. *J Biol Chem* 273: 19929–19932.

Paran N, De Silva FS, Senkevich TG, Moss B (2009) Cellular DNA ligase I is recruited to cytoplasmic vaccinia virus factories and masks the role of the vaccinia ligase in viral DNA replication. *Cell Host Microbe* 6: 563-569.

Poulin F, Gingras AC, Olsen H, Chevalier S, Sonenberg N (1998) 4E-BP3, a new member of the eukaryotic initiation factor 4E-binding protein family. *J Biol Chem* 273(22): 14002-14007.

Pause A, Belsham GJ, Gingras AC, Donze O, Lin TA, Lawrence JJr., Sonenberg N (1994) Insulin-dependent stimulation of protein synthesis by phosphorylation of a regulator of 5'-cap function *Nature* 371: 762-767.

Pascreau G, Delcros JG, Cremet JY, Prigent C, Arlot-Bonnemains Y (2005) Phosphorylation of maskin by Aurora-A participates in the control of sequential protein synthesis during Xenopus laevis oocyte maturation. *J Biol Chem* 280: 13415–13423.

Pelletier J, Sonenberg N (1988) Internal initiation of translation of eukaryotic mRNA directed by a sequence derived from poliovirus RNA. *Nature* 334: 320-325.

Pennington TH, Follett EA (1974) Vaccinia virus replication in enucleated BSC-1 cells: particle production and synthesis of viral DNA and proteins. *J Virol* 13: 488-493.

Pestova TV, Lorsch JR, Hellen CUT (2007) The mechanism of translation initiation in eukaryotes. In: M. B. Mathews NS, N. Sonenberg and J. W. B. Hershey, editor. Translational control in biology and medicine. Cold Spring Harbor, NY: Cold Spring Harbor Laboratory Press. pp. 87-128.

Peterson RT, Beal PA, Comb MJ, Schreiber SL (2000) FKBP12-rapamycin-associated protein (FRAP) autophosphorylates at serine 2481 under translationally repressive conditions. *J Biol Chem* 275: 7416-7423.

Piron M, Vende P, Cohen J, Poncet D (1998) Rotavirus RNA-binding protein NSP3 interacts with eIF4GI and evicts the poly(A) binding protein from eIF4F. *EMBO J* 17: 5811-5821.

Polacek C, Friebe P, Harris E (2009) Poly(A)-binding protein binds to the non-polyadenylated 30 untranslated region of dengue virus and modulates translation efficiency. *J Gen Virol* 90(Pt 3): 687–692.

Poncet D, Aponte C, Cohen J (1993) Rotavirus protein NSP3 (NS34) is bound to the 3′ end consensus sequence of viral mRNAs in infected cells. *J Virol* 67: 3159–3165.

Powis G, Bonjouklian R et al. (1994) Wortmannin, a potent and selective inhibitor of phosphatidylinositol-3-kinase. *Cancer Res* 54: 2419-23.

Prescott DM, Kates J, Kirkpatrick JB (1971) Replication of vaccinia wirus DNA In enucleated L-cells. *J Mol Biol* 59: 505-508.

Prévôt D, Darlix JL, Ohlmann T (2003) Conducting the initiation of protein synthesis: the role of eIF4G. *Biol Cell* 95: 141-156.

Proud CG (2004) Role of mTOR signaling in the control of translation initiation and elongation by nutrients. *Curr Top Microbiol Immunol* 279: 215-244.

Proud CG (2005) The eukaryotic initiation factor 4E-binding proteins and apoptosis. *Cell Death Differ* 12: 541–546.

Ptushkina M, von der Haar T, Karim MM, Hughes JM, McCarthy JE (1999) Repressor binding to a dorsal regulatory site traps human eIF4E in a high cap-affinity state. *EMBO J* 18: 4068–4075.

Pyronnet S, Imataka H, Gingras AC, Fukunaga R, Hunter T, Sonenberg N (1999) Human eukaryotic translation initiation factor 4G (eIF4G) recruits Mnk1 to phosphorylate eIF4E. *EMBO J* 18: 270-279.

Rahaus M, Desloges N, Wolff MH (2006) Varicella-zoster virus requires a functional PI3K/Akt/GSK-3α/β signaling cascade for efficient replication. *Cell Signal* 19: 312-320.

Raught B, Gingras AC, Gygi SP, Imataka H, Morino S, Gradi A, Aebersold R, Sonenberg N (2000) Serum-stimulated, rapamycin-sensitive phosphorylation sites in the eukaryotic translation initiation factor 4GI. *EMBO J* 19: 434–444.

Raught, B, Gingras AC, Sonenberg N (2001) The target of rapamycin (TOR) proteins. *PNAS* 98: 7037-44.

Raught B, Gingras AC (2007) Signaling to translation initiation. In: MB Mathews NS, N Sonenberg and JWB Hershey, editor. Translational control in biology and medicine. Cold Spring Harbor, NY: Cold Spring Harbor Laboratory Press. pp. 369-400.

Regad T, Chelbi-Alix MK (2001) Role and fate of PML nuclear bodies in response to interferon and viral infections. *Oncogene* 20: 7274–7286.

Rhoads RE (2009) eIF4E: New family members, new binding partners, new roles. *J Biol Chem* 284: 16711-16715.

Rinker-Schaeffer CW, Austin V, Zimmer S, Rhoads RE (1992) Ras transformation of cloned rat embryo fibroblasts results in increased rates of protein synthesis and phosphorylation of eukaryotic initiation factor 4E. *J Biol Chem* 267: 10659-10664.

Rivas C, Gil J, Melkova Z, Esteban M, Diaz-Guerra M (1998) Vaccinia virus E3L protein is an inhibitor of the interferon (IFN)-induced 2–5A synthetase enzyme. *Virology* 243: 406–414.

Rochester SC, Traktman P (1998) Characterization of the single-stranded DNA binding protein encoded by the vaccinia virus I3 gene. *J Virol* 72: 2917-2926.

Roper RL (2004) Rapid Preparation of Vaccinia Virus DNA Template for Analysis and Cloning by PCR. In: Isaacs SN, editor. Vaccinia Virus and Poxvirology Methods and Protocols. Philadelphia, PA: Humana Press. pp. 2849-2883.

Rosenwald B, Rhoads DB, Callanan LD, Isselbacher KJ, Schmidt EV (1993) Increased expression of eukaryotic translation initiation factors eIF-4E and eIF-2 alpha in response to growth induction by c-myc. *PNAS* 90(13): 6175-6178.

Rousseau D, Kaspar R, Rosenwald I, Gehrke L, Sonenberg N (1996) Translation initiation of ornithine decarboxylase and nucleocytoplasmic transport of cyclin D1 mRNA are increased in cells overexpressing eukaryotic initiation factor 4E. *PNAS* 93: 1065–70.

Rozen F, Edery I, Meerovitch K, Dever TE, Merrick WC, Sonenberg N (1990) Bidirectional RNA helicase activity of eucaryotic translation initiation factors 4A and 4F. *Mol Cell Biol* 10: 1134-1144.

Sarbassov DD, Ali SM, Kim DH, Guertin DA, Latek RR, Erdjument-Bromage H, Tempst P, Sabatini DM (2004) Rictor, a novel binding partner of mTOR, defines a rapamycin-insensitive and raptor-independent pathway that regulates the cytoskeleton. *Curr Biol*, 14: 1296-1302.

Sarbassov DD, Guertin DA, Ali SM, Sabatini DM (2005) Phosphorylation and regulation of Akt/PKB by the rictor-mTOR complex. *Science* 307: 1098–1101.

Savinova O, Jagus R (1997) Use of vertical slab isoelectric focusing and immunoblotting to evaluate steady-state phosphorylation of eIF2 alpha in cultured cells. *Methods* 11(4): 419-425.

Scheiflinger F, Dorner F, Falkner FG (1992) Construction of chimeric vaccinia viruses by molecular cloning and packaging. *PNAS* 89: 9977-9981.

Scheper GC, van Kollenburg B, Hu J, Luo Y, Goss DJ, Proud CG (2004) Phosphorylation of Eukaryotic Initiation Factor 4E Markedly Reduces Its Affinity for Capped mRNA. *J Biol Chem* 277: 3303-3309.

Schmelz M, Sodeik B, Ericsson M, Wolffe EJ, Shida H, Hiller G, Griffiths G (1994) Assembly of vaccinia virus: the second wrapping cisterna is derived from the trans Golgi network. *J Virol* 68(1): 130-147.

Schneider RJ, Mohr I (2003) Translation initiation and viral tricks. *Trends Biochem Sci* 28: 130-136.

Schneider R, Braunstein S, Xi Q, Formenti S (2005) Ionizing radiation controls protein synthesis through a novel Akt-independent pathway involving regulation of mTOR and 4E-BP1 stability. *Int J Radiat Oncol Biol Phys* 63: S146.

Schultz RM, Merriman RL, Andis SL, Bonjouklian R, Grindey GB, Rutherford PG, Gallegos A, Massey K, Powis G (1995) In vitro and in vivo antitumor activity of the phosphatidylinositol-3-kinase inhibitor, wortmannin. *Anticancer Res* 15(4): 1135-9.

Shatkin AJ, Manley JL (2000) The ends of the affair: Capping and polyadenylation. *Nat Struct Biol* 7: 838-842.

Shchelkunov SN, Marennikova SS, Moyer RW (2005) Orthopoxviruses pathogenic for humans. New York, NY: Springer Science + Business Media, Inc.

Shipkowitz NL, Bower RR, Appell RN, Nordeen CW, Overby LR, Roderick WR, Schleicher JB, Von Esch AM (1973) Suppression of herpes simplex virus infection by phosphonoacetic acid. *App Microbiol* 26: 264-267.

Shirokikh NE, Spirin AS (2008) Poly(A) leader of eukaryotic mRNA bypasses the dependence of translation on initiation factors. *PNAS USA* 105**:**10738-43.

Shuman S (2002) What messenger RNA capping tells us about eukaryotic evolution. *Nat Rev Mol Cell Biol* 3: 619-625.

Sieczkarski SB, Whittaker GR (2005) Viral entry. *Curr Top Microbiol Immunol* 285: 1–23.

Silva PN, Soares JA, Brasil JS, Nogueira SV, Andrade AA, de Magalhaes JC, Bonjardim MB, Ferreira PC, Kroon EG, Bruna- Romero O, Bonjardim CA (2006) Differential role played by the MEK/ ERK/EGR-1 pathway in orthopoxviruses vaccinia and cowpox biology. *Biochem J* 398: 83–95.

Smith GL (2002) The formation and function of extracellular enveloped vaccinia virus. *J Gen Virol* 83: 2915-2931.

Smith GL, Law M (2004) The exit of Vaccinia virus from infected cells. *Virus Res* 106: 189-197.

Soares JAP et al (2009) Activation of the PI3K/Akt pathway early during vaccinia and cowpox virus infections is required for both host survival and viral replication. *J Virol* 83: 6883-6899.

Sonenberg N, Morgan MA, Merrick WC, Shatkin AJ (1978) A polypeptide in eukaryotic initiation factors that crosslinks specifically to the 5'-terminal cap in mRNA. *PNAS* 75: 4843-4847.

Sonenberg N, Hinnebusch AG (2009) Regulation of translation initiation in eukaryotes: mechanisms and biological targets. *Cell* 136: 731-745.

Spriggs KA, Stoneley M, Bushell M, Willis AE (2008) Re-programming of translation following cell stress allows IRES-mediated translation to predominate. *Biol. Cell* 100: 27–38.

Stanford MM, Barrett JW et al. (2007) Oncolytic Virotherapy Synergism with ignaling Inhibitors: Rapamycin Increases Myxoma Virus Tropism for Human Tumor Cells. *J Virol* 81: 1251-1260.

Stebbins-Boaz B, Cao Q, de Moor CH, Mendez R, Richter JD (1999) Maskin is a CPEB-associated factor that transiently interacts with elF-4E. *Mol Cell* 4: 1017–1027.

Stephens LR, Eguinoa A, Erdjument-Bromage H, Lui M, Cooke F, Coadwell J, Smrcka AS, Thelen M, Cadwallader K, Tempst P, Hawkins PT (1997) The Gbg sensitivity of a PI3K is dependent upon a tightly associated adaptor, p101. *Cell* 89: 105–114.

Strudwick S, Borden KL (2002) The emerging roles of translation factor eIF4E in the nucleus. *Differentiation* 70: 10–22.

Stuart DT, Upton C, Higman MA, Niles EG, McFadden G (1993) A poxvirus-encoded uracil DNA glycosylase is essential for virus viability. *J Virol* 67: 2503–2512.

Suzan-Monti M, La Scola B, Raoult D (2006) Genomic and evolutionary aspects of Mimivirus. *Virus Res* 117: 145-155.

Svitkin YV, Ovchinnikov LP, Dreyfuss G, Sonenberg N (1996) General RNA binding proteins render translation cap dependent. *Embo J* 15: 7137-7146.

Svitkin YV, Herdy B, Costa-Mattioli M, Gingras AC, Raught B, Sonenberg N (2005) Eukaryotic translation initiation factor 4E availability controls the switch between cap-dependent and internal ribosome entry site-mediated translation. *Mol Cell Biol* 25: 10556-10565.

Tahara SM, Morgan MA, Shatkin AJ (1981) Two forms of purified m7G-cap binding protein with different effects on capped mRNA translation in extracts of uninfected and poliovirus-infected HeLa cells. *J Biol Chem* 256: 7691-7694.

Takahashi T, Hara K, Inoue H, Kawa Y, Tokunaga C, Hidayat S, Yoshino K, Kuroda Y, Yonezawa K (2000) Carboxyl-terminal region conserved among phosphoinositide-kinase-related kinases is indispensable for mTOR function in vivo and in vitro. *Genes Cells* 5: 765-775.

Tarun SZ, Sachs AB (1995) A common function for mRNA 5' and 3' ends in translation initiation in yeast. *Genes Dev* 9: 2997-3007.

Tarun SZ Jr, Wells SE, Deardorff JA, Sachs AB (1997) Translation initiation factor eIF4G mediates in vitro poly(A) tail-dependent translation. *Proc Natl Acad Sci* 94: 9046-9051.

Tattersall P, Ward DC (1976) Rolling hairpin model for replication of parvovirus and linear chromosomal DNA. *Nature* 263: 106-109.

Teranishi F, Takahashi N, Gao N, Akamo Y, Takeyama H, Manabe T, Okamoto T (2009) Phosphoinositide 3-kinase inhibitor (wortmannin) inhibits pancreatic cancer cell motility and migration induced by hyaluronan in vitro and peritoneal metastasis in vivo. *Cancer Sci* 100(4): 770-7.

Thoreen CC, Kang SA et al. (2009) An ATP-competitive Mammalian Target of Rapamycin Inhibitor Reveals Rapamycin-resistant Functions of mTORC1. *J Biol Chem* 284: 8023-8032.

Tilleray V, Constantinou C, Clemens MJ (2006) Regulation of protein synthesis by inducible wild-type p53 in human lung carcinoma cells. *FEBS Lett* 580: 1766–1770.

Tomoo K, Abiko F, Miyagawa H, Kitamura K, Ishida T (2006) Effect of N-terminal region of eIF4E and Ser65-phosphorylation of 4E–BP1 on interaction between eIF4E and 4E–BP1 fragment peptide. *J Biochem* 140: 237–246.

Tooze J, Hollinshead M, Reis B, Radsak K, Kern H (1993) Progeny vaccinia and human cytomegalovirus particles utilize early endosomal cisternae for their envelopes. *Eur J Cell Biol* 60(1): 163-178.

Topisirovic I, Guzman ML, McConnell MJ, Licht JD, Culjkovic B, Neering SJ, Jordan CT, Borden KLB (2003). Aberrant eukaryotic translation initiation factor 4E-dependent mRNA transport impedes the hematopoietic differentiation and contributes to leukemogenesis. *Mol Cell Biol* 23: 8992–9002.

Traktman P (1996) Poxvirus DNA replication. In: DNA Replication in Eukaryotic Cells. Cold Spring Harbor Laboratory Press. Pp. 775-798.

Tseng M, Palaniyar N, Zhang W, Evans DH (1999) DNA binding and aggregation properties of the vaccinia virus I3L gene product. *J Biol Chem* 274: 21637-21644.

Tsukiyama-Kohara K, Iizuka N, Kohara M, Nomoto A (1992) Internal ribosome entry site within hepatitis C virus RNA *J. Virol.* 66: 1476–1483.

Tuazon PT, Morley SJ, Dever TE, Merrick WC, Rhoads RE, Traugh JA (1990) Association of initiation factor eIF-4E in a cap binding protein complex (eIF-4F) is critical for and enhances phosphorylation by protein kinase C. *J Biol Chem* 265: 10617–10621.

Turner SJ, Domin J, Waterfield MD, Ward SG, Westwick J (1998) The CC chemokine monocyte chemotactic peptide-1 activates both the class I p85/p110 phosphatidylinositol 3-kinase and the class II PI3K-C2alpha. *J Biol Chem* 273: 25987-95.

van Eijl H, Hollinshead M, Rodger G, Zhang WH, Smith GL (2002) The vaccinia virus F12L protein is associated with intracellular enveloped virus particles and is required for their egress to the cell surface. *J Gen Virol* 83: 195-207.

Vende P, Piron M, Castagné N, Poncet D (2000) Efficient translation of rotavirus mRNA requires simultaneous interaction of NSP3 with the eukaryotic translation initiation factor eIF4G and the mRNA 3' end. *J Virol* 74: 7064-7071.

Virus Taxonomy: The Classification and Nomenclature of Viruses. The Seventh Report of the International Committee on Taxonomy of Viruses (2000) van Regenmortel MHV, Fauquet CM, Bishop DHL, Carstens EB, Estes MK, Lemon SM, Maniloff J, Mayo MA, McGeoch DJ, Pringle CR, Wickner RB, eds. VII Report of the ICTV. San Diego: Academic Press.

Vivanco I, Sawyers CL (2002) The phosphatidylinositol 3-Kinase AKT pathway in human cancer. *Nat Rev Cancer* 2: 489–501.

Vlahos CJ, Matter WF, Hui KY, Brown RF (1994) A specific inhibitor of phosphatidylinositol 3-kinase, 2-(4-morpholinyl)-8-phenyl-4H-1-benzopyran-4-one (LY294002). *J Biol Chem* 269: 5241-8.

Volpon L, Osborne MJ, Topisirovic I, Siddiqui N, Borden KL (2006) Cap-free structure of eIF4E suggests a basis for conformational regulation by its ligands. *EMBO J* 25: 5138–5149.

von der Haar T, Ball PD, McCarthy JE (2000) Stabilization of eukaryotic initiation factor eIF4E binding to the mRNA 5'-cap by domains of eIF4G. *J Biol Chem* 275: 30551-30555.

Vos JC, Stunnenberg HG (1988) Derepression of a novel class of vaccinia virus genes upon DNA replication. *EMBO J* 7(11): 3487-3492.

Walker EH, Pacold ME, Perisic O, Stephens L, Hawkins PT, Wymann MP, Williams RL (2000) Structural determinants of phosphoinositide 3-kinase inhibition by wortmannin, LY294002, quercetin, myricetin, and staurosporine. *Mol Cell* 6: 909-919.

Walsh D, Arias C, Perez C, Halladin D, Escandon M, Ueda T, Watanabe-Fukunaga R, Fukunaga R, Mohr I (2008) Eukaryotic translation initiation factor 4F architectural alterations accompany translation initiation factor redistribution in poxvirus-infected cells. *Mol Cell Biol* 28: 2648-2658.

Walsh D, Mohr I (2004) Phosphorylation of eIF4E by Mnk-1 enhances HSV-1 translation and replication in quiescent cells. *Genes Dev* 18**:** 660–672.

Walsh D, Perez C, Notary J, Mohr I (2005) Regulation of the translation initiation factor eIF4F by multiple mechanisms in human cytomegalovirus-infected cells. *J Virol* 79: 8057-8064.

Walsh D, Mohr I (2006) Assembly of an active translation initiation factor complex by a viral protein. *Genes Dev* 20: 461-472.

Wang C, Sarnow P, Siddiqui A (1993) Translation of human hepatitis C virus RNA in cultured cells is mediated by an internal ribosome-binding mechanism *J. Virol.* 67: 3338–3344.

Wang X, Flynn A, Waskiewicz AJ, Webb BLJ, Vries RG, Baines IA, Cooper JA, Proud CG (1998) The phosphorylation of eukaryotic initiation factor eIF4E in response to phorbol esters, cell stress and cytokines is mediated by distinct MAP kinase pathways. *J Biol Chem* 273: 9373-9377.

Wang G, Barrett JW et al. (2006) Infection of human cancer cells with myxoma virus requires Akt activation via interaction with a viral ankyrin-repeat host range factor. *PNAS* 103: 4640-46-45.

Wang X, Proud CG (2007) Methods for studying signal-dependent regulation of translation factor activity. In: J Lorsch, editor. Methods in enzymology Vol. 431 Translation initiation: Cell biology, high-throughput methods, and chemical-based approaches. USA: Elservier. pp. 113-142.

Ward DC, Reich E, Goldberg IH (1965) Base specificity in the interaction of polynucleotides with antibiotic drugs. *Science* 149: 1256-1263.

Welsch S, Doglio L, Schleich S, Krijnse Locker J (2003) The vaccinia virus I3L gene product is localized to a complex endoplasmic reticulum-associated structure that contains the viral parental DNA. *J Virol* 77: 6014-6028.

Werden SJ, Barrett JW *et al*. (2007) M-T5, the Ankyrin Repeat, Host Range Protein of Myxoma Virus, Activates Akt and Can Be Functionally Replaced by Cellular PIKE-A. *J Virol* 81: 2340-2348.

Wittek R, Moss B (1980) Tandem repeats within the inverted terminal repetition of vaccinia virus DNA. *Cell* 21: 277-284.

Wold MS (1997) Replication protein A: a heterotrimeric, single-stranded DNA-binding protein required for eukaryotic DNA metabolism. *Annu Rev Biochem* 66: 61-92.

World Health Organization (1999) Smallpox eradication: destruction of variola virus stocks. 52th World Health Assembly. Resolution A52/5.

Yang H, Masters SC, Wang H, Fu H (2001) The proapoptotic protein Bad binds the amphipathic groove of 14-3-3zeta. *Biochim Biophys Acta* 1547: 313-319.

Yu D, Ellis HM, Lee EC, Jenkins NA, Copeland NG, Court DL (2000) An efficient recombination system for chromosome engineering in Escherichia coli. *PNAS* 97: 5978-5983.

Yueh A, Schneider RJ (1996) Selective translation initiation by ribosome jumping in adenovirus-infected and heat-shocked cells. *Genes Dev* 10: 1557-1567.

Xi Q, Cuesta R, Schneider RJ (2004) Tethering of eIF4G to adenoviral mRNAs by viral 100k protein drives ribosome shunting. *Genes Dev* 18: 1997-2009.

Zaborowska I, Walsh D (2009) PI3K signaling regulates rapamycin-insensitive translation complex formation in vaccinia virus-infected cells. *J Virol* 83: 3988-3992.

Zappavigna V, Piccioni F, Villaescusa JC, Verrotti AC (2004) Cup is a nucleocytoplasmic shuttling protein that interacts with the eukaryotic translation initiation factor 4E to modulate Drosophila ovary development *PNAS* 101: 14800–14805.